# ANALYTICA CHIMICA ACTA

*International monthly devoted to all branches of analytical chemistry*
*Revue mensuelle internationale consacrée à tous les domaines de la chimie analytique*
*Internationale Monatsschrift für alle Gebiete der analytischen Chemie*



ELSEVIER PUBLISHING COMPANY

AMSTERDAM

*Anal. Chim. Acta*, Vol. 56, No. 1, 1–156, August 1971
**Published monthly**

## Publication Schedule for 1971

In the interests of rapid publication it has been found necessary to schedule 5 volumes for appearance in 1971. Since monthly publication will be maintained, this implies that 2 of the volumes will each consist of three issues, while 3 of the volumes will each consist of only 2 issues. The following provisional schedule applies:

| | | |
|---|---|---|
| Vol. **53**, No. **1** | January 1971 | |
| Vol. **53**, No. **2** | February 1971 | **(completing Vol. 53)** |
| Vol. **54**, No. **1** | March 1971 | |
| Vol. **54**, No. **2** | April 1971 | |
| Vol. **54**, No. **3** | May 1971 | **(completing Vol. 54)** |
| Vol. **55**, No. **1** | June 1971 | |
| Vol. **55**, No. **2** | July 1971 | **(completing Vol. 55)** |
| Vol. **56**, No. **1** | August 1971 | |
| Vol. **56**, No. **2** | September 1971 | |
| Vol. **56**, No. **3** | October 1971 | **(completing Vol. 56)** |
| Vol. **57**, No. **1** | November 1971 | |
| Vol. **57**, No. **2** | December 1971 | **(completing Vol. 57)** |

Subscription price: $17.50 or Dfl. 63.— per volume plus postage. Total subscription price for 1971: $87.50 or Dfl. 315.— plus postage. Additional cost for copies by airmail available on request. For subscribers in the U.S.A. and Canada, 2nd class postage paid at New York, N.Y. For advertising rates apply to the publishers.

Subscriptions should be sent to:

ELSEVIER PUBLISHING COMPANY P.O. Box 211, Amsterdam, The Netherlands

---

## GENERAL INFORMATION

*Languages*

Papers will be published in English, French or German.

*Submission of papers*

Papers should be sent to:

PROF. PHILIP W. WEST,
Coates Chemical Laboratories,
College of Chemistry and Physics,
Louisiana State University,
Baton Rouge 3,
La. 70803 (U.S.A.)

or to:

DR. A. M. G. MACDONALD,
Department of Chemistry,
The University,
P.O. Box 363
Birmingham B15 2TT (Great Britain)

*Reprints*

Fifty reprints will be supplied free of charge. Additional reprints (minimum 100) can be ordered at quoted prices. They must be ordered on order forms which are sent together with the proofs.

# INDUSTRIAL ELECTROCHEMICAL PROCESSES

*A Comprehensive Review of Past and Present Industrially Scaled Processes*

Edited by A. T. KUHN, Lecturer in Electrochemistry, University of Salford, Lancashire, England

**1971, xxiv + 632 pages, 56 tables, 144 illus., 1,805 lit.refs., Dfl. 165.00 (ca. $ 45.75)**
**ISBN 0-444-40885-1**

This book will provide newcomers with an excellent idea of the scope of the field, and the basic principles involved, together with the relative importance of each area. The professional electrochemist will find a concise and up to date review of the scientific background, while the chemical engineer or industrial electrochemist will find the fullest available bibliography on the process of interest to him. There is a listing of key Patents and references. The second part of the book reviews the major components of the technology, and a final chapter examines the development of the industry on a country by country basis.

The contributing authors have compiled what is unquestionably the most authoritative and fully researched book yet written on the subject.

CONTENTS:

Production of Elemental Fluorine by Electrolysis. Electrochemical Fluorination. The Chlor-Alkali Industry. Industrial Water Electrolysis. Electrolytic Heavy Water Manufacture. The Electrowinning of Metals. Electrorefining in Aqueous Electrolytes. Electrorefining in Molten Salts. Electrochemical Machining. The Electrolytic Finishing of Metals. Electroforming. The Electrodeposition of Paint. Electrodialysis. Miscellaneous Industrial Processes. Electrodes for Industrial Processes. Diaphragms and Electrolytes. Cell Design. An International Survey of Industrial Electrochemical Processes.

CONTRIBUTORS:

B. A. Cooke, D. Gilroy, P. F. Hart, A. W. D. Hills, G. Isserlis, C. Jackson, R. J. Kendrick, A. T. Kuhn, D. Lawson, N. N. Ness, A. L. L. Palluel, A. J. Rudge, D. H. Smith, G. S. Solt, J. M. Steele, E. V. Tuck, B. J. Woodhall, P. M. Wright.

---

**Elsevier**
Book Division, P.O. Box 3489
Amsterdam - The Netherlands

ANALYTICA CHIMICA ACTA
Vol. 56 (1971)

# ANALYTICA CHIMICA ACTA

*International monthly devoted to all branches of analytical chemistry*
*Revue mensuelle internationale consacrée à tous les domaines de la chimie analytique*
*Internationale Monatsschrift für alle Gebiete der analytischen Chemie*




ELSEVIER PUBLISHING COMPANY
AMSTERDAM

*Anal. Chim. Acta*, Vol. 56 (1971)

*Analytica Chimica Acta*
Elsevier Publishing Company, Amsterdam
Printed in The Netherlands



# DETERMINATION OF TRACES OF ARSENIC BY COPRECIPITATION AND X-RAY FLUORESCENCE

T. M. REYMONT AND R. J. DUBOIS
*Hercules Incorporated, Bacchus Works, Magna, Utah 84044 (U.S.A.)*

(Received 18th January 1971)

The well-known toxic effects of arsenic make the need for a sensitive trace analysis method imperative. Typical environmental monitoring programs for arsenic generate large numbers of samples. A wide range of other elements can be expected along with arsenic, and so the method must be adaptable to the varying compositions likely to exist with different types of materials to be tested. Therefore, the procedure must minimize the number of interfering elements. The levels of arsenic in the various samples of interest may run from tenths of a part per million to several hundred parts per million. Hence, to allow use of reasonably sized samples the method must be sensitive and linear over a range from a microgram or less up to several hundred micrograms.

Traces of arsenic are most frequently measured by the classical Gutzeit method or a modification[1]. After appropriate digestion, the arsenic is converted to arsine and distilled from solution. In the original semiquantitative approach, the arsine is trapped on paper strips coated with a mercury(II) halide. The extent of the staining of the paper caused by the unknown is visually compared to known samples. The Marsh test is based on distillation of the arsine into a heated capillary tube. The arsine is then decomposed to give a shiny mirror of arsenic, the length of which is compared to standards. A popular Gutzeit modification gives more quantitative results. The arsine is trapped in sodium hypobromite solution and determined by the molybdenum blue method. Another spectrophotometric method involves trapping arsine in silver diethyldithiocarbamate and reading. The arsenic may be converted to arsenic(III) chloride and distilled from an acid solution[2]. These procedures all are quite lengthy and require considerable care to eliminate interferences and especially to avoid losses of the volatile arsenic compound during the generation, distillation, and trapping.

Instrumental approaches for traces of arsenic include emission spectroscopy[3], atomic absorption[4], and X-ray fluorescence. The last mentioned has been used in several ways for traces of arsenic. In one procedure[5], after pretreatment arsenic is extracted with pyrrolidine dithiocarbamate in chloroform. The chloroform solution is then evaporated on filter paper and arsenic determined by X-ray fluorescence. The extraction is not too selective; lead directly interferes and large quantities of some other metals affect results by simple absorption of the arsenic K$\alpha$ X-rays.

Luke[6] proposed a preconcentration approach for arsenic and other elements based on precipitation with diethyldithiocarbamate with copper(II) as a coprecipitant. The precipitate is collected on filter paper and counted b X-ray fluorescence. Complexing agents are used to remove some interfering elements. In the same report

he suggested the possibility of the coprecipitation of various elements as the sulfide. This approach allowed more selectivity for arsenic than did the carbamate precipitation. Consequently, we have developed a method suitable for traces of arsenic precipitated as the sulfide.

## EXPERIMENTAL

### *Reagents*

*Standard arsenic solution* (100 *p.p.m.*) Dissolve 0.132 g of arsenic trioxide in 10 ml of 1 *M* sodium hydroxide, neutralize with 10 ml of 0.5 *M* sulfuric acid and dilute with water to 1 l.

*Molybdenum coprecipitant solution* (1000 *p.p.m.*) Dissolve 2.5217 g of $Na_2MoO_4 \cdot 2H_2O$ in 1 l of water containing 5 ml of sulfuric acid.

Interferent solutions containing 5000 p.p.m. of silver, bismuth, mercury(II), tin(IV), and antimony(III) were prepared by dissolving appropriate weights of the nitrates in water. A lead(II) solution (4800 p.p.m.) was prepared by dissolving the nitrate in water.

### *Apparatus*

A General Electric XRD-5S X-ray spectrometer was used with a molybdenum target X-ray tube and a lithium fluoride crystal. The K$\alpha$ line of arsenic was selected for measurement. The molybdenum target X-ray tube was selected for the analysis since its wavelength is shorter than the absorption wavelength for the arsenic K$\alpha$ line and the target lines do not interfere with the K$\alpha$ line of arsenic. Background and line counts were taken for 100 sec at 35.00° and 34.00° 2$\theta$, respectively. Counting was performed with a pulse-height analyzer.

The precipitates were collected on Millipore 25-mm diameter 2.0-$\mu$m polyvic filter papers and the Millipore microanalysis filter holder.

### *Procedure*

The general approach was the same for soil, water, air, or vegetation samples. For soil samples, oxidize 2–3 g of dried, finely ground soil with 5 ml of a mixture of two parts of bromine and three parts of carbon tetrachloride. After 15 min add 10 ml of concentrated nitric acid, and evaporate to dryness. Add 5 ml of concentrated sulfuric acid and heat to evolution of sulfur trioxide fumes to expel all nitric acid. Cool, dilute with water to about 75 ml and heat. Filter and make to volume with water. Take an aliquot, make 3.7 *M* with concentrated perchloric acid and add 200 $\mu$g of molybdenum. Precipitate arsenic and molybdenum as the sulfides with 5 ml of aqueous 2% (w/v) thioacetamide solution. After 15 min collect the precipitate on a filter, dry and count at 34.00° 2$\theta$. Count the background at 35.00° 2$\theta$ and correct. Determine the concentration of arsenic from the calibration curve.

## DISCUSSION AND RESULTS

The X-ray fluorescence method was based on collecting and measuring the arsenic as the 3+ and 5+ sulfides. The arsenic generally was freed in typical samples by digestion first with bromine–carbon tetrachloride, and then with nitric acid. This treatment dissolved and oxidized all the arsenic to the 5+ state and all organic ma-

terial was destroyed. During the sulfide precipitation step, some of the arsenic could be reduced to the 3+ state by the sulfide. After the nitric acid fume-off with sulfuric acid and dilution with water, insoluble materials such as silica, alumina, lead sulfate, calcium sulfate, etc., were removed by filtration.

After dilution of the filtrate, a portion was taken and reacidified before precipitation of the arsenic as the sulfide. The samples used in this study generally contained large amounts of lead. When sulfuric acid was used, more lead sulfate precipitated. Apparently lead sulfate was somewhat soluble in the concentrated sulfuric acid solution after the fuming with nitric acid and upon dilution insufficient time was allowed for the sulfate precipitate to grow before filtering. The reacidification to about 6 *M* with sulfuric acid was sufficient to accelerate this precipitate formation and bring down residual lead. When perchloric acid was selected for the acidification no lead precipitated from solution. The presence of a lead precipitate with the arsenic could not be tolerated. The lead Lα line at 1.175 Å significantly overlaps the arsenic Kα line at 1.177 Å.

Table I illustrates the effects of lead on the arsenic response at several levels of each metal with both sulfuric and perchloric acids. Samples were made up, carried through the digestion and filtration and then the appropriate acid was added before sulfide precipitation. With perchloric acid a 24-fold excess of lead in solution resulted in no lead precipitating or affecting the arsenic count. However, when sulfuric acid was used, a significant amount of lead was still present and the lead sulfide precipitate drastically affected the arsenic results.

Both arsenic(III) and arsenic(V) form sulfides that are insoluble in strong acid solutions. They do however dissolve at pH 7–8 or above and also in the presence of excess of sulfide. To ascertain more exactly the effect of acid strengths on the arsenic

TABLE I

EFFECT OF LEAD ON RECOVERY OF ARSENIC AS A FUNCTION OF ACID

| *As added*(μg) | *Pb added*(μg) | *Acid* | *X-ray* (*counts sec*$^{-1}$) |
|---|---|---|---|
| 0 | 160 | 3.7 *M* $HClO_4$ | 2 |
| 20 | 160 | 3.7 *M* $HClO_4$ | 276 |
| 20 | 320 | 3.7 *M* $HClO_4$ | 285 |
| 20 | 480 | 3.7 *M* $HClO_4$ | 277 |
| 20 | 480 | 6 *M* $H_2SO_4$ | 1530 |

TABLE II

EFFECT OF ACIDITY ON ARSENIC PRECIPITATION[a]

| *Acid strength* (*M*) | *As recovery* (%) |
|---|---|
| 0.74 | 99.4 |
| 1.5 | 100 |
| 2.9 | 100 |
| 3.7 | 100 |
| 4.4 | 99.3 |
| 5.9 | 98.5 |
| 7.4 | 80.8 |

[a] Acidity of solution from which the arsenic sulfide was precipitated adjusted with perchloric acid.

TABLE III

TIME REQUIRED FOR QUANTITATIVE PRECIPITATION OF $As_2S_3$ AND $As_2S_5$

| *Time (min)* | *As(III) recovery (%)* | *As(V) recovery (%)* |
|---|---|---|
| 1 | 31.3 | 31.8 |
| 5 | 95.4 | 91.4 |
| 10 | 101 | 98.7 |
| 15 | 100 | 99.3 |
| 20 | 98.2 | 102 |
| 25 | 99.2 | 99.8 |

sulfide precipitation, 10-$\mu$g samples were coprecipitated with 200 $\mu$g of molybdenum in solutions from 0.74 *M* to 7.4 *M* in perchloric acid. The results are shown in Table II. Complete recovery of arsenic was obtained up to 5.9 *M* acid. At 7.4 *M* acid low recoveries occurred. The X-ray fluorescence inspection of the resulting precipitates showed that the molybdenum sulfide completely precipitated at all acid strengths tested so that the low recovery of arsenic at the highest acid level was due to the solubility of the arsenic sulfide.

The sulfide of arsenic(V) is reported to form slowly. Arsenic(V) is slowly reduced to arsenic(III) with sulfide and if necessary, a rapid complete reduction can be accomplished by adding iodide to catalyze the reaction. There also was an apparent time factor for complete precipitation of the arsenic(III) sulfide. Therefore, a study was run with both arsenic(III) and arsenic(V) varying the time for which the precipitate was allowed to stand before the filtration and measurement. The results are shown in Table III. The arsenic(III) sulfide was recovered quantitatively from 10 min or longer, and the arsenic(V) sulfide from 15 min or longer. Therefore, there was no need to convert the arsenic from the 5+ state to 3+ state before precipitation as long as a 15-min precipitation time was allowed.

Excess of sulfide can dissolve the arsenic sulfides. To ensure that the sulfide was being precipitated quantitatively without redissolution, known arsenic samples were precipitated with 2%, 5% and 10% thioacetamide solutions. Complete recovery of arsenic was obtained with each thioacetamide concentration. Therefore, a 2% solution was used in subsequent work.

While arsenic(III) and (V) sulfides are insoluble in solutions up to at least 5.9 *M* in perchloric acid, many other metal sulfides are completely soluble even in weakly acidic solutions (below 1 *M*). In more strongly acidic solutions, only silver, mercury(II), bismuth, tin(IV), and antimony(III) were thought likely to precipitate and interfere with the arsenic determination. To determine any possible interferences, 10-$\mu$g amounts of arsenic were taken and the afore-mentioned metals were added each in a 50-fold excess. Precipitation of the sulfides was carried out over a range of acidities from 0.74 *M* to 7.4 *M* in perchloric acid. The results are shown in Table IV. At 7.4 *M* results were low owing to the partial solubility of the arsenic sulfide. Recoveries were high in solutions of 2.9–5.9 *M*. The 10% high recoveries were due primarily to the overlap of the bismuth L$\alpha$ line at 1.114 Å with the arsenic K$\alpha$ line at 1.177 Å. Pulse-height analysis minimizes this effect. Hence, the error caused by bismuth is quite small and would be insignificant even at a ten-fold excess. Based on fluorescence scans of the residues, mercury(II) sulfide was 95% dissolved in the 2.9 *M* acid and

TABLE IV

EFFECT OF ACIDITY ON RECOVERY OF ARSENIC IN 50-FOLD EXCESS OF Sb, Hg, Bi, Sn, AND Ag

| *Acid strength (M)*[a] | *As recovery (%)*[b] |
|---|---|
| 0.74 | 99.3 |
| 1.5 | 101 |
| 2.9 | 111 |
| 3.7 | 114 |
| 4.4 | 108 |
| 5.9 | 110 |
| 7.4 | 95.2 |

[a] Acidity of the solution from which the arsenic sulfide was precipitated adjusted with perchloric acid.
[b] Recovery of 10 μg of As(III) in the presence of 500 μg each of Sb(III), Hg(II), Ag, Sn(IV) and Bi(II).

completely dissolved in 3.7 *M* acid. The silver, antimony, and tin precipitated but caused little interference because their prime radiation lines are far removed from the Kα arsenic line.

Calibration data were obtained for standards containing both arsenic(III) and arsenic(V). A constant 200 μg of molybdenum was used as the coprecipitant. The sulfide precipitation was carried out in 3.7 *M* perchloric acid with 2% thioacetamide and a 15-min wait for complete precipitation. Linear calibration plots were obtained for both arsenic(III) and arsenic(V) standards from 1 μg to 350 μg of arsenic. The slopes were identical. On the basis of these data, the method is easily able to detect 1 μg of arsenic or less.

The efficiency of recovery was checked by using two soil samples that were previously found to contain 19.0 p.p.m. and 3.1 p.p.m. of arsenic. To each sample 100 p.p.m. of arsenic was added. In the first sample 119 p.p.m. arsenic was found; in the second 103 p.p.m. arsenic was found. The precision of this coprecipitation–X-ray method was determined by analyzing ten samples of soil. The replicate analyses of the soil sample showed the 95% confidence limit of the method to be ±0.6 p.p.m. at the 18-p.p.m. level.

SUMMARY

A new method for trace amounts of arsenic is described. After suitable sample preparation, arsenic is precipitated as the sulfide from a 3.7 *M* perchloric acid solution by means of a 2% thioacetamide solution with 200 μg of molybdenum as coprecipitant. The sulfide precipitation from highly acidic solution minimizes interferences. After 15 min the precipitate is filtered and the arsenic Kα line is counted by X-ray fluorescence. The method can detect less than a microgram of arsenic and is equally adaptable for arsenic in air, water, soil, or organic material.

RÉSUMÉ

On décrit une nouvelle méthode de dosage de l'arsenic, à l'état de traces. Après préparation de l'échantillon, l'arsenic est précipité comme sulfure, en milieu acide perchlorique 3.7 *M*, au moyen de thioacétamide à 2%, en présence de 200 μg

de molybdène comme coprécipitant. La précipitation comme sulfure, en milieu fortement acide diminue les interférences. Après 15 min, le précipité est filtré; la ligne Kα de l'arsenic est comptée par fluorescence aux rayons X. Cette méthode permet de déceler moins d'un microgramme d'arsenic et peut s'appliquer au dosage de l'arsenic dans l'air, l'eau, le sol ou dans des matières organiques.

ZUSAMMENFASSUNG

Es wird eine neue Methode für Spurenmengen Arsen beschrieben. Nach einer geeigneten Probenvorbereitung wird das Arsen als Sulfid aus 3.7 *M* Perchlorsäurelösung mit einer 2%-igen Thioacetamidlösung und mit 200 μg Molybdän als Mitfällungsmittel gefällt. Die Sulfidfällung aus stark saurer Lösung vermindert Störungen weitgehend. Nach 15 min wird der Niederschlag abfiltriert und die Arsen-Kα-Linie nach der Röntgenfluoreszenz-Methode gemessen. Es kann weniger als 1 μg Arsen nachgewiesen werden. Die Methode eignet sich für die Bestimmung von Arsen in Luft, Wasser, Boden und organischen Substanzen.

REFERENCES

1 N. H. FURMAN (Editor), *Scott's Standard Methods of Analysis*, 6th Edn., D. Van Nostrand, Princeton, N.J., 1962, pp. 118–127, pp. 135–137.
2 M. B. JACOBS, *The Analytical Chemistry of Industrial Poisons, Hazards, and Solvent*, 2nd Edn., Interscience, New York, 1949, pp. 242–244.
3 J. F. KOPP AND R. C. KRONER, *Appl. Spectrosc.*, 19 (1965) 155.
4 E. LAKENEN, *P & E Atomic Absorption Newsletter*, 5 (1966) 17.
5 F. J. MARCIE, *Environ. Sci. Tech.*, 1 (1967) 164.
6 C. L. LUKE, *Anal. Chim. Acta*, 41 (1968) 237.

*Analytica Chimica Acta*
Elsevier Publishing Company, Amsterdam
Printed in The Netherlands



# AMMONIUM 1-PYRROLIDINEDITHIOCARBAMATE AS A REAGENT FOR BISMUTH

HERBERT K. Y. LAU, HENRY A. DROLL AND PETER F. LOTT
*Chemistry Department, University of Missouri–Kansas City, Kansas City, Mo. 64110 (U.S.A.)*
(Received 25th February 1971)

The analytical application of the dithiocarbamate ion and its N-substituted compounds as reagents for inorganic analysis has been reviewed[1]; much is reported on the use of sodium diethyldithiocarbamate (NaDDTC) as a chromogenic reagent for heavy metals, and little is reported on the use of the 1-pyrrolidinedithiocarbamate ion, first prepared as the ammonium salt (APDC) by Malissa and Schoffmann[2]. APDC has received increasing attention as a reagent for the extraction of metals before their determination by atomic absorption spectrophotometry[3-5]. Advantages of APDC over NaDDTC are that it is more stable in acidic solutions under conditions where NaDDTC decomposes rapidly[2,6], that it reacts with more metals to form complexes that are easily extracted with organic solvents, and that the addition of ammonium ions does not add metal ions to the sample.

With NaDDTC and masking agents, Cheng *et al.*[7] developed a sensitive and selective spectrophotometric procedure for bismuth in the presence of certain metals. Concurrently, Bode[8] made a systematic study of metals that reacted with NaDDT and observed the high selectivity of NaDDTC for bismuth in the presence of masking agents. Encouraged by the work of Bode and the stability of the 1-pyrrolidinedithiocarbamate ion in aqueous solution, Kovacs and Guyer used sodium 1-pyrrolidinedithiocarbamate to determine bismuth spectrophotometrically in smelter zinc[9] and steel[10]. However, no study has been made of the use of APDC as a spectrophotometric reagent for the determination of bismuth in the presence of an excess of a large number of diverse ions and particularly for the determination of bismuth in alloys of tin and lead. The principal source of bismuth is the residue from the refining of lead. Tin and lead commonly interfere in the bismuth determination[11-14]. As a result, elaborate separation schemes such as internal electrolysis[15,16], ion-exchange[17] and distillation[16] have been developed. Recently, Kalt and Boltz[18] reported on the use of APDC as a reagent for the spectrophotometric determination of Cd, Co, Mo, and Bi; many ions interfered since neither masking agents nor separation methods were employed. Furthermore, no detailed atomic absorption studies exist for the determination of bismuth with APDC by organic extraction. The applicability of such a method has been mentioned[4,19] and has been used in the analysis of urine samples[20]. The determination of bismuth through its reaction with APDC followed by organic extraction should eliminate the uncertainty of chemical interferences when aqueous bismuth samples are aspirated directly into the flame. Sattur[21] found no evidence of chemical interference in the analysis of bismuth in non-ferrous alloys and biological samples; however, Bishop and Harris[22] observed an enhancement in the presence of tellurium,

and Husler[23] noticed a depression in a strong hydrochloric–nitric acid medium. The atomic absorbance of bismuth was also reported to be lower in the presence of calcium[23].

Reported herein is a detailed study of a spectrophotometric and atomic absorption method in which APDC and organic extractants are used for the selective determination of bismuth in the presence of a large number of diverse ions as well as in tin and lead alloys.

## EXPERIMENTAL

### *Apparatus*

Optical measurements were made with a Beckman D. U. Spectrophotometer and Bausch and Lomb 505 Recording Spectrophotometer.

A Perkin-Elmer model 303 Atomic Absorption Spectrophotometer with standard air–acetylene burner head and Perkin-Elmer bismuth intensitron lamp (operated at 8 mA) was used for the bismuth atomic absorption measurements. An Evans Electroselenium Ltd. (type 22941) high-spectral-output hollow-cathode tube (operated at 15 mA) was used for tin measurements.

Radiometric measurements were made with a Baird Atomic model 530 Spectrometer and a well-type sodium iodide–thallium activated crystal.

A Burrel model BB Wrist-Action Shaker operated at scale 10 was used to agitate samples.

### *Reagents*

*Standard* $1.000 \cdot 10^{-2}$ *M bismuth nitrate solution.* Dissolve 2.0898 g of pure bismuth metal in 40 ml of 4 *M* nitric acid, and dilute to 1 l with water. Prepare other bismuth solutions by dilution of this stock solution.

$2.5 \cdot 10^{-2}$ *M APDC solution.* Dissolve 0.4108 g of APDC in 100 ml of water. Prepare this solution weekly.

*Mixed masking solution* (0.15 *M EDTA*, 1 *M sodium citrate*, 4 *M ammonia*). Dissolve 50 g of EDTA and 294 g of sodium citrate in 267 ml of concentrated ammonia solution and dilute to 1 l with water.

0.6 *M Dibutylphosphate solution Eastman technical grade, app.* 55% *dibutyl, and* 45% *monobutyl.* Dissolve 208 ml of the dibutylphosphate and dilute to 1 l with chloroform.

Carrier-free bismuth-207 (as bismuth nitrate).

Foreign ion solutions, 0.1 *M*.

### *Preparation of calibration curves*

*Spectrophotometric procedure.* To a 125-ml separatory funnel containing 8 ml of concentrated hydrochloric acid, pipette a 50-ml sample containing 0–5 p.p.m. of bismuth. Pre-extract this solution (*ca.* 2 *M* in hydrochloric acid) for 5 min with 25 ml of the 0.6 *M* dibutylphosphate solution. Separate, discard the chloroform layer and add in turn 10 ml of the masking agent solution, 5 ml of 6 *M* sodium hydroxide and 2 ml of 2.5 *M* sodium cyanide solution. Adjust to pH 10.5 with 6 *M* sodium hydroxide and then add 2 ml of the APDC solution. Extract the yellow bismuth–APDC complex into 10.00 ml of chloroform by shaking vigorously for 5 min. Filter the organic layer

through a cotton plug in the stem of the separatory funnel into an optical cuvette and measure the absorbance at 360 nm. A reagent blank is run in the same manner. Linear calibration curves were obtained for 0.1–5 p.p.m. of bismuth at 360 nm, 380 nm and 400 nm.

*Atomic absorption procedure.* Into a 125-ml separatory funnel pipette a 50-ml sample containing 0–0.5 p.p.m. of bismuth and add 10 ml of the masking agent solution. If necessary, add base to make sure that the solution is basic before adding 2 ml of 2.5 *M* sodium cyanide solution. After adjusting to pH 9.5–10.5, add 6 ml of the APDC solution followed by 10.00 ml of MIBK. Extract the bismuth–APDC complex for 2 min; allow the layers to separate, and aspirate the upper layer directly into the flame of the atomic absorption spectrophotometer. The bismuth content was measured at 223.1 nm; a linear calibration curve was obtained for 0.01–0.5 p.p.m. A similar calibration curve was also prepared for 0–2.5 p.p.m. A similar calibration curve was also prepared for 0–2.5 p.p.m. bismuth.

## RESULTS

### *Bismuth–APDC complex*

Preliminary experiments showed that the reaction of a large excess of APDC with bismuth nitrate in acidic solution is fast and that a stable yellow precipitate is formed quantitatively. This yellow precipitate (m.p. 259–262°) is soluble in common organic solvents such as ethanol, acetone, ethyl ether, chloroform, butyl acetate, and methyl isobutyl ketone. A Yoe–Jones plot indicated the mole ratio of metal to ligand to be 1 : 3 and the gravimetric factor as well as the elemental analysis corresponded to a formula of $Bi(C_4H_8NCS_2)_3$. Gravimetric pH studies also showed that the complex is completely formed over the pH range 0–10. This information as well as a detailed i.r. structural study were recently presented[24], and will be published in the near future.

### *Extraction conditions*

The yellow bismuth–APDC complex which has an absorption maximum at 360 nm can be extracted into chloroform or MIBK from solutions of pH 0–12. The intensity of the yellow color decreases sharply beyond pH 12 and at pH 13.5 the organic layer is colorless. In studies of the extraction conditions, two extractable species of APDC were found (Fig. 1). The two species have absorption maxima at 261 nm and 281 nm respectively in the chloroform layer, and are most favorably extracted at pH 4 and 8. Probably they represent two different protonated species of the APDC molecule[24]. Since the masking agents function best in basic media, and since the absorbance contribution from the reagent at 360 nm is negligible above pH 9, the extraction of bismuth–APDC is limited to pH 9.5–11.5 for spectrophotometric determinations.

Radioactive $^{207}Bi$ was employed to determine the apparent distribution coefficients and the percentage of bismuth extracted into chloroform and MIBK as a function of pH. These results are reported in Table I. Over 99% of the bismuth was extracted into either solvent in the pH range pH 0–12.

To study the time required for extraction, standard bismuth samples were reacted with an excess of APDC in the presence of the masking agent at pH 10–10.5. The samples were then extracted by shaking for various times with either chloroform

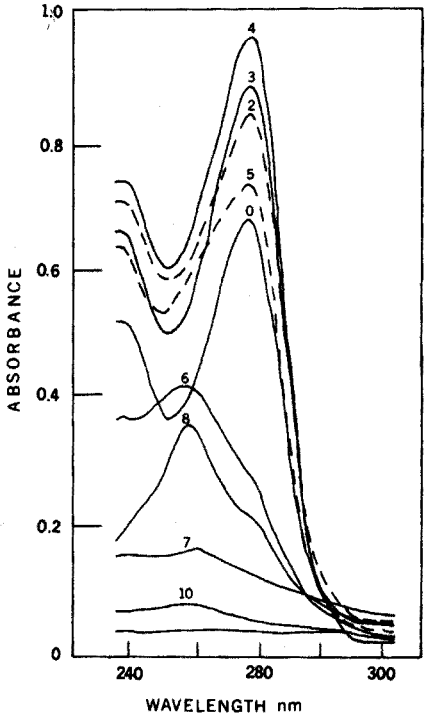


Fig. 1. Extraction of APDC into chloroform at different pH values. The number above each curve indicates the pH.

or MIBK. Without a pre-extraction with dibutylphosphate, the bismuth–APDC extraction appears to be complete in 15 sec. With the pre-extraction, it takes as long as 2 min to extract the bismuth–APDC complex and in actual analysis, a considerably longer extraction time was allowed.

*Study of interferences*

The dithiocarbamates are generally unselective reagents[1] forming complexes

TABLE I

EFFECT OF pH ON THE APPARENT DISTRIBUTION COEFFICIENT FOR $Bi(APDC)_3$

(A total of 50.00 ml of aqueous solution that included 25.00 ml of radioactive $2 \cdot 10^{-5}$ *M* $Bi^{3+}$, 10 ml of mixed masking agents, 2 ml of 2.5 *M* cyanide, various amounts of NaOH or HCl for pH adjustment and either 2 ml or 6 ml of APDC was extracted with 25.00 ml of $CHCl_3$ or MIBK)

| *pH* | | 0[a] | 4 | 6 | 10 | 12 | 14 |
|---|---|---|---|---|---|---|---|
| $CHCl_3$ | $K_d$ | 5150 | 4623 | 4889 | 1003 | 2026 | 0.170 |
| | % Bi extracted | 99.96 | 99.96 | 99.96 | 99.80 | 99.90 | 7.834 |
| MIBK | $K_d$ | 283 | 2223 | 6071 | 2028 | 715 | $3.75 \cdot 10^{-2}$ |
| | % Bi extracted | 99.30 | 99.91 | 99.97 | 99.90 | 99.72 | 1.871 |

[a] No masking agent or NaCN added.

TABLE II

IONS THAT REACT WITH APDC[a]

| | | | | | | | | | | | | | | | | |
|---|---|---|---|---|---|---|---|---|---|---|---|---|---|---|---|---|
| H | | | | | | | | | | | | | | | | |
| $\overline{Li}$ | $\overline{Be}$ | | | | | | | | | | | B | C | N | O | $\overline{F}$ |
| $\overline{Na}$ | $\overline{Mg}$ | | | | | | | | | | | $\overline{Al}$ | Si | P | S | $\overline{Cl}$ |
| $\overline{K}$ | $\overline{Ca}$ | $\overline{Sc}$ | $\overline{Ti}$ | $\underline{V}$ | $\underline{Cr}$ | $\underline{Mn}$ | $\underline{Fe}$ | $\underline{Co}$ | $\underline{Ni}$ | $\underline{Cu}$ | $\underline{Zn}$ | $\underline{Ga}$ | $\overline{Ge}$ | $\underline{As}$ | $\underline{Se}$ | $\overline{Br}$ |
| $\overline{Rb}$ | $\overline{Sr}$ | $\overline{Y}$ | $\overline{Zr}$ | $\underline{Nb}$ | $\underline{Mo}$ | Tc | (Ru) | (Rh) | $\underline{Pd}$ | $\underline{Ag}$ | $\underline{Cd}$ | $\underline{In}$ | $\underline{Sn}$ | $\underline{Sb}$ | $\underline{Te}$ | $\overline{I}$ |
| $\overline{Cs}$ | $\overline{Ba}$ | $\overline{La}$ | $\overline{Hf}$ | Ta | $\underline{W}$ | (Re)[b] | $\underline{Os}$ | (Ir) | $\underline{Pt}$ | $\underline{Au}$ | $\underline{Hg}$ | $\underline{Tl}$ | $\underline{Pb}$ | $\underline{Bi}$ | Po | At |
| Rb | Ra | Ac | $\overline{Th}$ | Pa | $\underline{U}$ | | | | | | | | | | | |
| | | | R.E.I. | | $\overline{La}$ | $\overline{Ce}$ | $\overline{Pr}$ | $\overline{Nd}$ | $\overline{Pm}$ | $\overline{Sm}$ | Eu | $\overline{Gd}$ | $\overline{Tb}$ | $\overline{Dy}$ | $\overline{Ho}$ | $\overline{Er}$ | Tm | Yb | Lu |
| | | | R.E.II. | | Ac | $\overline{Th}$ | Pa | $\underline{U}$ | Np | Pu | Am | Cm | | | | | | |

$\overline{NO_3^-}$ $\overline{H_2PO_4^-}$ $\overline{CNS^-}$ $\overline{S_2O_3^{2-}}$ $\overline{HPO_4^{2-}}$ $\overline{NO_2^-}$ $\overline{\text{Citrate}^-}$ $\overline{SO_3^-}$

$\overline{C_2O_4^{2-}}$ $\overline{C_4H_4O_6^{2-}}$ $\overline{CN^-}$ $\overline{HCO_3^-}$ $\overline{C_2H_3O_2^-}$ $\overline{SO_4^{2-}}$ $\overline{So_4^{2-}}$ $\overline{F^-}$

$\overline{Cl^-}$ $\overline{Br^-}$ $\overline{I^-}$ $\overline{P_2O_7^{4-}}$

[a] $\overline{\quad}$ Ions that show no visible reaction with APDC. ( ) Reaction very slow and probably incomplete. $\underline{\quad}$ Ions that react with APDC.

[b] Re has to be heated in order to observe any reaction.

TABLE III

EFFECT OF EDTA AND AMMONIUM CITRATE MIXTURE IN THE REACTION OF APDC AT pH 10.5[a,b]

| | | | | | | | | | | | |
|---|---|---|---|---|---|---|---|---|---|---|---|
| $\overline{V}$ | $\overline{Cr}$ | $\overline{Mn}$ | $\overline{Fe}$ | $\overline{Co}$ | $\overline{Ni}$ | $\underline{Cu}$ | $\overline{Zn}$ | $\overline{Ga}$ | Ge | $\overline{As}$ | $\overline{Se}$ |
| $\overline{Nb}$ | $\overline{Mo}$ | Tc | (Ru) | $\overline{Rh}$ | $\underline{Pd}$ | $\underline{Ag}$ | $\overline{Cd}$ | $\overline{In}$ | $\overline{Sn}$ | $\overline{Sb}$ | $\overline{Te}$ |
| Ta | $\overline{W}$ | (Re)[c] | $\underline{Os}$ | $\overline{Ir}$ | (Pt) | $\underline{Au}$ | $\underline{Hg}$ | $\overline{Tl}$ | $\overline{Pb}$ | $\underline{Bi}$ | Po |
| Pa | $\overline{U}$ | | | | | | | | | | |

[a] $\overline{\quad}$ Ions masked by EDTA + ammonium citrate at pH 10.5. ( ) Ions partially masked as judged by formation of a precipitate or color change. $\underline{\quad}$ Ions not masked.

[b] R.E. I and II showed no visible reaction.

[c] Re has to be heated to observe any reaction.

with a large number of metal ions, particularly the heavy metals. A detailed and systematic investigation was made of ions in aqueous solution that might react with APDC, and on the effect of EDTA and cyanide as masking agents. The results of the first part of the investigation, which supplement the result of other workers[2,19] on metal APDC complexes, are summarized in Table II. The effect of EDTA as a masking agent at pH 10.5 (using an ammonium citrate buffer) is shown in Table III. In the presence of EDTA and cyanide at pH 10.5, only thallium(III) and bismuth(III) gave a visible reaction with APDC, a phenomenon that is similar to the reaction of sodium diethyldithiocarbamate[8].

Some ions which may not form a colored product or a precipitate, may still be extractable into the organic phase and interfere in the bismuth determination. To

resolve the doubt, an interference study of all the cations and anions included in Table II was carried out following the previously described procedures. Each diverse ion was added in at least a 40-fold molar excess over the bismuth; only thallium(III) and to a small extent platinum(IV) interfered in the spectrophotometric method at 360 nm. No ions interfered in the atomic absorption method. In the spectrophotometric method, the slight interference of platinum(IV) can be circumvented by measuring the absorbance at 380 nm. The interference of thallium(III) can be easily removed by boiling the sample solution with 3 ml of saturated sulfite solution. The thallium(I) thus formed does not interfere; the excess of sulfur dioxide may be boiled off. Pre-extraction with dibutylphosphate was incorporated into the spectrophotometric study; the primary interference removed in this way was that due to the hydrolysis of tin.

*Optimal conditions for atomic absorption*

The instrumental conditions for maximal sensitivity were found to be an acetylene flow rate of 2.5 l $min^{-1}$ and an air flow rate of 21 l $min^{-1}$, with a burner height setting of 15 mm below the incident light beam. The above instrumental settings are not critical since the bismuth absorbance is not sensitive to small changes. Other optimal instrumental settings are a gain of 6.5, slit width of 0.3 mm, meter response of 2 and scale expansion of 5 on the Perkin-Elmer Instrument.

*Analysis of synthetic samples*

A series of fourteen synthetic solutions was prepared, each containing an equal amount of four diverse ions in large excess relative to the known amount of

TABLE IV

ANALYSIS FOR BISMUTH(III) IN THE PRESENCE OF FOREIGN IONS

| | *Foreign ions added* | | | | *Bi(III) found (p.p.m.)* | |
|---|---|---|---|---|---|---|
| | | | | | *Spectrophotometric*[a] | *Atomic absorption*[b] |
| 1. | Mn(II) | Ca(II) | Ba(II) | Se(IV) | 2.015 | 1.383 |
| 2. | La(III) | Mg(II) | Sm(III) | Au(III) | 2.123 | 1.411 |
| 3. | Zn(II) | $UO_2$(II) | Cu(II) | Ga(III) | 1.980 | 1.418 |
| 4. | Fe(III) | Ni(II) | Al(III) | Mo(VI) | 2.083 | 1.421 |
| 5. | V(V) | Dy(III) | Co(II) | Pd(II) | 2.048 | 1.418 |
| 6. | As(III) | Ti(IV) | Li(I) | Re(IV) | 2.051 | 1.393 |
| 7. | Cd(II) | Rh(III) | Ir(III) | Cr(III) | 2.132 | 1.372 |
| 8. | Ge(IV) | W(VI) | Sn(IV) | $P_2O_7^{4-}$ | 2.021 | 1.383 |
| 9. | $CNS^-$ | $NO_2^-$ | $SO_3^{2-}$ | $F^-$ | 2.103 | 1.399 |
| 10. | $Tart^{2-}$ | $HCO_3^{2-}$ | $C_2H_3O_2$ | $HPO_4^{2-}$ | 2.123 | 1.414 |
| 11. | $C_2O_4^{2-}$ | $ClO_3^-$ | $Br^-$ | $NO_3^-$ | 2.035 | 1.370 |
| 12. | Ba(II) | In(III) | Te(IV) | Be(II) | 1.980 | 1.381 |
| 13. | Pb(II) | Ag(I) | Hg(II) | Os(VIII) | 2.120 | 1.418 |
| 14. | Ru(III) | Ce(IV) | Th(IV) | Ho(III) | 2.090 | 1.379 |
| | Relative standard deviation (%) | | | | 2.85 | 1.39 |

[a] All samples contained 2.090 p.p.m. Bi(III) and over a 40-fold molar excess of each foreign ion.
[b] All samples contained 1.393 p.p.m. Bi(III) and over a 40-fold molar excess of each foreign ion.

bismuth. The samples were analyzed spectrophotometrically and by atomic absorption spectrophotometry following the described procedures. The results are reported in Table IV.

*Analysis of NBS samples*

Three NBS samples: the lead-base bearing metal, the solder, and the tin-base bearing metals were selected to test the applicability of the proposed methods for bismuth analysis.

The lead-base bearing metal, NBS 53d, contains an average of 9.92% Sb, 4.94% Sn, 0.268% Cu, 0.045% As, 0.002% Ni and 0.135% Bi. A 0.8-g sample was dissolved in 40 ml of 3 *M* nitric acid by slowly heating on a hot plate. After dissolution, 40 ml of 12 *M* hydrochloric acid was added and the solution was allowed to digest while being heated for 30 min. While still hot, the solution was transferred to a 250-ml volumetric flask and diluted to volume with water. White needle-like crystalline lead chloride precipitated on cooling and was allowed to settle for 2–4 h. For the spectrophotometric method, 25.00 ml of the sample was pipetted from the upper clear solution and pre-extracted once with 25 ml of 0.6 *M* dibutylphosphate in chloroform. Thereafter the normal spectrophotometric method was followed beginning with the addition of 10 ml of the mixed masking solution. The absorbance was measured at 380 nm. For the atomic absorption procedure, a 15-ml aliquot was used. After dilution to *ca.* 50 ml with water, the determination of bismuth was carried out as described under the atomic absorption procedure.

The solder alloy, NBS 127A, contains an average of approximately 70% Pb, and 30.03% Sn, 0.79% Sb, 0.129% As, 0.004% Cu, 0.002% Ni, 0.004% Ag and 0.036% Bi. A 2.9-g sample was slowly dissolved in 50 ml of 3 *M* nitric acid solution over a hot plate. When 10 ml of 12 *M* hydrochloric acid was added to the partially dissolved sample, the reaction became quite violent, but afterwards the solution turned clear as the heavy white crystalline precipitate of lead chloride formed. An additional 30 ml of 12 *M* hydrochloric acid was added, and the sample was heated until the initially formed lead chloride dissolved; it was then boiled slowly for 30 min. Dilution and further treatment for the spectrophotometric method were exactly the same as for the lead-base bearing metal. For the atomic absorption procedure, a 20-ml aliquot was diluted to *ca.* 50 ml with water, and then the atomic absorption procedure for bismuth was followed.

Tin-base bearing metal, NBS 54d, contains an average of 88.57% Sn, 7.04% Sb, 3.62% Cu, 0.62% Pb, 0.088% As, 0.027% Fe, 0.003% Ag, 0.002% Ni and 0.044% Bi. A 1.2-g sample was partially dissolved in 50 ml of 3 *M* nitric acid solution by heating on a hot plate. Then 10 ml of 12 *M* hydrochloric acid was carefully and slowly added to avoid too violent a reaction. Thereafter, an additional 30 ml of 12 *M* hydrochloric acid was added, and the solution was strongly heated, until dissolution was complete. The sample was then allowed to boil for at least 30 min. After cooling, the sample was transferred to a 250-ml volumetric flask and diluted to volume with water. The solution should be bluish and clear and without any precipitate. For the spectrophotometric method, two options for the determination of bismuth are possible. The 25.00-ml sample solution can be pre-extracted thrice before the determination of bismuth by following the previously described procedure. Emulsion formation at the interface of the organic solvent during the pre-extraction was

somewhat of a problem for this material. The material could be analyzed spectrophotometrically without the dibutylphosphate pre-extraction if the solution was rapidly manipulated immediately after adjustment to pH 10.5, to minimize the co-precipitation of bismuth with tin(IV) hydroxide. For the atomic absorption procedure, a 25-ml aliquot was used and after diluting to 50 ml, the bismuth determination was carried out as before.

## DISCUSSION

APDC is not a selective reagent, but by a suitable choice of masking agents and pH values, it can be made a very selective reagent for bismuth. Without the pre-extraction step in the spectrophotometric method, the primary interference remaining is the hydrolysis of tin. Whenever an aqueous sample contained an excess of tin and turned cloudy, a slightly lower bismuth–APDC absorbance was observed. Tin can be extracted without removing bismuth from a 2 *M* hydrochloric acid sample with dibutylphosphate in chloroform. Pre-extraction is unnecessary in the absence of tin; however, this step is incorporated into the general spectrophotometric procedure because appreciable amounts of lead are concurrently removed. Lead can be an interference if present in large excess. Experiments were performed on the aqueous layer after pre-extraction in order to evaluate the efficiency of tin extraction with dibutylphosphate in chloroform and to measure the amount of bismuth retained in the aqueous layer. The amount of tin was determined by atomic absorption spectrophotometry and the amount of bismuth was measured radiometrically with $^{207}Bi$. Results showed that over 99.88% of bismuth was retained in the aqueous layer while over 91% of tin was removed in one pre-extraction. Additional pre-extractions further lowered the tin content of the aqueous solution, but with decreasing efficiency. It is possible to improve the bismuth-APDC extraction (and so minimize the tin interference) by increasing the amount of APDC as in the atomic absorption method. However, a very large excess of APDC is not desirable in the spectrophotometric method, since the absorbance background caused by a large excess of APDC can be appreciable. The interference of antimony is highly pH-dependent particularly at a 40-fold molar excess. In a basic medium, appreciable amounts of antimony–APDC are extracted into chloroform and show up as a residual absorbance at 360 nm; at pH 10.5 and above, antimony is not extracted. In the atomic absorption method, none of the ions studied showed any interference in the bismuth determination. The enhancement of a bismuth absorption in the presence of tellurium, and the depression in the presence of calcium and in a mixed medium of strong hydrochloric and nitric acid, were not observed when the organic layer was aspirated into the burner. Those interferences occurred when the aqueous solution was aspirated directly into the flame[22,23]. The Boling burner showed essentially the same sensitivity as the standard single-slot burner.

The analysis of lead and tin alloys in NBS samples presents a tremendous challenge to the thiocarbamate method for the determination of bismuth. The complexing agent can no longer mask the lead interference completely, and the tin interference may not be completely removed by a single pre-extraction with dibutylphosphate in the spectrophotometric method. Therefore, lead was partially removed by crystallization as lead chloride from a hydrochloric acid solution and the tin by an

additional pre-extraction, if needed. In synthetic samples of tin and lead the removal of lead as lead chloride and of tin by as many as three pre-extractions was satisfactory since little or no bismuth was lost. Over 99% of the bismuth was recovered; this was confirmed radiometrically with bismuth-207.

*Reproducibility and accuracy*

Satisfactory results were obtained for the analysis of bismuth in the three NBS samples by both the spectrophotometric and atomic absorption methods (Table V). The spectrophotometric procedure shows a relative standard deviation of 2.85% and the atomic absorption method 1.39%, as indicated in Table IV.

TABLE V

ANALYSIS OF NBS SAMPLES (%)

| | 53*d* | 127*a* | 54*d* |
|---|---|---|---|
| Average NBS value | 0.135 | 0.036 | 0.044 |
| Spectrophotometric | 0.139 | 0.035 | 0.047 |
| | 0.141 | 0.035 | 0.046 |
| | 0.141 | 0.034 | 0.046 |
| Atomic absorption | 0.139 | 0.035 | 0.048 |
| | 0.141 | 0.035 | 0.049 |
| | 0.138 | 0.033 | 0.047 |

Since the spectrophotometric method is sensitive to 0.0042 mg $cm^{-2}$ for log $I_0/I = 0.001$ and the atomic absorption to 0.0082 mg $ml^{-1}$ at 1% absorption, the two procedures can be applied not only to alloys but also to agricultural and biological systems. The bismuth determination with APDC by the atomic absorption method is particularly important because of its high sensitivity, its inherent selectivity, and avoidance of the chemical interferences that occur when aqueous solutions are aspirated into the flame.

SUMMARY

A spectrophotometric method and an atomic absorption procedure have been developed for the determination of bismuth in the presence of a large number of foreign ions, and in lead- and tin-containing alloys. The ammonium salt of 1-pyrrolidinecarbodithioic acid (APDC) and organic extractants were used. Masking agents and separation methods were employed to improve the selectivity; APDC reactions, extraction conditions, and distribution coefficients are described.

RÉSUMÉ

Une méthode spectrophotométrique et une méthode par absorption atomique sont décrites pour le dosage du bismuth, en présence de nombreux ions étrangers, ainsi que dans des alliages contenant plomb et étain. On utilise la sel d'ammonium

de l'acide 1-pyrrolidinecarbodithioïque (APDC) et des extractants organiques. La sélectivité est améliorée par des réactifs de masquage et des méthodes de séparation. On examine les conditions d'extraction et les coefficients de partage.

ZUSAMMENFASSUNG

Für die Bestimmung von Wismut in Gegenwart einer grossen Zahl von Fremdionen sowie in blei- und zinnhaltigen Legierungen wurden eine spektrophotometrische Methoden und ein Atomabsorptionsverfahren entwickelt. Es wurden das Ammoniumsalz von 1-Pyrrolidindithiocarbamat (APDC) und organische Extraktionsmittel verwendet. Zur Verbesserung der Selektivität wurden Maskierungsmittel eingesetzt und Trennverfahren angewendet. APDC-Reaktionen, Extraktionsbedingungen und Verteilungskoeffizienten werden beschrieben.

REFERENCES

1 G. D. Thorn and K. A. Ludwig, *The Dithiocarbamates and Related Compounds*, Elsevier, New York, 1962.
2 H. Malissa and E. Schoffmann, *Mikrochim. Acta*, 1 (1955) 187.
3 G. D. Christian, *Anal. Chem.*, 41, No. 1 (1969) 24A.
4 W. Slavin, *Atomic Absorption Spectroscopy*, Interscience, New York, 1968; W. Slavin, *Atomic Absorption Newsletter*, 3 (1964) 141.
5 J. Ramirez-Munoz, *Atomic Absorption Spectroscopy*, Elsevier, New York, 1968.
6 E. Kovacs and H. Guyer, *Z. Anal. Chem.*, 13 (1959) 1964.
7 K. L. Cheng, R. H. Bray and S. W. Melsted, *Anal. Chem.*, 27 (1955) 24.
8 H. Bode, *Z. Anal. Chem.*, 143 (1954) 182; 144 (1955) 90 and 165.
9 E. Kovacs and H. Guyer, *Z. Anal. Chem.*, 186 (1962) 267.
10 E. Kovacs and H. Guyer, *Z. Anal. Chem.*, 187 (1962) 188.
11 W. W. Scott, *Standard Methods of Chemical Analysis, Vol. 1*, 5th Edn., Van Nostrand, New York, 165.
12 N. M. Lisicki and D. F. Boltz, *Anal. Chem.*, 27 (1955) 1722.
13 K. Kodama, *Methods of Quantitative Inorganic Analysis*, Interscience–John Wiley, New York, 1963, p. 164.
14 G. Charlot, *Colorimetric Determination of Elements*, Elsevier, New York, 1964, p. 186.
15 *Chemical Analysis of Metal*, American Society for Testing Materials, Philadelphia, 1956.
16 G. D'Amore and F. Corigliano, *Atti Soc. Peloritana Sci. Fis. Mat. Nat.*, 11 (1965) 239.
17 Z. Sulcek, P. Povondra and V. Kratochvil, *Collection Czech. Chem. Commun.*, 34 (1969) 3711.
18 M. B. Kalt and D. F. Boltz, *Anal. Chem.*, 40 (1968) 1087.
19 E. Lakanen, *Atomic Absorption Newsletter*, 2 (1966) 17.
20 J. B. Willes, *Anal. Chem.*, 34 (1962) 614.
21 T. W. Sattur, *Atomic Absorption Newsletter*, 5 (1966) 37.
22 C. T. Bishop and R. N. Harris, *Atomic Absorption Newsletter*, 8 (1969) 110.
23 J. W. Husler, *Atomic Absorption Newsletter*, 9 (1970) 31.
24 H. K. Y. Lau, P. F. Lott and H. A. Droll, *Pyrrolidinedithiocarbamic Acid and some of its Metal Complexes*, Inorganic Session of the 1970 Midwest ASC Meeting in Lincoln, Nebraska.

*Analytica Chimica Acta*
Elsevier Publishing Company, Amsterdam
Printed in The Netherlands



# EVALUATION OF SOME THREE-QUARTER-WAVE MICROWAVE CAVITIES FOR THE OPERATION OF ELECTRODELESS DISCHARGE LAMPS

D. O. COOKE, R. M. DAGNALL AND T. S. WEST
*Department of Chemistry, Imperial College of Science and Technology, London, S.W. 7 (England)*

(Received 10th April 1971)

Microwave-excited electrodeless discharge lamps have received considerable attention in the literature[1-3]. However, relatively little information is available regarding the performance and choice of microwave cavities for operation of these lamps. The importance of the correct choice of cavity and a knowledge of its behaviour under a wide variety of conditions may be appreciated when considering the cavity function. The role of the microwave cavity itself is to transfer the power from the microwave generator to the gas discharge. Thus, however well a lamp is prepared, its overall performance will to a large extent be dependent upon the particular microwave cavity in which it is to be operated. The use of the three-quarter-wave (Broida) type cavity has been recommended[4] in preference to the quarter-wave (Evenson) type because of the improved stability and freedom from tuning afforded. Winefordner *et al.*[5] have examined both the quarter-wave and three-quarter-wave cavities together with a tapered rectangular cavity. These workers also examined two types of stub radiators, the "A" and "C" type antennae, and they recommended the use of the tapered rectangular cavity or the "A" type antennae. However, in common with other workers they found the stub radiation method to be somewhat inefficient and utilised a quartz jacket with their "A" type antennae even in the case of a volatile element such as mercury. Winefordner[5] has criticised the three-quarter-wave Broida-type cavity on the grounds that it requires forced air cooling and is plagued with spurious discharges within the cavity, but outside the lamp. Neither of these criticisms appears to have been substantiated and indeed much of the more recent work[6,7] has been carried out with three-quarter-wave cavities.

The cavities evaluated in this study were the EMS 210L (Electro-Medical Supplies) which has been described elsewhere[4], together with two further types designated as BK-UT and BK-T (Beckman-RIIC) which have been briefly discussed previously[8,9]. The BK-UT cavity has special provision for air cooling and incorporates a solid base. The BK-T cavity has no built-in provision for cooling, but has two capacitive tuning stubs (of the type described by Aldous *et al.*[3]), both of which are provided with micrometer dials to enable resetting. The fourth cavity was a modified EMS 210L cavity denoted as ST; the modification consisted of the addition of an adjustable tuning stub of the type described by Fehsenfeld *et al.*[10] which is located on the coaxial connector.

The performance of the microwave cavities was assessed by comparison of the intensity and atomic absorption and atomic fluorescence spectroscopic measurements

over a wide range of microwave powers using a given lamp when operated in the four cavities. For this purpose, two elements and one compound of widely different boiling points were chosen to prepare lamps, namely, mercury, selenium and thallium chloride.

## EXPERIMENTAL

Spectroscopic evaluation was made with a modified Hilger & Watts "Uvispek" (H700) spectrophotometer with an atomic absorption attachment, the use of which has been described in a previous communication[9]. A premixed 10 cm air–propane flame (perforated plate burner) was used for a.a.s. and a Meker-type burner for a.f.s. The analytical signal was displayed on a Servoscribe recorder used on the 0–20 mV range.

### *Preparation and operation of the lamps*

The electrodeless discharge lamps were prepared by the same general method described previously[11]. The specific conditions used were as follows:

Selenium: metal, argon pressure 3 Torr, bulb length 4 cm.

Mercury: metal, argon pressure 0.1 Torr, bulb length 3 cm.

Thallium: thallium(I) chloride, argon pressure 3 Torr, bulb length 3 cm.

In all instances 8-mm (i.d.) quartz tubing was used. Microwave power for the sources was provided by a "Microtron 200" (Electro-Medical Supplies, Wantage, U.K.) microwave generator ($2450 \pm 25$ MHz) coupled with a reflected power meter (Electro-Medical Supplies). Initiation was achieved with a "Tesla" high-frequency vacuum tester. The lamps were located in position in the various cavities by means of a metal cap, which fitted neatly into the upper portion of the BK-T and BK-UT cavities and which rested above the EMS 210L and ST cavities.

Although it is to be expected[10] that tuning should be dependent on discharge characteristics and consequently be dependent upon the microwave power applied, a change in tuning characteristics with changing microwave power was generally impossible to detect. Consequently, apart from occasional checks, the cavities were tuned to give minimum reflected power at *ca.* 50 W.

### *Modulation*

Electronic modulation[12] was used throughout because it was considered that it is under such circumstances that these lamps would generally be utilised. Modulation at 100 Hz was provided electronically by a modulation unit Mk II (Electro-Medical Supplies), arbitrarily calibrated and set at position 5 for selenium and thallium, and position 4 for mercury lamps.

## EVALUATIÓN AND DISCUSSION

### *Selenium*

The efficiency of the cavities was shown to be in the order BK-UT>ST>EMS 210L>BK-T from a consideration of the microwave power level which provides the maximum lamp intensity and atomic fluorescence signal. Further evidence that the efficiency is in this order is provided by examination of the effect of microwave power

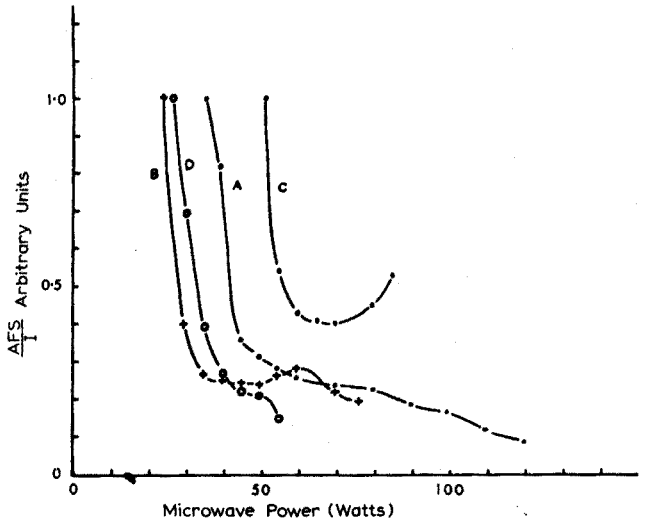


Fig. 1. Effect of microwave power ($P$–$R$) on the a.f.s. signal/intensity ratio for selenium with various cavities. (A) EMS 210L; (B) BK-UT; (C) BK-T; (D) ST.

on the ratio atomic fluorescence, signal/intensity for each cavity (Fig. 1). This ratio is seen initially to decrease rapidly with increasing microwave power showing some tendency to level off at high powers.

As might be expected with an element such as selenium (b.p. 685° at 760 Torr, vapour pressure 40 Torr at 506°), even at the lowest microwave power for which a discharge could be maintained, the vapour pressure was such that the atomic-absorption signal could not be seen to increase with increasing microwave power even when

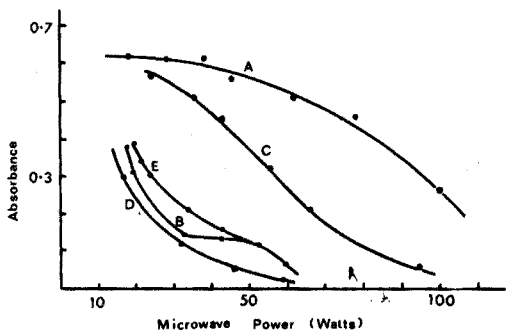


Fig. 2. Effect of microwave power ($P$–$R$) on the a.a.s. signal of selenium with various cavities. (A) EMS 210L; (B) BK-UT; (C) BK-T; (D) ST; (E) BK-UT strongly cooled.

the least efficient (BK-T) cavity was utilized (Fig. 2). Despite the efficiency order, the highest atomic fluorescence signal was obtained from the EMS 210L cavity, though the more efficient ST and BK-UT cavities would have provided a comparable signal had it proved possible to maintain a discharge at a sufficiently low microwave power. In general, a discharge could be maintained in the ST and BK-UT cavities at microwave-power levels approximately 15% lower than in the EMS 210L cavity. The use

of the cooling facility in the BK-UT cavity resulted in an increase in the analytical signals obtainable (Fig. 2), but the level resulting from the use of the EMS 210L cavity could not be attained even up to the point when strong cooling extinguished the discharge. Cooling was not applied to the ST cavity, but it is to be expected that a similar improvement would be obtained.

The performance of the BK-T cavity does, however, appear to be somewhat more complex. The more rapid decrease in the atomic absorption signal and considerably higher integrated line intensity at microwave powers above *ca.* 50 W, when compared with the EMS 210L cavity, would seem to contradict its position as the least efficient of the four cavities. This is, however, explained by considering the background radiation observed when this cavity is used for selenium. Figure 3 shows the background radiation for three of the cavities used; this was not measured for the ST cavity, but is probably similar in nature to the BK-UT cavity. The effect of the varying background radiation afforded by the various cavities is also evident from the dependence of the atomic absorption signal on slit width. However, background considerations alone do not explain the fact that a maximum is observed in the atomic fluorescence signal and that this maximum is appreciably below the maximum obtained with the

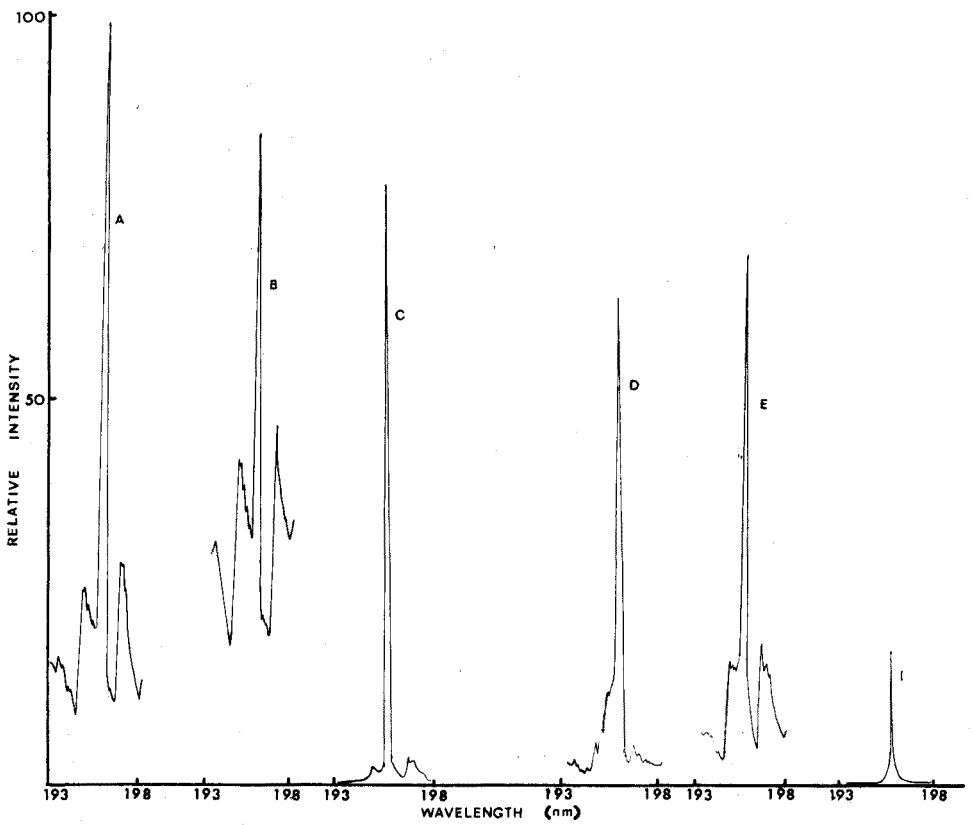


Fig. 3. Background radiation (193–198 nm) emitted by selenium lamp operated in various cavities. (A) EMS 210L, $P$–$R$ = 45 W; (B) BK-T, $P$–$R$ = 40 W; (C) BK-UT, $P$–$R$ = 41 W; (D) EMS 210L, $P$–$R$ = 116 W; (E) BK-T, $P$–$R$ = 118 W; (F) BK-UT, $P$–$R$ = 112 W.

EMS 210L cavity. Clearly an alternative process is required to explain why the maximal atomic fluorescence signal obtainable is not the same for all the cavities used. The presence of the tuning stubs in this particular cavity would seem not to improve the coupling efficiency, but rather to decrease it, apparently by absorbing microwave power; this phenomenon is discussed is greater detail in the section concerned with tuning facilities. When the EMS 210L cavity was used under optimal conditions, the detection limit (signal: noise = 1) by a.f.s. was 0.25 p.p.m. and by a.a.s. was 2.5 p.p.m. Se.

*Mercury*

The performance of the four cavities with respect to the variation in the a.f.s. and a.a.s. signal and lamp intensity (nebulising 100 p.p.m. and 1000 p.p.m. Hg for the a.f.s. and a.a.s. measurements, respectively, and taking all measurements at 253.7 nm) with microwave power (*P–R*) was examined. Figure 4 shows the performance of the

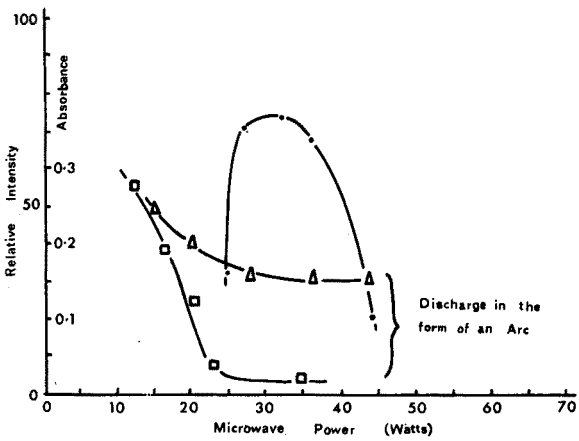


Fig. 4. Effect of microwave power (*P–R*) on lamp intensity (●), a.f.s. signal (□) and a.a.s. signal (△) of mercury with the BK-T cavity.

BK-T cavity which is typical of the cavities studied. As expected for an element of such volatility (b.p. 357° at 760 Torr, vapour pressure 40 Torr at 228.8°), no maximum could be observed in the variation of either the a.f.s. or a.a.s. signal with microwave power. The efficiency order is somewhat more obscure with mercury than selenium because of the absence of maxima in any of the analytical signals. The variation of the ratio of atomic fluorescence/signal intensity with microwave power is also rather complex; the increase in this ratio at high microwave powers is considerably more pronounced than in the case of selenium for both the EMS 210L and BK-T cavities. Furthermore, the gradient is negative for the ST cavity. Considering that no maximum, but only a steady decrease in the integrated line intensity was observed when this cavity was used, it can only be assumed that the ST cavity is the most efficient. The efficiency order in this instance is thus ST>BK-UT>EMS 210L>BK-T. In all instances the increase in the a.f.s. signal/intensity ratio at high microwave powers is brought about by a decrease in the integrated line intensity whilst the fluorescence signal is virtually constant. It can only be assumed therefore that there is a decrease in the line intensity

outside the absorption line profile of the atoms within the flame, whilst the intensity at the line centre remains approximately constant. This is almost certainly due to excessive line broadening, and the line intensity at the spectral bandpass used (0.01 nm) is no longer a measure of the integrated line intensity. When the BK-T cavity was tuned for maximal analytical signal, the detection limit by a.f.s. was 0.1 p.p.m. and by a.a.s. was *ca.* 10 p.p.m.

*Thallium*

The effect of microwave power on the atomic absorption signal with a 1000-p.p.m. thallium solution for the four cavities is shown in Fig. 5. As can be seen, there is little or no evidence of self-absorption/self-reversal effects even when using the more efficient cavities. A slit width of 0.1 mm (0.55 nm spectral bandpass) was used in all

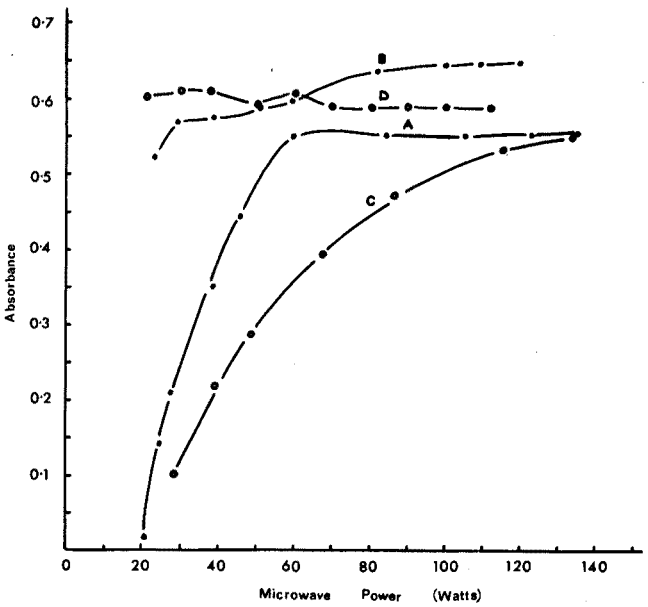


Fig. 5. Effect of microwave power ($P$–$R$) on the a.a.s. signal of thallium with various cavities. (A) EMS 210L; (B) BK-UT; (C) BK-T; (D) ST.

cases. For all the cavities, except the BK-T cavity, an increase in absorbance with increasing slit width up to 0.1 mm was observed. For the BK-T cavity a decrease in the absorption signal was observed above a slit width of 0.05 mm (0.28 nm spectral bandpass). The optimal atomic absorbance obtained with the BK-T cavity was still, however, below that of the other three remaining cavities. The BK-T cavity is thus again the least efficient. The position regarding the BK-UT and ST cavities is more obscure. The atomic absorbance signal with the ST cavity shows a slight decrease with increasing microwave power and this is the only cavity which shows any signs of increasing microwave power having an adverse effect on the line profile and hence the analytical signal. It is concluded, therefore, that this cavity is the most efficient and the order of efficiency in this instance is ST>BK-UT>EMS 210L>BK-T. Argon emission was visible in thallium lamps when operated at microwave powers ($P$–$R$) up to 60 W in the

ST cavity (and correspondingly higher in the other cavities). Above 60 W the discharge reverted from the so-called "skin effect" to a pale green discharge and then to the more characteristic bright green at *ca.* 100 W for both the ST and BK-UT cavities and at *ca.* 125 W for the EMS 210L cavity.

The performance of the thallium lamps (with 3 Torr argon) for a.f.s. studies, however, could only be described as poor. At a microwave power of 60 W no atomic fluorescence could be observed with the BK-T cavity, whilst only weak signals could be obtained with the other cavities even when up to 1000- p.p.m. solutions of thallium were nebulized. The magnitude of these signals at a power of 60 W confirmed the cavity efficiency order to be ST>BK-UT>EMS 210L>BK-T. It was noted that after *ca.* 2 h of operation in the bright green mode, a brown colouration could be observed on the inner walls of the lamp. This appeared to be a thin layer of thallium metal resulting from irreversible dissociation of the thallium(I) chloride. After *ca.* 20 h of operation the brown colouration reduced the transmission of the quartz walls by *ca.* 25% in the region 300.0–400.0 nm. However, quenching of the discharge by excess of free chlorine was not observed and no band emission attributable to chlorine could be detected. Heating the lamp to *ca.* 1000° for 2–3 min removed the brown colouration and resulted in a fresh deposit of white thallium(I) chloride, which indicates a buildup of chlorine within the lamp. In view of the poor results obtained in a.f.s. the effect of fill gas pressure on the performance of the thallium lamp was briefly examined.

The highest integrated line intensity and a.f.s. signal compatible with stability and long lifetime was obtained at a fill gas pressure of 10 Torr, the highest pressure for which a discharge could be maintained in the EMS 210L cavity used here. Higher pressures could be maintained in the ST and BK-UT cavities, but were not examined further. The highest pressure for which a discharge could be maintained again confirms the order of efficiency of the cavities as ST and BK-UT>EMS 210L>BK-T.

*Stability considerations*

The short-term stability of all lamps examined was similar when operated in all of the cavities, virtually always better than ±5% and often ±1%. Thallium lamps proved an exception when operated at high intensity (*P–R* 60 W) and stability was often very poor (± 20%). The drift rate, however, was not similar in all instances. The use of the BK-T cavity occasionally resulted in drift rates of up to 60% in 30 min although 15% per h was more normal. This is probably due to a drift in the tuning characteristics produced by heating effects. Indeed the original intensity could normally be regained by retuning the cavity. The drift rate was generally less than 2% per h for the other cavities.

*Cooling*

The cooling of electrodeless discharge lamps has been recommended by some workers[13,14]. There are two main reasons for the use of cooling; the first, and perhaps the most important, is to provide increased stability by improved insulation from draughts, particularly in the case of the "open" quarter-wave (Evenson) type cavity. In the case of the more shielded three-quarter-wave cavity, draughts are seldom a problem, although any apparatus should be well shielded from draughts because of their adverse effect on flame stability[15]. However the flow of cooling air must be accurately regulated or this itself can result in poor stability. The use of a preheated flow of air

has been reported[16] to improve both intensity and stability in certain circumstances.

The second reason for the utilisation of air cooling is to improve the analytical signal itself. For example, the vapour pressure within the lamp may be such that the discharge is constricted, completely extinguished, or has resulted in a broad or self-reversed line when operated at the normal operating temperature (*i.e.* the operating temperature without cooling). This is a direct consequence of incorrect lamp preparation and the problem is best rectified at the preparative stage either by choice of a more suitable (less volatile) compound or by decreasing the amount of element or compound used to prepare the lamp. A variation of fill gas pressure may also be useful, although this should generally be within the range 2–10 Torr, at least when the three-quarter-wave cavities of the type described here are used. Should it be impossible to rectify the situation at the preparative stage, then either air cooling or a less efficient cavity should be used. Although a less efficient cavity can often provide the greatest improvement, this would often not be available and air cooling can then provide a useful improvement in the analytical signal.

Air cooling may be applied to all the cavities examined in this study. The BK-T cavity has no provision for cooling, but air may be directed up through the base of the cavity and out through the top and viewing aperture, or, if a metal cap is in use, out through the viewing aperture alone. By far the best cooling facilities are those afforded by the BK-UT cavity. However, the improvement in analytical signal for selenium and mercury (Fig. 2) was insufficient to surpass the performance which could be obtained by using a less efficient cavity.

*Effects of tuning*

Of the four cavities examined, only the BK-UT cavity is completely without tuning facilities. The EMS 210L cavity has been stated[4] to possess the advantage of not requiring tuning, although the cavity does possess tuning facilities; in practice little change in performance could be observed when the tuning probe was used. Likewise variation of the electrode gap had little or no effect until the intensity was reduced by restriction of the viewing angle by the cylinder itself. The electrode gap normally used was 2.8 cm. No change in reflected microwave power was observed until the gap was less than 1.5 cm, when a small (10–20%) decrease was obtained. At this point the intensity was already reduced by the cylindrical electrode itself and analytical signals were consequently not examined.

The ST cavity has the same facilities as the EMS 210L with, in addition, an adjustable tuning stub, located on the coaxial connector. As with the EMS 210L, the tuning probe and variation of electrode gap had little or no effect. The sliding tuner also had less effect than might have been expected. The position giving minimum reflected power occurred when the tuning probe was very slightly extended. A decrease in the probe extension resulted in the lamp being extinguished, whilst an increase resulted in an increase in reflected power, the analytical signal behaving as if the microwave power had decreased. Consequently, for mercury an improvement in analytical performance could be obtained by using this cavity "out of tune". However, this improvement still did not match that which could be obtained from use of the EMS 210L cavity.

The BK-T cavity has two capacative tuning stubs. The use of a single capacative tuning stub in conjunction with an EMS 210L cavity has been recommended by

Aldous *et al.*[3] who claim improved warm-up times and spectral purity from lamps operating in such a cavity. This would tend to indicate that the use of a tuning stub of this type gave a more efficient cavity. The two tuning stubs used with the BK-T cavity apparently behave differently, although this is somewhat difficult to establish for certain because an identical cavity without tuning stubs was not available. It is possible, however, that the tuning stubs themselves are absorbing microwave power, and, in fact, the tuning stubs became extremely hot during operation. A discharge could not be maintained at all possible combinations of tuning stub positions. For selenium and thallium lamps minimum reflected power corresponded to the maximum a.f.s. signal. In the case of mercury this was not so because the lamp was already "over-run". The effect of the tuning stubs on the a.f.s. signal and reflected microwave power for mercury is shown in Fig. 6. The generator power was held constant at 25 W throughout

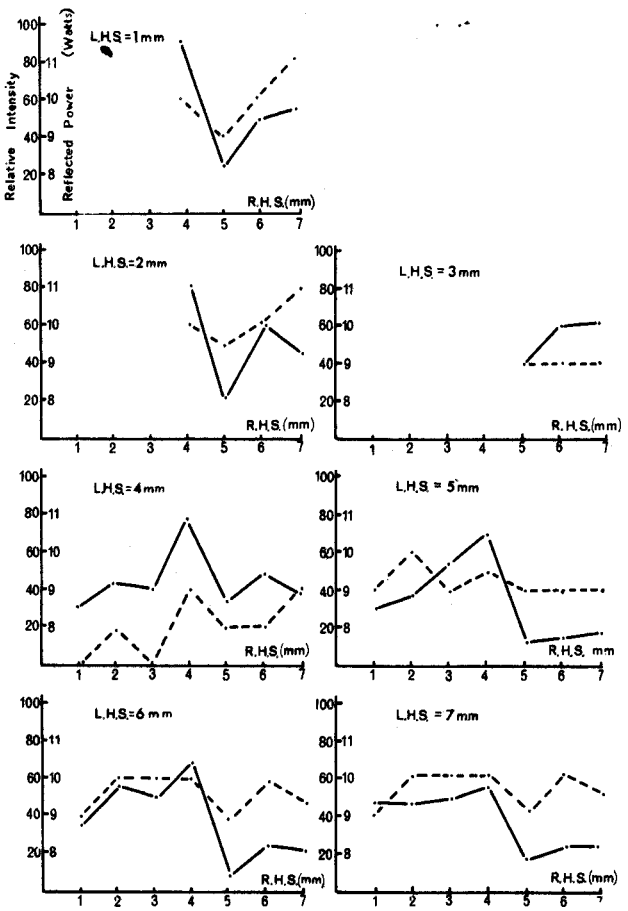


Fig. 6. Effect of tuning the BK-T cavity on the a.f.s. signal of mercury and reflected microwave power level. Lamp operated at microwave power of 25 W; L.H.S. and R.H.S. refer to the left and right hand tuning stubs respectively, when viewed facing the cavity viewing aperture; values in mm correspond to the distance of the capacitive tuning stubs from the cylindrical electrode. (·——·) Hg a.f.s.; (·– – –·– – –·) microwave reflected power.

this experiment. Similar results were obtained for selenium (generator power set at 40 W), except that a decrease in reflected power corresponded to an increase in a.f.s. signal and that the general effect of the tuning stubs was much less pronounced. It is particularly important to note that for lamps prepared from the more volatile compounds (*e.g.*, Hg, $AsI_3$, $SnI_4$, etc.), maximal analytical performance at low microwave powers is not necessarily indicated by the minimal reflected power.

*Cavity deterioration*

Microwave cavities are generally silver-plated because the current at microwave frequencies flows only through a very thin layer of the surface material and silver provides a cavity with a high $Q$ factor. However, the use of the silver results in a fairly rapid deterioration of the cavity walls, owing to the cumulative effect of oxide and sulphide formation, accelerated by the relatively high temperature at which the cavity operates. A further contribution is possibly afforded by the presence of ozone, which is produced by the far-ultraviolet radiation emitted by most discharge lamps. This deterioration results in a less efficient (lower $Q$) cavity. The stability of the lamps during the first 30 h of operation of a new cavity was particularly bad and was possibly a result of this initial deterioration. Beyond this, however, little problem was encountered. It might be of some advantage to use an element somewhat less subject to attack (*e.g.* rhodium), even perhaps at the expense of lowering the cavity $Q$ factor. Excessive deterioration has also been reported[5] from spurious discharges within the microwave field, but outside the lamp. No such discharges were experienced with any of the cavities used here, although the authors have frequently encountered this problem with the quarter-wave (Evenson) type cavity.

## DISCUSSION

The performance of four related three-quarter-wave cavities has been examined over a wide range of circumstances and an attempt has been made to explain the behaviour of electrodeless discharge lamps with regard to the parameters affecting lamp performance. The efficiency of the cavities has been shown to be ST > BK-UT > EMS 210L > BK-T. The difference in efficiency between the ST and BK-UT cavities is somewhat difficult to ascertain, the ST cavity being more efficient for mercury and thallium sources and slightly less efficient for the selenium lamp used. Maximal cavity efficiency is, however, not necessarily indicative of the most suitable conditions of operation for analytical atomic spectroscopic purposes, particularly for the more volatile elements. The effect was so marked with mercury sources that an improvement in the analytical a.a.s. and a.f.s. signal could even be obtained by tuning the least efficient (BK-T) cavity to minimal efficiency. Optimal cavity performance can be best achieved by correctly adjusting the microwave power; a change of $\pm 5$–10 W can result in a change of up to $\pm 90\%$ in the a.f.s. signal. However, optimal conditions ascertained for operation of a lamp in one particular microwave cavity will by no means be optimal for operation in another. Likewise, the optimal cavity for one lamp will not necessarily be the same for all lamps of that element. However, provided that the preparative parameters can be accurately controlled, it may prove possible to obtain maximal analytical performance from any type of microwave cavity merely by choosing the preparative conditions to suit the cavity concerned, though this may

often prove impracticable because of the difficulties encountered in introducing microgram quantities of material into the lamp blank[9]. It is also important to realise that the microwave power providing maximal integrated line intensity is seldom, if ever, that providing the optimal analytical signal; the optimal microwave power for a.f.s. studies is generally about 30% lower, whilst that for a.a.s. studies is still lower. The importance of optimising operating conditions on the basis of an analytical signal rather than the integrated line intensity is thus appreciated. The advantages of air cooling also have been examined and discussed.

Rather surprisingly, the differences in the a.a.s. and a.f.s. results obtained in different cavities was small. For the a.f.s. of selenium, the optimal choice of the microwave cavity (EMS 210L) resulted in an atomic fluorescence signal 2-fold that obtained with the least favourable cavity (BK-UT). A similar improvement was obtained when the a.a.s. sensitivities were compared. For mercury the BK-T cavity, in comparison to the least favourable ST cavity, gave a 3-fold a.a.s. and a.f.s. signal improvement when the BK-T cavity was tuned to minimal reflected power, and a 5-fold improvement when tuned to maximal analytical signal. For thallium, the differences in the a.a.s. sensitivities between the various microwave cavities was even less marked; the a.f.s. response was considerably more marked with the more usual (3 Torr argon fill gas) lamp because no signal could be detected with the BK-T cavity. However, the use of a lamp prepared with a higher fill gas pressure (10 Torr) resulted in a similar situation to that with mercury and selenium.

A less efficient cavity may prove useful for lamps of the more volatile elements in a.a.s. studies where line broadening is of considerable importance. The use of a more efficient cavity has the advantage that lamps having a wide range of internal pressures can still be operated and a wider range of lamp preparative conditions can therefore be dealt with.

We would like to thank Beckman-RIIC Ltd. for the award of a research grant to one of us (D.O.C.) and for the loan of apparatus to carry out this work.

SUMMARY

The effects of lamp preparation, modulation, stability, air cooling, cavity tuning and deterioration of cavity surfaces are considered on the analytical atomic absorbance and atomic fluorescence measurements of mercury, selenium and thallium, for four different types of three-quarter-wave resonant cavities. The efficiency of each cavity is compared and the advantages and disadvantages of each are evaluated with respect to their use in analytical atomic spectrometry.

ZUSAMMENFASSUNG

Für die analytischen Atomabsorptions- und Atomfluoreszenzmessungen von Quecksilber, Selen und Thallium wurden vier verschiedene Typen von Dreiviertelwellen-Resonanzhohlräumen eingesetzt und die Einflüsse von Lampenvorbereitung, Modulation, Stabilität, Luftkühlung, Hohlraumabstimmung und Abnutzung der Hohlraumoberflächen untersucht. Die Leistungsfähigkeiten der verschiedenen Hohlraüme werden miteinander verglichen und die Vor- und Nachteile eines jeden im Hinblick auf die Anwendung in der analytischen Atomspektrometrie ausgewertet.

REFERENCES

1 K. E. ZACHA, M. P. BRATZEL, JR. AND J. D. WINEFORDNER, *Anal. Chem.*, 40 (1968) 1733.
2 R. M. DAGNALL, K. C. THOMPSON AND T. S. WEST, *At. Abs. Newslett.*, 6 (1967) 117.
3 K. M. ALDOUS, D. ALGER, R. M. DAGNALL AND T. S. WEST, *Lab. Pract.*, (1970) 587.
4 R. M. DAGNALL, R. PRIBIL AND T. S. WEST, *Analyst*, 93 (1969) 281.
5 J. M. MANSFIELD, M. P. BRATZEL, JR., M. D. NORGORDON, D. N. KNAPP, K. E. ZACHA AND J. D. WINEFORDNER, *Spectrochim. Acta*, 23B (1968) 389.
6 G. B. MARSHALL AND T. S. WEST, *Anal. Chim. Acta*, 51 (1970) 179.
7 C. WOODWARD, *Anal. Chim. Acta*, 51 (1970) 548.
8 A. A. FISHER AND G. C. HAYWARD, Paper No. 16 presented at *21st Pittsburgh Conference of Analytical Chemistry and Applied Spectroscopy, March 1970.*
9 D. O. COOKE, R. M. DAGNALL AND T. S. WEST, *Anal. Chim. Acta*, 54 (1971) 381.
10 F. C. FEHSENFELD, K. M. EVENSON AND H. P. BROIDA, *Rev. Sci. Instr.*, 36 (1965) 294.
11 R. M. DAGNALL AND T. S. WEST, *Appl. Opt.*, 7 (1968) 1287.
12 R. F. BROWNER, R. M. DAGNALL AND T. S. WEST, Paper presented at *XIth Eastern Analytical Symposium, New York, U.S.A., 1968.*
13 R. F. BROWNER, R. M. DAGNALL AND T. S. WEST, *Anal. Chim. Acta*, 46 (1969) 207.
14 R. M. DAGNALL, G. F. KIRKBRIGHT, T. S. WEST AND R. WOOD, *Anal. Chim. Acta*, 47 (1969) 407.
15 K. C. THOMPSON AND P. C. WILDY, *Analyst*, 95 (1970) 776.
16 T. C. RAINS AND T. A. RUSH, *N.B.S. Technical Note No. 504*, July 1968–June 1969.

*Analytica Chimica Acta*
Elsevier Publishing Company, Amsterdam
Printed in The Netherlands



# DESCRIPTION ET PERFORMANCES D'UNE INSTALLATION POUR L'ETUDE DES SELS FONDUS PAR SPECTROPHOTOMETRIE D'ABSORPTION

G. LANDRESSE*
*Laboratoire de Chimie Analytique et Nucléaire, Université de Liège au Sart Tilman, B-4000 Liège (Belgique)*
(Reçu le 18 mars 1971)

Depuis quelques années, les études dans les solvants ionisés tels que les sels fondus, ont pris un essor considérable. Cet état de chose tient au fait que les solvants ionisés constituent un milieu radicalement différent de l'eau ou des solvants organiques non polaires et que l'étude des propriétés des solutés ouvre des perspectives intéressantes pour la connaissance de la matière; par ailleurs, la connaissance des réactions et, en général, des phénomènes physiques et chimiques dans les sels fondus est d'un intérêt pratique considérable étant donné qu'un certain nombre de procédés industriels importants sont directement concernés.

On a appliqué progressivement, dans l'étude des solutions dans les bains de sels fondus, les méthodes d'investigation bien établies pour l'étude des solutions aqueuses, et, si les bains de sels fondus constituent des solvants thermodynamiquement intéressants parce qu'ils permettent de couvrir un domaine de température étendu, il faut, en contrepartie, souligner que l'adaptation des différentes techniques pose en général un problème de mise au point délicat provenant justement de la plus ou moins haute température concernée.

Au laboratoire de Chimie Analytique et Nucléaire de l'Université de Liège, nous avons eu l'occasion de construire et de mettre au point une installation pour la spectrophotométrie d'absorption ultra-violette, visible et proche infrarouge des solutions dans les sels fondus dans un domaine allant de la température ordinaire jusque vers 800°. Il nous a paru utile de publier la description de cette installation qui, à notre avis, offre des possibilités intéressantes.

L'installation comporte deux parties essentielles: (*a*) les boîtes à gants pour la purification des bains de sels fondus et pour la préparation des solutions, et (*b*) l'appareil de spectrophotométrie et les accessoires.

## INSTALLATION DE PRÉPARATION DES BAINS FONDUS

Celle-ci se compose de deux boîtes à gants (Fig. 1), la première contenant une balance analytique au 0.1 de mg et une pompe de recyclage des gaz des boîtes à gants. Elle est raccordée à la ventilation générale qui maintient dans ces boîtes une dépression correspondant à 3 cm d'huile. La seconde boîte est équipée d'un four de préparation et d'un sas à vide. Cette boîte est directement reliée à une rampe à gaz

* Aspirant au Fonds National de la Recherche Scientifique.

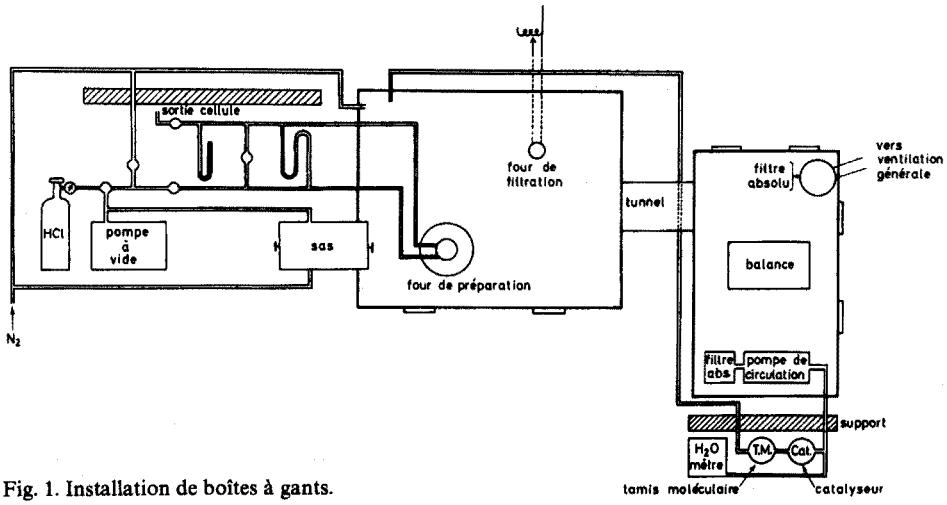


Fig. 1. Installation de boîtes à gants.

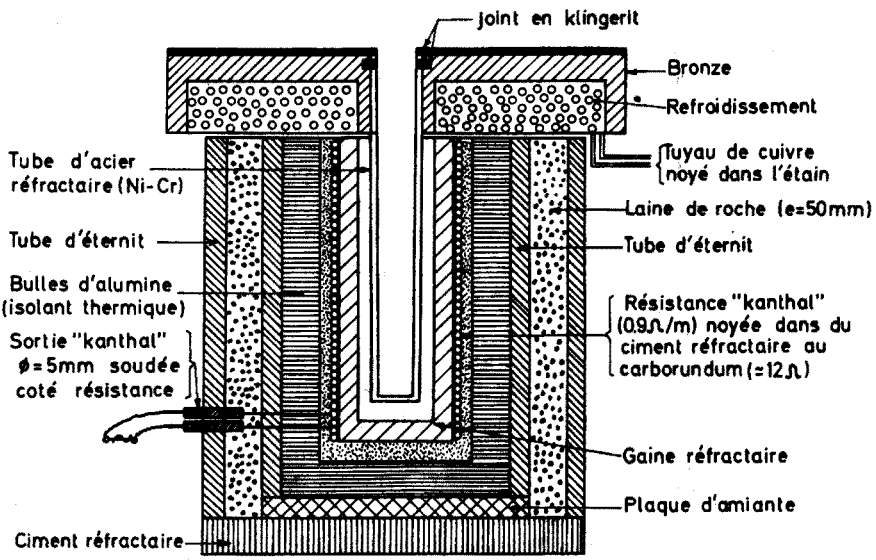


Fig. 2. Four de préparation.

requise pour la purification des bains fondus. Un autre circuit de gaz permet de maintenir dans les boîtes une atmosphère d'azote sec et pur. Nous allons décrire successivement ces différentes parties.

*Boîtes à gants*

Les boîtes à gants sont en cuivre; le volume total est de 800 l. La raison d'être de ces boîtes à gants est double: elles permettent d'abord le travail avec des bains fondus très hygroscopiques sans trop de risques d'hydratation étant donné qu'elles sont maintenues sous une atmosphère d'azote sec (nous aurons l'occasion

d'insister sur le fait que la purification des bains est un des points essentiels dans ce genre d'étude); en second lieu, désirant travailler avec des solutions d'uranium, elles offrent une protection radiobiologique efficace.

*Four de préparation*

Le four servant à la fusion et à la purification des solvants a été construit dans nos ateliers (Fig. 2); le tube en acier réfractaire destiné à contenir le bain thermostatique est fixé au fond de la boîte à gants au moyen d'un plateau en bronze équipé d'un serpentin de refroidissement. Un joint en klingerit assure l'étanchéité. Le fil de chauffage en Kanthal (15 Ω) est enroulé sur un tube en alumine et il est noyé dans un ciment au carborundum. L'ensemble est isolé thermiquement au moyen de billes creuses d'alumine contenues dans un premier tube en éternit, lui-même isolé par de la laine de roche; le tout est contenu dans un second tube en éternit. La régulation de la température du four est assurée par un "Proportional Temperature Controller SR1" de CNS Instr. Ltd (amplificateur magnétique commandé par un amplificateur proportionnel). La mesure de la température du four est effectuée par un thermocouple Fe/Fe Constantan et un millivoltmètre.

*Sas à vide*

La boîte est équipée d'un sas à vide destiné à l'introduction ou à la sortie d'objets de la boîte à gants sans introduire d'air ou d'humidité; il est constitué par un tube en plexiglas de 45 cm de long, 19 cm de diamètre et 5 mm de paroi, renforcé intérieurement par un grillage métallique pour réduire les risques d'implosion. Le sas est équipé de deux portes étanches à joints plats en caoutchouc, d'un manomètre, d'une entrée pour azote sec et d'une sortie raccordée à une pompe à vide.

*Purification des gaz constituant l'atmosphère des boîtes à gants*

Comme nous le verrons dans un paragraphe ultérieur, la préparation des échantillons pour la spectrométrie demande la manipulation des solvants au contact de l'atmosphère des boîtes à gants. Il est connu[1] que les mélanges de sels fondus contenant du lithium sont très hygroscopiques et il est, par exemple, pratiquement impossible d'obtenir un spectre convenable d'U(IV) et des mesures d'absorbance reproductibles si la manipulation du solvant a été faite dans une atmosphère contenant plus de 60 p.p.m. de vapeur d'eau. Cette eau produit, en effet, des ions oxydes en solution qui précipitent l'uranium(IV) sous forme d'$UO_2$. Il est dès lors indispensable d'apporter un soin particulier à la purification de l'atmosphère des boîtes à gants préparatives.

Le circuit de circulation et de purification du gaz, en l'occurence l'azote, pour les boîtes à gants est le suivant: une pompe à fort débit (1250 l $h^{-1}$) extrait l'azote de la boîte et l'envoie au travers d'un filtre absolu puis de deux tours en pyrex de 50 cm de haut et 10 cm de diamètre remplies l'une de tamis moléculaire 5 Å de formule $Ca_{4,5}Na_3[(AlO_2)_{12}(SiO_2)_{12}]\cdot 30\ H_2O$ destiné à éliminer l'eau et l'autre de catalyseur BASF (Cu finement dispersé sur $SiO_2$ fonctionnant à 150°) pour éliminer l'oxygène. La pompe de recyclage, à membranes souples, est de marque Austen; de façon à éviter les rentrées d'air et d'humidité par les joints et les fissures éventuelles dans les membranes, elle est installée à l'intérieur de l'une des boîtes à gants. Des teneurs en eau inférieures à 10 p.p.m. (18 v.p.m.), c'est-à-dire en dessous de la limite de détection de l'appareil à point de rosée Alnor, peuvent être obtenues dans les boîtes en dépression.

Après une demi-heure de manipulation, la teneur en eau passe à 17 p.p.m. et à 55 p.p.m. (100 v.p.m.) environ après plusieurs heures. Cette augmentation provient de la perméabilité à la vapeur d'eau des gants de néoprène utilisés.

Le recyclage est complété par un balayage d'azote sec.

*Système de sécurité*

Pour éviter une dépression ou une surpression trop forte dans les boîtes à gants, un système de manomètres à mercure et de relais agit sur le fonctionnement de la pompe à vide et de la pompe de recyclage.

*Rampe à gaz*

Une rampe à gaz permet soit de faire le vide, soit de faire barboter différents gaz, notamment HCl, dans la cellule de préparation du bain fondu. Les canalisations pénètrent dans les boîtes à gants au moyen de passages en Plastadur.

*Cellules de préparation*

Les cellules de préparation des bains (Fig. 3A et B) sont en quartz; c'est un matériau de choix: il est transparent, inerte et étanche au vide aux températures d'expérience. Le barbotage des gaz dans la cellule de préparation s'effectue soit par un capillaire latéral soudé à la cellule (type A), soit par un capillaire central muni d'un rodage qu'on introduit par un des trois rodages B7 de la tête de cellule (type B). Ce dernier système offre une meilleure résistance mécanique.

Les cellules de préparation servent également aux mesures électrochimiques. Dans ce type d'expérience, il suffit d'introduire les électrodes ad hoc par les rodages B7 de la tête de cellule.

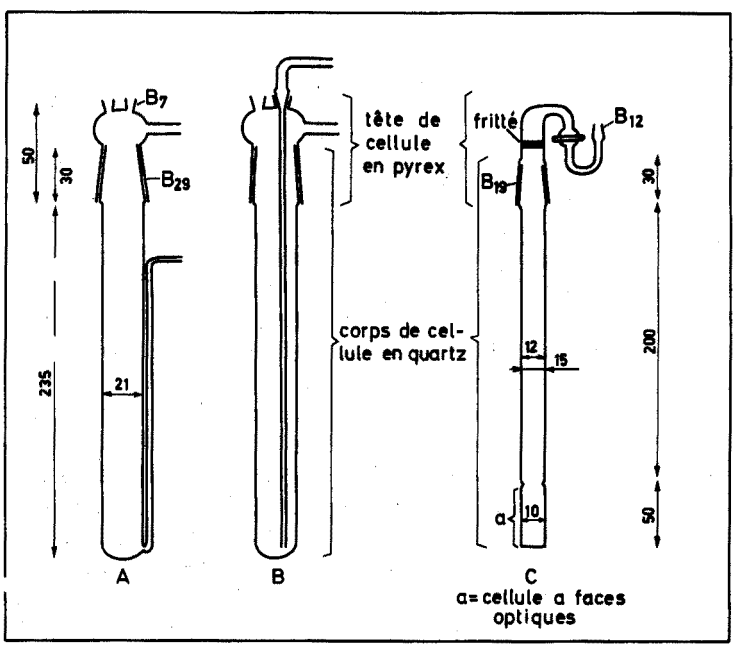


Fig. 3. (A et B) Cellules de préparation; (C) cellule spectrophotométrique.

## INSTALLATION DE MESURE

Celle-ci se compose d'un spectrophotomètre Cary 14 H, de deux fours installés dans une boîte à gants et d'une rampe à gaz.

*Spectrophotomètre Cary 14 H*

Le Cary 14 H est un spectrophotomètre à double faisceau enregistrant de 190 à 3000 nm. Il offre la possibilité d'installer deux fours dans le trajet optique et de mesurer des spectres directement sur des sels fondus. Le schéma de base comporte les éléments suivants: la source lumineuse → le hacheur → l'échantillon → le monochromateur → le détecteur → l'amplificateur de courant alternatif → l'enregistreur.

D'après Gruen[2], cette construction est celle qui convient le mieux pour l'étude des sels fondus jusqu'à 2200°. Le "chopper" hache le rayonnement provenant de la source lumineuse avant passage dans l'échantillon. L'appareil est pourvu d'un double monochromateur: un réseau échelette de 600 lignes/mm et un prisme de silice fondue de 30° d'angle au sommet. Les détecteurs sont un photomultiplicateur 1 P 28 pour l'u.v. et le visible et une cellule en PbS pour le proche i.r. Un système électronique amplifie uniquement le courant alternatif provenant de la source et il en résulte l'élimination du bruit de fond dû à l'émission de corps noir des échantillons à haute température. L'échelle des longueurs d'onde est précise à 0.29 nm près et reproductible à 0.05 nm près. Le pouvoir de résolution du monochromateur est d'environ 0.1 nm dans l'u.v. et le visible et de 0.3 nm dans l'i.r.

*Fours de mesure*

Les deux fours destinés à amener les deux cellules à échantillons (référence et solution) à une même température ont été construits dans nos ateliers d'après les plans de Morrey et Madsen[3]. Ces fours sont constitués respectivement

(*a*) d'un revêtement extérieur en laiton,

(*b*) d'un serpentin de cuivre noyé dans l'étain servant au refroidissement et relié à la canalisation d'eau,

(*c*) d'une couche de matériau multicellulaire pour l'isolation thermique,

(*d*) d'un bloc en nickel percé verticalement de neuf trous: l'un pour l'échantillon (central), un autre pour la sonde de thermorégulation et un troisième pour le thermocouple de mesure; les six derniers trous contiennent six carottes chauffantes constituées de fil de platine rhodié à 10% (6 $\Omega$ m$^{-1}$) de 20 $\Omega$ bobinées sur réfractaire.

L'ensemble est fermé par un couvercle en laiton refroidi par une circulation d'eau. Ces fours sont pourvus de fenêtres optiques au niveau de l'échantillon.

Le système de thermorégulation (tyratron au silicium) stabilise la température à $\pm 1°$. L'étalonnage des thermorégulateurs et des thermocouples (Pt/Pt rhodié) entre 150 et 800° a été effectué au moyen des points de fusion connus de In, Sn, Bi, Pb, Zn, Te, Sb, KCl et NaCl.

*Boîte à gants*

Les deux fours en question sont installés dans une boîte à gants en plexiglas à fond d'aluminium d'un volume de 160 l. Cette boîte, munie de quatre fenêtres optiques en quartz, est montée sur rails. Cette disposition permet aisément de retirer l'ensemble et de faire des mesures à température ordinaire et de passer rapidement aux mesures

sur sels fondus sans ajustement laborieux. La boîte à gants est à nouveau requise pour les mesures sur des substances radioactives. Elle est raccordée via un filtre absolu au circuit de ventilation qui y maintient une dépression équivalent à 3 cm d'huile. Les transferts se font au moyen d'un sas hermétique.

*Rampe à gaz de mesure*

La rampe à gaz est schématisée dans la Fig. 4. De conception simple, cette rampe étanche permet de contrôler aisément la nature et la pression de l'atmosphère

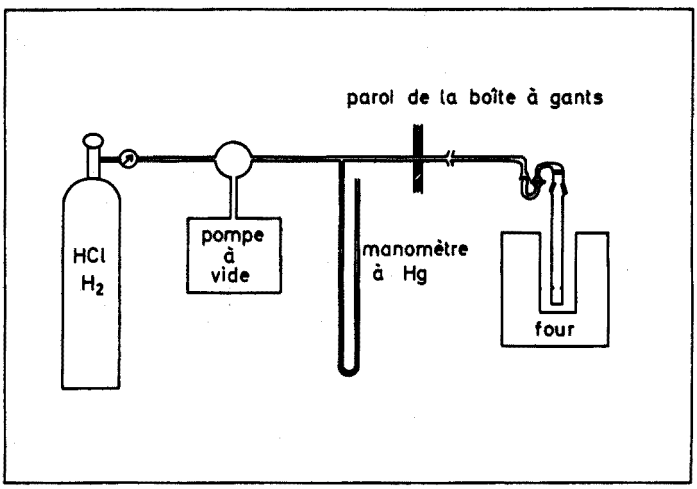


Fig. 4. Rampe à gaz de mesure.

en contact avec les bains fondus. La partie de la rampe proche de la cellule est rendue mobile par un jeu de rodages sphériques. Il y a lieu d'éviter le caoutchouc ou le PVC qui réagiraient avec HCl.

*Cellules spectrophotométriques*

Les cellules spectrophotométriques (Fig. 3C) sont en quartz optique (50 mm de hauteur et 10 × 10 mm de section carrée intérieure). Elles sont soudées à un tube de quartz de 20 cm de haut et 15 mm de diamètre extérieur, lui-même soudé à un rodage B 19 mâle en quartz. La tête de cellule est en pyrex et elle est pourvue d'un filtre en verre fritté. A mi-hauteur du tube en quartz, se trouvent deux ergots qui peuvent maintenir un bouchon de quartz.

Lors de nos premiers essais, les cellules devenaient opaques après quelques expériences. Cette corrosion provenait d'ions oxydes existant dans le bain et qui réagissent avec le quartz. Nous sommes parvenus à réduire considérablement cette corrosion en purifiant d'une part les solvants fondus et d'autre part en travaillant autant que possible en présence de HCl qui transforme $O^{2-}$ en $OH^-$, $H_2O$ ou $H_3O^+$. Dans ces conditions, les cellules spectrophotométriques ne présentent plus d'altération après plusieurs mois d'expérimentation à 450°.

## MANIPULATIONS

*Purification du solvant*

La méthode de purification adoptée est la suivante pour les bains ci-après:
(1) l'eutectique LiCl–KCl 58–42 mole %
(2) le mélange LiCl–KCl 70–30 mole %
(3) le mélange LiCl–CsCl 55–45 mole %
(4) l'eutectique ternaire NaCl–KCl–$MgCl_2$ 30–20–50 mole %.

Le sel est prépurifié et mis sous forme de "billes" selon la méthode décrite par Gruen et McBeth[4]. Ensuite, 30–50 g de sels sont introduits dans une cellule de préparation et mis sous vide à 300° pendant 24 h. Après cette période de séchage, le mélange est fondu sous HCl à 450°. On laisse barboter HCl dans le bain pendant 2 h environ puis HCl est éliminé et la cellule est rincée par l'azote. La purification est terminée par une électrolyse de 15 h sous tension de 1.25 V avec une cathode de tungstène et une anode de graphite (1.50 V dans le cas de NaCl–KCl–$MgCl_2$). Le bain est alors filtré sur laine de quartz disposée dans un four et condensé en plaque sur une nacelle de quartz. Le mélange refroidi est concassé et stocké en flacon hermétique.

*Mesures spectrophotométriques*

Des quantités exactement pesées de chlorures et de composé d'uranium ($Cs_2UCl_6$ ou $Cs_2UO_2Cl_4$) sont introduites dans la cellule de mesure qui est maintenue sous atmosphère d'azote pur et sec. L'ensemble est transféré par les sas dans l'installation de mesure. Toute la rampe de mesure est mise sous vide, y compris la cellule et le détendeur à gaz. On introduit alors la cellule dans le four, soit sous vide, soit sous une atmosphère d'HCl. Après fusion, la solution est prête pour les mesures spectrophotométriques. Celles-ci peuvent être réalisées à différentes températures (entre 400 et 550°) et sous différentes pressions d'HCl (entre 0 et 1 atm).

## PERFORMANCES DE L'INSTALLATION

La Fig. 5 montre les spectres d'U(IV) dans l'eutectique LiCl–KCl et dans le mélange LiCl–CsCl à 450°.

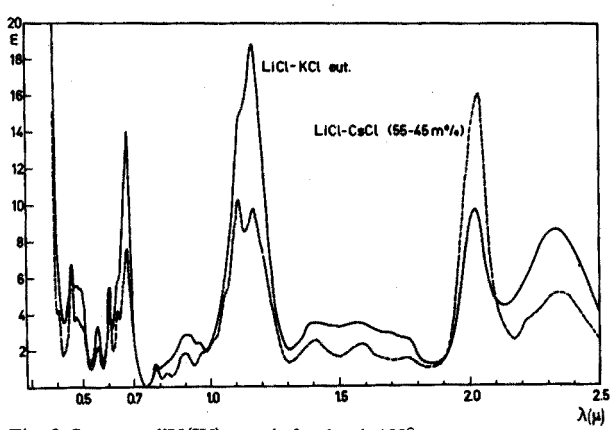


Fig. 5. Spectres d'U(IV) en sels fondus à 450°.

Nous avons vérifié la loi de Beer–Lambert ($A = \varepsilon lc$) pour l'U(IV) à 1.160 nm dans LiCl–KCl et à 1.105 nm dans LiCl–CsCl. La concentration en uranium est calculée d'après les pesées de solvant et de soluté en utilisant la densité du solvant aux températures d'expérience. Les résultats de ces expériences à 450° sont reportés sur la Fig. 6. La loi de Beer se vérifie parfaitement aux concentrations inférieures à $10^{-1}$ *M*. A partir de ces droites, on peut calculer aisément les valeurs de $\varepsilon$: 18.75 l $mol^{-1}$ $cm^{-1}$ dans l'eutectique LiCl–KCl et 10.4 l $mol^{-1}$ $cm^{-1}$ dans LiCl–CsCl (55–45 mole %).

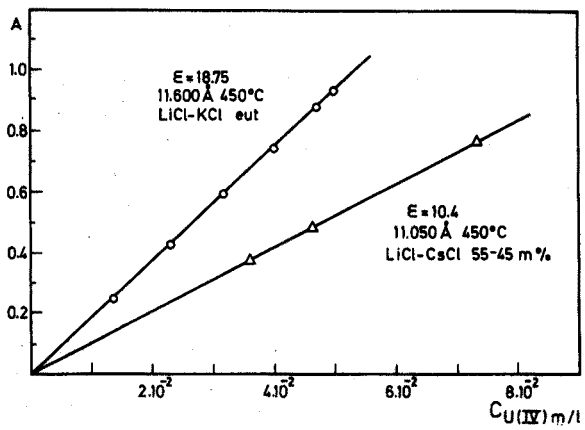


Fig. 6. Vérification de la loi de Beer–Lambert.

Nous avons pu, grâce à cette installation, étudier quantitativement la réaction de dismutation-amphotérisation de l'U(V) en présence de HCl dans les différents solvants. L'U(V) est formé dans le bain fondu par la réaction

$$UO_2^{2+} + 1/2\,H_2 \rightarrow UO_2^{+} + H^{+}$$

L'U(V) est traité par HCl et subit la dismutation selon la réaction suivante:

$$2\,UO_2^{+} + n\,HCl \underset{\text{vide}}{\overset{HCl}{\rightleftharpoons}} UO_2^{2+} + U^{4+} + 2\,W + n\,Cl^{-}$$

ou W désigne l'eau qui peut être présente sous trois formes $OH^-$, $H_2O$ et $H_3O^+$. Pour faciliter l'écriture, nous faisons abstraction des complexes chlorés de l'uranium.

Cette réaction est réversible: en éliminant HCl par pompage, on reforme U(V).

En étudiant le degré d'avancement de cette réaction en fonction de la pression d'HCl, nous avons pu préciser que dans l'eutectique LiCl–KCl, par exemple, aux pressions d'HCl supérieures à 60 mm Hg environ, les réactions principales sont

$$2\,UO_2^{+} + 6\,H^{+} \rightleftharpoons UO_2^{2+} + U^{4+} + 2\,H_3O^{+}$$

et

$$2\,UO_2^{+} + 4\,H^{+} \rightleftharpoons UO_2^{2+} + U^{4+} + 2\,H_2O$$

Cette dernière réaction devient d'ailleurs prépondérante entre 30 et 60 mm Hg; à partir de là, la réaction

$$2\,UO_2^{+} + 2\,H^{+} \rightleftharpoons UO_2^{2+} + U^{4+} + 2\,OH^{-}$$

commence à se manifester et cette dernière devient prépondérante aux pressions d'acide chlorhydrique inférieures à 30 mm Hg.

Les détails de cette étude quantitative seront publiés ultérieurement.

Nous remercions le Fonds National de la Recherche Scientifique et l'Institut Interuniversitaire des Sciences Nucléaires pour l'intérêt constant apporté à nos travaux et le soutien financier accordé à notre laboratoire.

RÉSUMÉ

Cet article décrit les parties essentielles d'une installation de spectrophotométrie d'absorption à haute température dans les sels fondus entre 300 et 2500 nm.

SUMMARY

The essential parts of a device for absorption spectrophotometry in the range 300–2500 nm at high temperature in molten salts are described. Application to uranium(IV) is discussed.

ZUSAMMENFASSUNG

Es werden die wesentlichen Teile einer Anlage beschrieben, mit der Salzschmelzen bei hohen Temperaturen im Bereich 300–2500 nm absorptionsspektrophotometrisch untersucht werden können. Die Anwendung auf Uran(IV) wird diskutiert.

BIBLIOGRAPHIE

1 W. J. Burkhard et J. D. Corbett, *J. Amer. Chem. Soc.*, 79 (1957) 6361.
2 D. M. Gruen, *Quart. Rev.*, *19* (1965) 349.
3 J. R. Morrey et A. W. Madsen, *Rev. Sci. Instr.*, 32 (1961) 799.
4 D. M. Gruen et R. L. McBeth, *J. Inorg. Nucl. Chem.*, 9 (1959) 290.

*Analytica Chimica Acta*
Elsevier Publishing Company, Amsterdam
Printed in The Netherlands



# SOLVENT EXTRACTION SEPARATIONS OF THE LANTHANIDES AND SELECTED METAL IONS WITH 1,1,1,2,2,3,3-HEPTAFLUORO-7,7-DIMETHYL-4,6-OCTANEDIONE

THOMAS R. SWEET AND DENNIS BRENGARTNER
*Department of Chemistry, The Ohio State University, Columbus, Ohio 43210 (U.S.A.)*
(Received 1st February 1971)

The $\beta$-diketone 1,1,1,2,2,3,3-heptafluoro-7,7-dimethyl-4,6-octanedione, H(fod), has been shown to be an effective chelating reagent for the lanthanides[1]. As a 0.10 *M* solution in carbon tetrachloride, H(fod) was found capable of extracting the lanthanides quantitatively from unbuffered aqueous solutions[2]. However, the separation factors reported were relatively small (1.1–3.5 for adjacent members).

The present work was undertaken to determine whether H(fod) could be used effectively to separate the lanthanides by a multiple solvent extraction technique such as Craig countercurrent distribution. For this purpose the extraction of the lanthanides with H(fod) from acetate-buffered solutions into benzene was studied. In addition, some transition and Group IIIA metals were investigated to gather information about the general applicability of this reagent for solvent extraction separations.

## EXPERIMENTAL

### *Apparatus*

The flame emission and atomic absorption measurements were made with a Perkin-Elmer Model 303 atomic absorption spectrophotometer with a flame emission accessory. The $\gamma$-activities of the lanthanide radioisotopes used were measured in a well crystal with a Nuclear Data Series 1100 analyzer system and associated readout equipment. The pH measurements were made with a Corning Model 12 pH meter and a semimicro combination electrode. Countercurrent distribution operations were performed on a 30-tube Craig-type apparatus (H.O. Post Scientific Instrument Company).

### *Reagents*

All chemicals used were analytical-reagent grade unless otherwise specified. Lanthanide nitrates were obtained from the Lindsay Division of American Potash and Chemical Company. Lanthanide radioisotopes (Union Carbide Company, Oak Ridge) had greater than 98% radiochemical purity. Comparison of the $\gamma$-spectra with literature values showed no extraneous photopeaks.

### *Procedure*

Solutions containing a 2 *M* total concentration of acetate were prepared from acetic acid and potassium acetate. The pH was adjusted to give a series of solutions

spaced 0.2–0.5 pH unit apart in the range of pH 1–7. The organic phase was 0.10 *M* H(fod) in benzene. All work was performed at $24 \pm 1°$.

For batch extractions, percent extraction *versus* pH curves were prepared for Cu(II), Fe(III), In(III), Ni(II), Tl(I), and Cd(II) in 1 *M* total acetate solutions. The extractions were performed by contacting a mixture of 5.0 ml of 2 *M* buffer and 5.0 ml of metal solution with 10.0 ml of 0.10 *M* H(fod) in benzene in a 30-ml glass bottle. The metal concentration was initially $5 \cdot 10^{-4}$ *M* in the aqueous phase.

The bottles were shaken for 1 h at medium speed. After settling for a few minutes, the pH of the aqueous phase was measured and recorded. No activity corrections were made. A 5.0-ml aliquot of each organic phase was placed in a 4-dram vial containing 5.0 ml of 1 *M* nitric acid. These vials were shaken for 1 h at medium speed. The organic layer was then removed with a suction tube. In this way, the metal ion was contained in aqueous solutions of a uniform background matrix and in the same concentration as in the organic phase in the original extraction. The samples were analyzed by atomic absorption with an air–acetylene flame and appropriate standards in the same medium as the samples.

A similar set of $\%E$ *versus* pH curves was prepared for all of the lanthanide series except lanthanum, cerium, and promethium. The aqueous solutions were $5 \cdot 10^{-3}$ *M* in metal and 1 *M* in total acetate. The procedure was essentially the same as above except for the determination steps. For the atomic absorption (Dy, Ho, Yb) and flame emission (Pr, Nd, Sm, Eu, Er, Tm, Yb, Lu) determinations, the aqueous phase used for the stripping of the extracted metal chelate also contained 1000 p.p.m. K as potassium nitrate to suppress ionization of the lanthanide in the flame. A nitrous oxide–acetylene flame was used. Radiotracers were used to analyze Eu, Gd, and Tb by counting an aliquot of each phase.

The Craig apparatus was designed to hold 10 ml of each phase in each tube. The apparatus was cleaned and filled with the aqueous buffer solution which had been presaturated with 0.10 *M* H(fod) in benzene. A 10-ml portion of the metal solution and 10 ml of the organic phase were equilibrated and the pH was readjusted to the desired value. The two-phase mixture was transferred into the first tube (tube 0) of the apparatus. The organic phase was then transferred to the next tube. Tube 0 was refilled with 10 ml of fresh organic phase, the apparatus was rocked to equilibrate the phases, and the sequence was repeated. After *n* transfers the apparatus was disassembled and the contents of each tube were placed in a labelled bottle.

The contents of the bottles were treated to concentrate the metal in one phase for the determination step. For flame analysis, base was used to put the metal into the organic phase in order to remove it from the high concentration of salts in the aqueous phase. The metal was subsequently back-extracted into a uniform aqueous phase for analysis.

## RESULTS AND DISCUSSION

Since protons are liberated in the reaction between the metal ion and the reagent, an effective pH buffer was necessary to hold the pH and hence the distribution ratio, *D*, constant in the countercurrent apparatus. *D* is defined as $[M]_{org}/[M]_{aq}$. It was found that an aqueous phase buffered with a concentration of 1 *M* in total

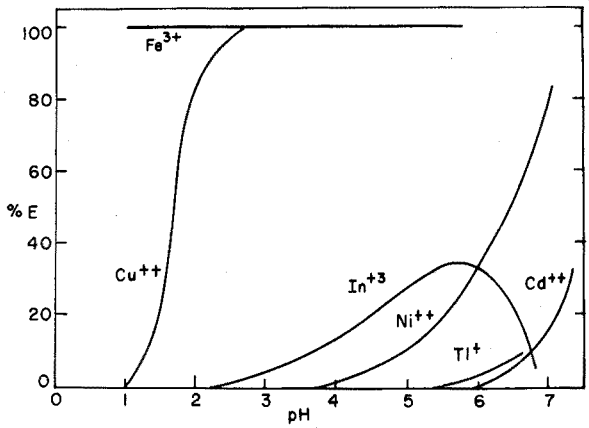


Fig. 1. % *E versus* pH for copper, indium, nickel, thallium, and cadmium extracted from one molar acetate buffer with 0.10 *M* H(fod) in benzene.

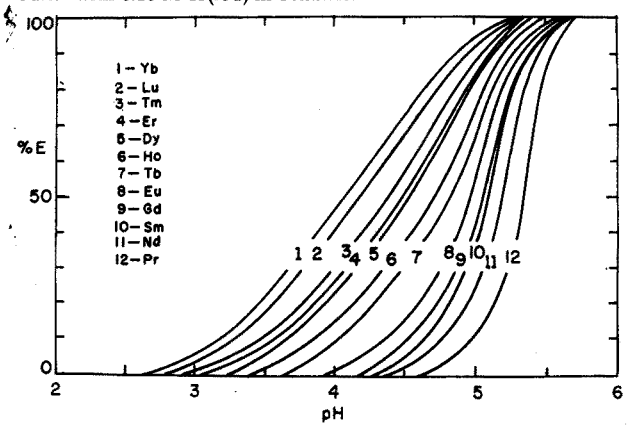


Fig. 2. % *E versus* pH for lanthanides extracted from one molar acetate buffer with 0.10 *M* H(fod) in benzene.

acetate would suffice for the metal concentrations employed. The acetate system was chosen because the $pK_a$ is about 4.7, which is near the middle of the extraction region for the lanthanides investigated. Hence, most extractions were performed in the region of high buffer capacity.

The precent extraction *versus* pH curves for the transition and Group IIIA metals investigated are shown in Fig. 1. From this graph and the corresponding plot for the lanthanides in Fig. 2, it can be seen that iron(III) can be selectively removed from all the other elements studied in a single extraction at pH 1.0. At a pH of about 2.85, copper(II) can be cleanly separated form the remaining metals except In(III), Lu(III), and Yb(III). Also investigated were Al(III), Ga(III), Cr(III), and Pt(IV), none of which was extracted to a detectable amount under the conditions used. It is possible that more than 1 h of shaking might be required to reach the maximum extraction for some of the elements. The arbitrary shaking time of 1 h was used to establish a limit for a separation of practical value.

All lanthanides studied were essentially completely extracted by pH 5.7. With the exception of the reversals of three adjacent pairs of metals, the series extracted in the order of decreasing radius of the tripositive ion. It is clear from Fig. 2 that a

simple one-stage separation of any lanthanide is not possible. The gradual change in the shape of these curves indicates that the species involved are not the same throughout the series. The reasons for this change are not obvious but involve the interplay of several factors, among which are (*a*) the regular decrease in ionic radius of the tripositive metal ions (the "lanthanide contraction") which causes stronger bonding in the chelate and accounts for the overall order of the extraction series. This decrease also causes stronger bonding with the competing hydroxide ion, (*b*) the metal–acetate formation constants, which reach a maximum value near the middle of the series[3], and (*c*) in the pH region investigated, both the acetate ion concentration and the ionic strength vary by several orders of magnitude.

Several authors[4,5] have discussed the effect of acetate buffers on the extraction of lanthanides with $\beta$-diketones. In unbuffered systems, a plot of log $D$ *versus* pH has a distinct region of linear + 3 slope[2]. In the 1 $M$ acetate system, this linear portion becomes curved upward with an average slope of less than + 3 and shifted to higher pH values. The vertical distance between the log $D$–pH curves of two metals, a measure of the separation that can be obtained, is less than in the same system without buffers. However, the pH stability introduced by the buffer is necessary in a multiple extraction technique in order to exploit the small differences in distribution properties.

Conditions for the countercurrent distribution were obtained from the batch extraction data. For a given set of lanthanides, a pH value was selected from Fig. 2 so as to bracket the 50% extraction value ($D = 1$). These values and the corresponding distribution ratios and separation factors, $B$ ($B = D_1/D_2$ at fixed pH), are listed in Table I, columns 1, 2, and 4. A time study showed that equilibrium was attained in less than 4 min for gadolinium(III), a representative lanthanide.

TABLE I

A SUMMARY OF THE RESULTS OF COUNTERCURRENT DISTRIBUTION STUDIES WITH 0.10 $M$ H(fod) IN BENZENE AND 1.0 $M$ ACETATE BUFFER FOR SELECTED MIXTURES OF LANTHANIDES

| *Lanthanides* | *Distribution ratio, D* | | *Separation factor, B* | |
|---|---|---|---|---|
| | *Predicted* | *Observed* | *Predicted* | *Observed* |
| Mixture No. 1, pH = 4.90 | | | | |
| Pr | 0.087 | 0.071 | | |
| | | | 8.4 | 9.4 |
| Eu | 0.73 | 0.67 | | |
| | | | 13.8 | 13.4 |
| Yb | 10.1 | 9.0 | | |
| Mixture No. 2, pH = 4.12 | | | | |
| Yb | 1.13 | 0.76 | | |
| | | | 1.27 | 1.13 |
| Lu | 0.89 | 0.67 | | |

The first countercurrent separation was made with a solution containing 0.01 $M$ praseodymium, 0.005 $M$ europium, and 0.005 $M$ ytterbium at pH 4.90 in 1 $M$ acetate buffer. The metal concentrations were determined by flame emission after thirty transfers. These elements were selected as they represented the center and ends of the extraction series and thus had relatively large separation factors. In addition, these elements had sufficient sensitivities for detection by flame emission after the dilution caused by the distribution process. No interelement interferences were observed in the detection step. From the metal concentrations detected, the amount

of metal in each tube was calculated and the fractional distribution was determined. The experimental distribution curves are presented in Fig. 3. The three ions were well separated with only about 5% overlap of praseodymium and europium. The distribution ratios and the separation factors observed in the countercurrent distribution are given in Table I, columns 3 and 5. The observed $D$ values were approximated with the equation $D=r_{max}/(n-r_{max})$, where $r_{max}$ is the number of the tube containing the maximum concentration of metal.

A second countercurrent run was performed to check the apparent reversal in the extraction order for the lutetium–ytterbium pair. A metal solution of 0.02 $M$ lutetium and 0.005 $M$ ytterbium in a pH 4.12 buffer was prepared and fractionated by thirty transfers. The procedure was exactly the same as for the first mixture. This run

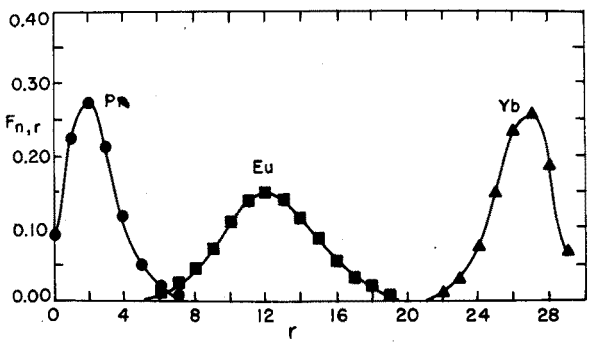


Fig. 3. Countercurrent distribution of praseodymium, europium, and ytterbium.

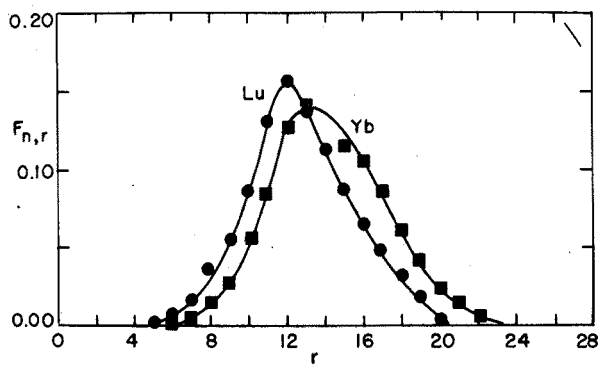


Fig. 4. Countercurrent distribution of lutetium and ytterbium.

confirmed the reversal of the general extraction order for lutetium and ytterbium in this buffer system. The experimental distribution curves are shown in Fig. 4.

The apparent reversals of the dysprosium–holmium and europium–gadolinium pairs were not investigated by this method. In order to provide an excess of the reagent over the stoichiometric amount for the *tris* chelate, the total metal concentration was limited to about 0.03 $M$ when the reagent concentration was 0.10 $M$. This concentration was too low for satisfactory measurements owing to the dilution caused by the distribution process along with the lower detection sensitivities for at least one member of each pair.

SUMMARY

1,1,1,2,2,3,3-Heptafluoro-7,7-dimethyl-4,6-octanedione (0.1 *M*) in benzene was used for the solvent extraction separation of the lanthanides and other selected metals from an aqueous phase containing 1 *M* total acetate in the pH range 1–7. A series of batch extractions was performed with the various metals and percent extraction *versus* pH curves were constructed. The lanthanides studied were completely extracted in the pH range of 5.7–7.0. Of the other metals that were investigated, only iron(III) and copper(II) were completely extracted. While the separation factors achieved for adjacent lanthanides were not large, the countercurrent distribution studies showed that such separations are feasible.

RÉSUMÉ

On propose l'utilisation de l'heptafluoro-1,1,1,2,2,3,3-diméthyl-7,7-octanedione-4,6 pour la séparation des lanthanides d'avec d'autres métaux par extraction dans un solvant. Des séries d'extractions ont été effectuées, avec divers métaux et á divers pH. Les élements des lanthanides examinés sont extraits quantitativement entre les pH 5.7 et 7.0. Parmi les autres métaux pris en considération, seuls fer(III) et cuivre(II) sont extraits complètement. Bien que les coefficients de séparation ne soient pas très grands, les études effectuées montrent que ces séparations sont possibles.

ZUSAMMENFASSUNG

Eine 0.1 *M* Lösung von 1,1,1,2,2,3,3-Heptafluor-7,7-dimethyl-4,6-octandion in Benzol wurde für die Verteilungstrennung der Lanthaniden und einiger anderer Metalle benutzt. Unter Verwendung einer wässrigen Phase mit 1 *M* Gesamtacetat im pH-Bereich 1–7 wurde mit den verschiedenen Metallen eine Reihe von einstufigen Extraktionen durchgeführt und die prozentuale Extraktion als Funktion des pH-Wertes aufgetragen. Die untersuchten Lanthaniden wurden im pH-Bereich 5.7–7.0 vollständig extrahiert. Von den anderen untersuchten Metallen konnten nur Eisen(III) und Kupfer(II) vollständig extrahiert werden. Wenn auch die für benachbarte Lanthaniden erzielten Trennfaktoren nicht gross waren, ergaben die Gegenstromverteilungsversuche, dass solche Trennungen ausführbar sind.

REFERENCES

1 R. E. SIEVERS, K. J. EISENTRAUT, D. W. MEEK AND C. S. SPRINGER, JR., *Volatile Rare Earth Chelates of β-Diketones*, Advances in Chemistry Series, No. 71, 1967.
2 T. R. SWEET AND D. BRENGARTNER, *Anal. Chim. Acta*, 52 (1970) 173.
3 S. P. SINHA, *Complexes of the Rare Earths*, Pergamon Press, London, 1966, p. 38.
4 S. D. BLAIR, *Master's Thesis*, The Ohio State University, 1968.
5 T. SHIGEMATSU, M. TABUSHI, M. MATSUI AND T. HONJYO, *Bull. Chem. Soc. Japan*, 42 (1969) 976.

*Analytica Chimica Acta*
Elsevier Publishing Company, Amsterdam
Printed in The Netherlands



# OBSERVATIONS SUR LE DOSAGE DU COBALT DANS LES METAUX FERREUX

R. BOULIN ET A. M. LEBLOND
*I.R.S.I.D., 78-St-Germain-en-Laye*
ET M. JEAN
*Centre d'Etudes Nucléaires de Saclay, 91-Gif-sur-Yvette (France)*

(Reçu le 17 mars 1971)

Les principaux réactifs du cobalt utilisés en vue de son dosage spectrophotométrique peuvent être classés quant à leurs sensibilités au moyen du coefficient d'extinction spécifique (Tableau I).

TABLEAU I

COEFFICIENTS D'EXTINCTION DES PRINCIPAUX RÉACTIFS DU COBALT

| *Réactif* | $b^a$ | $\lambda(nm)$ |
|---|---|---|
| Acide éthylènediamine tétracétique[1] | 0.0075 | 550–560 |
| Ion thiocyanique seul[2,3] | 0.03 | 630 |
| Ion thiocyanique et tétraphénylarsonium[4] | 0.03 | 620 |
| Ion thiocyanique et antipyrine[5] | 0.05 | 630 |
| Ion thiocyanique et diantipyrrylméthane[6] | 0.05 | 630 |
| Ion thiocyanique et triphényltétrazolium[7] | 0.07 | 620 |
| Diméthylglyoxime et *o*-dianisidine[8] | 0.14 | 435–440 |
| Phénanthrènequinone monoxime[9] | 0.29 | 470 |
| Sel de Nitroso-R[10,11] | 0.23 | 530 |
| | 0.35 | 430 |
| PAN[12] | 0.35 | 640 |
| PAR[13] | 0.35 | 550 |
| Quinolinazo R[14] | 0.52 | 570 |
| 2-Nitroso-1-naphtol[15] | 0.59 | 365 |
| Isonitrosomalonylguanidine[16] | 0.72 | 370 |

[a] Absorption d'une solution contenant 1 $\mu$g Co $ml^{-1}$ mesurée sous 1 cm de parcours optique.

L'examen des valeurs du coefficient d'extinction spécifique conduit à choisir entre le 2-nitroso-1-naphtol et l'isonitrosomalonylguanidine (NMG) pour la mesure de faibles quantités de cobalt.

Le NMG permet de mesurer 0.1 $\mu$g Co $ml^{-1}$ en cuve de 2 cm; en effet, l'absorption du complexe est de 0.15, déduction faite de l'absorption propre du NMG qui est de 0.20 pour une concentration de 0.2 g $l^{-1}$. Cette absorption ne varie pas sensiblement lorsque la concentration en cobalt augmente.

Pour faire la réaction en fiole de 100 ml il faut disposer de 10 $\mu$g de cobalt

(dans la prise d'essai). On pourra donc doser le cobalt dans les aciers utilisés pour la construction des réacteurs nucléaires dans lesquels la teneur en cobalt doit être inférieure à 0.020% soit 200 $\mu$g $g^{-1}$.

## CONDITIONS DE MESURE

Le complexe NMG–cobalt a son maximum d'absorption à 372 nm environ, et à cette longueur d'onde le colorant a une absorption propre de 0.10 à la concentration de 0.2 g $l^{-1}$ sous 1 cm de parcours optique (Fig. 1). Dissous en milieu acide perchlorique 0.3 *M*, le réactif est stable et sa solution limpide est quasi incolore.

Tenant compte de la composition du milieu réactionnel l'un de nous a recommandé les concentrations suivantes[16]: NMG 0.08 g $l^{-1}$, acétate d'ammonium 20 g $l^{-1}$, phosphate d'ammonium 8 g $l^{-1}$, et ions $NO_3^-$ 0.4 *M*.

L'étude entreprise a permis de constater que ces concentrations peuvent être multipliées par 2.5 sans inconvénient, excepté celles des ions $NO_3^-$ ; ceci permet de faire la réaction en fiole jaugée de 100 ou 250 ml selon la quantité de cobalt à mesurer, sans modifier les quantités de réactifs utilisés.

Une trop grande concentration de $NO_3^-$ fait évoluer l'absorption propre du colorant, alors que les ions $Cl^-$ ou $ClO_4^-$, à la même concentration de 1.35 *M*, sont sans action (Tableau II).

Dans le mode opératoire l'acide nitrique a été remplacé par l'acide perchlorique à la même concentration molaire.

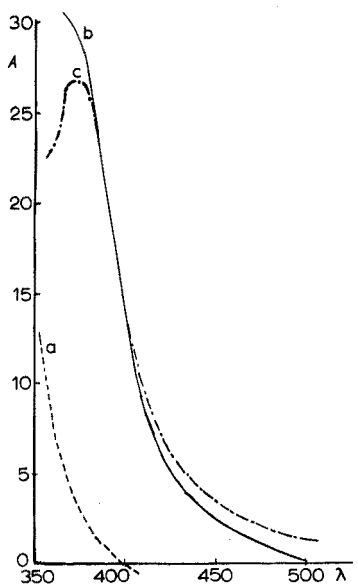


Fig. 1. Courbe d'adsorption. Cuve 1 cm. (----) Terme 0 par rapport à l'eau; (——) terme 2 par rapport à l'eau; (—·—·—) terme 2 par rapport au terme 0. Terme 0 = 0.2 g $l^{-1}$ de NMG; terme 2 = 0.2 g $l^{-1}$ de NMG + 0.32 $\mu$g $ml^{-1}$ de Co.

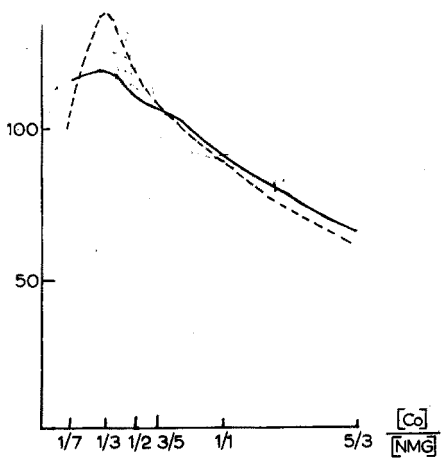


Fig. 2. Composition du complexe. (----) Sans fer; (——) avec fer. Mesures effectuées à 370 nm; cuve de 1 cm.

TABLEAU II

VARIATION DES ABSORPTIONS SELON LES ACIDES EN PRÉSENCE
(Absorption mesurée par rapport à l'eau)

| *Ions* | *Temps (min)* | | | | |
|---|---|---|---|---|---|
| | 0 | 35 | 110 | 185 | 280 |
| $NO_3^-$ | 0.145 | 0.165 | 0.211 | 0.254 | 0.300 |
| $Cl^-$ | 0.116 | 0.115 | 0.114 | 0.113 | 0.109 |
| $ClO_4^-$ | 0.120 | 0.116 | 0.115 | 0.115 | 0.114 |

Les conditions énoncées antérieurement[16] conviennent; il faut veiller à conserver le rapport massique 5/2 des sels d'ammonium (acétate et phosphate) et le rapport de la somme des sels d'ammonium et des ions $H^+$ (l'acidité doit être inférieure à 12 meq). La température n'a pas d'influence notable.

*Constitution du complexe*

Par la méthode des variations continues, en présence de fer (1 mg), ou sans fer, la constitution du complexe s'établit selon le rapport de 3 molécules-grammes d'isonitrosomalonylguanidine pour 1 atome-gramme de cobalt (Fig. 2); le rapport est le même que celui du complexe nitroso-R–cobalt[15].

INFLUENCE DES ÉLÉMENTS

Le fer a peu d'influence sur la mesure du cobalt. Ainsi, la courbe (Fig. 3) comporte les absorptions du cobalt (0.25 mg) (défalcation faite des absorptions des témoins avec fer et exempts de cobalt), en fonction de la quantité de fer (Technique de la NF A06-311); en définitive la coloration est peu sensible au fer, au delà de 1 mg de fer environ (4 $\mu$g $ml^{-1}$), contrairement au complexe avec le sel de nitroso-R (Fig. 4).

On constate que l'absorption ne change pas en présence de 4 mg, ou de 50 mg, de fer pour une même concentration en cobalt (1 mg $l^{-1}$). Une série de mesures à cobalt

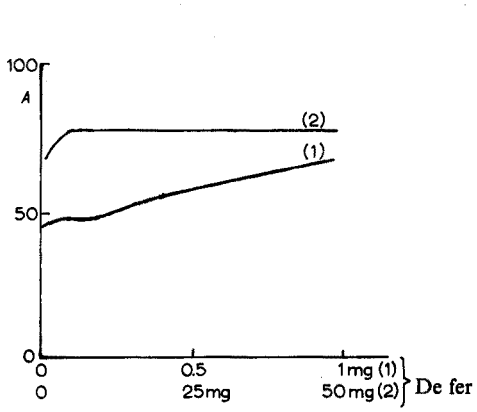


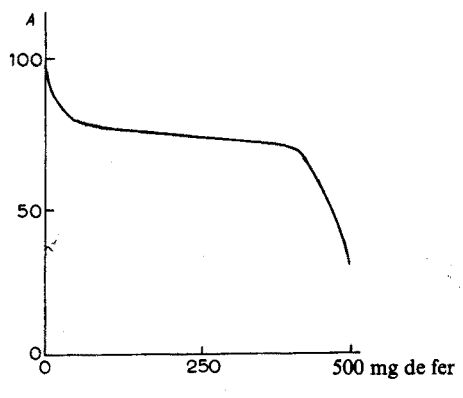


Fig. 3. Influence du fer sur la mesure. NMG. Co 1 $\mu$g $ml^{-1}$. $\lambda$ 370 nm.

Fig. 4. Influence du fer sur la mesure. Nitroso-R. Co 1 mg. $\lambda$ 550 nm.

croissant de 25 à 500 $\mu$g, en présence de 50 mg (0.2 mg $ml^{-1}$) de fer par essai, a permis de vérifier que la courbe des absorptions en fonction du cobalt présent est bien une droite (Technique de la N.F. A06-311). On arrive à une absorption de 1.2 pour 500 $\mu$g de cobalt (2 $\mu$g $ml^{-1}$).

Des essais plus poussés montrent qu'il est possible de mesurer 0.4 $\mu$g Co $ml^{-1}$ en présence de 2 mg Fe $ml^{-1}$. Cependant, il est préférable de séparer le fer dès que sa concentration dépasse 1.5 mg $ml^{-1}$.

Le nickel doit être séparé dès que sa concentration atteint 20 $\mu$g $ml^{-1}$ dans la fiole de mesure, car il bloque partiellement la formation du complexe.

Le chrome oxydé par l'acide perchlorique lors de la mise en solution absorbe à 370 nm. Il doit être éliminé sous forme de chlorure de chromyle en l'absence de nickel dès que sa concentration dépasse 20 $\mu$g $ml^{-1}$.

Le cuivre doit être séparé dès la même concentration. Si la teneur en manganèse est importante (supérieure à 1%) la mise en solution est faite en absence de phosphate (stabilisant la valence III du manganèse). Ces ions $PO_4^{3-}$ doivent être ajoutés avant de faire la mesure.

Le tungstène, le molybdène, le vanadium ne gênent pas.

## SÉPARATIONS

La séparation du nickel se fait par échange d'ions en milieu chlorhydrique (10 *M*): fer et cobalt sont fixés, le nickel n'est pas retenu, ainsi que le chrome. Le cobalt est élué sélectivement en milieu chlorhydrique 4 *M*[17]

Si la teneur en cobalt est inférieure à 0.100%, la prise d'essai est importante (0.5 à 1 g) et il faut séparer la majorité du fer sous forme de chlorure dans l'éther isopropylique; sinon le fer sature l'échangeur d'ion et le cobalt n'est pas fixé lors de la séparation du nickel.

## RÉSULTATS

### *Etalonnage*

Soit *y* l'absorption de la solution à mesurer et *x* la concentration en cobalt de la

TABLEAU III

DOSAGE DU COBALT DANS DIFFÉRENTS ACIERS

| *Echantillon* | *Teneur certifiée* (%) | *Teneur trouvée* (%) |
|---|---|---|
| BCS 271 | 0.012 | 0.013, 0.013, 0.013 |
| 273 | 0.021 | 0.022, 0.0223 |
| 275 | 0.059 | 0.060[a] |
| 276 | 0.027 | 0.028 |
| 327 | 0.002 | 0.0062, 0.0065[b] |
| BAM 2CrNiMoS | 0.219 | 0.223, 0.207, 0.219 0.214[c] |

[a] Après séparation du fer, ce résultat montrant que la séparation convient, même s'il s'agit de quantités relativement élevées de fer.
[b] Après séparation du fer.
[c] Après séparation du nickel.

même solution, exprimée en $\mu g\ ml^{-1}$, on obtient une fonction de la forme:

$$y = bx + a$$

dans laquelle $b$ est le coefficient angulaire de la droite d'étalonnage ou le coefficient d'extinction spécifique défini dans l'introduction, et $a$ est annulé par le mode de mesure.

Dans les conditions définies précédemment, nous avons obtenu, sur une solution de cobalt, les valeurs suivantes pour $b$: 0.781, 0.815, 0.820, 0.809, 0.819, 0.784, 0.773, 0.763, 0.772 et 0.764 dont la moyenne est 0.790 et l'écart type 0.019.

La loi de Beer est vérifiée dans le domaine de concentration de 0.2–1.2 $\mu g\ ml^{-1}$.

Différents échantillons types d'acier, analysés par des manipulateurs différents ont conduit aux résultats du Tableau III.

## DOSAGE SPECTROPHOTOMÉTRIQUE DU COBALT

*Principe*

Après mise en solution de la prise d'essai à l'aide de mélanges d'acides appropriés, le cobalt peut être séparé, si nécessaire, du fer par extraction du chlorure et du nickel par échange sur résine anionique.

On forme ensuite le complexe cobalt–isonitrosomalonylguanidine, dont on mesure l'absorption.

*Domaine d'application*

La mesure est applicable aux quantités de cobalt comprises entre 10 et 500 $\mu g$, ce qui permet, en adaptant les prises d'essai et les dilutions, de doser des teneurs en cobalt comprises entre 0.010 et 25%.

On peut doser, sans séparation, les teneurs supérieures à 0.020% dans le fer pur et à 1.3% dans le nickel.

*Réactifs*

*Mélange acide de mise en solution.* Solution aqueuse de 300 ml acide perchlorique ($d = 1.67$) et 150 ml d'acide phosphorique ($d = 1.71$) $l^{-1}$.

*Mélange acide dilué.* Diluer 5 fois la solution ci-dessus (200 ml $l^{-1}$).

*Isonitrosomalonylguanidine* (2 $g\ l^{-1}$). Peser 2 g de réactif dans un bécher de 100 ml, ajouter un peu d'eau pour obtenir une pâte, puis 25 ml d'acide perchlorique ($d = 1.67$). Agiter pour dissoudre et diluer à un litre avec de l'eau distillée.

*Solution étalon de cobalt* (1 $g\ l^{-1}$). Dans un bécher de 250 ml, dissoudre 1 g de cobalt pur dans 80 ml d'acide chlorhydrique ($d = 1.19$) et 20 ml d'acide nitrique. Chauffer. Refroidir après dissolution et porter le volume à 1 l (en fiole jaugée). Cette solution est stable 3 mois. Les solutions plus diluées doivent être préparées le jour de l'emploi.

*Solution étalon de cobalt* (100 $mg\ l^{-1}$). Diluer 10 fois la solution à 1 g $l^{-1}$.

*Solution étalon de cobalt* (4 $mg\ l^{-1}$). 40 ml solution à 100 mg $l^{-1}$ cobalt + 200 ml mélange acide $l^{-1}$.

*Appareillage*

Colonne de verre pyrex: diamètre intérieur 10 mm; longueur 100 mm; munie

d'un robinet à voie droite de 2 mm permettant de régler l'écoulement de l'éluat. Pour régler aisément le débit de l'éluat on peut coiffer l'extrémité inférieure de la colonne d'un bout de tube de polythène convenablement étiré afin d'obtenir un débit de 1 ml $min^{-1}$. Le robinet est seulement utilisé pour le passage du liquide.

Introduire un tampon de laine de quartz ou de "chloro fibre Rovyl" que l'on tasse légèrement en bas de la colonne; puis la résine Dowex AG 1-X8 (100–200 mesh, forme $Cl^-$) en suspension dans l'eau (environ 4 ml de résine dans la colonne); enfin, un autre tampon sur la résine pour la maintenir en place.

*Mode opératoire*

*Prises d'essai*

1 g si la teneur présumée en cobalt est inférieure à 0.050%; 0.5 g si elle est inférieure à 0.5%; et 0.25 g si supérieure à 0.5%.

*Mise en solution*

(*a*) *Aucune séparation n'est nécessaire* (*Co* > 0.050% *et Ni* < *aux limites admissibles*). Introduire la prise d'essai dans une fiole conique de 250 ml à large ouverture. Ajouter 20 ml de mélange acide et 5 ml d'acide nitrique conc. ($d = 1.40$). (Les aciers dont la teneur en manganèse est supérieure à 1% sont dissous dans 6 ml d'acide perchlorique ($d = 1.67$) au lieu de 20 ml de mélange acide (afin d'éviter la formation du complexe violet entre les ions Mn(III) et $PO_4^{3-}$). L'acide phosphorique (3 ml pour 100 ml de solution A) est ajouté avant de compléter au volume.) Couvrir la fiole d'un verre de montre et chauffer. Si l'échantillon se dissout difficilement ajouter 10 ml d'acide chlorhydrique conc. ($d = 1.19$).

Après dissolution totale, retirer le verre de montre et poursuivre le chauffage jusqu'à fumées blanches, abondantes, remplissant la fiole. (A ce stade le chrome est oxydé en Cr(VI) et la solution prend une teinte orangée; si tel est le cas, ajouter goutte à goutte de l'acide chlorhydrique conc. pour éliminer le chrome sous forme de chlorure de chromyle et poursuivre le chauffage jusqu'à fumées blanches pour éliminer l'acide chlorhydrique.) Refroidir, ajouter 25 à 50 ml d'eau pour dissoudre les sels. Chauffer modérément si la dissolution est lente. Filtrer la silice si nécessaire puis transvaser en fiole de: 100 ml si la teneur présumée en cobalt est inférieure à 0.2%; 250 ml si la teneur présumée en cobalt est comprise entre 0.2 et 2% (ajouter 30 ml de mélange acide avant de compléter au volume); 500 ml si la teneur présumée en cobalt est supérieure à 2% (ajouter 80 ml de mélange acide). Amener au volume avec de l'eau distillée (solution A).

(*b*) *Une séparation est nécessaire.* Teneurs limites en nickel nécessitant une séparation:

| | | | |
|---|---|---|---|
| Prise d'essai: 1 g: | Ni supérieur à 1% | | |
| 0.5 g: | teneur en | Co < 0.2 | Ni > 4% |
| | | 0.2 < Co < 0.5% | Ni > 20% |
| 0.250 g: | | 0.5 < Co < 2 | Ni > 40% |
| | | 2 < Co < 10 | Ni > 80% |

Introduire la prise d'essai dans un bécher de 250 ml. Ajouter 20 ml d'acide chlorhydrique conc. et 5 ml d'acide nitrique conc. Couvrir d'un verre de montre et chauffer. Après dissolution complète, retirer le verre de montre et évaporer la solution à sec.

*Séparation du fer* ($Co < 0.050\%$)

Ajouter au résidu ci-dessus 10 ml d'acide chlorhydrique 9 $N$ (3+1). Chauffer légèrement jusqu'à dissolution des sels. Refroidir.

Introduire la solution dans une ampoule à séparation de 250 ml. Rincer le bécher avec 15 ml d'acide chlorhydrique 9 $N$ (3+1). Ajouter dans l'ampoule 25 ml d'éther isopropylique. Agiter pour extraire le fer, décanter, soutirer la phase aqueuse dans un bécher de 100 ml. Ajouter 5 ml d'acide chlorhydrique 9 $N$ (3+1) dans l'ampoule, agiter, décanter et soutirer la phase aqueuse dans le bécher de 100 ml contenant la première portion. Retirer la phase organique.

Ajouter 1 ml d'acide nitrique conc. au contenu du bécher et chauffer avec précaution pour chasser l'éther isopropylique, puis amener à siccité.

*Séparation du nickel*

Préparation des solutions à traiter. (*a*) Teneur en cobalt inférieure à 0.050%: pas de dilution avant échange. (*b*) Teneur en cobalt supérieure à 0.050%: les sels obtenus sont dissous dans 20 ml d'acide chlorhydrique ($d = 1.19$), puis introduits dans la fiole jaugée convenable, suivant la teneur en cobalt:

| *Teneur en cobalt* | *Volume de la fiole jaugée (ml)* | *Partie aliquote à séparer (ml)* |
|---|---|---|
| $0.05\% < Co < 0.2\%$ | 100 | 20 |
| $0.2\% < Co < 2\%$ | 250 | 25 |
| $2\% < Co < 4\%$ | 500 | 25 |
| $4\% < Co < 10\%$ | 500 | 10 |

Compléter au volume par de l'eau. La partie aliquote prélevée est évaporée à sec dans un bécher de 100 ml.

(1) *Fixation du cobalt.* Les résidus obtenus sont repris par 5 ml d'acide chlorhydrique 10 $N$ (5+1) (chauffer doucement si nécessaire), introduire la solution au sommet de la colonne (la résine doit être préalablement lavée avec 15 ml d'acide chlorhydrique 10 $N$ (5+1)). Le débit du liquite à échanger est réglé à 1 ml $min^{-1}$.

Après écoulement complet de la solution, rincer le bécher et la colonne avec 5 ml d'acide chlorhydrique 10 $N$ (5+1). Effectuer un second lavage avec 5 ml d'acide chlorhydrique 10 $N$ (5+1) pour éliminer la totalité du nickel dans l'effluent.

(2) *Elution du cobalt.* Pour éluer le cobalt, laver la résine avec 20 ml d'acide chlorhydrique 4 $N$ (1+2) que l'on introduit en 4 fois 5 ml, en laissant écouler la totalité de la solution entre chaque addition. L'éluat est recueilli dans un bécher de 100 ml. Un peu de fer est élué avec le cobalt (teinte jaune de l'éluat).

(3) *Régénération de la résine.* Eluer le fer restant, en lavant la résine avec 2 fois 25 ml d'acide chlorhydrique 0.5 $N$ (1+96), la rincer avec de l'eau distillée et enfin laver avec 15 ml d'acide chlorhydrique 10 $N$ (5+1).

*Préparation de la solution B (après séparation)*

Après séparation du fer: reprendre le résidu par 5 ml d'acide chlorhydrique 10 $N$ (5+1) et chauffer modérément si nécessaire jusqu'à dissolution. Ajouter 5 ml

d'acide perchlorique 7.2 *N* (3+2) puis chauffer jusqu'à fumées blanches. (L'emploi de l'acide perchlorique seul évite la formation de complexe entre le manganèse(III) et $PO_4^{3-}$).

Après séparation du nickel: ajouter 5 ml d'acide perchlorique 7.2 *N* puis chauffer jusqu'à fumées blanches.

Refroidir, ajouter 10 ml d'eau distillée après dissolution des perchlorates, ajouter 5 ml d'acide phosphorique 13.5 *N* (3+7). Introduire en fiole jaugée de 50 ml. Rincer le bécher et compléter au volume avec de l'eau distillée : on obtient une solution B.

*Mesure*

| *Teneur en cobalt* | *Volume de la solution A (ml)* | *Partie aliquote de mesure (ml)* |
|---|---|---|
| 0.05% < Co < 0.2% | 100 | 10 |
| 0.2% < Co < 2% | 250 | 5 |
| 2% < Co < 4% | 500 | 5 |
| 4% < Co < 10% | | |

Lorsque la teneur en cobalt est supérieure à 4% il est nécessaire de prévoir une dilution intermédiaire de 10 ml de solution A dans une fiole de 50 ml dans laquelle on a ajouté 5 ml de mélange acide ; cette nouvelle solution (B) sera utilisée ci dessous.

| *Teneur en cobalt* | *Volume de solution B (ml)* | *Partie aliquote de mesure (ml)* |
|---|---|---|
| Co < 0.2% | 50 | 20 |
| 0.2% < Co < 4% | 50 | 10 |
| 4% < Co < 10% | 50 | 5 |

*Dosage.* Prélever deux parties aliquotes de solution A (ou B), les introduire chacune dans une fiole jaugée de 100 ml et compléter à 25 ml si nécessaire avec du mélange acide dilué.

(i) Essai. Dans une des fioles jaugées de 100 ml introduire successivement en agitant, 10 ml de solution d'isonitrosomalonylguanidine, 10 ml de solution d'acétate d'ammonium (500 g $l^{-1}$), 20 ml de solution d'hydrogénophosphate d'ammonium (diammonique) (100 g $l^{-1}$), 10 ml d'acide perchlorique ($d = 1.67$). Compléter à 100 ml avec de l'eau distillée.

(ii) Témoin de teinte (il sert de référence et permet de compenser l'absorption des ions colorés). Dans la seconde fiole jaugée de 100 ml, introduire successivement en agitant, 10 ml de solution d'acétate d'ammonium (500 g $l^{-1}$), 20 ml de solution d'hydrogénophosphate d'ammonium (100 g $l^{-1}$), 10 ml d'acide perchlorique ($d = 1.67$). Compléter à 100 ml avec de l'eau distillée.

(iii) Mesurer la différence d'absorption entre l'essai et le témoin de teinte, 30 min après dilution au volume, à 370 nm, en cuve de 1 cm.

*Etalonnage*

Dans 6 fioles jaugées de 100 ml introduire:

0 5 10 15 20 25 ml de solution de cobalt à 4 mg $l^{-1}$,
25 20 15 10 5 0 ml de mélange acide dilué, soit
0 20 40 60 80 100 $\mu$g de cobalt.

Opérer selon (i)

Mesurer la différence d'absorption entre les différents termes et le terme 0 (témoin) à 370 nm, en cuve de 1 cm.

L'absorption du témoin (0) mesurée à 370 nm, en cuve de 1 cm, par rapport à l'eau est comprise entre 0.10 et 0.15. Il faut en tenir compte lors des mesures d'absorption du complexe.

*Expression des résultats*

La quantité de cobalt contenu dans la fiole de 100 ml est obtenue: soit en se rapportant à la droite d'étalonnage, soit par calcul à l'aide du coefficient d'extinction spécifique en tenant compte des dilutions et parties aliquotes employées.

TABLEAU IV

PRISES D'ESSAI RECOMMANDÉES EN FONCTION DES TENEURS EN COBALT ET EN NICKEL

| *Prise d'essai* (*g*) | *Teneur présumée en cobalt* | *Teneur au delà de laquelle le nickel est séparé* |
|---|---|---|
| 1 | Co < 0.050% | 1% |
| 0.5 | 0.05 < Co < 0.2% | 4% |
| | 0.2 < Co < 0.5% | 20% |
| 0.250 | 0.4 < Co < 2% | 40% |
| | Co > 2% | 80% |

RÉSUMÉ

Le dosage spectrophotométrique du cobalt dans les aciers, au moyen de l'isonitrosomalonylguanidine, a été reconsidéré. Son mode opératoire est étendu aux aciers à faible teneur en cobalt, et à ceux contenant des éléments d'alliage nécessitant une séparation. Le domaine des matériaux technologiques se trouve ainsi couvert, de 8% à moins de 0.01%.

SUMMARY

The spectrophotometric determination of cobalt in steels with isonitrosomalonylguanidine has been studied afresh, and the method has been extended to low cobalt steels and to those containing alloying elements in concentrations sufficiently high to necessitate their separation. The range of technological materials containing from 8% to below 0.01% is now covered.

ZUSAMMENFASSUNG

Das Prinzip der spektrophotometrischen Bestimmung von Kobalt in Stählen durch Isonitrosomalonylguanidin wurde erneut in Betracht gezogen. Der Verwendungsbereich des Verfahrens wurde auf Stähle mit niedrigem Kobaltgehalt ausge-

dehnt, sowie auch auf Stähle, die einen solchen Gehalt an Legierungsbestandteilen aufweisen, dass ein Trennungsverfahren unbedingt erforderlich ist. So ist es möglich den Kobaltgehalt der, zu technologischen Zwecken, hergestellten Legierungen, in einem Bereich zwischen 8 % und weniger als 0.01 % zu bestimmen.

BIBLIOGRAPHIE

1 H. GOTO ET J. I. KOBAYASHI, *Sci. Rept. Res. Inst. Tohoku Univ.*, A6 (1954) 551.
2 M. NAMIKI, Y. KAKITA ET H. GOTO, *Sci. Rept. Res. Inst. Tohoku Univ.*, A 14 (1962) 309.
3 S. TRIBALAT ET C. ZELLER, *Bull. Soc. Chim. France*, (1962) 2041.
4 H. E. AFFSPRUNG, N. A. BARNES ET H. A. POTRAZ, *Anal. Chem.*, 23 (1951) 1680.
5 E. SUDO, *Sci. Rept. Res. Inst. Tohoku Univ.*, A6 (1954) 324.
6 A. K. BABKO ET V. N. DANILOVA, *Zavodsk. Lab.*, 30 (1964) 1198.
7 A. ALEXANDOV, P. VASSILEVA-ALEXANDROVA ET E. KOVATCHOVA, *Mikrochim. Acta*, 3 (1967) 579.
8 J. SCHERZER ET V. RONA, *Rev. Chim. (Bucharest)*, 11 (1960) 712.
9 K. C. TRIKHA, M. KATYAL ET R. P. SINGH, *Talanta*, 14 (1967) 977.
10 B.I.S.R.A., *J. Iron Steel Inst. (London)*, 176 (1954) 63.
11 K. H. KOCH, K. OHLS, E. SEBASTIANI ET G. RIEMER, *Z. Anal. Chem.*, 312 (1970) 307.
12 K. L. CHENG ET R. H. BRAY, *Anal. Chem.*, 27 (1955) 782.
13 M. I. ZABOEVA, G. N. ZUS ET M. P. DOROFEEVA, *Zavodsk. Lab.*, 35 (1969) 1158.
14 N. N. BASARGIN, A. V. KADOMTSEVA ET V. I. PETRASHEN, *Zavodsk. Lab.*, 35 (1969) 16.
15 E. B. SANDELL, *Colorimetric Determination of Traces of Metals*, 3ème Edn., Interscience, New York, 1959, p. 415.
16 M. JEAN, *Anal. Chim. Acta*, 6 (1952) 278.
17 P. DE GÉLIS, *Circulaire d'Informations Techniques du Centre de Documentation de la Sidérurgie*, 1969, no. 5, p. 1303.

*Analytica Chimica Acta*
Elsevier Publishing Company, Amsterdam
Printed in The Netherlands



# SPECTROPHOTOMETRIC DETERMINATION OF SMALL AMOUNTS OF NITRATE AND NITRITE BY CONVERSION TO NITROTOLUENE AND EXTRACTION INTO TOLUENE

M. K. BHATTY AND A. TOWNSHEND
*Chemistry Department, Birmingham University, P.O. Box 363, Birmingham B15 2TT (England)*
(Received 30th March 1971)

The determination of small amounts of nitrate has always been a particularly difficult problem for the analytical chemist. Only spectrophotometric methods seem to have been generally used for this purpose, and even the best of these methods suffer from certain disadvantages. Those procedures based on the nitration of organic compounds are often experimentally difficult, requiring reaction with a solid nitrate sample (*e.g.* the phenol-2,4-disulphonic acid procedure[1]), or distillation of the nitro compound (the 2,4-xylenol procedure[1]). Even the chromotropic acid method[2,3], in which nitration proceeds smoothly in aqueous solution, is subject to serious interference from bromate, bromide, titanium and nitrite. The method which uses the oxidizing action of nitrate to give a yellow oxidation product of brucine[1], gives variable day-to-day colour development and does not give linear calibration plots at the wavelength of maximal absorbance. The determination of nitrate by measurement of its absorbance at 210 nm is rapid and simple[4], but is subject to interference by the numerous other species that absorb at this wavelength. The extraction methods utilizing crystal violet[5], Nile Blue A[6] and tetraphenylphosphonium chloride[7] are also subject to various interferences.

In the present paper, a novel method for the spectrophotometric determination of small amounts of nitrate is described. It is based on the rapid nitration of toluene by nitrate in 56% (v/v) sulphuric acid, and subsequent extraction of the nitrotoluene into the residual toluene, as a molecular complex between the two species. This complex has an absorbance maximum at 284 nm, which is quite distinct from that of either single component, and which can be monitored to give a measure of the original nitrate concentration. The few interferences are easily eliminated. The method can be extended to the determination of nitrite or of nitrite–nitrate mixtures simply by oxidizing nitrite to nitrate with bromine water.

## EXPERIMENTAL

All inorganic reagents used were of analytical-reagent or microanalytical-reagent grade.

### *Standardization procedure for nitrate*

To each of a series of 25-ml volumetric flasks transfer 1–5 ml aliquots of a $0.3 \cdot 10^{-3}$ *M* sodium nitrate solution, and make up to 5 ml with distilled water. Add

5 ml of toluene and 15 ml of (3 + 1) sulphuric acid. Shake the stoppered flasks, covered by paper or other material to reduce heat losses, for 5 min, and allow to cool to room temperature. Measure the absorbance of each toluene layer at 284 nm in stoppered silica 1-cm cells against that of a blank extract. Construct a calibration graph.

*Determination of nitrate* (1–18 *p.p.m.*)

Take 5 ml of test solution, and treat as in the standardization procedure. If it is necessary to remove interfering species, this should be done in the following sequence:

*Nitrite.* Add 0.1 g of urea to the 5 ml of test solution, followed by 0.1 g of sodium carbonate. Heat to boiling. (Alternatively, allow to stand at room temperature for 8 h.) Cool before proceeding further.

*Bromide, iodide, thiocyanate.* Add 0.1 g of silver sulphate. When the precipitate has coagulated (10 min), add the toluene, etc.; there is no need to filter off the precipitate.

*Sulphite.* Shake the toluene extract with 1 ml of 10 % sodium carbonate solution before measuring the absorbance of the toluene.

*Mercury(II).* Shake the toluene extract for 5 min with 1 ml of 10 % sulphuric acid containing 0.1 g of EDTA (acid form) before measuring the absorbance of the toluene.

*Determination of nitrite* (0.8–14 *p.p.m.*)

Transfer an aliquot of test solution (4.8 ml) to a 25-ml volumetric flask. Add 0.1 ml of saturated bromine water, followed after 5 min by 0.1 ml of 90 % formic acid. When the excess of bromine has been destroyed, add 0.1 g of silver sulphate. When the precipitate has coagulated, determine the nitrate as described above. From the concentration of nitrate measured, calculate the original nitrite concentration.

*Determination of nitrite and nitrate in admixture*

Determine nitrate alone on a 5-ml portion of test solution, using the procedure described above to destroy nitrite.

On a second aliquot (containing less than $1.5 \cdot 10^{-6}$ moles of nitrite plus nitrate), oxidize the nitrite to nitrate as described above, and measure the total nitrate concentration. Ascertain the nitrite concentration by difference.

## RESULTS AND DISCUSSION

Mononitrotoluenes, dissolved in isooctane, show well-defined absorbance peaks with maxima at 207 and 250 nm. When dissolved in toluene, however, it was found that all three mononitrotoluenes give a single strong absorption peaking at 284 nm. (Owing to the high absorbance of the solvent at lower wavelengths, the spectrophotometer gives a plateau at such wavelengths, often extending to 283 nm.) It is well-known that aromatic nitro compounds are good $\pi$-acceptors, whereas aromatic hydrocarbons act as $\pi$-donors. Thus it is probable that toluene and the nitrotoluenes interact to form a molecular or "charge-transfer" complex, in which the spectral properties of the acceptor nitrotoluene molecules are modified quite considerably. The absorbances of the molecular complexes of sulphur dioxide and iodine with aromatic hydrocarbon donors have previously been used as a measure of sulphur

dioxide[8] and iodine[9] concentration. In the work described here, it was shown that nitrate may be determined by its nitration of toluene followed by extraction of the nitrotoluene into toluene.

*Reaction conditions*

The extent and speed of nitration were dependent on the acidity and temperature. At 25°, no nitration was observed in 11 or 38% (v/v) sulphuric acid, and incomplete reaction in 56 or 75% sulphuric acid, for a 5-min reaction of 62 μg of nitrate in 20 ml of the acid. In order to carry out experiments at 25°, the solutions had to be cooled after mixing with the strong sulphuric acid. It was found, however, that if an attempt was made to retain the heat of mixing, nitration proceeded more readily. Best reaction times were achieved with (3 + 1) sulphuric acid; the reaction temperature was

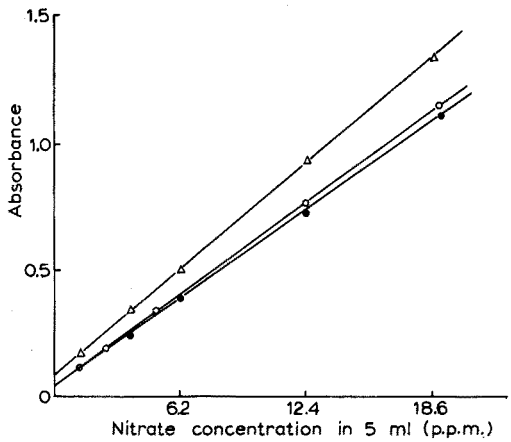


Fig. 1. Absorbance of toluene extracts for nitrate from 56% $H_2SO_4$ at 25° (●) and 70° (△) and from 75% $H_2SO_4$ at 25° (○).

TABLE I

RELATIVE ABSORBANCES FOR VARIOUS NITRATION AND MOLECULAR COMPLEX FORMATION SYSTEMS WITH 62 μg OF NITRATE IN 56% (v/v) SULPHURIC ACID (20 ml)

| *System* | *Wavelength of maximum absorbance (nm)* | *Absorbance after reaction at* | |
|---|---|---|---|
| | | 25° | 70° |
| Benzene | 278 | 0.52 | 0.98 |
| Toluene | 284 | 0.72 | 0.93 |
| *o*-Xylene | 287 | 0.63 | 0.88 |
| *m*-Xylene | 288 | 0.68 | 0.75 |
| *p*-Xylene | 292 | 0.30 | 0.41 |
| Cyclohexene | 310 | — | 0.07 |
| Phenol, 1% (w/v) in isooctane | 347 | 0.20 | 0.30 |
| | 284 | 0.21 | 0.27 |
| Phenol, 1% (w/v) in toluene | 352 | 0.35 | — |
| | 287 | 0.74 | — |

65–70°, with a final acid concentration of 56% (v/v). A hot 75% acid solution gave low recoveries, and the aqueous phase turned yellow on addition of the toluene. A comparison of calibration graphs at various acidities and temperatures is given in Fig. 1.

A number of common aromatic compounds were examined as alternatives to toluene. The spectral characteristics, after reaction at 25° and *ca.* 70° are given in Table I. In all instances, absorbances were higher after reaction at 70° than at 25°, although there was only a small difference for *m*-xylene. Benzene gave the greatest absorbance, but toluene is to be preferred because of its lower volatility and lesser toxicity. Phenol, although usually readily nitrated, gave only small absorbances; when phenol was dissolved in toluene, the spectral data indicate that the toluene was preferentially nitrated. The low absorbance obtained when *p*-xylene was used is probably a direct reflection of the difficulty of nitration.

As shown in Fig. 1, the nitrate calibration graph is a straight line for 1–18 p.p.m. in the original 5 ml of test solution, with recoveries decreasing at higher concentrations. The apparent molar absorptivity in the organic phase is 4,200 l $mol^{-1}$ $cm^{-1}$. A comparison with values calculated or quoted for other procedures for nitrate is given in Table II. Results for the determination of 12.4 p.p.m. of nitrate showed a maximal deviation of $\pm 2\%$ (6 results).

TABLE II

APPARENT MOLAR ABSORPTIVITIES OF METHODS FOR NITRATE DETERMINATION

| *Reagent* | *Apparent molar absorptivity* ($l\ mol^{-1}\ cm^{-1}$) | *Reference* |
|---|---|---|
| Brucine | 1,500 | 1 |
| Phenol-2,4-disulphonic acid | 10,000 | 1 |
| Chromotropic acid | 18,000 (?)[b] | 2 |
| Mineral acid[a] | 9,000 | 4 |
| Nile blue | 3,100 | 6 |
| Tetraphenylphosphonium chloride | 2,240 | 7 |
| Present method | 4,200 | |

[a] Direct u.v. measurement.
[b] Assuming 1-cm cells were used.

*Interferences*

Most spectrophotometric methods for nitrate suffer from many interferences. In the present method, only nitrite, sulphite, iodide, bromide, thiocyanate and mercury(II) interfered, out of a large number of common species tested (Table III). Iodide, bromide and thiocyanate, which not only gave absorbing toluene extracts but caused reduction of nitrate were readily removed by precipitation from the test solution with silver sulphate. Complete precipitation occurred within 10 min. Sulphite, which extracts as a molecular complex of sulphur dioxide with toluene[8], is rapidly back-extracted into a sodium carbonate solution. Mercury(II) (added as its chloride), the only interfering metal ion, appears to extract as a halide complex[8]. It may be back-extracted into an acidic EDTA solution. The extraction is a little slow, but is complete after shaking for 5 min.

TABLE III

EFFECT OF DIVERSE IONS[a]

| *Ion*[b] | *Absorbance* | *Absorbance after treatment to eliminate interference (see text)* |
|---|---|---|
| — | 0.93 | 0.93 |
| $NO_2^-$ | 1.56 | 0.95[c] |
| | | 1.8[d] |
| $SO_3^{2-}$ | 1.20 | 0.91 |
| $Br^-$ | 0.40 | 0.93 |
| $I^-$ | >2.0 | 0.93 |
| $SCN^-$ | 1.00 | 0.94 |
| $Hg^{2+}$ | 1.40 | 0.94 |

[a] Acetate, $CO_3^{2-}$, $F^-$, $Cl^-$, $CN^-$, $S^{2-}$, $SO_4^{2-}$, $PO_4^{3-}$, $ClO_4^-$, $Ag^+$, $Cu^{2+}$, $Cd^{2+}$, $Zn^{2+}$, $Pb^{2+}$, $Fe^{3+}$, $Co^{2+}$, $Ni^{2+}$, $Mn^{2+}$ and $Cr^{3+}$ all gave absorbances of 0.92–0.95.
[b] Ten-fold molar concentration compared to nitrate.
[c] Urea treatment.
[d] Sulphamic acid treatment.

Nitrite interferes in almost all spectrophotometric methods for nitrate, and the present method is no exception. However, it is readily removed from the test solution by heating with urea and sodium carbonate. If no heating is used, complete destruction takes about 8 h. Sodium azide and cystine, when used to destroy nitrite, instead lead to absorbances somewhat greater than that obtained from the equivalent amount of nitrate. Sulphamic acid causes even greater absorbances, when used for this purpose (Table III).

*Determination of nitrite*

It is also possible to adapt the nitrate method to the determination of nitrite after oxidation to nitrate. Several oxidants were investigated for this purpose, including bromine, hydrogen peroxide, ammonium persulphate and potassium permanganate. Removal of the excess of these oxidants was necessary, otherwise higher results were usually obtained. Since an excess of bromine was most easily removed, this oxidant was employed. Bromine rapidly oxidized nitrite, and the excess of bromine was destroyed simply by the addition of formic acid. Bromide was then precipitated by silver sulphate before the nitration procedure was carried out. The calibration graph obtained in this way was identical to that obtained by the procedure for the determination of nitrate.

The determination of nitrate and nitrite in one sample is also possible. The nitrate is determined on one aliquot after destruction of nitrite with urea; nitrite is oxidized to nitrate in another aliquot, and the total nitrate concentration determined. A 5-ml solution containing 31 $\mu$g of nitrate and 23 $\mu$g of nitrite gave quantitative recoveries of both ions.

## CONCLUSIONS

The method described above is specific for the determination of microgram amounts of nitrate. It is simple to carry out, requires minimal pretreatment of the sample, and takes only a few minutes. No expensive reagents are required, and there

are no problems of reagent purity or instability. The method can be extended to the determination of nitrite and nitrate–nitrite mixtures, and should be widely applicable to determinations in numerous matrices.

The authors thank Professor R. Belcher for his interest and encouragement. M. K. B. thanks the Chemistry Department, Birmingham University, for the provision of research facilities, the Government of Pakistan and the P.C.S.I.R. for leave of absence, and the Nuffield Foundation for the award of a fellowship.

SUMMARY

Nitrate (1–18 p.p.m. in 5 ml of aqueous solution) is determined by conversion to nitrotoluene in 56% sulphuric acid at 70°, and extraction into toluene of a molecular complex of nitrotoluene with that solvent, followed by measurement of the absorbance of the complex at 284 nm. The few interferences ($NO_2^-$, $Br^-$, $I^-$, $SCN^-$, $SO_3^{2-}$ and $Hg^{2+}$) are easily eliminated. Nitrite (0.8–14 p.p.m.) may also be determined, after oxidation to nitrate with bromine water. The method takes only a few minutes.

RÉSUMÉ

On propose un dosage de nitrate (1–18 p.p.m. dans 5 ml de solution aqueuse) par transformation en nitrotoluène et extraction dans le toluène; on mesure finalement l'absorption du complexe moléculaire formé à 284 nm. Les quelques interférences ($NO_2^-$, $Br^-$, $I^-$, $SCN^-$, $SO_3^{2-}$ et $Hg^{2+}$) sont facilement éliminées. Les nitrites (0.8–14 p.p.m.) peuvent être également dosés après oxydation en nitrate par l'eau de brome. Cette méthode est rapide et ne prend que quelques minutes.

ZUSAMMENFASSUNG

Nitrat (1–18 p.p.m. in 5 ml wässriger Lösung) wird bestimmt, indem es in 56%iger Schwefelsäure bei 70° zu Nitrotoluol umgesetzt, dieses als Molekülkomplex mit Toluol extrahiert und die Extinktion des Komplexes bei 284 nm gemessen wird. Die geringen Störungen ($NO_2^-$, $Br^-$, $J^-$, $SCN^-$, $SO_3^{2-}$ und $Hg^{2+}$) werden leicht eliminiert. Nitrit (0.8–14 p.p.m.) kann nach Oxydation zum Nitrat mit Bromwasser ebenfalls bestimmt werden. Die Ausführung dauert nur wenige Minuten.

REFERENCES

1 See M. J. TARAS, in D. F. BOLTZ, *Colorimetric Determination of Non-Metals*, Interscience, New York, 1958, pp. 135–152.
2 P. W. WEST AND G. L. LYLES, *Anal. Chim. Acta*, 23 (1960) 227.
3 J. J. BATTEN, *Anal. Chem.*, 36 (1964) 939.
4 R. BASTIAN, R. WEBERLING AND F. PALILLA, *Anal. Chem.*, 29 (1957) 1795.
5 Y. YAMAMOTO, S. UCHIKAWA AND K. AKABORI, *Bull. Chem. Soc. Japan*, 37 (1964) 1718.
6 G. POKORNY AND W. LIKUSSAR, *Anal. Chim. Acta*, 42 (1968) 253.
7 D. T. BURNS, A. G. FOGG AND A. WILLCOX, *Mikrochim. Acta*, (1971) in press.
8 M. K. BHATTY AND A. TOWNSHEND, *Anal. Chim. Acta*, (1971) in press.
9 T. C. J. OVENSTON AND W. T. REES, *Anal. Chim. Acta*, 5 (1951) 123.

*Analytica Chimica Acta*
Elsevier Publishing Company, Amsterdam
Printed in The Netherlands



# INSTRUMENTAL NEUTRON ACTIVATION ANALYSIS OF ROCKS WITH A LOW-ENERGY PHOTON DETECTOR

J. HERTOGEN* AND R. GIJBELS**
*Institute for Nuclear Sciences, State University, Ghent (Belgium)*
(Received 1st April 1971)

A general feature of the Ge(Li) $\gamma$-spectra of neutron irradiated silicate rocks, taken a few days or more after the irradiation, is the high peak density in the energy region below 400 keV. Multiple spectral interferences then often prevent the optimal acquisition of information, owing to the propagation of errors in correcting the data. This is especially inconvenient for radionuclides which only have useful $\gamma$-rays in this energy region.

When small ultra-high resolution Ge(Li) detectors became available, one could expect that some results of the instrumental neutron activation analysis (i.n.a.a.) technique in this field would improve considerably[1]. Preliminary results for rocks with a "low-energy photon detector" having a FWHM of 0.75 keV at the 122.0 keV peak of $^{57}$Co were reported by Dran *et al.*[2]. Zielinsky and Frey[3] determined rare earth element abundances in volcanic rocks with this detector after a chemical group separation, whereas Zoller and Gordon[4] used it for atmospheric pollutants. De Bruin and Korthoven[5] discussed the determination of palladium in platinum with a similar detector. In a recent article, Rosenberg and Wiik[6] discussed the i.n.a.a. of eleven lanthanide elements in lunar samples, using such a planar X-ray detector with a FWHM of 0.95 keV at the 63 keV peak of $^{169}$Yb.

The purpose of the present work was to establish the usefulness of a low-energy photon detector of high resolution in the quantitative analysis of silicate rocks. Some peculiarities of the spectra obtained are pointed out, with special emphasis on spectral interferences in comparison with conventional Ge(Li) detectors. The problem of reproducible counting geometry and photon attenuation is also considered.

## *Detector and electronics*

The detector used in this work was a low-energy photon detector, Ortec Model 8013-10425. This low-capacitance planar Ge(Li) detector has an active diameter of 10 mm, a sensitive depth of 5 mm and an active volume of *ca.* 0.4 cm$^3$. The insensitive layer at the radiation incident face was removed and the intrinsic region covered with a gold electrode of 10–20 nm thickness. This results in an essentially "windowless" detector. The frontal face of the detector housing consists of a thin beryllium window (0.13 mm) at a distance of 5 mm from the diode. A similar detector

* Navorsingsstagiair of the NFWO.
** Research Associate of the IIKW.

and its characteristics have been described in detail by Palms *et al.*[7].

Further stages in the measuring chain were: a cooled FET Ortec Model 117 preamplifier, an Ortec Model 450 research amplifier (2.0-$\mu$sec differentiating and integrating time constants) and an Intertechnique DIDAC 4000-channel analyzer.

One has to avoid the presence of high-Z material near the detector, otherwise the $\gamma$-spectra could be complicated by fluorescent X-rays. For example, intense Ba-K X-ray fluorescent radiation is observed when glass counting vials are used. Hence, the detector was not shielded. The plexiglass sample holder was attached directly to the detector housing in order to have a strict control over the counting geometry.

*Detector efficiency and system resolution*

For the absolute detection efficiency calibration of the detector (see Fig. 1) a set of sources was counted. It is perhaps more convenient to use one or two single radionuclides with $\gamma$-rays covering the whole energy region of interest, both for routine energy calibration and for relative detection efficiency calibration. Precision

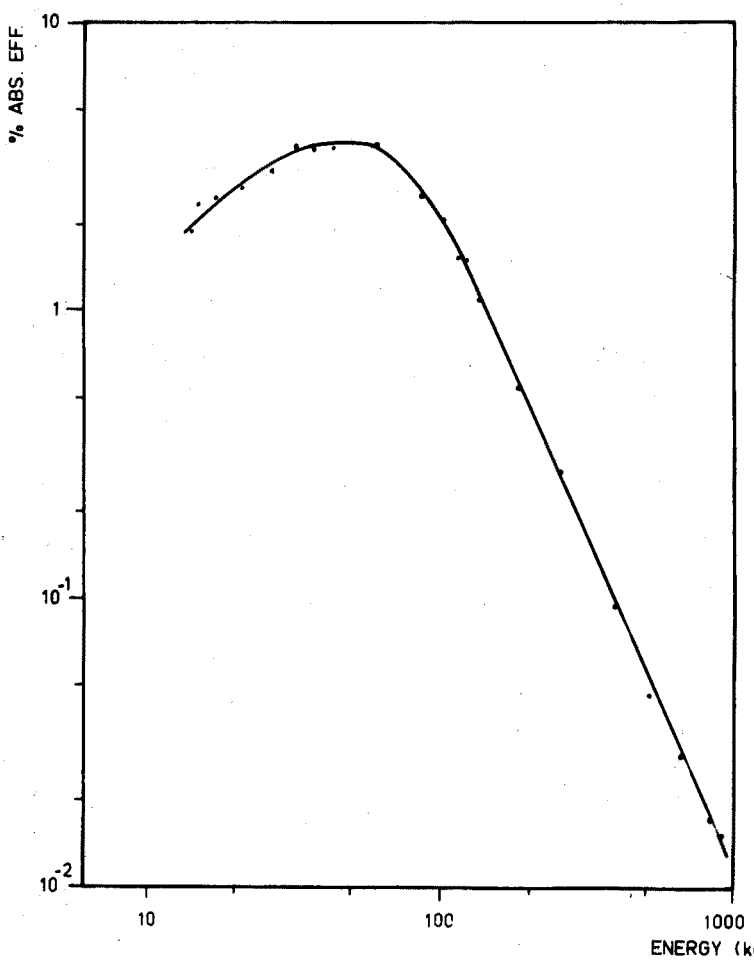


Fig. 1. Absolute photo-peak efficiency of the low-energy photon detector, measured with calibrated I.A.E.A. sources at a distance of 10 mm above the detector surface[8].

data of $\gamma$-ray energies and of their relative intensities have been reported for radionuclides such as $^{75}Se$[9], $^{133}Ba$[10] and $^{182}Ta$[11-13], which are very suitable for the low-energy region.

The resolution as a function of the photon energy is given in Table I. As the resolution is also determined by the electronic circuitry, the measurements were performed in nearly the same experimental conditions as for the actual sample countings, *i.e.* 2.0 $\mu$sec amplifier time constants, a maximum amplifier output voltage of 10 V and an analog-to-digital conversion slope of 10 V for 4000 channels. The counting rate was kept low and the base line restorer was operated in the "Low" position.

The following points are closely related to the resolution and the efficiency.

*The peak-to-background ratio.* The usefulness of low-energy peaks in conventional Ge(Li) spectra is limited because the peaks are superimposed upon high Compton and Bremsstrahlung continua. This often results in rather poor counting statistics and occasionally introduces errors in the peak area determination. In spectra obtained with low-energy photon detectors, several factors enhance the peak-to-background ratio appreciably. First, there is the overall effect of peak-width narrowing caused by the much better resolution. The beryllium window also markedly lowers the absorption of soft $\gamma$-rays in the detector housing. Moreover, the detection yield for high-energy $\gamma$-rays is very low. One can calculate that 81% of a parallel beam of 500-keV $\gamma$-rays, perpendicular to the detector surface, are not detected with the 5-mm thick detector. For a 50-mm long double open-ended coaxial detector this figure drops to 12%. The same calculation for 1-MeV $\gamma$-rays gives, respectively, 86% and 22%.

Table II lists the results of an experiment in which sources of $^{241}Am$, $^{57}Co$ (both in the presence of a $^{137}Cs$ source) and of $^{75}Se$ were counted, once with the low-energy photon detector and once with a 40-cm$^3$ coaxial Ge(Li) detector (resolution 2.2 keV at 1333 keV).

TABLE I

SYSTEM RESOLUTION *vs.* ENERGY

| | *Energy (keV)* | *FWHM (eV)* | *Gain (keV/chan.)* |
|---|---|---|---|
| $^{57}Co$ | 14.4 | 285 | 0.10 |
| $^{241}Am$ | 26.4 | 318 | — |
| $^{241}Am$ | 59.5 | 403 | — |
| Au-K$\alpha$1 | 68.8 | 434 | — |
| $^{182}Ta$ | 100.1 | 460 | — |
| $^{57}Co$ | 122.0 | 507 | — |
| $^{75}Se$ | 135.9 | 543 | — |
| $^{182}Ta$ | 179.4 | 630 | — |
| $^{75}Se$ | 264.3 | 760 | — |
| $^{113m}In$ | 391.4 | 868 | — |
| $^{137}Cs$ | 661.8 | 1102 | 0.20 |
| $^{54}Mn$ | 834.8 | 1376 | 0.37 |
| $^{60}Co$ | 1173.1 | 1533 | — |
| $^{60}Co$ | 1332.4 | 1690 | — |

TABLE II

PEAK-TO-BACKGROUND RATIO FOR SMALL AND LARGE DETECTORS

| *Peak counted* | *(keV)* | *Peak-to-background ratio* | |
|---|---|---|---|
| | | *Low-energy photon detector (0.10 keV/chan.)* | *40 cm³ Ge(Li) (0.25 keV/chan.)* |
| $^{241}Am^{a}$ | 59.5 | 48.7 | 2.8 |
| $^{57}Co^{a}$ | 121.9 | 57.8 | 11.9 |
| | 136.3 | 14.8 | 4.6 |
| $^{75}Se$ | 121.0 | 13.6 | 2.3 |
| | 135.9 | 30.3 | 9.9 |

[a] In the presence of a $^{137}Cs$ source.

*The energy range covered.* As a rule one can assume that for an optimal computer reduction of the γ-spectra, it is required that at least five channels span one FWHM[14]. If this criterion is applied to a peak at 100 keV in the actual experimental conditions, *i.e.* 0.460 keV FWHM at 100 keV and a 4000-channels memory, this implies that approximately only the region from 0 to 400 keV can be measured. However, the fast decrease in the efficiency makes this limitation rather insignificant for the i.n.a.a. of rocks. Above 400 keV only the useful $^{140}La$ (486.8 keV) and the $^{181}Hf$ (482.2 keV) lines are thus "lost".

*Ge–K X-ray escape and Au–K X-ray fluorescence phenomena*

*Ge–K X-ray escape peaks.* In spectra obtained with the small detector, intense lines are accompanied by small peaks about 10 keV lower, owing to the Ge–K X-ray escape effect (Kα: 9.9 keV; Kβ: 11.0 keV). The escape peak ratio has been measured previously by Palms *et al.*[7] (up to 60 keV) and by Ungrin and Johns[15] (from 40 keV to 411 keV) for "windowless" detectors of a smaller size than the one used here. Ungrin and Johns explained the occurrence of escape peaks in terms of the absence of an insensitive front layer. They also derived a theoretical expression for the escape peak ratio, which is a good fit to the experimental points. Some numerical values are summarized in Table III. From this one can conclude that the escape phenomenon may present problems when X-rays are used for quantitative determinations.

TABLE III

Ge–K X-RAY ESCAPE PEAK EFFICIENCIES

| *Energy (keV)* | | *Escape peak area/photo-peak area* | |
|---|---|---|---|
| | | *Present work* | *Palms et al.*[7] |
| In-Kα | 24.1 | 0.0527 | 0.0580 |
| In-Kβ | 27.5 | 0.0341 | 0.0302 |
| Ba-Kα | 32.0 | 0.0228 | 0.0213 |
| $^{241}Am$ | 59.5 | 0.0054 | 0.0050 |
| $^{57}Co$ | 121.9 | 0.0015 | 0.0014[a] |

[a] Predicted by Ungrin and Johns[15].

TABLE IV

Au–K X-RAY FLUORESCENCE EFFECT

| *Sample* | *Cooling time (d)* | *Au-Kα1 (counts/h)* |
|---|---|---|
| G-2 | 7 | *ca.* 4000 |
| G-2 | 20 | *ca.* 500 |
| Trachyte | 25 | *ca.* 1500 |
| BCR-1 | 33 | *ca.* 550 |

*Au–K X-ray fluorescence.* The Au–K X-rays appeared in all the spectra obtained with the small detector (Kα2 : 66.98 keV ; Kα1 : 68.79 keV ; Kβ′1 : 77.97 keV ; Kβ′2 : 80.17 keV). This is a result of the excitation of the gold-electrode atoms by intense β-emitters or by γ-rays with energies near the K absorption edge. They interfere seriously with some photopeaks of $^{182}$Ta (67.7 keV), $^{153}$Gd (69.6 keV), $^{153}$Sm (69.6 keV) and it is rather difficult to correct for their contribution. The data of Table IV give an idea about the amount of this effect for the experimental conditions used in this work (see *Spectral interferences*).

*Sample mounting*

As expected, these small detectors are very sensitive to geometry parameters. The change in efficiency of the detector was measured while a source was moved along the central axis of the detector housing and in a plane at *ca.* 5 mm above the beryllium window, *i.e.* the usual counting position. A solution of $^{182}$Ta in a vial of the same size as the actual samples (see below) was counted in this experiment. The vertical source to detector distance is highly critical as can be seen from Fig. 2. The data of Fig. 3 correspond to two directions, perpendicular to each other. The asymmetrical and slightly distorted pattern of Fig. 3 is presumably due to a non-axial detector mounting.

Whereas counting geometry is a general problem in γ-ray spectrometry, self-absorption effects need special attention when low-energy photons are measured. If one uses an appropriate standard rock as monitor, it is permissible to neglect the differences in attenuation between monitor and samples, insofar as they are due to compositional variations. The variations in density, however, create problems that are less easily avoided.

Hence, there is a need to obtain sources of the same geometrical shape and the same density, irrespective of their specific volume. In this work the problem was solved by pressing equal amounts of a mixture of graphite and rock powder into pellets of identical dimensions (diameter: 12.7 mm, thickness: 4.5 mm). A hydraulic press (Applied Research Laboratories) was modified so as to obtain pellets of constant thickness. The pressure used was 8,000 p.s.i. Graphite was chosen as binder as it is available in very pure quality. Moreover, it has two additional advantages: it lowers the differences in "bulk composition" and it acts as a lubricant in the pressing procedure. After rock fragments had been ground in an agate mortar, 1 g of the powdered sample and 0.3 g of graphite (Pechiney, "Poudre Pastillable") were homogenized in a polyethylene vial with a Turbula mixer (System Schatz, type T2A). A plexiglass sphere

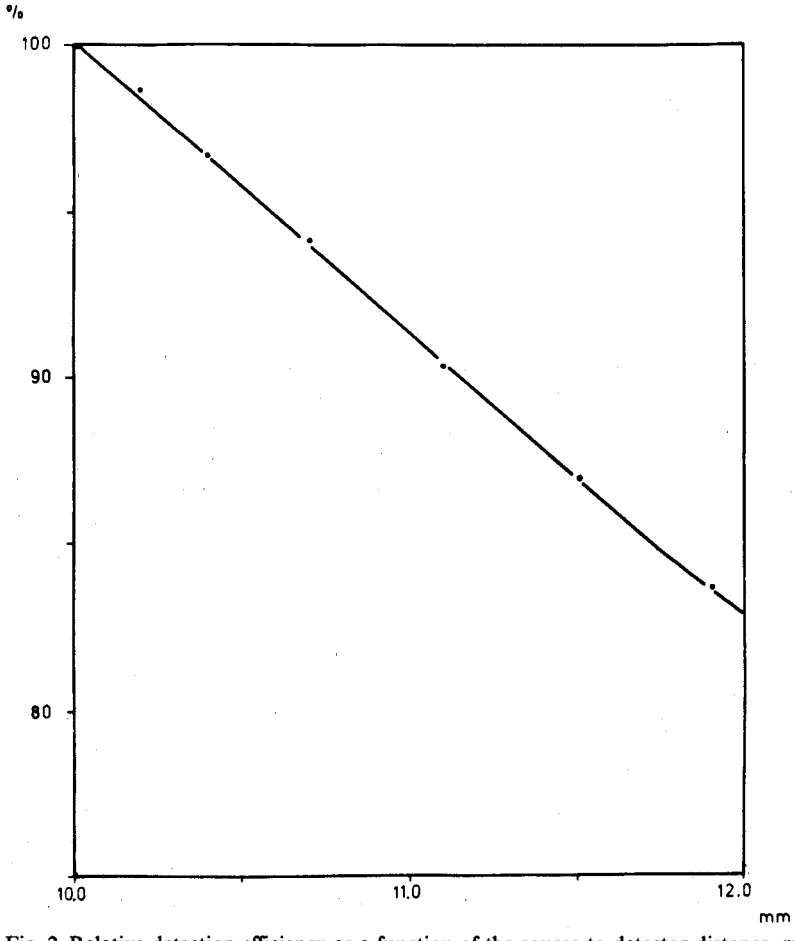


Fig. 2. Relative detection efficiency as a function of the source-to-detector distance, measured along the detector axis.

was added to avoid clustering of the mixture. Some problems did arise here regarding the inner shape of the vials. A cylindrical one appeared not to be ideal, for a fraction of the powder was trapped in the edges. After being weighed, the pellets were tightly sealed in a Mylar foil. This was achieved by gently pressing the foil and the pellet into a well in a heated copper block. When prepared in this way, the pellets could easily be handled after the irradiation and counting vials became superfluous.

The advantages of this pelletizing technique are obvious, but it is also a potential source of systematic errors. Heterogeneities in the mixture of rock powder and graphite have to be avoided by choosing appropriate mixing conditions. As pointed out in a review article of Stakheev and Kuznetsov[16], this problem is quite complex. The optimal mixing time turns out to be a function of the actual experimental conditions, such as the particle size, the cohesion properties and the relative amounts of the mixture components, the form of the container, the type of mixer, etc. It is,

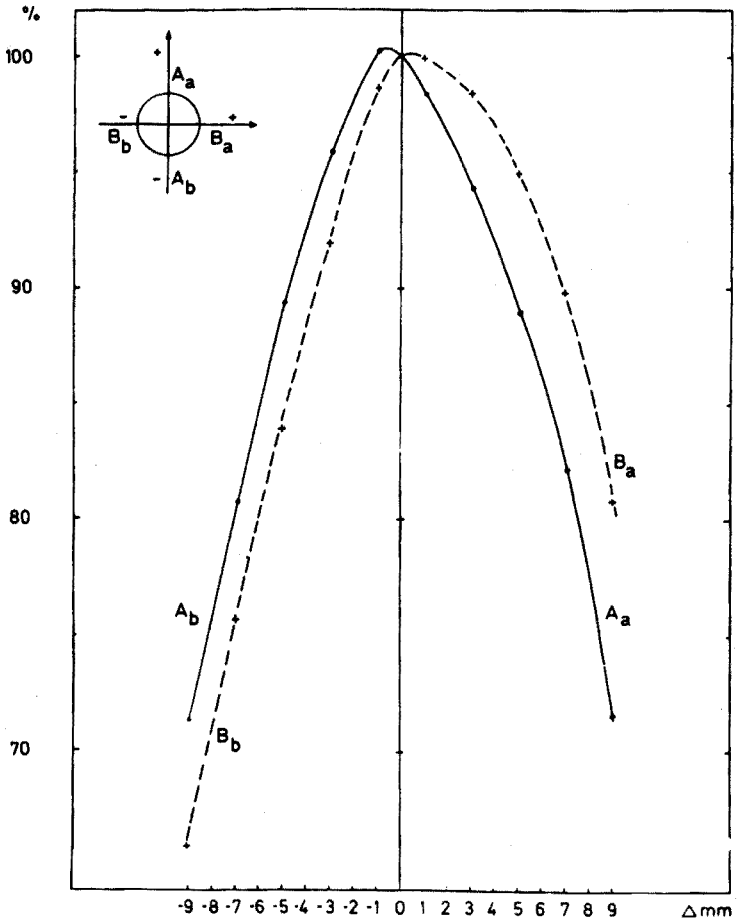


Fig. 3. Relative change of the detection efficiency for lateral deplacements of a source with respect to the central axis (measured in a plane at 10 mm above the detector surface).

however, almost impossible to establish the optimal mixing time for such complex material as silicate rocks and for each particular sample. Thus a rather arbitrary mixing time of 4 h was chosen. If the foregoing may be considered as less important, the results for trace elements could be highly affected when contamination occurs during the pelletizing procedure. In order to check this, a pellet of pure graphite, sealed in a Mylar foil, was irradiated and counted several times with a large Ge(Li) detector and with the small detector. Evidence was found for 37.29-min $^{38}$Cl and 35.87-h $^{82}$Br, which are due to chlorine and bromine impurities in the Mylar foil. Small peaks of 2.58-h $^{56}$Mn and 15.0-h $^{24}$Na also appeared. In practice these impurities could hardly be considered as true contaminations.

*Spectral interferences and abundance determination*

With its extremely high resolution, a low-energy photon detector is an appropriate instrument for a detailed study of interferences in $\gamma$-spectra. The following results are intended to complete the data listed by Gordon *et al.*[1], who described the

use of a conventional Ge(Li) detector for i.n.a.a. of silicate rocks. The effect of mutual interference is strongly dependent on the relative abundances of the elements, and to a lesser extent also on the activation and cooling time and on the thermal-to-epithermal neutron flux ratio in the irradiation site. In order to have a wide range of $\gamma$-ray spectra, ten different samples were irradiated: the U.S.G.S. standard rocks BCR-1 and G-2, which were used as reference material, and a series of volcanic rocks from the Canary Islands, namely quartz trachytes, alkalinized gabbros, alkaline olivine basalts and a hawaiite.

The samples were irradiated in the Thetis Research Reactor of the Institute: initially for 5 min ($\phi_{th}/\phi_{epi}=28$) and then for 6 h ($\phi_{th}/\phi_{epi}=24$) at a thermal flux of about $10^{12}$ n cm$^{-2}$ sec$^{-1}$. Each standard rock and each sample was irradiated separately during 5 min together with a copper foil as flux monitor. The counting scheme is given in Table V.

In a related series of countings, standard and sample pellets were measured in the same geometry. It has indeed been found[17] that the spectrum shape is a function of the source-to-detector distance, owing to coincidence summing effects and possibly to other phenomena which are influenced by the average solid angle between detector and incident radiation (*e.g.* edge effects). The maximum fractional analyzer dead-time was limited to *ca.* 10%. Indeed, at a fractional dead-time of 20%, for instance, a systematic error of at least $-5\%$ was observed in the live-time mode of counting.

After the counting the content of the MCA-memory was transferred via an interface to that of a DEC PDP-9 computer for reduction of the spectra and Calcomp-plotting. The program[18] consisted mainly in a peak search and peak area determination routine. The peak area was calculated by the total peak area method, a linear shape of the background being assumed. A procedure in which a constant number of channels is added for a given peak, was not regarded as optimal. In such a procedure, it is supposed that the peak parameters are identical in standard and sample spectrum, but small gain and baseline shifts can occur, since counting times are quite long and a series of related measurements can extend over several days.

For the identification of the $\gamma$-lines, three $\gamma$-ray energy compilations were used to fulfill the need for precise and complete data, namely those of Filby *et al.*[19], Pagden *et al.*[20] and Dams and Adams[21]. The $\gamma$-energies listed here are taken from

TABLE V

| *Cooling time* | *Counting time* | *Radionuclides measured* |
|---|---|---|
| *5-min irradiation* | | |
| 15 min | 10 min | $^{51}$Ti, $^{60m}$Co |
| 1 h | 30 min | $^{139}$Ba, $^{152m_1}$Eu, $^{165}$Dy |
| *6-h irradiation* | | |
| 7 d | 30 min | $^{140}$La, $^{153}$Sm, $^{239}$Np(U), $^{47}$Sc |
| 15 d | 2 h | $^{51}$Cr, $^{59}$Fe, $^{131}$Ba, $^{141}$Ce, $^{147}$Nd, $^{152g}$Eu, $^{153}$Gd, $^{160}$Tb, $^{169}$Yb, $^{170}$Tm, $^{177}$Lu, $^{181}$Hf, $^{182}$Ta, $^{233}$Pa(Th) |
| *ca.* 22 d | 5 h | |
| *ca.* 35 d | 8 h | |

TABLE VI

SPECTRAL INTERFERENCES IN THE $\gamma$-RAY SPECTRA OF SILICATE ROCKS (UP TO 400 keV)[a]

| *Radionuclide* | $E_\gamma$ (*keV*) (*ref.* 21) | $I_\gamma$[b] (*ref.* 20) | *Interferences low-energy photon detector* | *Additional interferences large detector* |
|---|---|---|---|---|
| $^{47}$Sc (3.43 d) | *159.4* | 73. | | $^{175}$Hf(156.7+161.3) $^{152g}$Eu-(161.7) $^{182}$Ta(156.4) $^{169}$Yb(156.0) $^{131}$Ba(157.0) |
| $^{51}$Ti (5.79 min) | *320.1* | 95.5 | | |
| $^{51}$Cr (27.8 d) | *320.1* | 9. | $^{147}$Nd(319.4) | |
| $^{59}$Fe (45.1 d) | *142.5* | 0.8 | | $^{141}$*Ce(145.4)* $^{175}$Yb(144.7) $^{233}$Pa(145.4) |
| | *192.3* | 2.5 | | $^{169}$Yb(197.8) $^{160}$Tb(197.2) $^{182}$Ta(198.4) |
| $^{60m}$Co (10.5 min) | *58.5* | 2. | | $^{165}$*Dy(Ho-Kβ′1+2:53.9+55.3)* |
| $^{131}$Ba (11.5 d) | 92.3 | <0.1 | $^{147}$Nd(91.1) $^{169}$Yb(93.6) $^{233}$Pa(U-Kα2:94.7) | *cf.* $^{147}$Nd(91.1) |
| | *124.0* | 26. | $^{154}$*Eu(123.3)* | $^{152g}$*Eu(121.8)*[c] |
| | 133.7 | <0.1 | $^{181}$Hf(133.1) | *cf.* $^{181}$Hf(133.1) |
| | 137.3 | <0.1 | $^{181}$Hf(136.2+136.9) | |
| | 157.0 | 0.9 | | *cf.* $^{47}$Sc(159.4) |
| | *216.1* | 19. | $^{160}$*Tb(215.6)* | |
| | 373.1 | 13. | | $^{233}$Pa(375.2) $^{152g}$Eu(367.6) |
| $^{139}$Ba (83 min) | *165.8* | 21.7 | | |
| $^{140}$La (40.27 h) | 131.0 | 0.5 | $^{169}$Yb(130.5) | |
| | 242.0 | 0.6 | | $^{152g}$Eu(244.7) |
| | 266.5 | 0.5 | | $^{182}$Ta(264.1) |
| | *328.5* | 21. | | |
| $^{141}$Ce (32.5 d) | *145.4* | 49. | $^{175}$Yb(144.7) $^{233}$Pa(145.4) | $^{59}$*Fe(142.5)* |
| $^{147}$Nd (11.1 d) | *91.1* | 27. | $^{131}$Ba(92.3) | $^{182}$*Ta(100.1+84.7)* $^{170}$Tm-(84.3) $^{169}$Yb(84.2+93.6) $^{175}$Hf(89.6) $^{153}$Sm(89.5+97.5+103.2) $^{160}$*Tb(87.2+93.9)* $^{233}$*Pa-(86.8+103.8;+U-Kα1+2: 98.5+94.7)* $^{153}$Gd(97.5+103.2) |
| | 120.5 | 0.5 | $^{152g}$Eu(121.8) | *cf.* $^{131}$Ba(124.0) |
| | 319.4 | 2. | $^{51}$Cr(320.1) | |

*(continued)*

TABLE VI *(continued)*

| *Radionuclide* | $E_\gamma$ *(keV)* *(ref. 21)* | $I_\gamma{}^b$ *(ref. 20)* | *Interferences low-energy photon detector* | *Additional interferences large detector* |
|---|---|---|---|---|
| $^{145}$Sm (340 d) | 61.2 | 12.9 | $^{175}$Hf(Lu-K$\beta'$1 : 61.3) | *cf.* $^{169}$Yb(63.1) |
| $^{153}$Sm (47.1 h) | *69.7* | 4.6 | *Au-K$\alpha$1(68.8)* | *cf.* $^{169}$Yb(63.1) |
| | 75.4 | 0.2 | $^{233}$Pa(75.3) $^{161}$Tb(74.6) | |
| | 83.4 | 0.2 | $^{175}$Hf(89.6) | *cf.* $^{147}$Nd(91.1) |
| | 89.5 | 0.2 | | |
| | 97.5 | <0.1 | | $^{239}$*Np(106.3 + Pu-K$\alpha$2 : 99.5)* $^{182}$*Ta(100.1)* |
| | *103.2* | 27. | $^{239}$Np(Pu-K$\alpha$1 : 103.6) | $^{233}$*Pa(U-K$\alpha$1 + 2 : 98.4 + 94.7; 103.8)* $^{153}$Gd(97.5 + 103.2) |
| $^{152m_1}$Eu (9.35 h) | *121.8* | 5. | $^{152g}$*Eu(121.8)* $^{147}$Nd(120.5) | $^{154}$*Eu(123.3)* $^{131}$*Ba(124.0)* |
| | 344.2 | 1.7 | $^{152g}$Eu(344.2) $^{175}$Hf(343.6) $^{181}$Hf(345.9) $^{24}$Na(347DE) | $^{233}$Pa(340.5) |
| $^{152g}$Eu (12.2 y) | *121.8* | 29.4 | $^{147}$Nd(120.5) | *cf.* $^{131}$Ba(124.0) |
| | *244.7* | 7.6 | | $^{154}$Eu(248.0) $^{131}$Ba(239.8 + 246.8 + 249.4) $^{233}$Pa(248.3) |
| | 271.0 | 0.1 | $^{233}$Pa(271.5) | |
| | 296.0 | 0.4 | | $^{160}$Tb(298.6) $^{233}$Pa(299.9) |
| | *344.2* | 28.5 | *cf.* $^{152m_1}$Eu(344.2) | |
| $^{153}$Gd (236 d) | 68.2 | 0.2 | $^{182}$Ta(W-K$\beta'$2 : 69.1) Au-K$\alpha$1 (68.8) | *cf.* $^{169}$Yb(63.1) |
| | 69.7 | 4.3 | $^{153}$Sm(69.7) | |
| | *97.4* | 51.5 | $^{233}$*Pa(U-K$\alpha$1 : 98.5)* $^{153}$Sm-(97.4) | *cf.* $^{147}$Nd(91.1) |
| | *103.2* | 39.0 | $^{233}$*Pa(103.8)* $^{153}$Sm(103.2) | |
| $^{160}$Tb (73 d) | *86.8* | 12. | $^{233}$*Pa(86.6)* | *cf.* $^{147}$Nd(91.1) |
| | 197.0 | 5.1 | $^{169}$Yb(197.8) $^{182}$Ta(198.4) | |
| | 215.6 | 4. | $^{131}$Ba(216.1) | |
| | 230.7 | 0.1 | $^{182}$Ta(229.3) $^{175}$Hf(229.6) | |
| | *298.6* | 26.3 | $^{233}$*Pa(299.9)* | $^{152g}$Eu(296.0) |
| | 309.5 | 0.9 | | $^{233}$Pa(311.9) $^{169}$Yb(307.6) |
| $^{165}$Dy (2.36 h) | *94.7* | 3.7 | | |
| | *47.5* (Ho-K$\alpha$1) | | $^{152m_1}$Eu(Sm-K$\beta'$1 + 2 : 45.4 + 46.6) | |
| | *46.7* (Ho-K$\alpha$2) | | | |
| $^{166}$Ho (26.9 h) | 80.6 | <0.1 | Au-K$\beta'$2(80.2) + ? | $^{153}$Sm(83.4) $^{182}$Ta(84.7) |
| $^{170}$Tm (129 d) | *84.3* | 3.4 | $^{182}$*Ta(84.7)* $^{169}$Yb(84.2) | *cf.* $^{147}$Nd(91.1) |
| $^{169}$Yb | *63.1* | 57.3 | $^{175}$Hf(Lu-K$\beta'$2 : 62.9) | $^{175}$Hf(Lu-K$\beta'$1 : 61.3) $^{145}$Sm-(61.2) |



*(continued)*

TABLE VI *(continued)*

| *Radionuclide* | $E_\gamma$ *(keV)* (*ref.* 21) | $I_\gamma$[b] (*ref.* 20) | *Interferences low-energy photon detector* | *Additional interferences large detector* |
|---|---|---|---|---|
| (30.6 d) | | | | $^{181}$*Hf(Ta-Kβ′1+2:65.2+ 67.0)* |
| | | | | $^{182}$*Ta(65.7+67.7+W-Kβ′1+2:67.2+69.1)* $^{153}$Gd(69.7) |
| | 93.6 | 2.3 | $^{160}$Tb(93.9)$^{233}$Pa(U-Kα2:94.7) | |
| | 109.8 | 17.8 | $^{233}$Pa(U-Kβ3+1:110.4+111.3) | $^{233}$Pa(U-Kβ2:114.6)$^{182}$Ta-(116.4+113.7)$^{175}$Yb(113.8) |
| | 118.2 | 1.7 | | $^{177}$Lu(113.0)$^{175}$Hf(113.8) |
| | *130.5* | 11.2 | $^{140}$La(131.0) | *cf.* $^{181}$Hf(133.1) |
| | *177.1* | 20.2 | | $^{182}$*Ta(179.4)* |
| | 197.9 | 34.9 | $^{160}$Tb(197.0)$^{182}$Ta(198.4) | |
| | 261.1 | 1.6 | | $^{182}$Ta(264.1) |
| | 307.6 | 10.8 | | $^{233}$Pa(311.9) |
| | *50.7* (Tm-Kα1) | | $^{170}$Tm(Yb-Kα2:51.3) | |
| | *49.7* (Tm-Kα2) | | $^{152g}$Eu(Gd-Kβ′2:50.0) | *others* |
| $^{177}$Lu (6.75 d) | 113.0 | 4.4 | *cf.* $^{169}$Yb(109.8) | |
| | *208.4* | 7.5 | $^{169}$Yb(207.4)$^{239}$Np(209.8) | |
| $^{175}$Hf (70.0 d) | 89.6 | 3.4 | | *cf.* $^{147}$Nd(91.1) |
| | 113.8 | 0.2 | *cf.* $^{169}$Yb(109.8) | |
| | 229.6 | 0.6 | $^{182}$Ta(229.3)$^{160}$Tb(230.7) | |
| | 343.5 | 84.0 | *cf.* $^{152m_1}$Eu(344.2) | |
| | 54.1 (Lu-Kα1) | | $^{160}$Tb(Dy-Kβ′2:53.5)<br>$^{177}$Lu(Hf-Kα2:54.6) | |
| | 53.0 (Lu-Kα2) | | $^{160}$Tb(Dy-Kβ′2:53.5)<br>$^{170}$Tm(Yb-Kα1:52.4) | *others* |
| $^{181}$Hf (44.6 d) | *133.1* | 40.0 | $^{131}$Ba(133.7) | $^{169}$*Yb(130.5)* |
| | *136.2* | 6.0 | $^{177}$Lu(136.7) | |
| | *136.9* | 1.7 | | |
| | 345.9 | 13.0 | *cf.* $^{152m_1}$Eu(344.2) | |
| $^{182}$Ta (115.1 d) | 42.7 | 0.2 | $^{131}$Ba(Cs-Kα:30.8)+? | |
| | 65.7 | 2.8 | $^{181}$Hf(Ta-Kβ′1:65.2) | |
| | *67.7* | 41.7 | $^{182}$Ta(W-Kβ′1:67.2)<br>*Au-Kα2(67.0)*<br>$^{181}$*Hf(TaKβ′2:67.0)* | *cf.* $^{169}$Yb(63.1) |
| | 84.7 | 1.5 | $^{170}$Tm(84.3) | *cf.* $^{147}$Nd(91.1) |
| | *100.1* | 14.2 | $^{233}$Pa(U-Kα1:98.5) | |
| | 113.7 | 1.9 | | |
| | 116.4 | 0.5 | *cf.* $^{169}$Yb(109.8) | |
| | *152.4* | 7.2 | | |
| | 156.4 | 2.8 | $^{169}$Yb(156.0) | |
| | 179.4 | 3.3 | | $^{169}$Yb(177.1) |
| | 198.4 | 1.5 | $^{169}$Yb(197.9)$^{160}$Tb(197.0) | |
| | *222.1* | 8.0 | | |
| | 229.7 | 4.0 | $^{169}$Yb(230.7)$^{175}$Hf(229.6) | |
| | 264.1 | 3.8 | | |
| | *59.3* (W-Kα1) | | $^{169}$Yb(Tm-Kβ′2:59.0) | *others* |

*(continued)*

TABLE VI *(continued)*

| *Radionuclide* | $E_\gamma$ *(keV)* *(ref. 21)* | $I_\gamma$[b] *(ref. 20)* | *Interferences low-energy photon detector* | *Additional interferences large detector* |
|---|---|---|---|---|
| $^{233}$Pa | 75.3 | 0.8 | $^{161}$Tb(74.7) | |
| (27 d) | 86.6 | 1.7 | $^{160}$Tb(87.2) | |
| | 103.8 | 0.7 | $^{153}$Gd(103.2)$^{153}$Sm(103.2) $^{239}$Np(Pu-Kα1 : 103.6) | *cf.* $^{147}$Nd(91.1) |
| | 145.4 | 0.4 | $^{141}$Ce(145.4)$^{175}$Yb(145.2) | $^{59}$Fe(142.5) |
| | 271.5 | 0.3 | $^{152g}$Eu(271.0) | |
| | 299.9 | 6.3 | $^{160}$Tb(298.6) | $^{152g}$Eu(296.0) |
| | *311.8* | 34.0 | | $^{169}$Yb(307.6)$^{160}$Tb(309.5) |
| | 340.3 | 3.9 | | *cf.* $^{152m_1}$Eu(344.2) |
| | 375.2 | 0.6 | $^{131}$Ba(373.1) | |
| | *98.4* (U-Kα1) | | $^{153}$*Gd(97.5)* $^{239}$Np(Pu-Kα2 : 99.5) $^{182}$Ta(100.3) | *cf.* $^{147}$Nd(91.1) |
| | *94.7* (U-Kα2) | | $^{169}$*Yb(93.6)* $^{160}$Tb(93.9) | |
| $^{239}$Np | *106.3* | 21.9 | | *cf.* $^{153}$Sm(103.2) |
| (2.35 d) | 106.5 | <0.1 | | |
| | 228.2 | 11.3 | | |
| | 277.8 | 13.5 | | |

[a] The peaks listed in column 2 include only those which are frequently observed in γ-ray spectra of irradiated silicate rocks. Among the spectral interferences (columns 4 and 5) some peaks are mentioned that are not listed in column 2. Interferences with photon energies below 60 keV have not explicitly been listed for the large detector; as a reminder the indication "others" is shown. Peaks that are suitable for quantitative determinations have been italicized in column 2; prominent peaks which interfere with such an "analytical" peak, are italicized in the fourth and fifth columns.

[b] The absolute intensities (number of photons per 100 decays) are calculated from decay schemes, using experimental data on conversion where possible.

[c] Two small peaks often appear at *ca.* 125 keV and 127 keV. They are sum peaks of $^{182}$Ta(67.7 keV) and respectively the $^{182}$Ta(W-Kα2 : 57.97 keV) and $^{182}$Ta(W-Kα1 : 59.31 keV) X-rays.

Dams and Adams[21], whereas the X-ray energies are from Bearden[22].

In Table VI the spectral interferences up to 400 keV are summarized for the main radionuclides that appeared in the spectra of neutron-activated silicate rocks. For the data under the heading "large detector", the use of a detector with a resolution of about 4 keV at 1333 keV was assumed, although large detectors are now available with a much better resolution. Table VI can hardly be more than a generalization. One has to check for each particular case whether or not a certain peak will present a real problem.

It was also tempting to investigate whether X-rays could be useful in the i.n.a.a. of silicate rocks. In this respect, special attention was paid to $^{170}$Tm and $^{166}$Ho, which cannot readily be determined from the areas of their γ-peaks at 84.3 keV and 80.6 keV, but which appear to have quite high internal conversion coefficients. Radionuclides such as $^{175}$Hf and $^{169}$Yb are also interesting, since they decay by electron capture.

From the large amount of peaks (some 45 in the energy region 25–70 keV) only a few appeared to be more or less useful; these are listed explicitly in Table VI. Figure 4 shows the complex structure of the X-ray spectrum below 70 keV.

Figures 5 and 6 show low-energy photon spectra of different rocks.

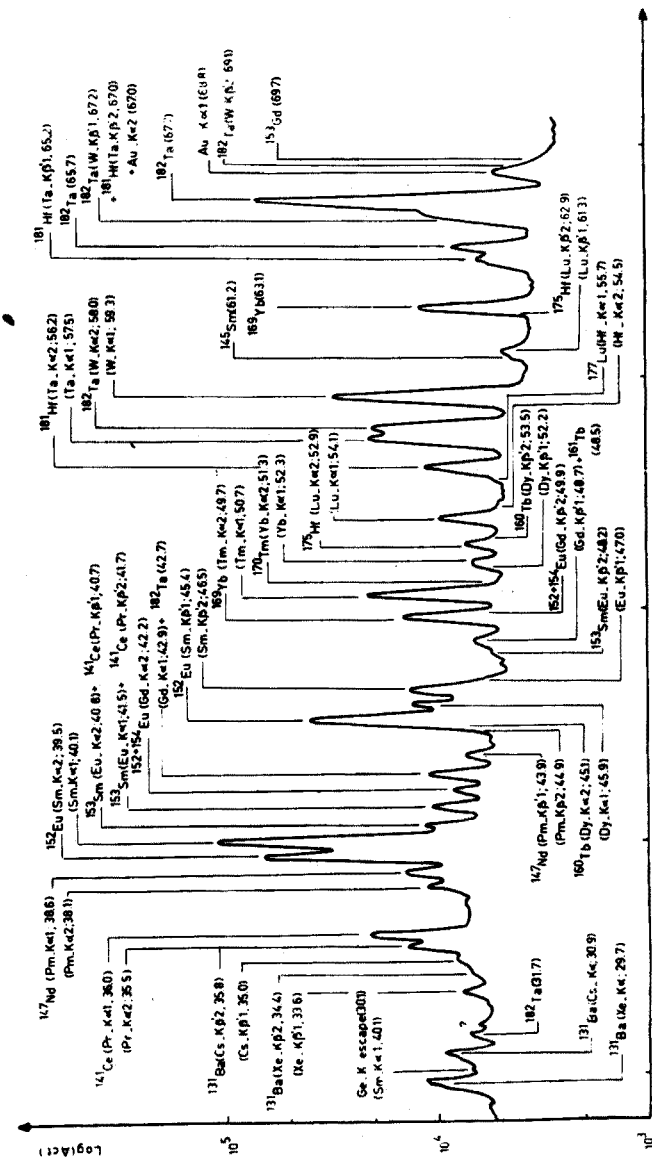


Fig. 4. X-Ray spectrum (below 70 keV) of a hawaiite, taken with the low-energy photon detector 1 month after the irradiation (1-g sample, irradiated for 6 h at a nominal flux of $10^{12}$ n cm$^{-2}$ sec$^{-1}$; counting time 8 h).

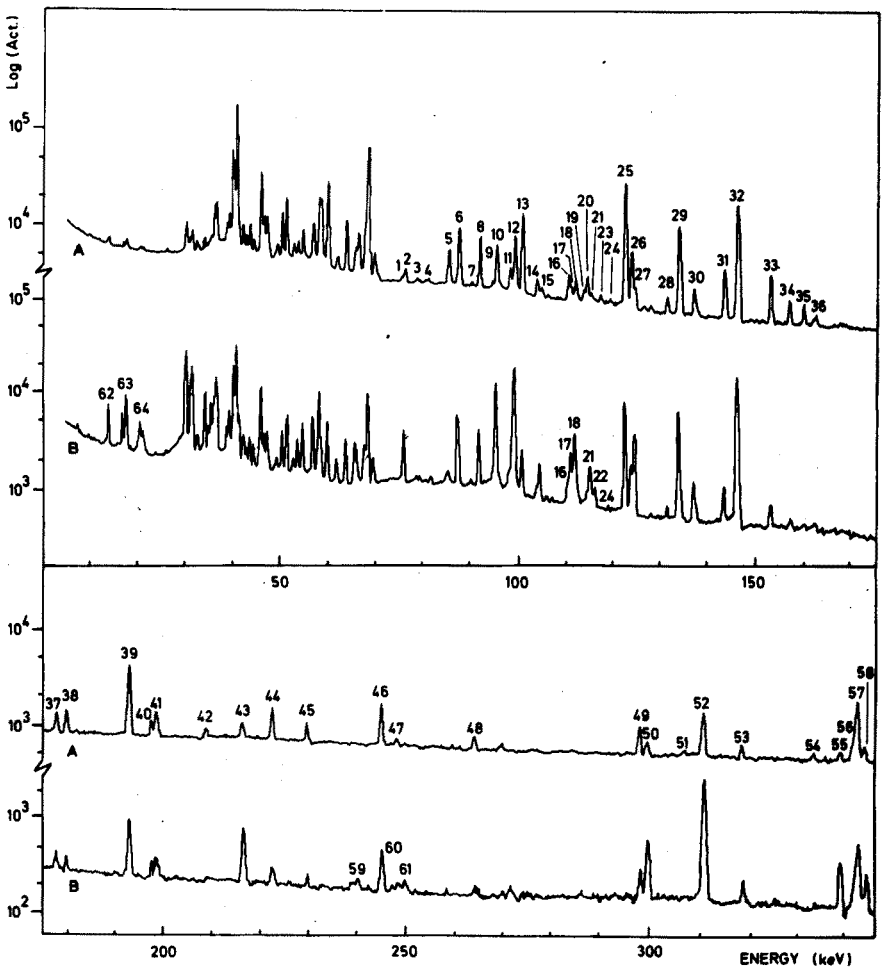


Fig. 5. Low-energy photon spectrum of a hawaiite (A) and of G-2 (B), measured 1 month after the irradiation (same conditions as for Fig. 4; for the identification of the peaks below 70 keV see Fig. 4).

1. $^{161}$Tb(74.6)
2. $^{233}$Pa(75.3)
3. Au-K$\beta'$1(78.0)
4. Au-K$\beta'$2(80.2)
5. $^{182}$Ta(84.7) + $^{170}$Tm(84.3)
6. $^{160}$Tb(86.8) + $^{233}$Pa(86.6)
7. $^{175}$Hf(89.6)
8. $^{147}$Nd(91.1)
9. $^{169}$Yb(93.6)
10. $^{233}$Pa(U-K$\alpha$ 2:94.6)
11. $^{153}$Gd(97.5)
12. $^{233}$Pa(U-K$\alpha$ 1:98.4)
13. $^{182}$Ta(100.1)
14. $^{153}$Gd(103.2)
15. $^{233}$Pa(103.8)
16. $^{169}$Yb(109.8)
33. $^{182}$Ta(152.4)
34. $^{182}$Ta(156.4) + $^{169}$Yb(156.0)
35. $^{47}$Sc(159.4)
36. $^{175}$Hf(161.3) + $^{152s}$Eu(161.4)
37. $^{169}$Yb(177.1)
38. $^{182}$Ta(179.4)
39. $^{59}$Fe(192.3)
40. $^{160}$Tb(197.0) + $^{169}$Yb(197.9)
41. $^{182}$Ta(198.4)
42. $^{177}$Lu(208.4)
43. $^{131}$Ba(216.0) + $^{160}$Tb(215.6)
44. $^{182}$Ta(222.1)
45. $^{182}$Ta(229.7) + $^{160}$Tb(230.7)
46. $^{152s}$Eu(244.4)
47. $^{152s}$Eu(248.0) + $^{233}$Pa(248.3)
48. $^{182}$Ta(264.1)

17. $^{233}$Pa(U-K$\beta$ 3:110.4)
18. $^{233}$Pa(U-K$\beta$1:111.3)
19. $^{177}$Lu(113.0)
20. $^{182}$Ta(113.7)
21. $^{233}$Pa(U-K$\beta$2:114.6)
22. $^{233}$Pa(U-K$\delta$1, 2:115.4)
23. $^{182}$Ta(116.4)
24. $^{169}$Yb(118.2)
25. $^{152s}$Eu(121.8)
26. $^{154}$Eu(123.1)
27. $^{131}$Ba(124.0)
28. $^{169}$Yb(130.5)
29. $^{181}$Hf(133.1)+$^{131}$Ba(133.7)
30. $^{181}$Hf(136.2+136.9)
31. $^{59}$Fe(142.5)
32. $^{141}$Ce(145.4)
49. $^{160}$Tb(298.6)
50. $^{233}$Pa(299.9)
51. $^{169}$Yb(307.6)
52. $^{233}$Pa(311.8)
53. $^{51}$Cr(320.1)
54. $^{59}$Fe(334.8)
55. $^{233}$Pa(340.3)
56. $^{175}$Hf(343.5)
57. $^{152s}$Eu(344.2)
58. $^{181}$Hf(345.9)
59. $^{131}$Ba(239.8)
60. $^{131}$Ba(246.8)
61. $^{131}$Ba(249.4)
62. $^{233}$Pa(U-L$\alpha$:13.6)
63. $^{233}$Pa(U-L$\beta$:17)
64. $^{233}$Pa(U-L$\gamma$:20)

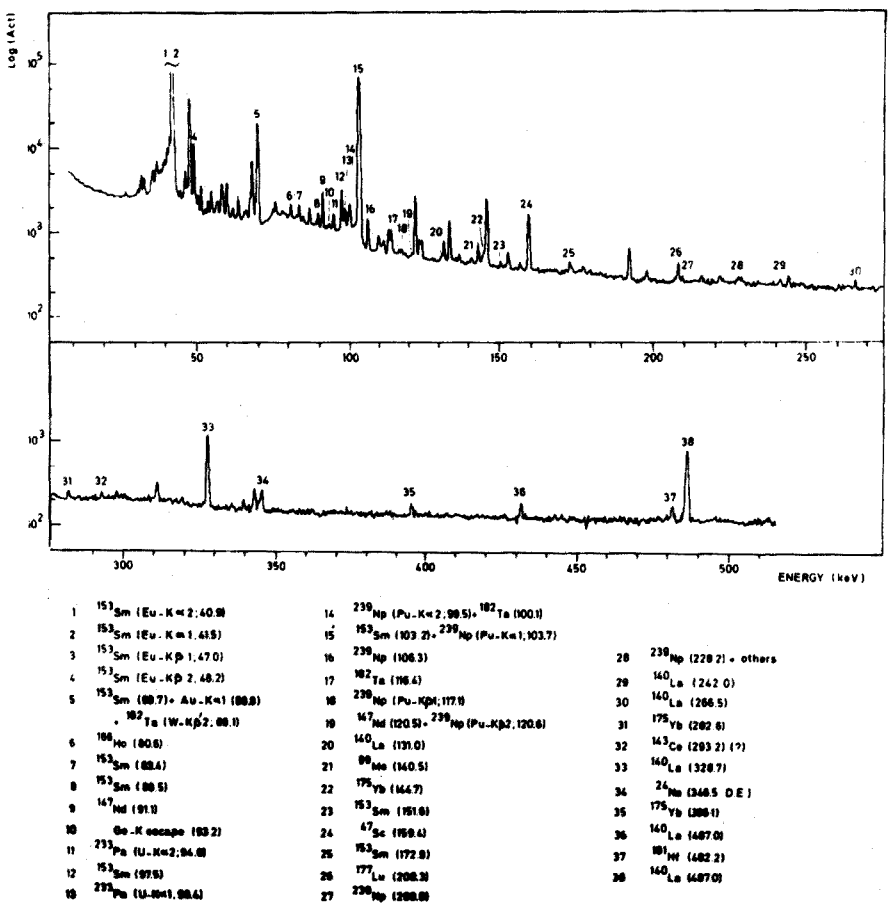


Fig. 6. Low-energy photon spectrum of a hawaiite, measured 7 days after the irradiation. Only the typical peaks are indicated; for the identification of the other peaks, see Fig. 4 and Fig. 5 (1-g sample, irradiated for 6 h at a nominal flux of $10^{12}$ n cm$^{-2}$ sec$^{-1}$; counting time 30 min).

For some radionuclides, namely $^{131}$Ba, $^{153}$Gd, $^{160}$Tb and $^{170}$Tm, single corrections for interfering activity have to be applied. In all cases, the particular contribution can be calculated from a pure peak of the interfering radionuclide, if the relative intensities of the peaks are known. A survey of Table VI shows that one needs pure spectra of $^{152g+154}$Eu (for $^{131}$Ba), $^{182}$Ta (for $^{170}$Tm) and $^{233}$Pa (for $^{153}$Gd and $^{160}$Tb), although information on other radionuclides may be useful in many instances. When measuring the pure spectra, several requirements need to be fulfilled: the "sample" must resemble the rock samples with respect to shape, matrix composition and density. This is important in connection with self-absorption of low-energy photons and geometry-dependent effects (see above). This resemblance can be achieved in the following way. An appropriate amount of radioactive tracer in a suitable amount of solution (*ca.* 250 $\mu$l) is spotted on a mixture of non-activated rock powder and graphite (1 g rock powder and 0.3 g graphite). After the solvent has been evaporated, this mixture is pressed into pellets. In order to avoid contamination of the press die with radioactive material, the mixture is packed in a Mylar foil before pelletizing.

## DISCUSSION

For the measurement of short-lived radionuclides, a large detector is superior to the low-energy photon detector, except for $^{165}$Dy (see below). Most of the short-lived species mainly emit $\gamma$-rays of higher energy ($^{24}$Na, $^{27}$Mg, $^{28}$Al, $^{42}$K, $^{49}$Ca, $^{52}$V, $^{56}$Mn). Besides the $^{165}$Dy lines, peaks of $^{51}$Ti, $^{60m}$Co, $^{139}$Ba, $^{152m_1}$Eu, $^{153}$Sm, $^{155}$Sm and $^{239}$U were observed in the spectra obtained with the small detector, but were not useful in most cases.

Longer-lived radionuclides such as $^{47}$Sc, $^{51}$Cr, $^{59}$Fe, $^{131}$Ba, $^{181}$Hf and $^{233}$Pa can also be measured with the small detector, but the results are not better than with a conventional Ge(Li) detector.

The advantage of the low-energy photon detector is clearly demonstrated in the determination of the geochemically very interesting group of the *lanthanides.*

The precision of the *lanthanum* results match those obtained with a large detector, but for several other elements the results obtained with the small detector are much better.

*Cerium*

The 145.4-keV line of $^{141}$Ce is well separated from the $^{59}$Fe 142.5-keV peak. It is, however, recommended to postpone the determination of cerium until 4.2-d $^{175}$Yb (144.7 keV) has decayed.

*Neodymium*

The 91.1-keV peak of 11.1-d $^{147}$Nd shows up very clearly in all the spectra and is free from any serious interference. The standard deviation on the peak area is generally about 1% (based on counting statistics). This is the case for the 5-h counting, 2 or 3 weeks after irradiation.

*Samarium*

With a conventional Ge(Li) detector, the presence of $^{239}$Np and especially $^{233}$Pa interferes with the measurement of $^{153}$Sm (103.2 keV). In order to keep the $^{233}$Pa

interference low, the counting must be performed within a few days after the irradiation, since the activity in the vicinity of 100 keV is then essentially due to $^{153}Sm$[1]. The latter limitation does not hold for the small detector, since the 103.2-keV peak of $^{153}Sm$ is well separated from the $^{233}Pa$ and $^{239}Np$ activities, with the possible exception of a small Pu-K$\alpha$1 contribution from $^{239}Np$ (103.6 keV). This allows the sample to be counted after the decay of $^{24}Na$ and results in a very favourable peak-to-background ratio: the counting statistics for this peak in BCR-1 improve to 0.32%.

Samarium can also be determined after a short irradiation. It should be noted that with the small detector the 104.2-keV peak of 21.9-min $^{155}Sm$ is well separated from the 103.2-keV peak of $^{153}Sm$. With a large Ge(Li) detector the peaks are not resolved and hence it is recommended to wait for the decay of $^{155}Sm$, in order to avoid faulty decay corrections.

*Europium*

The advantage of the small detector here lies in the fact that the intense 121.8-keV line of $^{152g}Eu$ (12.2 y) can be used without a correction for $^{131}Ba$ (124.1 keV), even when the barium content is rather high (*e.g.* in G-2). The line connecting the left and right boundaries of the 121.8-keV peak does not completely coincide with the continuous background of the spectrum. This is due to the 123.3-keV peak of $^{154}Eu$ and will not lead to systematic errors.

*Gadolinium*

It is almost impossible to determine this element by means of a large detector, as appears from the data of Table VI. From spectra obtained with the small detector, the $^{153}Gd$ activity can be measured from the 97.5-keV and 103.2-keV peaks. In both cases corrections have to be made for $^{233}Pa$ contributions, caused by the U-K$\alpha$1 X-ray (98.46 keV) and the 103.8-keV $\gamma$-ray. Obviously one has to account for possible remaining $^{153}Sm$ activity. Theoretically, gadolinium can also be determined by measuring the activity of 7.2-d $^{161}Tb$, which is formed in the reaction

$$^{160}Gd(n,\gamma)^{161}Gd \xrightarrow[3.73\ min]{\beta^-} {}^{161}Tb\,.$$

The 48.5-keV and 74.9-keV peaks of $^{161}Tb$ appear in the spectra obtained with the small detector, but they cannot be used for quantitative purposes.

*Terbium*

Although the 879.3-keV peak of $^{160}Tb$ is free from direct interferences in the spectra of large detectors, there are some problems with this peak, owing to the often intense $^{46}Sc$ 889.4-keV line and to the Compton edges of $^{59}Fe$ (1099.5 keV) and $^{46}Sc$ (1120.5 keV). The 962.6+966.0 keV peaks of $^{160}Tb$ are also commonly used after a correction for $^{152g}Eu$ (964.0 keV). This contribution to the complex peak is, however, generally more than 50%. Therefore, the 86.8-keV peak of $^{160}Tb$ in the spectra obtained with the small detector is likely to give more reliable results, even when some $^{233}Pa$ (86.6 keV) activity has to be removed (typically a few per cent).

*Dysprosium*

The dysprosium abundances are determined from the 94.7-keV peak of 2.36-h

$^{165}$Dy after the 5-min irradiation. A point of interest was to know whether or not 22.4-min $^{233}$Th (Pa-K$\alpha$1 : 95.86 keV) interfered. This possibility could be eliminated because the more intense 86.6-keV $\gamma$-peak of $^{233}$Th was not observed at the time $^{165}$Dy was measured. As $^{165}$Dy has to be counted in the presence of considerable $^{56}$Mn and $^{24}$Na activities, the better peak-to-background ratio in spectra obtained with the small detector is an important improvement compared with a large detector.

*Holmium*

The 80.6-keV line of 26.9-h $^{166}$Ho shows up rather weakly in spectra taken 4 d and 7 d after the 6-h irradiation. Moreover, this peak is subjected to complex interference which has not yet been identified completely (*e.g.* Au-K$\beta'$2: 80.17 keV). The Er-K$\alpha$ X-rays cannot be used, for they coincide with the Tm-K$\alpha$ X-rays ($^{169}$Yb), although it is perhaps possible to obtain some information by following the decay. Even with a low-energy photon detector it remains difficult to obtain data for the holmium content within reasonable precision limits.

*Thulium*

In the conventional Ge(Li) spectra thulium can hardly be determined from the unique 84.3-keV peak of $^{170}$Tm. In the spectra with the small detector only the $^{182}$Ta 84.7-keV $\gamma$-ray is left as an interference. Hence, the small detector is able to give acceptable Tm-values when the Ta/Tm ratio is not too unfavourable. The $^{170}$Tm Yb-K$\alpha$ X-rays are obscured by the Tm-K$\alpha$1 ($^{169}$Yb) and the Dy-K$\beta'$1 ($^{160}$Tb) X-rays.

*Ytterbium*

Gordon *et al.*[1] have already described the difficulties in the evaluation of precise values for ytterbium with conventional Ge(Li) detectors. Serious problems arose for both 4.2-d $^{175}$Yb and 30.6-d $^{169}$Yb. The absolute intensities of the $^{175}$Yb $\gamma$-transitions are quite low and none of the prominent peaks of $^{169}$Yb is free from interference. The epithermal neutron activation technique of Brunfelt and Steinnes[23] was also not successful with regard to ytterbium. However, the low-energy photon detector allows ytterbium to be determined from $^{169}$Yb with good precision. The standard deviation on the 63.1-keV peak was 0.85% for BCR-1 and 2.0% for G-2. If the hafnium content of the sample is high, it is perhaps better not to use the 63.1-keV peak, because of the possible interference from the Lu-K$\beta'$2 ($^{175}$Hf) 62.95-keV X-rays.

One can also use the 130.5-keV and 177.1-keV $\gamma$-peaks and the 50.73-keV Tm-K$\alpha$1 peak of $^{169}$Yb, without the necessity of removing interfering activities.

*Lutetium*

The 208.4-keV activity may be due to 6.75-d $^{177}$Lu and 155-d $^{177m}$Lu. If one takes into account the rate of formation of the two nuclides, this peak can be totally assigned to $^{177}$Lu : the capture cross-sections are 7 barn for $^{177m}$Lu, 315 barn for $^{177}$Lu and 1740 barn for the 0.16-msec $^{177}$Lu level, which produces 6.75-d $^{177}$Lu nuclides[24,25]. The small detector resolves the 208.4-keV peak almost completely from the 209.8-keV $^{239}$Np line and reduces the peak statistics from *ca.* 20% for a large detector to *ca.* 10%. As can be seen from Table VI, the use of the $^{177}$Lu 113.0-keV peak remains more than questionable in the case of rocks.

To summarize the situation for the rare earths, the low-energy photon detector

gives data for neodymium and gadolinium; this is interesting from the geochemical point of view, since it allows possible anomalous behaviour of cerium and europium to be established more clearly. Secondly, high precision values for at least one of the heavy rare-earth elements, namely for ytterbium, are obtainable, which is an important improvement compared to a conventional Ge(Li) detector.

The advantages of this small detector are again well illustrated in the instrumental determination of *tantalum* and *uranium*.

*Tantalum*

In thermal neutron-irradiated samples, only relatively high tantalum contents can be determined precisely when a large detector is used. In this case the 1189.0-keV, 1221.4-keV and 1231.0-keV peaks of $^{182}$Ta are quite intense. For lower tantalum abundances one inevitably has to determine the area of the highly disturbed 67.7-keV and 100.3-keV peaks. The small detector also cannot thoroughly resolve these peaks from interfering species: the 67.7-keV line has to be corrected for the Ta-K$\beta'$2 ($^{181}$Hf), as well for the small Au-K$\alpha$2 (gold electrode) contributions and the 100.3-keV peak is slightly affected by the U-K$\alpha$1 ($^{233}$Pa) X-ray. Nevertheless, these peaks are much more reliable than those obtained in conventional Ge(Li) spectra. The $^{182}$Ta (W-K$\alpha$1 : 59.31 keV) peak can also be used after a small correction for $^{169}$Yb (Tm-K$\beta'$2 : 58.97 keV).

*Uranium*

The uranium abundances are determined from the 106.3-keV peak of 2.35-d $^{239}$Np, which is produced via the reaction

$$^{238}\mathrm{U}(\mathrm{n},\gamma)^{239}\mathrm{U} \xrightarrow[23.54\ \mathrm{min}]{\beta^-} {}^{239}\mathrm{Np}.$$

The best results are obtained 7 d after the irradiation. The precision can be partly expressed in terms of the counting statistics of the peak area, which were 4% for BCR-1 (1.8 p.p.m.) and 1.7 % for a quartz trachyte (6.6 p.p.m.).

The epithermal neutron activation procedure of Brunfelt and Steinnes[23] also proved to be very advantageous with respect to tantalum and uranium. In this connection, it may be stated that in the "reactor" neutron activation technique, the precision of the tantalum and uranium values is a function of the thermal-to-epithermal neutron flux ratio in the irradiation site.

As this article has been concentrated on the technique as such, a discussion of the results of the Fuerteventura samples is beyond its scope. Nevertheless, some results are presented in Table VII in order to establish the reliability of the small detector for quantitative work. The results obtained with the small detector are compared with those obtained with a large Ge(Li) detector (Ortec double open-ended coaxial detector, active volume 35 cm$^3$, resolution 2.2 keV at 1332 keV). As test cases, iron, thorium, hafnium and europium were chosen, because those elements can be determined quite precisely with a large Ge(Li) detector.

The above approach is somewhat unconventional, but serves the present purpose of demonstrating that the low-energy photon detector can be used for quantitative analysis. The agreement of the results with those obtained with a large Ge(Li) detector is satisfactory and suggests that problems of geometry and self-absorption

TABLE VII

COMPARISON OF SOME RESULTS FROM THE PHOTON DETECTOR WITH THOSE FROM A 35-cm$^3$ Ge(Li) DETECTOR

(Figures in brackets represent the per cent standard deviation, based on counting statistics. The results of each measurement are listed separately)

| Sample \ $E_\gamma$(keV) | Fe(%) ($^{59}$Fe measured) | | | |
|---|---|---|---|---|
| | 142.5[a] | 192.5[a] | 1098.6[b] | 1291.5[b] |
| Hawaiite[c] | 9.49(2.5), 9.00(2.3) | 8.94(1.7), 8.90(1.6) | 8.47(0.7), 8.46(0.7) | 8.64(0.7), 8.62(0. |
| Basanitoid[c] | 9.40(3.1), 9.55(2.4) | 9.44(1.9), 9.51(1.6) | 9.50(0.7), 9.46(0.7) | —, 9.58(0. |
| Alkaline olivine basalt[c] | 8.56(2.5), 8.40(2.4) | 8.59(1.6), 8.47(1.6) | 8.40(0.7), 8.73(0.7) | 8.51(0.7),— |
| Quartz trachyte(II)[d] | 1.27(9.9), 1.00(8.9) | 1.20(6.2), 1.06(4.6) | 1.09(1.2),— | 1.25(1.3),— |
| Quartz trachyte(II)[d] | 2.60(8.4), 2.14(7.1) | 2.31(4.9), 2.22(4.2) | 2.23(1.0),— | 2.58(1.1),— |
| | Hf(p.p.m.) ($^{181}$Hf measured) | | | |
| | 133.1[a] | 136.2+136.9[a] | 482.2[b] | |
| Hawaiite[c] | 11.6(1.3), 11.6(1.5) | 11.1(8.7), 11.8(9.7) | 11.9(7.6), 11.0(7.4) | |
| Basanitoid[c] | 5.50(2.1), 5.42(1.8) | 5.20(14), 5.63(12) | 5.89(9.1), 5.75(9.3) | |
| Alkaline olivine basalt[c] | 4.47(1.8), 4.47(1.9) | 4.21(13), 4.70(12) | 4.85(9.3), 4.47(10) | |
| Quartz trachyte(I)[d] | 9.62(1.1), 9.64(0.9) | 9.95(6.1), 9.05(6.5) | 9.72(1.6),— | |
| Quartz trachyte(I)[d] | 32.8(0.9), 32.9(0.8) | 33.8(5.3), 33.2(4.0) | 33.3(1.5),— | |
| | Eu(p.p.m.) ($^{152g}$Eu measured) | | | |
| | 121.8[a] | 1407.5[b] | | |
| Hawaiite[c] | 5.24(0.8), 5.24(0.7) | 5.30(3.2), 5.31(2.9) | | |
| Basanitoid[c] | 2.75(1.1), 2.78(0.8) | —, 2.98(3.3) | | |
| Alkaline olivine basalt[c] | 2.25(1.0), 2.25(0.8) | 2.20(3.7), — | | |
| Quartz trachyte(I)[d] | 0.93(1.4), 0.89(1.1) | 0.93(3.6), — | | |
| Quartz trachyte(II)[d] | 4.44(1.0), 4.33(0.8) | 4.58(2.6), — | | |
| | Th(p.p.m.) ($^{233}$Pa measured) | | | |
| | 311.9[a] | 311.9[b,e] | | |
| Hawaiite[c] | 8.40(4.5), 8.80(5.0) | 7.91(6.8), 8.65(7.1) | | |
| Basanitoid[c] | 4.79(7.8), 4.39(7.3) | 4.66(9.6), — | | |
| Alkaline olivine basalt[c] | 2.30(8.8), 2.48(10) | 2.95(12), 2.70(14) | | |
| Quartz trachyte(II)[d] | 34.7(1.3), 33.8(1.1) | 33.5(0.6), — | | |
| Quartz trachyte(II)[d] | 26.1(1.5), 25.7(1.4) | 25.7(0.8), — | | |

[a] Low-energy photon detector.
[b] 35-cm$^3$ Ge(Li) detector.
[c] BCR-1 used as a standard.
[d] G-2 used as a standard.
[e] Measured 1–2 months after the irradiation, *i.e.* not in optimal conditions.

of low-energy photons which are more acute in the case of the small detector can be kept under control.

We are grateful to Prof. Dr. J. Hoste for his interest in this work and to Dr. P. De Paepe for the supply of the rock samples.

SUMMARY

The usefulness of a small low-energy photon Ge(Li) detector for instrumental neutron activation analysis of silicate rocks was investigated. In order to avoid systematic errors caused by self-absorption of low-energy photons and by the counting geometry, a sample pelletizing technique is proposed. The spectral interferences in spectra taken with the small Ge(Li) detector and with a large one were compared and a definite advantage for a small detector was found for the determination of Ce, Nd, Sm, Eu, Gd, Tb, Dy, Tm, Yb, Lu, Ta and U.

RÉSUMÉ

On examine l'utilité d'un petit détecteur Ge(Li) pour l'analyse par activation neutronique instrumentale des silicates. On propose une technique permettant d'éviter des erreurs systématiques due à une self-absorption de photons de faible énergie. Ce petit détecteur présente des avantages pour le dosage de Ce, Nd, Sm, Eu, Gd, Tb, Dy, Tm, Yb, Lu, Ta et U.

ZUSAMMENFASSUNG

Es wurde die Anwendbarkeit eines kleinen Ge(Li)-Detektors für Photonen niedriger Energie bei der instrumentellen Neutronenaktivierungsanalyse von Silikatgesteinen untersucht. Zur Vermeidung systematischer Fehler durch Selbstabsorption der niedrigenergetischen Photonen und durch die Zählgeometrie wird ein Probenpelletierverfahren vorgeschlagen. Die spektralen Störungen bei Spektren, die mit dem kleinen Ge(Li)-Detektor und mit einem grossen aufgenommen worden waren, wurden miteinander verglichen. Es wurde ein deutlicher Vorteil des kleinen Detektors bei der Bestimmung von Ce, Nd, Sm, Eu, Gd, Tb, Dy, Tm, Yb, Lu, Ta und U festgestellt.

REFERENCES

1 G. E. Gordon, K. Randle, G. G. Goles, J. B. Corliss, M. H. Beeson and S. S. Oxley, *Geochim. Cosmochim. Acta*, 32 (1968) 369.
2 J. C. Dran, R. Gijbels and G. E. Gordon, in *M.I.T. Laboratory for Nuclear Science, Chemistry Progress Report, M.I.T.-905-133, Section IV, D*, 1968.
3 R. A. Zielinsky and F. A. Frey, *Contrib. Mineral. Petrol.*, 29 (1970) 242.
4 W. H. Zoller and G. E. Gordon, *Anal. Chem.*, 42 (1970) 257.
5 M. de Bruin and P. J. M. Korthoven, in *Proc. Symposium on Semiconductor Detectors for Nuclear Radiation, München, May 11–13, 1970*, p. 174.
6 J. Rosenberg and H. B. Wiik, *Radiochem. Radioanal. Letters*, 6 (1971) 45.
7 J. M. Palms, P. Venugopala Rao and R. E. Wood, *Nucl. Instr. Methods*, 64 (1968) 310.
8 J. Deneef, private communication.

9 T. S. NAGPAL AND R. E. GAUCHER, *Nucl. Instr. Methods*, 89 (1970) 311.
10 Y. GURFINKEL AND A. NOTEA, *Nucl. Instr. Methods*, 57 (1967) 173.
11 U. GRUBER, R. KOCH, B. P. MAIER AND O. W. B. SCHULTZ, *Z. Naturforsch.*, 20a (1965) 929.
12 E. J. SEPPI, H. HENDRIKSON, F. BOEHM AND J. W. M. DUMOND, *Nucl. Instr. Methods*, 16 (1962) 17.
13 D. H. WHITE, R. E. BIRKETT AND T. THOMSON, *Nucl. Instr. Methods*, 77 (1970) 261.
14 R. L. HEATH, in J. R. DE VOE, *Modern Trends in Activation Analysis*, National Bureau of Standards, Washington, D.C., 1969, p. 965.
15 J. UNGRIN AND M. W. JOHNS, *Nucl. Instr. Methods*, 70 (1969) 112.
16 YU. I. STAKHEEV AND YU. N. KUZNETSOV, *Zavodsk. Lab.*, 36 (1970) 1.
17 R. GIJBELS, J. C. DRAN, H. ERTEN, W. ZOLLER, J. FASCHING AND G. E. GORDON, in *M.I.T. Laboratory for Nuclear Science, Chemistry Progress Report, M.I.T.-905-133*, 1968, p. 32.
18 J. OP DE BEECK, private communication.
19 R. H. FILBY, A. I. DAVIS, G. G. WAINSCOTT, W. A. HALLER AND W. A. CASSATT, *Gamma-ray Energy Tables for Neutron Activation Analysis*, WSUNRC-97, October 1969, Report Washington State University.
20 I. M. H. PAGDEN, G. J. PEARSON AND J. M. BEWERS, *Isotope Catalogue for Instrumental Activation Analysis (1970)*, Atlantic Oceanographic Laboratory, Bedford Institute, Dartmouth, Canada, to be published.
21 R. DAMS AND F. ADAMS, *J. Radioanal. Chem.*, 7 (1971) 127.
22 J. A. BEARDEN, *Rev. Mod. Phys.*, 39 (1967) 78.
23 A. O. BRUNFELT AND E. STEINNES, *Anal. Chim. Acta*, 48 (1969) 13.
24 C. M. LEDERER, J. M. HOLLANDER AND I. PERLMAN, *Table of Isotopes*, 6th Edn., John Wiley, New York, 1968.
25 N. E. HOLDEN, F. W. WALKER, D. T. GOLDMAN AND J. R. STEHN, *Chart of the Nuclides*, 10th Edn., General Electric Co., December 1968.

*Analytica Chimica Acta*
Elsevier Publishing Company, Amsterdam
Printed in The Netherlands



# FLUORESCENCE AND PHOSPHORESCENCE OF 5- AND 8-AMINOQUINOLINE

STEPHEN G. SCHULMAN AND LOWELL B. SANDERS*

*Department of Pharmaceutical Chemistry, College of Pharmacy, University of Florida, Gainesville, Fla. 32601 (U.S.A.)*

(Received 29th March 1971)

The aminoquinolines are of considerable industrial importance as intermediates in the preparation of dyes and drugs. Notably 8-aminoquinoline is the aromatic nucleus of the antimalarial pamaquine and is of analytical interest as a chelating agent. To date, several studies of the absorption spectra of aminoquinolines have been carried out[1-3] but although most of the isomers show fluorescence, no systematic study of their fluorescences has been undertaken.

Studies of the luminescences of the aminoquinolines in different solvents and at different pH can yield information leading to new methodology for the analyses of these compounds and can serve to elucidate chemical and physical processes occurring in the lowest excited states, subsequent to excitation and preceding emission. In the latter context it is known that in arylamines, excitation to the lowest excited singlet state is generally accompanied by intramolecular charge transfer from the amino group to the aromatic ring[4]. It is of interest to compare the excited state $pK_a^*$ values and the solvent dependence of aminoquinoline fluorescence bands with those of quinolines substituted with other electron-donating groups; especially with those of the corresponding hydroxyquinolines[5-9].

In this study, the fluorescence and phosphorescence spectroscopy of 5- and 8-aminoquinoline, the two aminoquinoline isomers which are hardly or not at all fluorescent in aqueous solutions, is discussed.

## EXPERIMENTAL

5- and 8-Aminoquinoline (K and K Laboratories Inc., Plainview, N.Y.) were purified by multiple recrystallization from chloroform followed by vacuum sublimation. The purities of these compounds were established by the excellent agreement of the corrected excitation spectra with the electronic absorption spectra. Mallinckrodt reagent-grade perchloric and sulfuric acids and Matheson Coleman and Bell Spectroquality chloroform, *n*-heptane, *p*-dioxane and acetonitrile were employed in these studies without further purification. Ethanol was distilled under low pressure, to remove traces of benzene, before employment as a solvent. Sodium hydroxide solutions were prepared by dilution of the concentrated carbonate-free solution with distilled deionized water.

* Department of Chemistry, University of Florida, Gainesville, Fla. 32601, U.S.A.

Absorption spectra were taken on a Beckman DB spectrophotometer. Fluorescence spectra were taken on a Perkin-Elmer MPF-2A fluorescence spectrophotometer whose monochromators were calibrated against the line emission spectrum of xenon. Emission and excitation spectra were corrected for the wavelength dependent response of monochromators, phototube and lamp by means of a Perkin-Elmer corrected spectra accessory employing a rhodamine B quantum counter. Quantum yields of fluorescence were calculated by the relative method of Parker and Rees[10], with quinine hydrogen sulfate in 0.1 *N* sulfuric acid as a standard.

Phosphorescence spectra were taken at 77°K on an Aminco spectrophotofluorimeter with a rotating can phosphoroscope to isolate the phosphorescence. Phosphorescence spectra were uncorrected. Moreover, cracking of the acidic and basic ethanol solutions upon which spectra were taken prevented the estimation of even approximate phosphorescence efficiencies.

## RESULTS AND DISCUSSION

The principle absorption and fluorescence characteristics of 5- and 8-aminoquinoline, at room temperature and in several solvents are presented in Table I.

TABLE I

LOW ENERGY ABSORPTION MAXIMA ($\bar{\nu}_a$), FLUORESCENCE MAXIMA ($\bar{\nu}_f$) AND QUANTUM YIELDS OF FLUORESCENCE ($\phi_f$) OF THE AMINOQUINOLINES AT ROOM TEMPERATURE

(Spectral maxima are reported in $\mu m^{-1}$ ($cm^{-1} \cdot 10^{-4}$))

| | *5-Aminoquinoline* | | | *8-Aminoquinoline* | | |
|---|---|---|---|---|---|---|
| | $\bar{\nu}_a$ | $\bar{\nu}_f$ | $\phi_f$ | $\bar{\nu}_a$ | $\bar{\nu}_f$ | $\phi_f$ |
| 18 *M* $H_2SO_4$ | — | — | — | — | — | — |
| $1.0 \cdot 10^{-2}$ *M* $HClO_4$ | — | — | — | — | — | — |
| pH 7 Buffer | 2.96 | 1.93 | 0.001 | — | — | — |
| Ethanol | 2.90 | 1.94 | 0.01 | — | — | — |
| Acetonitrile | 2.90 | 2.06 | 0.01 | 2.90 | 2.10 | 0.01 |
| Chloroform | 2.93 | 2.08 | 0.02 | 2.91 | 2.14 | 0.01 |
| *p*-Dioxane | 2.88 | 2.09 | 0.07 | 2.83 | 2.15 | 0.01 |
| *n*-Heptane | 2.96 | 2.26 | 0.26 | 2.93 | 2.28 | 0.002 |

Neither the 5- nor the 8-isomer fluoresces in fluid solutions in concentrated or dilute acid and in neutral aqueous solutions the 8-isomer is still non-fluorescent while the 5-isomer shows a fluorescence which is very weak. In low dielectric media, however, both isomers fluoresce with weak to moderate intensity.

The Stokes' shifts calculated from the data of Table I, which demonstrate an increase with increasing solvent polarity and hydrogen bonding capability of the solvent, indicate that the long wavelength absorption and fluorescence bands of the neutral molecules arise from $\pi$–$\pi^*$ transitions and that changes in hydrogen bonding and solute–solvent dipole interactions are substantial on going from the ground state to the lowest excited singlet state. In the case of 5-aminoquinoline it would appear that hydrogen-bond donor capability of the solvent is most important in determining

the energy of solvent relaxation after excitation since water and ethanol produce the largest Stokes' shifts while acetonitrile which is more polar than ethanol but is strictly a hydrogen-bond acceptor does not produce as large a Stokes' shift relative to the shift in *n*-heptane which is neither polar nor hydrogen-bonding. The Stokes' shift in acetonitrile, chloroform and *p*-dioxane, which are all hydrogen-bond acceptors, are comparable even though the polarities of chloroform and dioxane are not as great as that of acetonitrile. For 8-aminoquinoline fluorescence was not observed in a wide enough variety of solvents for a comparable breakdown of excited state solvent effects to be evaluated.

The quantum yields of fluorescence in the various solvents fell with increasing solvent polarity and hydrogen bonding capability for 5-aminoquinoline. Again, the solvents with the greatest hydrogen-bond donor capabilities yielded the lowest quantum yields for 5-aminoquinoline and in dilute acid solutions where proton transfer to the ring nitrogen is complete, the fluorescence of 5-aminoquinoline is completely quenched. In the solvent series acetonitrile, chloroform, *p*-dioxane, the quantum yields were lower than in *n*-heptane with the yields decreasing in order of increasing polarity rather than hydrogen-bond acceptor strength. However, even though *p*-dioxane is non-polar, it does have substantial C–O bond dipole moments which may be of greater importance on the microscopic level than gross dielectric properties. Consequently, it is probably too soon to draw rigid conclusions regarding the relative importances of dipole–dipole interactions *versus* hydrogen-bonding acceptor properties of the solvent in providing a mechanism of internal conversion. Insufficient data are available for any conclusions to be drawn about the nature of solvent dependent quenching of the neutral 8-aminoquinoline; however, it is extremely interesting that the quantum yield of fluorescence in *n*-heptane is considerably lower than in more polar and hydrogen-bonding solvents, which is opposite to the case observed for 5-aminoquinoline. It is interesting to speculate that for 8-aminoquinoline hydrogen-bonding donor interaction and the absence of hydrogen-bonding acceptor interaction in the excited state are responsible for fluorescence quenching.

The substantial shifts of the long wavelength absorption spectra of 5- and 8-aminoquinoline in solutions of varying pH[3] suggest that the fluorescence arises from a $^1L_a$ state[11] of naphthalene perturbed by the heterocyclic nitrogen and amino groups. This conclusion results from the great sensitivity predicted for the position of the $^1L_a$ excited state to substituents in quinoline ring atoms corresponding to the α-positions in naphthalene, owing to the transverse polarization of the $^1L_a \leftarrow {}^1A$ transition in naphthalene. Thus protonation of the nitrogen atoms of aminoquinolines corresponds to variation of the substituents in α-positions of naphthalene. The $^1L_b$ transitions of 5-aminoquinoline and 8-aminoquinoline which lie at 3.17 and 3.15 $\mu m^{-1}$, respectively, do not vary much with protonation. This is a result of the relative insensitivity of the longitudinally polarized $^1L_b \leftarrow {}^1A$ transition of naphthalene to α-substituents. These results are interesting because in quinoline itself, it is the $^1L_b$ state which is the lowest excited singlet state. Apparently, the mixing of charge transfer from the amino group to the aromatic ring with the transition from the ground state to the weakly perturbed $^1L_a$ state of quinoline, is sufficient to lower the energy of the $^1L_a$ state below that of the $^1L_b$ state relative to the ground state in the 5- and 8-aminoquinolines.

At reduced temperatures (*i.e.*, a dry ice–acetone bath) it was possible to observe

moderately intense fluorescence from the doubly charged cations, singly charged cations and neutral species derived from the aminoquinolines. At dry ice temperature, the singly charged cations were present in ice containing $1.0 \cdot 10^{-2}$ *M* perchloric acid while the neutral species were studied in ice prepared from a borate buffer of pH 10.2. The doubly charged cations were first studied in 18 *M* sulfuric acid. This solvent did not set to an ice but became very viscous at the temperature of the dry ice–acetone bath. However, these viscous solutions of cold sulfuric acid containing the aminoquinolines were fluorescent. Moreover, when the acid was diluted to 3.6 *M* with water and then immersed in the dry ice–acetone bath, it did freeze and solutions of the aminoquinolines in these concentrated acid ices yielded fluorescence spectra essentially identical with those taken in the viscous sulfuric acid solutions. The fluorescences observed for 5- and 8-aminoquinoline in media of varying acidity and at the dry ice–acetone bath temperature are presented in Table II.

TABLE II

FLUORESCENCE MAXIMA ($\bar{\nu}_f$) OF THE AMINOQUINOLINES AT ~233°K (DRY ICE–ACETONE BATH) AND IN MEDIA OF DIFFERENT ACIDITIES

(Spectral maxima are reported in $\mu m^{-1}$ ($cm^{-1} \cdot 10^{-4}$))

| | $\bar{\nu}_f$ | |
|---|---|---|
| | *5-Aminoquinoline* | *8-Aminoquinoline* |
| 18 *M* $H_2SO_4$ | 2.68 | 2.76 |
| 3.6 *M* $H_2SO_4$ | 2.67 | 2.74 |
| $1.0 \cdot 10^{-2}$ *M* $HClO_4$ | 1.83 | 2.14 |
| pH 10.2 Buffer | 2.05 | 2.36 |

That the emissions listed in Table II are truly fluorescences and not phosphorescences can be established by two lines of reasoning. First, the room-temperature fluorescences of Table I are similar in position to the low-temperature emissions of the neutral species observed in pH 10.2 buffer. Although the low-temperature emissions of the neutral species are at higher frequencies than the corresponding emissions in polar solvents at room temperature, it must be borne in mind that no solvent relaxation can occur in the rigid medium, thus the Stokes' shifts in ice should be smaller than those for even weakly polar solvents under fluid circumstances. Second, the shifts of the fluorescence spectra in the rigid media, resulting from protonation, are comparable in magnitude to the shifts of the corresponding long wavelength absorption maxima in fluid solutions, upon conversion from one prototropic form to the other. The pH dependences of phosphorescence frequencies are much smaller than those observed here[12]. No phosphorescence was observed at any acidity in the dry ice–acetone media.

The ground-state $pK_a$ values of the aminoquinolines, the long wavelength absorption maxima and the fluorescence maxima of the various prototropic forms derived from the aminoquinolines can be employed to estimate the dissociation constants of the doubly protonated and singly protonated aminoquinolines in the lowest

excited singlet state, with the aid of the Förster cycle[13] at 25°.

$$pK_a - pK_a^* = 2.10 \cdot 10^{-3} (\bar{\nu}_A - \bar{\nu}_B) \quad (1)$$

where $pK_a$ and $pK_a^*$ are the ground and lowest excited singlet state dissociation constants corresponding to the same equilibrium and $\bar{\nu}_A$ and $\bar{\nu}_B$ are the approximate positions of the O–O bands (in $cm^{-1}$) of acid and conjugate base, respectively, and are calculated by averaging the positions of the absorption and fluorescence maxima, respectively. From $pK_a$ values[2], the absorption data[3] and the fluorescence data in Table II, the $pK_a^*$ values of the doubly charged cations derived from 5- and 8-aminoquinoline, are estimated to be $-16.6$ and $-12.6$, respectively. The $pK_a^*$ values of the singly charged monocations (protonated at the ring nitrogen) are estimated to be 10.9 and 10.0 for the 5- and 8-isomer, respectively. It must be remembered that these values are not quantitative, as the fluorescence measurements were made in rigid media and the effect of solvent relaxation subsequent to excitation, in fluid solutions, is not accounted for in the present calculations. Although it is known that in some cases the effect of solvent relaxation can outweigh the effect of polarization of the electronic transition in determining the value of $pK_a^*$ relative to $pK_a$[14], in cases where $pK_a^*$ calculated in the absence of solvent relaxation is very different from $pK_a$, $pK_a$ is at least qualitatively accurate[9]. Thus the values calculated here are probably not in error, relative to the thermodynamic $pK_a^*$ by more than 3–4 units. In any event, the extremely negative values of $pK_a^*$ for the dications suggest that they may even be fluorescent in fluid solutions, but their great acidities preclude their formations even in the most concentrated acid media. Moreover, the high acidities of the dications in the excited state relative to the ground state as well as the low acidities of the excited ring-protonated monocations relative to their ground states, indicate that upon excitation to the lowest excited singlet state charge transfer occurs from the exocyclic nitrogen and to the heterocyclic nitrogen. This situation is perfectly analogous to that in 5- and 8-hydroxyquinolines. The failure of the monocations to fluoresce in fluid solutions is apparently due to diffusion limited quenching by the solvent involving hydrogen bonding-assisted internal conversion and possibly some intersystem crossing to the lowest triplet state.

In ethanolic solutions made 1.8 *M* with sulfuric acid and at 77°K, the doubly charged cations were found to phosphoresce as well as fluoresce. Isolation of the phosphorescences was accomplished by means of rotating shutter. 5-Aminoquinoline demonstrated a O–O phosphorescence band at 2.29 $\mu m^{-1}$ and other intense vibronic maxima at 2.18 and 2.05 $\mu m^{-1}$. The O–O vibronic feature of the 8-aminoquinoline dication occurred at 2.25 $\mu m^{-1}$ with other vibronic features at 2.14 and 2.04 $\mu m^{-1}$. The monocations are not phosphorescent since no emission was observed with the rotating shutter in place in dilute acidic ethanol media.

In ethanolic media 1.0 *M* in sodium hydroxide, however, weak emissions with blurred vibrational structure were observed, with the rotating shutter in place, with maxima at 2.20 $\mu m^{-1}$ and 2.46 $\mu m^{-1}$ for 5- and 8-aminoquinoline respectively. These emissions were coincident with the only emissions observed when the shutter was removed, and are believed to be delayed fluorescence originating from the neutral aminoquinolines. The blue shifts of these emissions (0.10–0.15 $\mu m^{-1}$) relative to the fluorescences observed at dry ice–acetone temperatures are reasonable for fluorescence shifts resulting from the depopulation of "hot-bands" as the temperature is

lowered. The phosphorescences of the dications, however, occur some 0.4–0.6 $\mu m^{-1}$ to the red of the corresponding fluorescences. These results are in contrast to the 5- and 8-hydroxyquinolines in which no phosphorescence or delayed fluorescence is observed at any pH[8]. Consequently, structural analogies should not be carried too far in predicting the luminescence properties of molecules.

The authors are grateful to Professor J. D. Winefordner for allowing them to use his phosphorimetric equipment.

SUMMARY

5-Aminoquinoline and 8-aminoquinoline fluoresce moderately to weakly in low dielectric media but not in strongly hydrogen-bonding or acidic aqueous media. At low temperatures and in rigid media moderately intense fluorescence is observed in aqueous media at all pH values. Quenching of the aminoquinoline fluorescences in fluid media is believed to be due primarily to hydrogen bonding in the lowest excited singlet state. The fluorescences of the aminoquinolines arise from the $^1L_a$ states in the respective molecules. Calculation of approximate excited singlet state $pK_a^*$ values indicates that upon excitation to the $^1L_a$ state the amino group becomes a weaker base while the heterocyclic ring nitrogen becomes a stronger base. Phosphorescence is observed for the doubly protonated cations of both aminoquinolines but not for the singly protonated or neutral species. Both neutral species exhibit delayed fluorescence at 77°K.

RÉSUMÉ

L'amino-5-quinoléine et l'amino-8-quinoléine présentent une fluorescence moyenne à faible, en milieu faiblement diélectrique. On observe une fluorescence relativement intense en milieu aqueux, à tous les pH. Une étude théorique est effectuée sur les phénomènes de fluorescence et de phosphorescence des aminoquinoléines.

ZUSAMMENFASSUNG

5-Aminochinolin und 8-Aminochinolin fluoreszieren mässig bis schwach in niedrigdielektrischen Medien, jedoch nicht in stark wasserstoffbindenden oder sauren wässrigen Medien. Bei tiefen Temperaturen und in unterkühlten Medien wird eine mässig intensive Fluoreszenz in wässrigen Medien bei allen pH-Werten beobachtet. Die Fluoreszenzlöschung der Aminochinoline in flüssigen Medien wird hauptsächlich auf Wasserstoffbindung im niedrigsten angeregten Singulettzustand zurückgeführt. Die Fluoreszenz der Aminochinoline stammt von den $^1L_a$-Zuständen in den betreffenden Molekülen. Die Berechnung der ungefähren $pK_a^*$-Werte für die angeregten Singulettzustände ergibt, dass durch Anregung zum $^1L_a$-Zustand die Aminogruppe eine schwächere Base, der Ringstickstoff eine stärkere Base wird. Phosphoreszenz wird bei den doppelt protonierten Kationen beider Aminochinoline beobachtet, jedoch nicht bei den einfach protonierten und neutralen Spezies. Beide neutralen Spezies zeigen verzögerte Fluoreszenz bei 77°K.

REFERENCES

1 E. A. STECK AND F. C. NACHOD, *Z. Phys. Chem.*, 15 (1958) 372.
2 E. V. BROWN AND A. C. PLASZ, *J. Heterocyclic Chem.*, 7 (1970) 335.
3 S. G. SCHULMAN, *J. Pharm. Sci.*, 60 (1971) 371.
4 A. WELLER, *Progress in Reaction Kinetics*, 1 (1961) 187.
5 R. E. BALLARD AND J. W. EDWARDS, *J. Chem. Soc.*, (1964) 4868.
6 S. F. MASON, J. PHILP AND B. E. SMITH, *J. Chem. Soc.*, (1968) 3051.
7 S. G. SCHULMAN AND Q. FERNANDO, *Tetrahedron*, 24 (1968) 1777.
8 M. GOLDMAN AND E. L. WEHRY, *Anal. Chem.*, 42 (1970) 1178.
9 S. G. SCHULMAN, *Anal. Chem.*, 43 (1971) 285.
10 C. A. PARKER AND W. T. REES, *Analyst*, 85 (1960) 587.
11 J. PLATT, *J. Chem. Phys.*, 17 (1949) 484.
12 S. G. SCHULMAN AND J. D. WINEFORDNER, *Talanta*, 17 (1970) 607.
13 T. FÖRSTER, *Z. Elekrochem.*, 54 (1950) 42.
14 S. G. SCHULMAN, P. T. TIDWELL, J. J. CETORELLI AND J. D. WINEFORDNER, *J. Amer. Chem. Soc.*, 93 (1971) 3179.

*Analytica Chimica Acta*
Elsevier Publishing Company, Amsterdam
Printed in The Netherlands



# LOWEST EXCITED SINGLET STATE $pK_a^*$ VALUES OF THE ISOMERIC AMINOPYRIDINES

S. G. SCHULMAN, A. C. CAPOMACCHIA AND M. S. RIETTA

*Department of Pharmaceutical Chemistry, College of Pharmacy, University of Florida, Gainesville, Fla. 32601 (U.S.A.)*

(Received 16th February, 1971)

The aminopyridines are of analytical interest because of their wide applications as intermediates in the preparation of drugs and dyestuffs.

Recently, there has been a study of the fluorescences of the three isomeric aminopyridines in various solvents[1]. In the latter study, equilibrium constants ($pK_a^*$) for the dissociation, in the lowest excited singlet state, of the monoprotonated aminoquinolines (protonated in the ring) were evaluated from the Förster cycle[2], the average of the long wavelength absorption maximum and fluorescence maximum of each species being used as the 0–0 vibronic band of that species.

Excited state $pK_a^*$ values evaluated from the Förster cycle often yield valuable information about intramolecular charge transfer accompanying excitation and about molecular relaxation processes involving the vibrations of the excited molecule and the reorientation of the solvent cage subsequent to excitation. However, owing to the approximations concerning equal entropies of protonation in ground and exited states and the similarities of the vibrational makeup of ground and excited states of acid and conjugate base, inherent in the Förster cycle, the $pK_a^*$ values calculated from the thermodynamic cycle are frequently not in good agreement with those determined by fluorimetric titration. From the analytical point of view, $pK_a^*$ values determine the optimal pH range of fluorimetric analyses (when excited state prototropism is fast compared with fluorescence) and the selectivity to be obtained in fluorimetric analysis of multicomponent samples[3]. In this context $pK_a^*$ values determined from the Förster cycle are unreliable and those determined by fluorimetric titration alone are suitable for analytical purposes. Moreover, the averaging of absorption and emission maxima to obtain the 0–0 band (an attempt to correct for vibrational discrepancies in ground and excited states) is not valid if the energy associated with reorientation of the solvent cage, after excitation, is not identical for acid and conjugate base[4]. Consequently, it was decided to evaluate the $pK_a^*$ values for all conjugate acid–base pairs derived from the aminopyridines by fluorimetric titrations and by Förster cycle calculations, by means of the shifts in absorption maxima alone, the shifts in fluorescence maxima alone and the shifts in averages of absorption and fluorescence maxima, upon protonation.

## EXPERIMENTAL

2-Aminopyridine, 3-aminopyridine and 4-aminopyridine were purchased from Eastman Organic Chemicals Inc., Rochester, N.Y., K and K Laboratories Inc.,

Plainview, N.Y. and Pfaltz and Bauer, Inc., Flushing, N.Y. The 2- and 3-isomers were purified by one recrystallization each from chloroform, while the 4-isomer was triply recrystallized from chloroform. Acidic solutions were made from Mallinckrodt reagent-grade perchloric acid and sulfuric acid. Basic solutions were prepared by dilution of carbonate-free sodium hydroxide with water. Absorption spectra were taken on a Beckman DB spectrophotometer while fluorescence spectra were taken on a Perkin-Elmer MPF-2A fluorescence spectrophotometer, operated in the ratio-recording mode. Fluorescence spectra were not corrected for the wavelength dependence of the monochromators and the R-106 multiplier phototube; however, the monochromators were calibrated against the line emission spectrum of the xenon lamp.

Fluorimetric titrations were effected by plotting the relative fluorescence intensity of each fluorescing species as a function of pH or Hammett acidity[5]. Förster cycle calculations of $pK_a^*$ were effected by utilizing the relationship

$$pK_a^* = pK_a - 2.10 \cdot 10^{-3} (\bar{\nu}_a - \bar{\nu}_b) \quad (1)$$

where $pK_a^*$ and $pK_a$ are the dissociation constants (at 25°) of the corresponding acid–base reaction in the lowest excited singlet and ground states, respectively, and $\bar{\nu}_a$ and $\bar{\nu}_b$ are the wavenumbers of the electronic transitions of acid and conjugate base, respectively. Values of $pK_a^*$ were calculated for $\bar{\nu}_a$ and $\bar{\nu}_b$ being taken as the wavenumbers of the long wavelength $\pi$–$\pi^*$ absorption maxima, the fluorescence maxima and the average of the two latter quantities, respectively.

## RESULTS AND DISCUSSION

### *Electronic spectra*

The absorption and fluorescence maxima of the various prototropic species derived from the aminopyridines are listed in Table I. Notable among these data is the observation of an extremely weak fluorescence from the singly protonated 4-aminoquinoline in dilute acid solutions and the failure of the doubly charged cation of 3-aminopyridine to fluoresce even in 18 *M* sulfuric acid. No fluorescence was reported by Weisstuch and Testa[1] for the 4-isomer in dilute acid while the fluorescence reported, by these authors, for the doubly charged cation of the 3-isomer in 10 *M* hydrochloric acid appears to be due to the singly charged cation. 3-Aminopyridine in concentrated acid exhibits a weak fluorescence, similar in position to that of the monocation in

TABLE I

LONG WAVELENGTH $\pi$–$\pi^*$ ABSORPTION MAXIMA ($\bar{\nu}_{abs}$) AND FLUORESCENCE MAXIMA ($\bar{\nu}_f$) OF THE PROTOTROPIC SPECIES DERIVED FROM THE AMINOPYRIDINES

| | *Doubly charged cation* (18 $MH_2SO_4$) $\bar{\nu}_{abs}$ ($cm^{-1}$) $\bar{\nu}_f$ ($cm^{-1}$) | *Singly charged cation* (0.1 *M* $HClO_4$) $\bar{\nu}_{abs}$ ($cm^{-1}$) $\bar{\nu}_f$ ($cm^{-1}$) | *Neutral species* ($10^{-3}$ *M* $N_aOH$) $\bar{\nu}_{abs}$ ($cm^{-1}$) $\bar{\nu}_f$ ($cm^{-1}$) |
|---|---|---|---|
| 2-Aminopyridine | $3.89 \cdot 10^4$ | $3.31 \cdot 10^4$ $2.77 \cdot 10^4$ | $3.45 \cdot 10^4$ $2.85 \cdot 10^4$ |
| 3-Aminopyridine | $3.83 \cdot 10^4$ | $3.15 \cdot 10^4$ $2.53 \cdot 10^4$ | $3.46 \cdot 10^4$ $2.76 \cdot 10^4$ |
| 4-Aminopyridine | $3.90 \cdot 10^4$ $2.91 \cdot 10^4$ | $3.80 \cdot 10^4$ $2.79 \cdot 10^4$ | $4.10 \cdot 10^4$ $2.92 \cdot 10^4$ ($3.77 \cdot 10^4$) |

dilute acid. This fluorescence shifts gradually (about 1000 $cm^{-1}$) as the medium is changed from dilute to very concentrated acid. The blue shift is believed to be due to the change in solvent composition, and the quenching of the singly protonated 3-aminopyridine fluorescence in moderately concentrated perchoric acid solutions will later be shown to be due to diffusion-limited static quenching.

2-Aminopyridine was also found to undergo a small blue shift as the solvent medium was changed from dilute to concentrated acid. However, no quenching accompanied the increase in acid concentration. The shift of the absorption spectrum of 2-aminopyridinium ion on protonation should be accompanied by a corresponding shift of comparable magnitude of the fluorescence spectrum if the excited doubly charged cation is generated. Since no such large shift of the fluorescence spectrum was observed, it is assumed that the excited doubly charged cation derived from 2-aminopyridine is too strong an acid to exist in 18 *M* sulfuric acid.

The nature of the lowest $\pi$–$\pi^*$ transition of the neutral species derived from 4-aminopyridine also presents a problem. The long wavelength $\pi$–$\pi^*$ transition of 4-aminopyridine occurs in dilute sodium hydroxide at $4.10 \cdot 10^4$ $cm^{-1}$. A shoulder is present on the long wavelength side of this band at $3.77 \cdot 10^4$ $cm^{-1}$. This shoulder has also been observed in low dielectric media and has been assigned to the $\pi$–$\pi^*$ transition of pyridine[1]. However, the shoulder shifts towards the red with increasing solvent polarity and hydrogen-bond donor capacity and is very intense for a typical symmetry-forbidden $\pi$–$\pi^*$ transition. It is quite possible, however, that the shoulder represents the $^1L_b$ band of pyridine partially submerged in the more intense $^1L_a$ band envelope and is therefore the lowest $\pi$–$\pi^*$ absorption.

*$pK_a^*$ values obtained from the Förster cycle*

The $pK_a^*$ values of the aminopyridines, calculated from the Förster cycle (eqn. 1), the ground state $pK_a$ values[6], and the data of Table I, are presented in Table II. These data indicate that the doubly charged cations of all of the aminopyridines are stronger acids in the lowest excited singlet state than in the ground state. Moreover,

TABLE II

LOWEST EXCITED SINGLET STATE $pK_a^*$ VALUES CALCULATED FROM THE FÖRSTER CYCLE (EQN. 1), THE SPECTRAL DATA OF TABLE I AND THE GROUND-STATE $pK_a$ VALUES

| | $pK_a^*$ *calculated from shift, upon dissociation, of* | | | |
|---|---|---|---|---|
| | $pK_a$ | *Absorption maxima* | *Fluorescence maxima* | *Average of abs. and fluor. maxima* |
| *2-Aminopyridine* | | | | |
| Doubly charged cation | −7.6 | −19.8 | | |
| Singly charged cation | 6.9 | 9.8 | 8.8 | 9.4 |
| *3-Aminopyridine* | | | | |
| Doubly charged cation | −1.5 | −15.8 | | |
| Singly charged cation | 6.0 | 12.5 | 10.8 | 11.7 |
| *4-Aminopyridine* | | | | |
| Doubly charged cation | −6.3 | − 8.4 | −8.6 | −8.5 |
| Singly charged cation | 9.2 | $8.6 < pK_a^* < 15.5$ | 11.9 | $10.2 < pK_a^* < 13.7$ |

the very negative values of the doubly charged cations of the 2- and 3-isomers, derived from absorption data alone, support the conclusion that these species, in the lowest excited singlet state, are too strongly acidic to exist in the strongest acid medium employed in these studies ($H_0$ −10). Consequently, no fluorescence was observed from these species. The doubly charged excited cation of the 4-isomer is, however, accessible in concentrated sulfuric acid (and just barely so in the most concentrated perchloric acid solutions employed). $pK_a^*$ values for the doubly charged cation of 4-aminopyridine calculated from absorption shifts alone, fluorescence shifts alone and the averaging technique were in very good agreement, indicating that the vibrational structures of ground and excited states are similar and that solvent relaxation subsequent to excitation is nearly identical for the doubly protonated and singly protonated cations. The spectral shifts and $pK_a^*$ values of doubly protonated 4-aminopyridine are in agreement with the theoretical model of Mason[7] which predicts that dissociation of this species occurs from the amino nitrogen. The data of Table II indicate that in the lowest excited singlet state the monoprotonated aminopyridinium ions are weaker acids than in the ground state. Mason's benzyl carbanion model[7] and other studies of nitrogen heterocyclics[8] suggest that in this case dissociation occurs from the nitrogen atom in the pyridine ring. The $pK_a^*$ values of the monocations of the 2- and 3-isomers determined from fluorescence shifts tend to be somewhat lower than those determined from absorption shifts, which suggests differences in the vibrational makeup of ground and excited states or differences in solvent cage reorganization for acid and conjugate base, subsequent to excitation. Owing to the uncertainty of the nature of the lowest excited singlet absorption of the neutral species derived from the 4-isomer, only a range can be given for the $pK_a^*$ value calculated from the absorption spectral shift. However, the fluorescence shift of the 4-aminopyridinium ion upon dissociation permits a better estimate of $pK_a^*$, that value being 11.9.

*Variations of relative quantum yields of fluorescence with acidity*

Fluorimetric titrations of the doubly protonated cations of 2-aminopyridine and 3-aminopyridine were not possible owing to the strongly acidic natures of these excited species and the rapidities of their prototropic dissociations compared with their respective rates of radiative deactivation. Fluorimetric titration of the doubly charged 4-isomer, in concentrated sulfuric acid, however, yielded a $pK_a^*$ value of −8.5, in excellent agreement with the data of Table II. In concentrated perchloric acid, the fluorescence of the monoprotonated 2-aminopyridinium ion was not quenched as the acidity of the medium was varied. However, the fluorescence of the monoprotonated 3-aminopyridinium ion was quenched in moderately concentrated perchloric acid solutions, with half quenching occurring at $H_0$ −1.5. Since the ground state $pK_a$ value of the doubly protonated 3-isomer is −1.5, it is believed that the quenching of 3-aminopyridinium ion fluorescence is static (*i.e.* quenching occurs as a result of the ground state reaction). This circumstance is probably due to the diffusion-limited nature of the acid–base reaction, the reaction in the excited state being too slow to compete with fluorescence.

In neutral and dilute basic solutions, the fluorescenses of all three of the aminopyridines shift towards the blue without quenching. The midpoints in the blue shiftings occur at pH values corresponding to the ground-state $pK_a$ values for dissociation of the monoprotonated pyridinium ions. Consequently for all three iso-

mers, excited state prototropism must be too slow to compete with fluorescence for deactivation of the lowest excited singlet state, and the ground-state thermodynamics apparently govern the conversion of fluorescences from those of the monoprotonated species to those of the neutral species.

In basic solutions (pH 11) the fluorescence of the neutral aminopyridines is quenched. Quenching is virtually complete for all isomers at pH 14. Half quenching occurs for the 2-isomer at pH 12.0, for the 3-isomer at pH 12.4 and for the 4-isomer at pH 13. Because of the weak fluorescence of the neutral 4-aminopyridine, the latter value is a rough estimate. No changes in absorption or excitation spectra were observed in the pH range 11–14. It is believed that these quenching phenomena are due to excited-state dissociation of the aminoquinolines to form anions, the protons being lost from the neutral amino groups. Similar processes have been observed in the naphthylamines[9]. While the anions are too strongly basic to exist in aqueous solutions in the ground state, the charge transfer from the amino group to the ring occurring upon excitation enhances the acidities of the pyridines in the excited state. Consequently, the $pK_a^*$ values of 12.0, 12.4 and 13 are assigned to the lowest excited states of the neutral 2-, 3- and 4-aminopyridines, respectively.

Owing to the very weak fluorescence observed for 4-aminopyridine, except in the most concentrated sulfuric acid solutions, fluorimetry would not be a method of choice for the analysis of this compound.

SUMMARY

Dissociation constants for the various prototropic forms of the three isomeric aminopyridines were determined from shifts in absorption spectra, shifts in fluorescence spectra and variations of fluorescence intensity with pH and Hammett acidity. The $pK_a^*$ values obtained indicate that charge transfer from the amino nitrogen to the ring nitrogen occurs upon excitation. The excited doubly charged cations of the 2- and 3-isomers are too strongly acidic to equilibrate with their conjugate bases within the lifetime of the excited state. Quenching of aminopyridine fluorescences in basic solutions is attributed to formation of non-fluorescent anions in the excited state. The weak fluorescence of 4-aminopyridine makes fluorimetry unsuitable as a method of analysis for this compound.

RÉSUMÉ

Une étude est effectuée sur les constantes de dissociation des diverses formes prototropiques de trois aminopyridines isomères, par des mesures d'absorption et de fluorescence. Les valeurs $pK_a^*$ obtenues montrent que le transfert de charge de l'azote amino à l'azote cyclique se fait par excitation. La faible fluorescence de l'amino-4-pyridine n'est pas suffisante pour permettre une analyse par fluorimétrie.

ZUSAMMENFASSUNG

Die Dissoziationskonstanten für die verschiedenen prototropen Formen der drei isomeren Aminopyridine wurden bestimmt, indem die Verschiebungen in den Absorptionsspektren und in den Fluoreszenzspektren sowie die Änderungen der

Fluoreszenzintensität mit dem pH-Wert und der Hammett-Acidität ausgewertet wurden. Die erhaltenen $pK_a^*$-Werte zeigen, dass bei der Anregung ein Charge-transfer vom Aminostickstoff zum Ringstickstoff auftritt. Die angeregten doppelt geladenen Kationen der 2- und 3-Isomeren sind zu stark sauer, um mit ihren konjugierten Basen innerhalb der Lebensdauer des angeregten Zustandes zum Gleichgewicht zu kommen. Die Fluoreszenzlöschung der Aminopyridine in basischen Lösungen wird der Bildung von nichtfluoreszierenden Anionen im angeregten Zustand zugeschrieben. Wegen der schwachen Fluoreszenz von 4-Aminopyridin ist die Fluorimetrie keine geeignete Analysenmethode für diese Verbindung.

## REFERENCES

1 A. WEISSTUCH AND A. C. TESTA, *J. Phys. Chem.*, 72 (1968) 1982.
2 T. FÖRSTER, *Z. Elektrochem.*, 54 (1950) 42.
3 S. G. SCHULMAN AND J. D. WINEFORDNER, *Talanta*, 17 (1970) 607.
4 S. G. SCHULMAN, P. T. TIDWELL, J. J. CETORELLI AND J. D. WINEFORDNER, *J. Amer. Chem. Soc.*, 93 (1971) 3179.
5 M. PAUL AND F. LONG, *Chem. Rev.*, 57 (1957) 1.
6 A. ALBERT, in A. R. KATRITZKY, *Physical Methods in Heterocyclic Chemistry, Vol. 1*, Academic Press, New York, 1963, p. 73.
7 S. F. MASON, *J. Chem. Soc.*, (1960) 219.
8 A. WELLER, *Progress in Reaction Kinetics, Vol. 1*, Pergamon Press, London, 1961, p. 187.
9 H. BOAZ AND G. K. ROLLEFSON, *J. Amer. Chem. Soc.*, 72 (1950) 3435.

*Analytica Chimica Acta*
Elsevier Publishing Company, Amsterdam
Printed in The Netherlands



# DETERMINATION OF DIFFUSION COEFFICIENTS FROM INSTANTANEOUS CURRENT MEASUREMENTS AND THE KOUTECKY EQUATION

JERRY L. JONES* AND HERBERT A. FRITSCHE, JR.**
*Department of Chemistry, Texas A & M University, College Station, Texas 77840 (U.S.A.)*
(Received 15th March 1971)

Many fundamental electrochemical investigations require accurate values of ionic or molecular diffusion coefficients. Such investigations are frequently carried out under conditions which do not satisfy the requirements of the Nernst expression[1] or the limiting laws[2-4]. Hence, diffusion coefficients calculated from these latter expressions may be in error when attempts are made to apply them to more realistic conditions. Only the tracer technique[5,6] has been shown to predict values of the diffusion coefficient which are in agreement with polarographic data[7,8]. Heyrovský and Kůta[9] have discussed the feasibility of determining diffusion coefficients from polarographic data but most attempts at such determinations have met with only limited success[10,11]. Among the more successful attempts are those of Los and Murray[12,13] who derived a polarographic current equation for oscillographic methods. They concluded, and later demonstrated, that diffusion coefficients calculated by their expression from currents measured during the first two seconds of drop life should agree with corresponding tracer values.

This investigation describes a simple method for the determination of diffusion coefficients by means of instantaneous polarographic current data from first drops. The results agree well with the corresponding tracer values. An iterative computer technique and an IBM 7094 computer were used to solve the Koutecky polarographic current equation for the diffusion coefficient. Special consideration has been given to the experimental satisfaction of the assumptions made in the derivation of the current-time equation with special care given to the back-pressure effect and the problems associated with depolarization of the dropping mercury electrode.

## THEORY

The electrochemical determination of diffusion coefficients requires the use of a satisfactory polarographic current expression. The Koutecký equation[14,15] is considered by many investigators to be the most rigorously derived polarographic current equation that considers spherical diffusion to a dropping mercury electrode.

---

* Current address: Department of Chemistry, Central Washington State College, Ellensburg, Wash. 98926, U.S.A.
** Current address: Department of Clinical Pathology, M. D. Anderson Hospital and Tumor Institute, University of Texas at Houston, Houston, Texas 77025, U.S.A.

The Koutecký equation is

$$i = 706\, nD^{\frac{1}{2}} m^{\frac{2}{3}} t^{\frac{1}{6}} C(1 + 39D^{\frac{1}{2}} t^{\frac{1}{6}} m^{-\frac{1}{3}} + 150\, Dt^{\frac{1}{3}} m^{-\frac{1}{3}})$$

where $i$ is the instantaneous current in $\mu$A, $n$ is the number of moles of electrons involved in the overall electrode reaction of one mole of depolarizer, $D$ is the diffusion coefficient in $cm^2\ sec^{-1}$, $C$ is the depolarizer concentration in $mmole\ l^{-1}$, $m$ is the flow rate of mercury through the capillary in $mg\ sec^{-1}$ and $t$ is the drop life in sec.

The use of this equation for the calculation of diffusion coefficients requires that the assumptions made in its derivation be experimentally satisfied. Unless this is done the results will either be in error or only fortuitously correct[16]. The important assumptions embodied are: (*a*) the electrochemical reaction must be diffusion-controlled, (*b*) a spherical mercury drop working electrode must be used, (*c*) negligible concentration polarization should exist and, (*d*) the flow rate of mercury must be constant throughout the drop life.

Diffusion control is experimentally exhibited at all potentials by reversible systems and occurs after the limiting current has been reached among irreversible systems. Convection currents are removed by precise temperature regulation and isolation of the cell from vibration to prevent mechanical mixing. Maxima which may exist should be suppressed by lowering the flow rate of mercury. Caution must be exercised when the use of chemical maximum suppressors is necessary in diffusion coefficient studies[17,18]. Migration currents are made negligible with the use of an appropriate supporting electrolyte.

Spherical mercury drops are produced with capillaries having a diameter up to at least 0.1 mm[19]. Measurements at the end of a drop life are preferred because the capillary shielding effect is negligible[20]. Concentration polarization and concomitant problems associated with the past history of the solution in the vicinity of the electrode are eliminated by measuring instantaneous currents on first drops with a vertical capillary[21,22].

The capillary flow rate of mercury is ordinarily not constant throughout the drop life because of a time-dependent back-pressure effect. Failure to recognize this may introduce considerable error into ordinary polarographic determinations of diffusion coefficients. The error is smaller at the end of a drop life, however, and may be made negligible by careful selection of the capillary orifice and height of the mercury column[23]. In reality, then, the instantaneous flow rate is not equal to the average flow rate; the latter is ordinarily obtained by measuring the weight of several drops. But when the back-pressure effect is made negligible, the instantaneous flow rate near the end of the drop life will approach the value of the average flow rate.

If one assumes that the Poiseuille–Hagen laws[9] apply, then the instantaneous flow rate, $m_t$, can be expressed by

$$m_t = kg\rho(h_c - h_b) \tag{1}$$

where

$$k = \frac{r_c^4\, \rho\pi}{8\, l_c\, v} \tag{2}$$

The instantaneous flow rate is in units of $g\ sec^{-1}$ when the constant $k$ is in cm sec and $h_c$ and $h_b$, the mercury heights corresponding to effective or measured pressure and

back pressure, respectively, are in cm. The constant $g$ is the acceleration due to gravity in cm $sec^{-2}$ and $\rho$ is the density of mercury in g $cm^{-3}$. Included in the constant $k$ are the values for $\pi$; $r_c$, the radius of the capillary in cm; $l_c$, the length of the capillary in cm; and $v$, the viscosity of mercury in dyne $cm^{-2}$.

The instantaneous back pressure, $h_b$, can be written as

$$h_b = 2\gamma(g\rho r_t)^{-1} \tag{3}$$

where

$$r_t = (3m_t t/4\pi\rho)^{\frac{1}{3}} \tag{4}$$

The interfacial tension at a mercury–solution interface is given by $\gamma$ in dynes $cm^{-1}$, $t$ is the time elapsed, in sec, since the birth of the drop and $r_t$ is the radius of the drop, assuming spherical drop behavior, in cm at any time $t$.

A combination of eqns. (3) and (4) gives

$$h_b = k_2\gamma(m_t t)^{-\frac{1}{3}} \tag{5}$$

where

$$k_2 = (2/g\rho)(4\pi\rho/3)^{\frac{1}{3}}. \tag{6}$$

Substitution of eqn. (5) into eqn. (1) yields

$$m_t = kg\rho h_c - kg\rho k_2\gamma(m_t t)^{-\frac{1}{3}} \tag{7}$$

The first term in eqn. (7) is the flow rate independent of back pressure, $m_h$, where

$$m_h = kg\rho h_c \tag{8}$$

For a given capillary, the flow rate independent of back pressure is a function of $h_c$ only and can be determined experimentally from $g$, $\rho$, $h_c$, and $r_c$. The radius of the capillary can be determined from drop weight data.

A similar expression can be derived for the average flow rate, $\bar{m}$, in the same manner. In this case the average radius of the drop, $\bar{r}$, must be substituted into the back-pressure term. Now

$$\bar{r} = \tfrac{3}{4}(3\bar{m}t_d/4\pi\rho)^{\frac{1}{3}} \tag{9}$$

where $t_d$ is the drop life in sec. The average flow rate is therefore

$$\bar{m} = kg\rho h_c - (\tfrac{4}{3})kg\rho k_2\gamma(\bar{m}t_d)^{-\frac{1}{3}} \tag{10}$$

Again, the first term in eqn. (10) is the flow rate independent of back pressure, $m_h$.

The second terms in eqns. (7) and (10) express the influence of back pressure on the flow rate of mercury. This correction is larger in the case of the average flow rate than for the instantaneous flow rate.

Consideration of eqns. (7) and (10) also shows that the instantaneous flow rate will be somewhat larger than the average flow rate at the end of the drop life, although during the early part of the drop life $m_t$ will be smaller than $\bar{m}$. This back-pressure term is a function of interfacial tension, flow rate, time and the constant, $k$, but it is independent of $h_c$ for a given capillary.

Equation (7) reveals that for a given capillary the back-pressure correction term will be a function of time only if all other parameters are held constant. This term

will have its largest value early in the drop life but as the drop grows this term becomes small. Therefore at the end of the drop life the back-pressure term makes its smallest contribution to the flow rate. If the value of $m_h$ is made large compared to the second term then the contribution of the back pressure to the flow rate is made small, especially near the end of the drop life. This condition can be met by a proper choice of $h_c$ and $r_c$. During the latter part of the drop life, then, both $m_t$ and $\bar{m}$ approach $m_h$ and the experimental value of $m$ can be assumed to approximate quite closely the almost constant flow rate exhibited near the end of the drop life.

Kůta and Smoler[24] state that if the flow rate can be kept high, *i.e.* on the order of 2 mg $sec^{-1}$, the back-pressure correction will lie within the range of experimental error of the recording polarograph and may be neglected. Thus the requirement that the flow rate be constant near the time of current measurement can be met by careful experimentation.

## EXPERIMENTAL

### *Electrical measurements*

A Sargent Model XXI polarograph was used to record conventional polarograms and a Sargent Model FS polarograph was used for precision measurements of maximum currents on single drops. The recorder pen speed was 1 sec for full scale deflection, which is sufficient for accurate current measurement provided that the drop time is greater than about 2 sec[25]. Recorder current calibration was accomplished by applying the bridge potential to a 100 kΩ (±0.05%) General Radio standard resistor. The potential across the resistor was first adjusted to give a recorder pen deflection that was approximately equal to that given by the test solution, and the potential was then measured with a potentiometer. The magnitude of the current flowing at a particular value of recorder pen displacement was calculated from Ohm's law. The current in μA divided by the deflection in mm gave the true sensitivity factor for a selected instrument sensitivity setting. The potential of the working electrode was controlled with a Sargent IR compensator which is similar to the one described by Arthur and Vanderkam[26].

Temperatures were regulated at 25.00±0.02°. The cell, reference and counter electrodes have been described previously[27]. The cell and dropping mercury assembly were cushioned to prevent mechanical mixing. Current measurements were made with the constant temperature bath momentarily turned off to prevent mechanical noise and a.c. interference induced in the recorder. A cathetometer was used to measure mercury column heights (±0.04 mm).

### *Reagents*

Triply distilled mercury was used for the working electrode. Analytical-grade lead(II) nitrate, zinc(II) nitrate, and thallium(I) nitrate were used to prepare the depolarizer solutions. Thallium solutions were standardized by a potassium iodate titration and zinc and lead solution concentrations were determined titrimetrically with EDTA solutions. All other chemicals used in this investigation were reagent grade. Distilled water was passed through a thoroughly seasoned ion-exchange column before use. Matheson prepurified nitrogen was used without further purification.

*Procedure*

*Polarographic current measurement.* Normal, well-defined polarograms were obtained for each depolarizer. Mercury flow rates were made as high as possible without causing maxima of the second kind. These were always less than 2 mg $sec^{-1}$. A point on the limiting current plateau of the wave was chosen for measurement of maximum currents on single drops and the polarographic bridge was set at this potential. Several drops were allowed to form and fall with the circuit open to insure the absence of any depletion effects. As a selected drop just began to grow the circuit was closed and the instantaneous current was recorded on this drop and serial drops. Six measurements were made in this manner for each depolarizer. Drop times were measured and average flow rates were determined from drop weight data for each depolarizer solution with the circuit closed. After subtractive correction for the residual current, the instantaneous current, drop time, average flow rate, depolarizer concentration and number of electrons involved in the electrochemical reaction were substituted into the Koutecký equation for calculation of the diffusion coefficient.

*Iterative computer technique.* The Bolzano bisection iterative computer technique was used to solve the Koutecký equation for the diffusion coefficient. The method is based on the theorem that if $f(x)$ is a real function, that is, continuous between $x=a$ and $x=b$, where $a$ and $b$ are real numbers, and if $f(a)$ and $f(b)$ are of opposite signs, then there is a real root, $x=p$, between $a$ and $b$. The Bolzano bisection technique goes further and predicts that the root lies midway between $a$ and $b$, say at $p_1$. The theorem is then applied to the subintervals. If $f(a)$ and $f(p_1)$ are of the same sign the root does not lie in this interval, but in the region of $f(p_1)$ and $f(b)$. Once the correct interval is found it is bisected and the new root, $p_2$, is predicted by bisection of the new interval. The iteration is continued until the product becomes zero, that is, $f(p_i)=0$ or until the difference between iteration values becomes very small, so that $p_i-p_{i+1}$ approaches zero. This method is similar to that of false position[28,29]. The computer program was written in double precision to eliminate roundoff error. A Fortran IV listing of the program and the variable names are available from the authors.

## RESULTS AND DISCUSSION

*Average flow rate*

As mentioned earlier, if an agreement between experimental currents and currents predicted by the Koutecký equation is to be obtained, the effects of back pressure must not be present. To assess the importance of the back pressure, diffusion coefficients were determined on a depolarizer at varying mercury column heights. The radius of the capillary was $3.26 \cdot 10^{-3}$ cm and the length of the capillary was 16.8 cm. The results are shown in Table I. The diffusion coefficient increased only slightly with increasing flow rates and all values agreed with the tracer values to within 2%. It appears that under these experimental conditions the effect of back pressure is negligible. However, this test must be performed with each new capillary and depolarizer solution to be examined in order to insure the absence of back-pressure interference. If a dependence does occur, the height of the mercury column, and hence the average flow rate, must be adjusted to minimize it or another capillary must be selected.

*Depolarizer diffusion coefficients*

The diffusion coefficients of lead(II), zinc(II), and thallium(I) were determined

TABLE I

INFLUENCE OF AVERAGE FLOW RATE OF MERCURY ON CALCULATED DIFFUSION COEFFICIENT OF LEAD(II)

(Diffusion coefficients were measured under the following conditions: supporting electrolyte, 0.100 *M* HCl and 0.100 *M* KCl; depolarizer, 0.962 m*M* $Pb(NO_3)_2$; length of capillary, 16.8 cm; radius of capillary, $3.26 \cdot 10^{-3}$ cm; applied voltage, $-1.00$ V *vs.* saturated calomel electrode.)

| $h_c$ (*cm*) | $t_d$ (*sec*) | $\bar{m}$ (*mg sec*$^{-1}$) | $i$ (*μA*) | *Diffusion coefficient* $\cdot 10^5$ |
|---|---|---|---|---|
| 54.0 | 4.79 | 1.747 | 8.97 | 0.960 |
| 48.0 | 5.77 | 1.456 | 8.28 | 0.958 |
| 38.0 | 6.92 | 1.214 | 7.63 | 0.953 |
| 28.5 | 8.92 | 0.938 | 6.83 | 0.953 |

TABLE II

POLAROGRAPHIC DIFFUSION COEFFICIENTS IN AQUEOUS SOLUTION[a]

(Supporting electrolytes were 0.100 *M* potassium chloride and 0.100 *M* hydrochloric acid for Pb(II), 0.100 *M* potassium chloride for Tl(I), and 1.00 *M* ammonium chloride and 1.00 *M* ammonium hydroxide for Zn(II).)

| *Ion* | *Concentration* (*mM*) | $t_d$ (*sec*) | $\bar{m}$ (*mg sec*$^{-1}$) | $i$ (*μA*) | *Diff. coeff.* $\cdot 10^5$ | *Tracer diff. coeff.*[a] $\cdot 10^5$ |
|---|---|---|---|---|---|---|
| Pb(II) | 0.962 | 4.79 | 1.747 | 8.97 | 0.960 | 0.963 |
| | 1.198 | 4.83 | 1.743 | 11.13 | 0.954 | |
| | 1.051 | 5.49 | 1.561 | 9.39 | 0.963 | |
| Tl(I) | 1.102 | 6.93 | 1.212 | 6.41 | 1.85 | 1.84 |
| | 1.216 | 6.89 | 1.216 | 6.42 | 1.82 | |
| | 1.101 | 6.61 | 1.274 | 6.57 | 1.86 | |
| Zn(II) | 0.674 | 5.13 | 1.224 | 5.27 | 1.02 | 1.02 |
| | 0.724 | 5.16 | 1.219 | 5.61 | 1.00 | |

[a] Tracer diffusion coefficients for Zn(II) and Pb(II) are taken from ref. 5. The value for Tl(I) is from ref. 6.

in the respective electrolytes; the values are given in Table II. The capillary that was characterized in the study mentioned previously was used. Each diffusion coefficient value represents the average of six measurements on first drops. Currents were of the order of 5–10 μA and the range of repetitive current measurements was not greater than 0.02 μA; this range of less than 0.4% of the mean is an indication of the overall reproducibility of each measurement. The range, or estimated error, for each value of the diffusion coefficient entered in Table II is ±1.5% of the reported mean value. The calculated diffusion coefficients agree with the mean values of tracer diffusion coefficients to within less than 2% in all cases. Considering that the uncertainty in the tracer values themselves is 1–2%, the tracer values have been essentially reproduced by the polarographic technique.

*Koutecky equation*

Some investigators state that the last term in the equation is negligible and, since the entire equation is difficult to solve by normal methods, the last term is

usually dropped. The entire equation is easily solved by a computer technique. For comparison, when the data in Table II were used to recalculate diffusion coefficients from the Koutecký equation without the last term, the diffusion coefficient of lead(II) was higher by approximately 0.5% and those for zinc(II) and thallium(I) were higher by approximately 1.0%. Thus it can be concluded that the third term may not always be negligible as some authors believe[30].

The authors gratefully acknowledge the partial financial support of Texas A&M University through a Graduate College Research Fellowship and the Fund for Organized Research.

SUMMARY

Disagreements between experimental polarographic currents and those predicted by the Koutecký equation often arise from failure to consider depolarizer concentration depletion and the influence of back pressure on the time-dependent flow rate of mercury from the dropping mercury electrode. The magnitudes of these effects have been made negligible by measuring maximum currents on first drops and by adjusting the capillary constants. With proper consideration of the assumptions implicit in the mathematical model and careful experimental measurements, the use of the Koutecký current–time relationship has yielded polarographic diffusion coefficients for lead(II), zinc(II), and thallium(I) which agree with tracer values within 2%. The use of all three terms in the equation is shown to be justified. A computer program which utilized the Bolzano bisection reduced tedious calculations.

RÉSUMÉ

On examine les différences obtenues entre courants polarographiques expérimentaux et courants calculés par l'équation de Koutecký. Les écarts observés sont négligeables si les courants maxima sont mesurés sur les premières gouttes et si les constantes du capillaire sont ajustées. On a pu ainsi obtenir des valeurs á 2% près pour les mesures polarographiques du plomb, du zinc et du thallium(I). Un programme d'ordinateur, utilisant la bisection de Bolzano permet d'éviter des calculs fastidieux.

ZUSAMMENFASSUNG

Unterschiede zwischen den experimentellen polarographischen Strömen und jenen, die nach der Koutecký-Gleichung zu erwarten sind, entstehen häufig dadurch, dass die Verarmung der Depolarisatorkonzentration und der Einfluss des Gegendrucks auf die zeitabhängige Fliessgeschwindigkeit des Quecksilbers aus der tropfenden Quecksilberelektrode nicht berücksichtigt werden. Diese Effekte konnten durch Messung der Maximalströme bei den ersten Tropfen und Anpassung der Kapillarkonstanten vernachlässigt werden. Bei geeigneter Berücksichtigung der im mathematischen Modell enthaltenen Voraussetzungen und bei sorgfältigen experimentellen Messungen ergab die Anwendung der Koutecký-Strom–Zeit-Beziehung polarographische Diffusionskoeffizienten für Blei(II), Zink(II) und Thallium(I), die mit Tracer-

Werten innerhalb 2% übereinstimmten. Es wird gezeigt, dass die Anwendung aller drei Glieder in der Gleichung gerechtfertigt ist. Ein Computerprogramm unter Anwendung der Bolzano-Bisektion verminderte langwierige Berechnungen.

REFERENCES

1 W. NERNST, *Z. Phys. Chem. (Leipzig)*, 2 (1888) 613.
2 L. GOSTING AND H. HARNED, *J. Amer. Chem. Soc.*, 73 (1951) 159.
3 L. ONSAGER, *Ann. N. Y. Acad. Sci.*, 46 (1945) 241.
4 T. WILLIAMS AND C. MONK, *Trans. Faraday Soc.*, 57 (1961) 447.
5 J. WANG AND F. POLESTRA, *J. Amer. Chem. Soc.*, 76 (1954) 1528.
6 J. WANG AND F. POLESTRA, *J. Amer. Chem. Soc.*, 76 (1954) 1584.
7 A. FONDS, A. BRINKMAN AND J. LOS, *J. Electroanal. Chem.*, 14 (1967) 43.
8 R. BEARMAN, *J. Phys. Chem.*, 66 (1962) 2072.
9 J. HEYROVSKÝ AND J. KŮTA, *Principles of Polarography*, Academic Press, New York, 1966, p. 106.
10 D. TURNHAM, *J. Electroanal. Chem.*, 10 (1965) 19.
11 H. STRELOW AND M. VON STACKELBERG, *Z. Elektrochem.*, 57 (1953) 342
12 J. LOS AND D. MURRAY, *Advances in Polarography, Vol. 2*, Pergamon Press, New York, 1960, p. 425.
13 J. LOS AND D. MURRAY, *Advances in Polarography, Vol. 2*, Pergamon Press. New York, 1960, p. 437.
14 J. KOUTECKÝ, *Czech. J. Phys.*, 2 (1953) 50.
15 D. R. CROW AND J. V. WESTWOOD, *Polarography*, Methuen, London, 1968, p. 19.
16 J. LINGANE, *J. Amer. Chem. Soc.*, 75 (1953) 788.
17 C. TANFORD, *J. Amer. Chem. Soc.*, 74 (1952) 211.
18 G. RUSSELL, *J. Polarog. Soc.*, 11 (1965) 7.
19 G. SMITH, *Trans. Faraday Soc.*, 47 (1952) 63.
20 J. MACDONALD AND F. WETMORE, *Trans. Faraday Soc.*, 47 (1951) 533.
21 W. HANS, W. HENNE AND E. MEURER, *Z. Elektrochem.*, 58 (1954) 836.
22 W. HANS AND W. HENNE, *Naturwissenschaften*, 40 (1953) 524.
23 J. HEYROVSKÝ AND J. KŮTA, *Principles of Polarography*, Academic Press, New York, 1966, p. 94.
24 J. KŮTA AND I. SMOLER, *Progress in Polarography, Vol. 1*, Interscience, New York, 1962, p. 43.
25 H. MCKENZIE AND M. TAYLOR, *Australian J. Chem.*, 11 (1958 260.
26 P. ARTHUR AND R. K. VANDERKAM, *Anal. Chem.*, 33 (1961) 765.
27 J. L. JONES AND H. A. FRITSCHE, *J. Electroanal. Chem.*, 12 (1966) 334.
28 G. KORN AND T. KORN, *Mathematical Handbook for Scientists and Engineers*, McGraw-Hill, New York, 1961, p. 631.
29 K. KUNZ, *Numerical Analysis*, McGraw-Hill, New York, 1957, p. 4.
30 L. MEITES, *Polarographic Techniques*, Interscience, New York, 2nd Edn., 1965, p. 116.

*Analytica Chimica Acta*
Elsevier Publishing Company, Amsterdam
Printed in The Netherlands



# POLAROGRAPHIC DETERMINATION OF CHLORAMPHENICOL

KJETIL FOSSDAL AND EINAR JACOBSEN
*Department of Chemistry, University of Oslo, Blindern, Oslo 3 (Norway)*

(Received 6th April 1971)

Chloramphenicol is an extremely valuable antibiotic, and titrimetric[1], spectrophotometric[2-8] and chromatographic[9-14] procedures have been outlined for its determination in pharmaceuticals and biological materials. However, these methods are time-consuming and besides, the solubility characteristics of chloramphenicol make isolation by liquid–liquid extraction difficult. On the other hand, polarographic methods are rapid and less susceptible to interference and should be advantageous for routine analysis of chloramphenicol.

Polarographic methods for the determination of chloramphenicol depend upon the reducibility of the nitro group. According to Hess[15] the drug is reduced in two steps in acidic medium, the first step being well defined. Hess recommended 0.2 *M* phthalate buffer pH 4 as supporting electrolyte, in conjunction with a large concentration of thymol to suppress a maximum on the curve. However, the polarographic wave is partly deformed by this surfactant and later workers have recommended gelatine[16] and methylene blue[17] as maximum suppressors. With methylene blue, the wave height is said to be proportional to the concentration in the range 40–500 $\mu$g ml$^{-1}$.

Preliminary experiments indicated that the drug is more reversibly reduced when ionic surfactants are used as maximum suppressors. The present work was carried out in order to examine the electroreduction of chloramphenicol more carefully and to investigate the application of polarography to routine analysis of the drug.

## EXPERIMENTAL

### *Equipment*

Polarograms were recorded with a Metrohm E 261 R Polarecord connected to a Metrohm E 393 a.c. modulator. An Ag/AgCl/saturated KCl electrode served as reference electrode and a tungsten electrode was employed as auxiliary electrode. All a.c. polarograms were obtained with an amplitude of 10 mV r.m.s. The capillary characteristics of the dropping mercury electrode, measured in 0.1 *M* potassium nitrate (open circuit) at a mercury height of 45.7 cm, were $m = 2.950$ mg sec$^{-1}$ and $t = 2.44$ sec. All experiments were performed at $25 \pm 0.1°$. Dissolved air was removed from the solutions by bubbling oxygen-free nitrogen through the cell for 10 min and passing it over the solution during the electrolysis.

Cyclic voltammetry, chronopotentiometry and coulometry were performed with a versatile solid-state instrument constructed in this laboratory following the design of Goolsby and Sawyer[18]. A Mosely 7030 AM X-Y recorder and a Honeywell

Electronic 194 strip-chart recorder were used in conjunction with the instrument. A three-electrode assembly was used for all measurements. A Metrohm E410 hanging mercury drop was used as working electrode for the cyclic voltammetric and chronopotentiometric experiments, and a mercury pool was employed for the controlled-potential coulometric measurements. The reference electrode was an aqueous silver/silver chloride electrode and a platinum coil served as auxiliary electrode. These electrodes were isolated in glass tubes with fine-porosity fritted glass discs. The shield tubes were filled with the supporting electrolyte used in the sample solution. The solution was stirred with a magnetic stirrer and a Teflon stirring bar.

*Chemicals*

Chloramphenicol (D-threo-2-dichloroacetamido-1-(4-nitrophenyl)propane-diol-(1,3)) was obtained (99 % pure) from Apothekernes Laboratorium, Oslo, Norway. A 1 m*M* stock solution was prepared by dissolving the appropriate amount of the commercial product in distilled water.

Decylamine (Koch-Light, Ltd, England) was used as maximum suppressor. A 1 % stock solution was prepared by dissolving 1 g of the amine in 100 ml of distilled water containing an equivalent amount of perchloric acid. All other chemicals were reagent grade and were used without further purification. The pH of all solutions was determined with a Beckman Zeromatic pH meter.

## RESULTS

*Polarography*

Polarograms of 0.5 m*M* chloramphenicol recorded from acidic solutions exhibit a large maximum, which is hard to suppress by common surfactants. Experiments showed, however, that the maximum was easily suppressed by decylamine. Moreover, the half-wave potential and the limiting current were unaffected even when the amount of this surfactant was increased to 0.003%.

The effect of pH on the first polarographic wave was investigated by recording polarograms of 0.5 m*M* chloramphenicol in dilute acids, acetate, phthalate and citrate buffers; 0.003 % decylamine was added to each solution. A well defined wave was obtained from all electrolytes. The reversibility of the electrode reaction was tested for each polarogram by determining the value $E_{\frac{1}{4}} - E_{\frac{1}{4}}$. Some data are given in Table I.

TABLE I

POLAROGRAPHIC DATA OF 0.5 m*M* CHLORAMPHENICOL IN VARIOUS ELECTROLYTES WITH 0.003% DECYLAMINE PRESENT

| *Supporting electrolyte* | *pH* | $E_{\frac{1}{4}}$ (*V*) | $E_{\frac{1}{4}} - E_{\frac{1}{4}}$ (*mV*) |
|---|---|---|---|
| HCl/NaCl | 1.6 | −0.16 | −32 |
| HCl/NaCl | 2.0 | −0.18 | −30 |
| Acetate | 3.7 | −0.25 | −32 |
| Acetate | 5.0 | −0.30 | −28 |
| Acetate | 6.3 | −0.38 | −30 |
| Phthalate | 3.7 | −0.31 | −60 |
| Citrate | 7.5 | −0.43 | −52 |

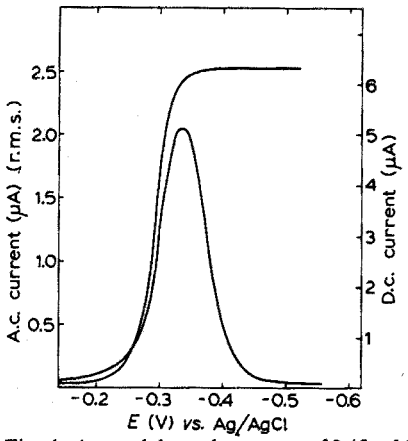


Fig. 1. A.c. and d.c. polarograms of 0.45 m*M* chloramphenicol in 0.5 *M* acetate buffer pH 4.7 with 0.003% decylamine present.

According to Hess[15] the slope of the plot of log $i/(i_d - i)$ *vs.* the potential was −91 mV for polarograms recorded from phthalate buffer pH 4 with thymol as maximum suppressor. It is interesting to note that this value decreased to −60 mV when decylamine was used to suppress the maximum, and it decreased to −28 mV when acetate buffer was used as supporting electrolyte. Because the steepest wave was obtained from acetate buffers, 0.5 *M* acetate buffer pH 4.7 and 0.003% decylamine were used as supporting electrolyte in the following experiments. The half-wave potential in this electrolyte was $E_{\frac{1}{2}} = -0.287$ V *vs.* Ag/AgCl.

The d.c. polarographic step was followed by an a.c. polarographic wave (Fig. 1), indicating that a fast electron-transfer is involved in the overall electrode reaction. The summit potential, $E_s$, was 40 mV more negative than the half-wave potential.

The effect of drop time was investigated by recording polarograms of 0.5 m*M* chloramphenicol in 0.5 *M* acetate buffer at various heights of the mercury column. The value $i \cdot h^{-\frac{1}{2}}$, where $h$ is the height of the column after correction for the "back-pressure", was constant, indicating that the d.c. current was diffusion-controlled. However, the height of the a.c. wave increased linearly with increasing height of the column, which implies that the concentration of the depolarizer responsible for the a.c. current is time-dependent and that the a.c. current is partly controlled by the rate of a slow reaction[19,20].

The temperature coefficient (determined in the range 25–45°) of the d.c. current, +1.27% per degree, and that of the a.c. peak current, +0.95% per degree, implies that the current is controlled essentially by diffusion.

In acetate buffers the half-wave potential of chloramphenicol was shifted −47 mV per pH unit to more negative values with increasing pH. The number of hydrogen ions, $Z$, consumed in the electrode reaction is given by

$$\Delta E_{\frac{1}{2}}/\Delta \mathrm{pH} = -0.059\ Z/\alpha n_a$$

where $\alpha$ is the transfer coefficient. The value $\alpha n_a$ calculated from the equation

$$E = E_{\frac{1}{2}} - (0.059/\alpha n_a) \log (i/i_d - i)$$

was 1.97, which gives the value $Z = 1.6$. Consequently, two hydrogen ions probably participate in the rate-determining step of the electrode reaction.

The second polarographic step of chloramphenicol previously reported by Hess[15] is only poorly developed at pH 4.7. The wave is obviously due to an irreversible reduction but it was not possible to obtain reproducible values for the half-wave potential and limiting current.

TABLE II

POLAROGRAPHIC DATA FOR THE REDUCTION OF VARIOUS AMOUNTS OF CHLORAMPHENICOL IN 0.5 *M* ACETATE BUFFER pH 4.7

| *Concn.* (*mM*) | *Amount of decylamine* (%) | $i_d$ ($\mu A$) | $i_d/C$ ($\mu A\ mmole^{-1}$) |
|---|---|---|---|
| 1.740 | 0.0030 | 24.8 | 14.3 |
| 0.994 | 0.0030 | 14.2 | 14.3 |
| 0.806 | 0.0030 | 12.0 | 14.9 |
| 0.621 | 0.0030 | 9.20 | 14.8 |
| 0.497 | 0.0030 | 7.50 | 15.0 |
| 0.248 | 0.0015 | 3.75 | 15.1 |
| 0.0994 | 0.0015 | 1.50 | 15.1 |
| 0.0750 | 0.0015 | 1.10 | 14.7 |
| 0.0500 | 0 | 0.710 | 14.2 |
| 0.0100 | 0 | 0.140 | 14.0 |
| 0.0075 | 0 | 0.110 | 14.7 |
| 0.0050 | 0 | 0.070 | 14.0 |
| 0.0025 | 0 | 0.035 | 14.0 |
| 0.0010 | 0 | 0.015 | 15.0 |
| | | Mean | 14.58 |

Polarograms recorded from 0.5 *M* acetate buffer pH 4.7 with various amounts of chloramphenicol present, showed that the d.c. current increased linearly with concentration. Decylamine was used as maximum suppressor. No maximum was observed at concentrations of the drug below 0.05 m*M* and no decylamine was added to these solutions. The results (Table II) indicate that chloramphenicol can be determined by polarography in the entire concentration range $10^{-6}$ to $2 \cdot 10^{-3}$ *M* which corresponds to 0.3–600 $\mu$g $ml^{-1}$. The diffusion current constant, $I = i_d/Cm^{\frac{2}{3}}t^{\frac{1}{6}}$, calculated from the data in Table II, is $I = 6.10$.

The height of the a.c. polarographic wave is much lower than the corresponding d.c. current. Moreover, it is not proportional to the concentration. Hence, a.c. polarography has no advantage over conventional d.c. polarography for the determination of chloramphenicol.

*Cyclic voltammetry*

Voltammetric experiments were performed at a hanging mercury drop electrode. Reproducible waves were obtained provided that the mercury drop was exchanged between each potential sweep. If the potential sweep was repeated at the same mercury drop, the peak heights decreased and the peak potentials were shifted to

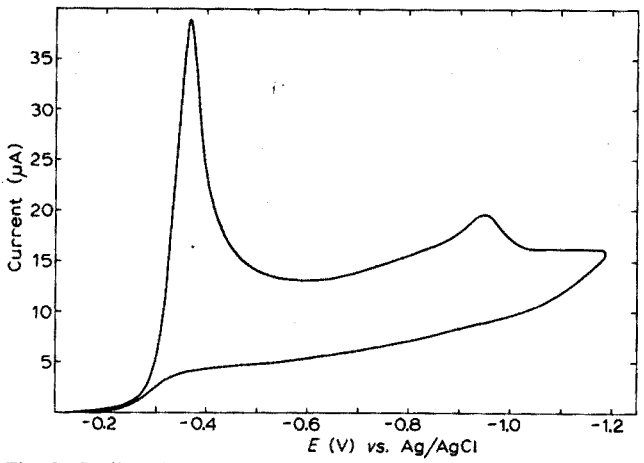


Fig. 2. Cyclic voltammogram of 0.5 m*M* chloramphenicol in 0.5 *M* acetate buffer pH 4.7 at a mercury electrode. Scan rate, 0.2 V $sec^{-1}$.

more negative values, indicating that the reduction product was adsorbed at the electrode.

Voltammograms recorded at fast scan rates exhibited two cathodic peaks at potentials corresponding to the two polarographic steps (Fig. 2). At slower scan rates the second peak was split into two peaks (Fig. 3), indicating that this electrode reaction involved a slow step. No anodic peak resulting from reoxidation of the reduction product was observed at any scan rate. Voltammetric data obtained from acetate buffer pH 4.7 are given in Table III.

Values of $\alpha n_a$ may be calculated from cyclic voltammetric data relating peak potential and the logarithm of the scan rate in the relationship

$$(E_p)_2 - (E_p)_1 = (0.059/2\alpha n_a) \log (v_1/v_2)$$

where $(E_p)_1$ and $(E_p)_2$ are the two peak potentials for a given reaction, $v_1$ and $v_2$ the appropriate scan rates and $n_a$ the number of electrons in the rate determining step.

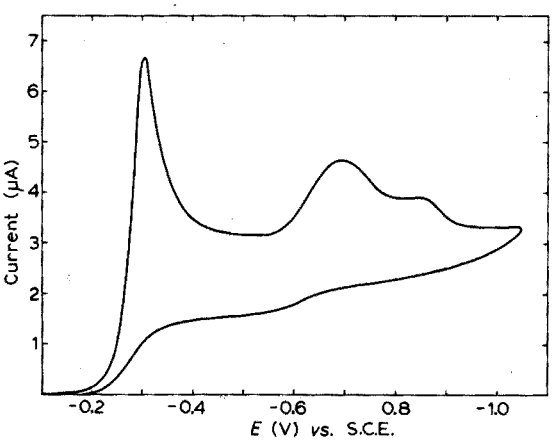


Fig. 3. Cyclic voltammogram of 0.5 m*M* chloroamphenicol in 0.5 *M* acetate buffer pH 4.7 at a mercury electrode. Scan rate, 0.0083 V $sec^{-1}$.

TABLE III

VOLTAMMETRIC DATA FOR THE REDUCTION OF 0.5 *M* CHLORAMPHENICOL IN 0.5 *M* ACETATE BUFFER pH 4.7

| *Scan rate* $v_1 (V\ sec^{-1})$ | *First wave* | | | *Second wave* | | |
|---|---|---|---|---|---|---|
| | $-E_p$ (*V*) | $i_p$ ($\mu A$) | $i_p v^{-\frac{1}{2}}$ ($\mu A\ V^{-\frac{1}{2}}\ sec^{\frac{1}{2}}$) | $-E_p$ (*V*) | $i_p$ ($\mu A$) | $i_p v^{-\frac{1}{2}}$ ($\mu A\ V^{-\frac{1}{2}}\ sec^{\frac{1}{2}}$) |
| 0.50 | 0.415 | 45.75 | 65 | 0.988 | 10.5 | 14.9 |
| 0.20 | 0.368 | 38.25 | 86 | 0.950 | 6.8 | 15.2 |
| 0.10 | 0.345 | 27.88 | 88 | 0.918 | 5.3 | 16.8 |
| 0.033 | 0.328 | 17.25 | 95 | 0.875 | 2.6 | 14.3 |
| 0.016 | 0.313 | 10.00 | 78 | 0.760, 0.865 | | |
| 0.0083 | 0.303 | 6.95 | 76 | 0.705, 0.850 | | |
| 0.0033 | 0.298 | 4.47 | 78 | 0.660, 0.830 | | |
| 0.0016 | 0.293 | 3.17 | 79 | 0.643, 0.815 | | |

The values of $\alpha n_a$ for the first wave calculated from the data in Table III at scan rates of 0.0016–0.0083 V $sec^{-1}$ (a time scale comparable to the polarographic data) was 2.1, which is close to the value calculated from the polarographic wave ($\alpha n_a = 1.97$) and indicates that four electrons are involved in the electrode reaction. However, the value $\alpha n_a$ calculated from faster sweep rates decreased with increasing sweep rate, which indicates that a slow one- or two-electron transfer is involved in the overall reaction.

The calculated values of $\alpha n_a$ for the second and third voltammetric wave were 0.3 and 0.6, respectively, indicating that the poorly developed second polarographic wave is due to two slow one-electron transfer reactions.

The current function, $i_p/v^{\frac{1}{2}}$, of the first wave was constant at scan rates below 0.02 V $sec^{-1}$, indicating that the current became diffusion-controlled at slow scan rates.

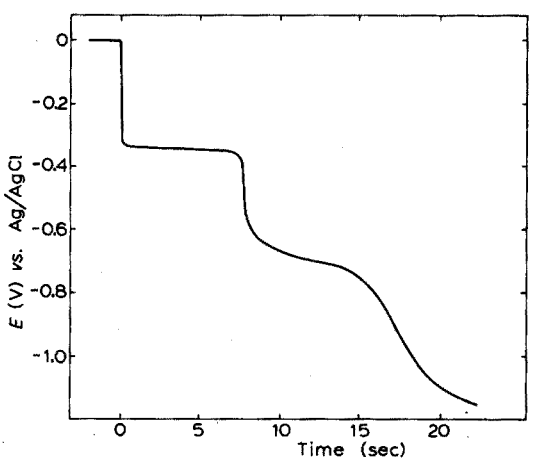


Fig. 4. Chronopotentiogram of 0.5 m*M* chloramphenicol in 0.5 *M* acetate buffer at a mercury electrode. Current, 7.0 $\mu$A.

TABLE IV

CHRONOPOTENTIOMETRIC DATA FOR THE REDUCTION OF 0.5 m$M$ CHLORAMPHENICOL IN 0.5 $M$ ACETATE BUFFER pH 4.7

| *Current* ($\mu A$) | $\tau$ (*sec*) | $E_{t=0}$ ($V$) | $E_{\tau/4}$ ($V$) |
|---|---|---|---|
| 10 | 2.68 | −0.352 | −0.353 |
| 9 | 3.50 | −0.345 | −0.348 |
| 8 | 4.80 | −0.343 | −0.345 |
| 7 | 7.66 | −0.338 | −0.340 |
| 6 | 16.55 | −0.333 | −0.335 |
| 5 | 27.95 | −0.328 | −0.330 |
| 4 | 44.0 | −0.323 | −0.325 |
| 3 | | −0.315 | |
| 2 | | −0.303 | |
| 1 | | −0.283 | |

*Chronopotentiometry*

The reduction of chloramphenicol in acetate buffer pH 4.7 gave rise to two-step chronopotentiograms (Fig. 4). The first wave was well defined and the quarter-wave potential was close to the peak potential of the first cyclic voltammetric wave (Table IV). Reproducible data were obtained provided that the mercury drop was exchanged between each run. The second chronopotentiometric wave was less well defined; accurate data were hard to obtain and are not included in the Table. The quarter wave potential of the second wave, $E_{\tau/4}$, was about −0.74 V.

No reverse (anodic) chronopotentiometric wave was observed, which indicates a highly irreversible process. The potential–time relationship for such processes is given by[21]

$$E = (0.059/\alpha n_a)\,[\log nFC^0 k^0_{fh} i_0^{-1} + \log (\tau^{\frac{1}{2}} - t^{\frac{1}{2}})\tau^{-\frac{1}{2}}]$$

where $E$ is the potential of the working electrode, $\alpha$ the transfer coefficient, $n_a$ the number of electrons in the rate-controlling step, $F$ the faraday, $k^0_{fh}$ the forward heterogeneous rate constant, $i_0$ the current density, $C^0$ the concentration of the active species in the bulk of the solution, $\tau$ the transition time and $t$ the time after the electrolysis is started. At $t=0$ the equation reduces to:

$$E_{t=0} = (0.059/\alpha n_a) \log nFC^0 k^0_{fh} i_0^{-1}$$

By applying a constant current and recording the potential of the working electrode as a function of time, $E_{t=0}$ can be obtained by extrapolation of the potential–time curve to zero.

A plot based on this equation for the first chronopotentiometric wave of chloramphenicol in acetate buffer pH 4.7 is illustrated in Fig. 5. The slope of the line is 0.062 which gives the value $\alpha n_a = 0.95$. This experiment indicates that the rate-determining charge-transfer step involves two electrons.

*Coulometry*

Coulometric reductions at controlled potential of chloramphenicol in 0.5 $M$ acetate buffer pH 4.7 were performed to determine the number of electrons involved

in the overall electron-transfer reactions. The experiments were carried out in the absence of air with a small electrolysis cell and a mercury pool as working electrode.

The potential of the mercury pool was first controlled at $-0.50$ V *vs.* Ag/AgCl. In this experiment 9.15 coulombs were consumed in the reduction of $2.5 \cdot 10^{-5}$ mole of chloramphenicol which yields the value $n = 3.8$ for the first electrode reaction. The experiment was repeated with a new solution containing the same amount of chloramphenicol and with the potential of the working electrode controlled at $-1.00$ V; 14.94 coulombs were consumed in this reduction, corresponding to a value of $n = 6.2$. These experiments clearly demonstrate that four electrons are involved in the first polarographic step and that the second step involves two electrons.

## CONCLUSION

It is evident from the experimental results that a slow electron-transfer reaction is involved in the reduction of chloramphenicol. The galvanostatic experiment established that two electrons are involved in the rate-determining step and the shift in half-wave potentials with increasing pH indicates that two hydrogen ions are consumed in the reaction. On the other hand, coulometric experiments established that four electrons are consumed in the overall reduction and hence, the following reduction mechanism may be postulated for the first polarographic wave

$$R\text{-}NO_2 + 2H^+ + 2e^- \xrightarrow{\text{slow}} R\text{-}NO + H_2O$$

$$R\text{-}NO + 2H^+ + 2e^- \xrightarrow{\text{fast}} R\text{-}NHOH$$

The fast reduction of the nitroso group is probably responsible for the appearance of an a.c. polarographic wave and the preceding slow reduction of the nitro group explains the drop-time dependence of the a.c. current.

The second reduction wave of chloramphenicol involves two electrons and is probably due to a further reduction of the hydroxylamine group to the amine.

$$R\text{-}NHOH + 2H^+ + 2e^- \xrightarrow{\text{slow}} R\text{-}NH_2 + H_2O$$

This reduction is highly irreversible, and the polarographic wave is only poorly defined. Cyclic voltammetric experiments indicate that the reduction occurs in two steps and that the first one-electron reduction to an intermediate radical species is the rate-determining step.

## ANALYTICAL APPLICATIONS

Polarograms of chloramphenicol recorded from 0.5 *M* acetate buffer pH 4.7 with 0.003% decylamine present exhibit a very well-defined wave. The current is diffusion-controlled and proportional to the concentration in the entire range $10^{-6}$–$10^{-3}$ *M*. Obviously, this supporting electrolyte is much better than the phthalate buffer previously recommended for polarographic determination of the drug in pharmaceuticals[17].

Alessandro[22] recommends a spectrophotometric method for the determination of chloramphenicol in milk. However, the procedure is very time-consuming and

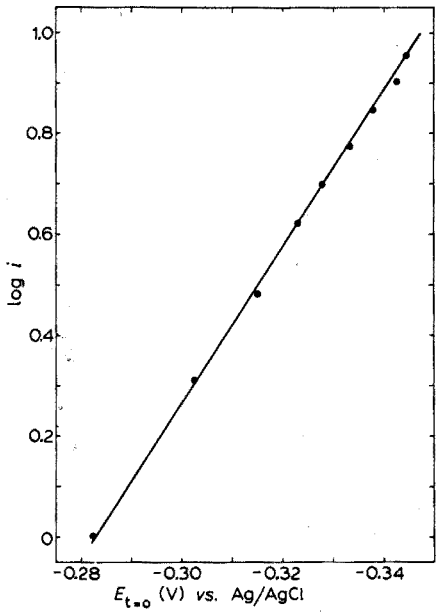


Fig. 5. Galvanostatic studies of the reduction of 0.5 m*M* chloramphenicol in 0.5 *M* acetate buffer pH 4.7. The current is given in $\mu$A.

includes isolation of the drug by a series of extractions. Preliminary experiments showed that a polarographic wave of chloramphenicol is observed even in the presence of milk. Hence, a few experiments were performed in order to modify the polarographic method for determination of the drug in milk without any preceding and time-consuming separation.

Experiments showed that the proteins present in milk are surface-active and that the polarographic wave of chloramphenicol is partly distorted by the adsorbed layer on the electrode. The limiting current is depressed and the wave is shifted to more negative potentials. However, in acetate or phosphate buffer with pH 6–7 a

TABLE V

POLAROGRAPHIC DETERMINATION OF CHLORAMPHENICOL IN MILK
(Supporting electrolyte, 1 : 1 mixture of milk and 0.5 *M* phosphate buffer pH 6.4)

| *Concn.* (*mM*) | *Concn. in pure milk* ($\mu g\ ml^{-1}$) | *Current* $i_d$ ($\mu A$) | $i_d/C$ ($\mu A\ mM^{-1}$) |
|---|---|---|---|
| 0.100 | 65.0 | 0.92 | 9.2 |
| 0.080 | 52.0 | 0.715 | 8.9 |
| 0.050 | 32.5 | 0.440 | 8.8 |
| 0.010 | 6.5 | 0.089 | 8.9 |
| 0.0075 | 4.87 | 0.068 | 9.0 |
| 0.0050 | 3.25 | 0.047 | 9.4 |
| 0.0025 | 1.63 | 0.038 | 15 |
| 0.0010 | 0.65 | 0.030 | 30 |

well-defined polarographic wave is obtained even in the presence of 50% milk. In these mixtures the half-wave potential is $-0.60$ V *vs.* Ag/AgCl, the slope of the plot of $\log i/i_d - i$ *vs.* the potential is $\pm 0.070$ and the diffusion current is still about 65% of the value obtained in the absence of milk.

In a series of experiments equal volumes of milk and buffer pH 6.4 containing various amounts of chloramphenicol were mixed and transferred to a polarographic cell. The air was removed with nitrogen and a polarogram recorded.

The results (Table V) show that the drug can be determined in milk in the concentration range 3–60 $\mu$g ml$^{-1}$ with a relative deviation of a few %. At lower concentration the current is not proportional to the concentration. However, the current is perfectly reproducible and by using a standard curve the concentration of the drug can be estimated even in the range 0.3–3 $\mu$g ml$^{-1}$.

SUMMARY

The electroreduction of chloramphenicol has been studied by polarography, cyclic voltammetry, chronopotentiometry and coulometry. The experimental results lead to the conclusion that the drug undergoes a slow 2-electron reduction of the nitro group which is followed by a fast 2-electron reduction to hydroxylamine. At more negative potentials the hydroxylamine group is further reduced to the amine. In acetate buffer pH 4.7 with 0.003% decylamine present, the drug produces a very well-defined, diffusion-controlled 4-electron polarographic wave. The current is proportional to the concentration and permits the drug to be determined by polarography in the concentration range 0.3–600 $\mu$g ml$^{-1}$. A rapid polarographic method for the determination of chloramphenicol in milk is proposed.

RÉSUMÉ

Une étude est effectuée sur l'électroréduction du chloramphénicol, par polarographie, voltammétrie cyclique, chronopotentiométrie et coulométrie. Les résultats expérimentaux conduisent à la conclusion qu'il se produit une réduction lente (à 2 électrons) du groupe nitro, suivie d'une réduction rapide (à 2 électrons) en hydroxylamine. Le groupe hydroxylamine est ensuite réduit en amine à des potentiels plus négatifs. Un dosage polarographique est proposé, en milieu tampon pH 4.7, avec 0.003% de décylamine, pour des concentrations de 0.3 à 600 $\mu$g ml$^{-1}$, en particulier dans le lait.

ZUSAMMENFASSUNG

Die elektrochemische Reduktion von Chloramphenicol wurde durch Polarographie, cyclische Voltammetrie, Chronopotentiometrie und Coulometrie untersucht. Aus den experimentellen Ergebnissen ist zu schliessen, dass das Arzneimittel einer langsamen 2-Elektronenreduktion der Nitrogruppe unterliegt, auf die eine schnelle 2-Elektronenreduktion zum Hydroxylamin folgt. Bei negativeren Potentialen wird die Hydroxylamingruppe weiter zum Amin reduziert. In Acetatpuffer pH 4.7 mit einem Gehalt von 0.003% Decylamin ruft das Mittel eine sehr gut definierte, diffusionskontrollierte polarographische 4-Elektronenstufe hervor. Der Strom ist

der Konzentration proportional und erlaubt die Bestimmung des Arzneimittels durch Polarographie im Konzentrationsbereich 0.3–600 $\mu$g $ml^{-1}$. Eine rapidpolarographische Methode für die Bestimmung von Chloramphenicol in Milch wird vorgeschlagen.

REFERENCES

1 P. N. PANDEY AND V. CHANDRA, *Z. Anal. Chem.*, 231 (1961) 35.
2 F. M. FREEMAN, *Analyst*, 81 (1956) 299.
3 K. KAKEMI, T. ARITA AND S. OHASHI, *Yakugaku Zasshi*, 82 (1962) 342.
4 J. JACQUET AND F. CHARTON, *Compt. Rend. Acad. Agr. France*, 49 (1963) 373.
5 R. C. SHAH, P. V. RAMAN AND B. M. SHAH, *J. Pharm. Sci.*, 52 (1963) 167.
6 D. W. O'GORMAN HUGHES AND L. K. DIAMOND, *Science*, 144 (1964) 296.
7 R. C. SHAH, P. V. RAMAN AND P. V. SHETH, *Indian J. Pharm.*, 30 (1968) 68.
8 D. S. MASTERSON, *J. Pharm. Sci.*, 57 (1968) 305.
9 P. D. SHAW, *Anal. Chem.*, 35 (1963) 1580.
10 G. L. RESNICK, D. CORBIN AND D. H. SANDBERG, *Anal. Chem.*, 38 (1966) 582.
11 R. SABA, D. MONNIER AND F. R. KHALIL, *Pharm. Acta Helv.*, 42 (1967) 335.
12 Y. T. LIN, K. T. WANG AND T. I. WANG, *J. Chromatog.*, 21 (1966) 158.
13 R. ROUSSELET AND R. PARIS, *Ann. Pharm. Franc.*, 22 (1964) 249.
14 M. YAMAMOTO, S. IGUCHI AND T. AOYAMA, *Chem. Pharm. Bull. (Tokyo)*, 15 (1967) 123.
15 G. B. HESS, *Anal. Chem.*, 22 (1950) 649.
16 C. RUSSU, I. CRUCEANU, D. MONCIU AND V. BARCARU, *Farmaco, Ed. Prat.*, 20 (1965) 22.
17 F. SUMMA, *J. Pharm. Sci.*, 54 (1965) 442.
18 A. D. GOOLSBY AND D. T. SAWYER, *Anal. Chem.*, 39 (1967) 411.
19 G. H. AYLWARD AND J. W. HAYES, *J. Electroanal. Chem.*, 8 (1964) 442.
20 E. JACOBSEN, *Anal. Chim. Acta*, 35 (1966) 447.
21 P. DELAHAY, *New Instrumental Methods in Electrochemistry*, Interscience, New York, 1954.
22 A. ALESSANDRO, *Boll. Lab. Chim. Provinciali (Bologna)*, 14 (1963) 355.

*Analytica Chimica Acta*
Elsevier Publishing Company, Amsterdam
Printed in The Netherlands



# STANDARDISATION OF DILUTE AQUEOUS BROMINE SOLUTIONS FOR REACTION KINETICS BY INCREMENTAL POTENTIOMETRIC TITRATION WITH THIOSULPHATE

R. E. EVANS AND D. R. MARSHALL
*Department of Chemistry, University College of North Wales, Bangor (Wales)*

(Received 15th March 1971)

The kinetics of very fast bromination reactions can be measured potentiometrically by using very dilute bromine solutions with concentrations down to *ca.* $10^{-8}$ $M$[1]. When second-order kinetics are measured, it is necessary to know the actual bromine concentration. Even when pseudo-first order kinetics are employed, and the bromine concentration is not required in calculations, it is necessary to know initially that the bromine concentration is much less than that of the substrate, and some knowledge of the bromine concentration is desirable.

Bromine is usually determined titrimetrically after first liberating an equimolar amount of iodine from added potassium iodide, but for kinetics this method clearly cannot be used directly. A practicable variant, however, is to produce a bromine concentration high enough for this conventional determination by adding a drop of pure bromine to the reaction solution at the end of each kinetic run, and measuring the potential produced at an indicator electrode relative to that measured at the beginning of the kinetic run. The final concentration is then determined by adding potassium iodide and titrating the liberated iodine with thiosulphate, and the initial concentration is calculated from this value and the difference in potentials[2]. This method is a variant of the widely used incremental addition technique. The method is simplest to apply if bromide ions are always present in a constant concentration much greater than that of bromine, when the Nernst equation simplifies to

$$E = E' + (RT/2F) \ln [Br_2] \quad (1)$$

and the potential change is given by

$$\Delta E = E_2 - E_1 = (RT/2F) \ln [Br_2]_2/[Br_2]_1 \quad (2)$$

In practice, however, this method suffers from the drawback that it is only possible to tell whether or not the initial bromine concentration is kinetically suitable when it is too late to alter it.

This drawback could be avoided by withdrawing samples of the initial bromine solution before substrate is added to start the reaction, and determining the bromine concentration in the samples by some suitable method, but transfer of samples of very dilute bromine solutions often leads to extensive loss of bromine by evaporation or by reaction with trace impurities, and sample transfer is not, therefore, reliable.

The necessary very dilute bromine solutions of suitable concentrations can, however, be prepared and standardised without any of these difficulties by using other incremental methods. The most direct is incremental addition of standard bromine solution, when the final bromine concentration is found by simultaneous solution of eqn. (3) (giving the value of the increment)

$$\Delta[Br_2] = [Br_2]_2 - [Br_2]_1 \quad (3)$$

together with eqn. (2). Further additions can then be made if it is necessary to adjust the concentration.

This incremental addition method has three defects. One, common to all such methods, is that the accuracy is affected greatly by errors in the measurement of $\Delta E$. A second defect, peculiar to the use of volatile solutes, is that a standard bromine solution does not remain standard for long under most conditions, owing to evaporation. This, however, is a different source of evaporative error from that mentioned before, as evaporation during the *addition* of the standard bromine solution is effectively compensated. The bromine solution is both standardised and used by delivery from a syringe, and errors due to evaporation in the two operations thus largely cancel. The third defect is that incremental addition to produce very dilute standard bromine solutions must use very dilute solutions throughout. Trace impurities in reaction vessels and solutions commonly consume significant proportions of such low concentrations for some time, making the method somewhat time-consuming. Furthermore, when extremely low bromine concentrations are used, the electrode response to concentration changes may be less than the theoretical Nernst slope[1], when accurate determinations are not possible.

The second and third defects can be overcome by using instead a technique of incremental subtraction, in which much higher bromine concentrations are used, and known amounts of bromine are removed by quantitative titration with a suitable reductant. Sodium thiosulphate is a suitable reductant, and it has been established that accurately standard bromine solutions over a wide range of concentrations may be prepared by this means.

Thiosulphate is commonly titrated against iodine, which in weakly acidic solution oxidises thiosulphate quantitatively to tetrathionate. In alkaline solutions iodine is a more powerful oxidant, and when the hydrogen ion concentration is sufficiently low will oxidise thiosulphate to sulphate[3]. The redox potential of bromine, however, is such that even in acidic solution bromine will oxidise thiosulphate to sulphate[3,4]. The stoichiometry of this last reaction has been investigated over a wide range of bromine concentration, to establish the validity and accuracy of this analytical method.

## EXPERIMENTAL

### *Chemicals and equipment*

Chemicals were of AnalaR grade. Water was redistilled from alkaline permanganate to remove reducing impurities. Standard sodium thiosulphate solutions were freshly prepared and stabilised, and were standardised against potassium iodate.

The apparatus was that used for kinetic measurements. The reaction vessel was a cylindrical glass vessel having four necks fitted with Quickfit sockets to accom-

modate the electrodes and a spiral glass stirrer, and to allow access for addition of reagents. The capacity of the cell was about 150 ml. The cell normally contained 100 ml of reaction solution, which was kept at 25° by immersion in a thermostat.

The reference electrode was an E.I.L. screened glass electrode kept at constant potential by added perchloric acid (usually 0.1 *M*). (The use of a glass reference electrode[5] eliminates liquid junctions, and by having a very high impedance limits current flow and prevents polarisation of the indicator electrode.) The indicator electrode was of bright platinum (5 mm square). The cell potential was measured by means of an E.I.L. Model 23A pH meter. The output current from the meter was fed through an accurate decade resistance box, and the potential developed across this resistor was applied to a Control Instruments "Hi-speed" potentiometric chart recorder. By choice of a suitable value for the decade resistor, it was possible to arrange full scale deflection on the chart for any desired range of cell potential. The potential calibration of the circuit was checked periodically against a calibrated potential source, fed by a Mallory cell and giving 0–100 mV to within 0.05 mV. This source was itself calibrated against a Pye precision vernier potentiometer or against a Solartron LM 1426 digital voltmeter, each using a Weston standard cell.

The stability and sensitivity of the recorder were within 0.1 % and its linearity within 0.2 % of the full scale deflection, limiting the effective accuracy of measurements made within the full scale deflection. It was sometimes convenient to back-off part of larger changes in cell potential with the calibrated potential source (see Fig. 1), and the accuracy of measurement was then mainly dependent on the accuracy of the potential source, namely within about 0.05 mV. Over periods of 10–15 min, registered potentials fluctuated slowly over a range of about 0.05 mV cell potential, so that spot readings were liable to errors of this order, but averaged values were more reliable than this,

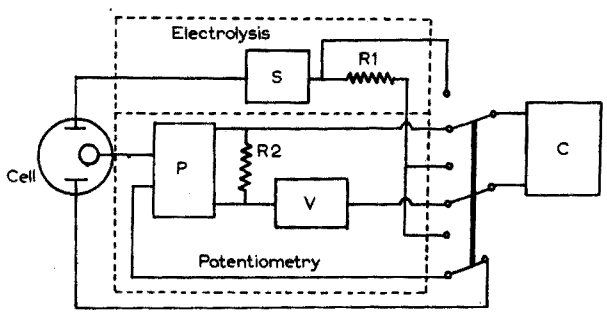


Fig. 1. Circuit used for incremental electrolysis and incremental potentiometric titration. (S) Steady current source; (P) pH meter; (V) calibrated variable potential source; (C) chart recorder.

as were small potential changes recorded on an expanded scale over a period of a minute or less.

## RESULTS

### *Stoichiometry of the bromine–thiosulphate reaction*

When sodium thiosulphate solution (0.1 *M*) was titrated against a solution of bromine (0.09 *M*) and sodium bromide (1 *M*), the volume required was only one eighth of that needed when potassium iodide was first added to the bromine solution.

(This procedure was adopted to compensate for evaporative losses during transfer of bromine solution.) When the end-points were observed potentiometrically, successive ratios found were 7.98, 8.00, 7.96, and 8.04. The molar ratio of bromine to thiosulphate was thus 4.00, corresponding to quantitative oxidation of thiosulphate to sulphate.

To verify that the stoichiometry remained constant even at low bromine concentrations, an initial bromine concentration of *ca.* $10^{-6}$ *M* was established in the reaction vessel. When a steady potential was obtained after reaction of any oxidisable impurities in the vessel, standard bromine solution was added from an "Agla" micrometer syringe, causing the potential to rise sharply. Freshly prepared, stabilised sodium thiosulphate solution (0.001 *M*) was titrated into the vessel from another syringe until the potential fell to its original value, and the stoichiometry was calculated (Table I).

TABLE I

STOICHIOMETRY OF BROMINE OXIDATION OF THIOSULPHATE IN DILUTE SOLUTIONS

| $10^6 \cdot$ *moles* $Br_2$ *(initial)* | $10^6 \cdot$ *moles* $Br_2$ *added* | *Thiosulphate (ml, 0.001008 M)* | *Stoichiometry* |
|---|---|---|---|
| 0.711 | 1.37 | 0.338 | 4.02 |
| 0.711 | 1.37 | 0.336 | 4.05 |
| 0.711 | 1.37 | 0.345 | 3.94 |
| 0.680 | 1.37 | 0.338 | 4.03 |
| 0.680 | 1.35 | 0.336 | 4.00 |
| 0.525 | 1.40 | 0.350 | 3.97 |
| | | Mean stoichiometry | = 4.002 |
| | | Standard error | = 0.017 |

Error caused by loss of bromine from the standard solution was overcome by frequent restandardisation.

In separate experiments the amount of sulphate produced in the reaction was measured volumetrically by a standard microchemical method. Sodium thiosulphate solution (10 ml, $5.10 \cdot 10^{-4}$ *M*) was oxidised with pure bromine (1 drop; excess), and the excess of bromine was removed by addition of ascorbic acid. The solution was titrated photometrically with barium perchlorate and Dimethylsulphonazo III indicator[6], and found to contain $1.012 \cdot 10^{-5}$ mole sulphate, *i.e.* 1.984 moles per mole of thiosulphate used (theory requiring 2 moles).

Thus, over the range of concentrations used, the reaction is quantitatively:

$$S_2O_3^{2-} + 4Br_2 + 5H_2O = 2SO_4^{2-} + 10H^+ + 8Br^-$$

*Incremental titration of bromine*

If a bromine solution is partly titrated with $V$ ml of $M$ molar thiosulphate giving a total volume $V_t$,

$$(Br_2)_1 - (Br_2)_2 = 4VM/V_t \qquad (4)$$

where $(Br_2)$ denotes a total (analytical) bromine concentration, *i.e.* $[Br_2] + [Br_3^-]$.

Insertion of numerical values into eqn. (2) and conversion to decadic logarithms gives the value of $\Delta E$ in millivolts:

$$\Delta E = 29.5 \log [Br_2]_2/[Br_2]_1$$

or

$$(Br_2)_2/(Br_2)_1 = \text{antilog}\,(\Delta E/29.5) \quad (5)$$

Combination of eqns. (4) and (5) gives the values of the bromine concentration before, $(Br_2)_1$, and after, $(Br_2)_2$, the addition of thiosulphate, the generally used form being

$$(Br_2)_2 = (4MV/V_t)\,\text{antilog}\,(\Delta E/29.5)/[1 - \text{antilog}\,(\Delta E/29.5)] \quad (6)$$

The application of these equations was tested by adding a number of successive measured quantities of standard thiosulphate solution to a suitable bromine solution containing relatively large concentrations of bromide and perchloric acid. From the potential change produced by each addition were calculated the initial and final bromine concentrations, $(Br_2)_{i(n)}$ and $(Br_2)_{f(n)}$. Since $(Br_2)_{f(n)}$ and $(Br_2)_{i(n+1)}$ refer to the same bromine solution, but are independent determinations of the bromine concentration, a series of checks on the reproducibility of the method was obtained (Table II).

TABLE II

REPRODUCIBILITY OF BROMINE DETERMINATIONS WITH SMALL INCREMENTS
($V_t$ = 100 ml. Thiosulphate $1.008 \cdot 10^{-3}$ $M$)

| *Addition number* | $V$ (*ml*) | $-\Delta E$ (*mV*) | $10^6\,(Br_2)_{f(n)}$ | $10^6\,(Br_2)_{i(n+1)}$ |
|---|---|---|---|---|
| 1 | 0.020 | $2.0_7$ | $4.6_0$ | $4.5_8$ |
| 2 | 0.020 | $2.4_8$ | $3.7_7$ | $3.8_8$ |
| 3 | 0.020 | $2.9_8$ | $3.1_3$ | $3.5_4$ |
| 4 | 0.020 | $3.3_1$ | $2.7_3$ | $2.4_8$ |
| 5 | 0.020 | $5.0_6$ | $1.6_7$ | $1.7_7$ |
| 6 | 0.020 | $7.7_9$ | $0.9_7$ | – |

TABLE III

REPRODUCIBILITY OF BROMINE DETERMINATIONS WITH LARGER (COMBINED) INCREMENTS

| *Addition number* | $\Sigma V$ (*ml*) | $-\Delta E$ (*mV*) | $10^6\,(Br_2)_{original}$ |
|---|---|---|---|
| 1 | 0.020 | $2.0_7$ | $5.4_1$ |
| 2 | 0.040 | $4.5_5$ | $5.4_0$ |
| 3 | 0.060 | $7.5_3$ | $5.4_3$ |
| 4 | 0.080 | $10.8_4$ | $5.6_5$ |
| 5 | 0.100 | $15.9_0$ | $5.6_7$ |
| 6 | 0.120 | $23.6_9$ | $5.7_4$ |
| | | | Mean = 5.55 |
| | | | $\sigma$ = 0.15 (2.8%) |

The results have also been calculated differently (Table III), the readings at each incremental stage being used to calculate an (independent) value for the bromine concentration obtained at the end of the series of additions, giving a different form of check on reproducibility.

A further independent verification of the method was obtained by coulometry,

when bromine generated by electrolysis provided incremental additions to a bromine solution in the way that added standard bromine solution did in the earlier experiments. A steady current generator giving an output of about 0.7 mA generated bromine by electrolysis of acidified sodium bromide solution (0.1 $M$ $HClO_4$, 0.1 $M$ NaBr) in the reaction vessel, which was provided with a second platinum electrode for the purpose. The circuit (Fig. 1) could be switched to the usual potential measuring function. A bromine concentration of about $10^{-6}$ $M$ was first established. Then a further quantity of bromine was generated, the quantity being found from the chart record, which showed the duration and magnitude of the current by recording the potential drop across a suitable precision resistor R1. By switching to the potential measuring circuit the increase in potential caused by the generation of more bromine was found in the usual way. The final bromine concentration was found from this incremental addition, for which

$$(Br_2)_2 - (Br_2)_1 = (Br_2)_2\,[\text{antilog}\,(\Delta E/29.5) - 1]/\text{antilog}\,(\Delta E/29.5)$$

Since 1 coulomb will produce $5.18 \cdot 10^{-6}$ moles of bromine, in 100 ml of solution a current of $I$ amps will produce in time $t$ sec a quantity

$$(Br_2)_2 - (Br_2)_1 = 5.18 \cdot 10^{-5}\, It$$

Hence the final concentration is given by

$$(Br_2)_2 = 5.18 \cdot 10^{-5}\, It\ \text{antilog}\,(\Delta E/29.5)/[\text{antilog}\,(\Delta E/29.5) - 1] \qquad (7)$$

This concentration was immediately measured again by incremental subtraction through titration with thiosulphate, the two values being, of course, independent. Several such pairs of determinations were carried out (Table IV).

TABLE IV

REPRODUCIBILITY OF BROMINE CONCENTRATIONS DETERMINED INDEPENDENTLY BY INCREMENTAL ELECTROLYSIS AND BY INCREMENTAL TITRATION

| *Current (mA)* | *Time (sec)* | *ΔE (mV)* | $10^6 \cdot (Br_2)$ *after electrolysis* | |
|---|---|---|---|---|
| | | | *By incremental electrolysis* | *By incremental titration* |
| 0.728 | 60.05 | $16.5_2$ | 3.11 | 3.14 |
| 0.728 | 59.65 | $13.5_6$ | 3.43 | 3.43 |
| 0.727 | 51.05 | $10.4_2$ | 3.44 | 3.45 |
| 0.730 | 54.45 | $11.8_3$ | 3.41 | 3.46 |
| 0.727 | 35.75 | $8.0_8$ | 2.87 | 2.84 |
| 0.733 | 72.5 | $14.5_7$ | 4.03 | 4.02 |
| 0.728 | 29.75 | $15.2_0$ | 1.61 | 1.71 |

## DISCUSSION

It is clear that under all the experimental conditions used the reaction between bromine and thiosulphate ions is quantitatively:

$$S_2O_3^{2-} + 4Br_2 + 5H_2O = 2SO_4^{2-} + 10H^+ + 8Br^-$$

The two ultimate standards used for bromine determination, the iodine–thiosulphate reaction and quantitative electrolysis, are independent, and show complete agreement. The agreement in the results in Table IV is independent of the Nernst slope value for the electrode, and so is independent of any systematic anomalies of electrode behaviour. In most experiments, bromine was always present in excess, but even in the first experiments with 0.1 *M* solutions, when bromine was completely reduced, the stoichiometry was exactly the same. This is to be expected from the large free energy change calculated for the reaction[4].

The accuracy of the titrations depends largely on the accuracy with which potential changes can be measured. This is found generally in incremental titrations, owing to the exponential relationship between potential and concentration functions. (The most suitable measuring system might be a precision digital voltmeter reading to 0.01 mV, with print-out of the reading every few seconds, but this was not available.) In contrast, even the relatively large volumes of titrant added in the stoichiometry experiments (Table I) produced a dilution error of only 0.04 mV, certainly no larger than the likely end-point errors of the order of 0.1 mV (corresponding to about 0.4 % of the titre). In general, titrant volumes did not exceed 0.1 % of the total volume, the corresponding changes then being less than 0.013 mV at 25°, corresponding to an error of less than 0.1 % in the final bromine concentration.

Other minor sources of potential change when titrant is added are the production of bromide ions by the reduction of bromine and, when a glass reference electrode is used, the simultaneous formation of hydrogen ions. These potential changes may be calculated from the Nernst equation, reduced to the form

$$E = (RT/F) \ln ([S]_2/[S]_1) = 59.0 \log ([S]_2/[S]_1) \quad (8)$$

where S represents the ions concerned. Thus, a suitable bromine concentration before titration might be $10^{-5}$ *M*. If this is almost wholly reduced, the addition concentrations of bromide and hydrogen ions produced will be $8 \cdot 10^{-5}$ and $1 \cdot 10^{-4}$ *M*, respectively. If the solution contains 0.1 *M* concentrations of each ion, the corresponding potential changes will be a decrease for the indicator electrode of 0.020 mV and an increase for the glass reference electrode of 0.025 mV, resulting in a decrease of cell potential of 0.045 mV. This corresponds to an underestimate of 0.36 % in the eventual bromine concentration, and can be neglected if it is within the experimental error, or if it is otherwise acceptable. If, however, the concentrations of bromide and hydrogen ions were each 0.01 *M*, instead of 0.1 *M*, the corresponding decrease of cell potential would be 0.454 mV, and the underestimate of final bromine concentration 4.5 %. Such a large error in bromine concentration would be unacceptable when second-order kinetics were employed, and it would be necessary to calculate the correction. The amounts of bromide and hydrogen ions produced in the titration may, of course, be calculated from the amount of thiosulphate used, and it can then easily be seen whether or not a correction is necessary.

Another small source of error is the change in the proportion of bromine complexed in the form of tribromide anions. This will be roughly an order of magnitude smaller than the errors produced by ionic concentration changes, however, and so may usually be neglected.

The results in Table II were obtained under unfavourable conditions. The volumes of thiosulphate added, though small, were liable to errors of only *ca.* 1 %, but

much larger errors in the measured potential changes were likely. The agreement between the last two columns is poor, suggesting substantial measuring errors.

The same measurements, however, yield the values in Table III, for which the standard deviation (2.8%) would often be acceptable in kinetic experiments. This shows that the method gives better results when larger potential changes are used, as is to be expected. The values for the original bromine concentration in Table III increase somewhat as the working bromine concentration falls, which suggests that at the lowest concentrations the indicator electrode might have been slightly less sensitive towards concentration changes than is required by the Nernst equation; these figures may, nevertheless, give a realistic estimate of the level of error to be expected under many conditions.

In the electrolysis experiments this last possible source of error was eliminated, as was discussed earlier, and the agreement shown in Table IV is surprisingly good.

Although only thiosulphate has been used, the method could obviously be applied generally, for other reductants, with appropriate alterations to the stoichiometry numbers. Arsenite might be used instead of thiosulphate, for example. The choice of reductant would depend partly on the possible effects of the oxidation products in the final solution, since any products which might produce side effects, such as complex formation, must be avoided. Sulphate ions are likely to be generally acceptable in this respect.

We thank the Science Research Council for a research studentship to R.E.E.

SUMMARY

Aqueous bromine in the concentration range $10^{-1}$–$10^{-6}$ $M$ oxidizes thiosulphate quantitatively to sulphate. This reaction can be used to standardise very dilute bromine solutions by addition of a measured but insufficient quantity of relatively concentrated standard thiosulphate solution. The fall in bromine–bromide redox potential at an inert indicator electrode caused by the addition allows the final bromine concentration to be found. The method can be applied in the measurement of fast bromination kinetics.

RÉSUMÉ

Le brome en solution aqueuse ($10^{-1}$ à $10^{-6}$ $M$) oxyde quantitativement le thiosulfate en sulfate. Cette réaction permet d'étalonner des solutions très diluées de brome, par addition d'une quantité déterminée, mais insuffisante de thiosulfate étalon. La chute de potentiel rédox brome–bromure à une électrode indicatrice inerte permet de déterminer la concentration en brome. Cette méthode peut s'appliquer à des mesures de cinétiques rapides de bromation.

ZUSAMMENFASSUNG

Wässrige Bromlösung im Konzentrationsbereich $10^{-1}$–$10^{-6}$ $M$ oxydiert Thiosulfat quantitativ zu Sulfat. Diese Reaktion kann für die Einstellung sehr verdünnter Bromlösungen ausgenutzt werden, indem eine abgemessene, aber un-

zureichende Menge relativ konzentrierter Standard-Thiosulfat-Lösung hinzugefügt wird. Der durch die Zugabe bewirkte Abfall des Brom–Bromid-Redoxpotentials an einer inerten Indikatorelektrode ermöglicht die Bestimmung der verbliebenen Bromkonzentration. Die Methode kann für die Messung der Kinetik schneller Bromierungsreaktionen angewendet werden.

REFERENCES

1 R. P. BELL AND D. J. RAWLINSON, *J. Chem. Soc.*, (1961) 63.
2 J. R. ATKINSON AND R. P. BELL, *J. Chem. Soc.*, (1963) 3260.
3 J. W. MELLOR, *A Comprehensive Treatise on Inorganic and Theoretical Chemistry, Vol. X*, Longmans, 1930, pp. 497, 498.
4 L. CAMON, *Rev. Acad. Cienc. Exact., Fis.-Quim. Nat., Zaragoza*, 14 (1959) 95; *Chem. Abstr.*, 57 (1962) 3073g.
5 R. P. BELL AND R. R. ROBINSON, *Proc. Roy. Soc.*, 270 (A) (1962) 411.
6 R. BUDESINSKY, *Anal. Chim. Acta*, 39 (1967) 375.

*Analytica Chimica Acta*
Elsevier Publishing Company, Amsterdam
Printed in The Netherlands



# KOLORIMETRISCHE BESTIMMUNGSMETHODEN FÜR DIE VINYLPHOSPHATINSEKTIZIDE DICROTOPHOS (DIMETHYL-(2-DIMETHYLCARBAMOYL-1-METHYL-VINYL)-PHOSPHAT) UND MONOCROTOPHOS (DIMETHYL-(2-METHYLCARBAMOYL-1-METHYL-VINYL)-PHOSPHAT)

JORGE ROSALES UND ROLAND DOUSSE
*CIBA-GEIGY AG, Werk Monthey (U.S.A.)*
UND ALFRED BECKER
*CIBA-GEIGY AG, Basel (Schweiz)*

(Eingegangen den 31. März 1971)

Die Entwicklung des Insektizids Phosphamidon (Dimethyl-(2-chloro-2-diäthylcarbamoyl-1-methyl-vinyl)-phosphat) erfolgte 1957. Diesem Präparat sind die später entdeckten Enolphosphate Dicrotophos (Dimethyl-(2-dimethylcarbamoyl-1-methyl-vinyl)-phosphat) und Monocrotophos (Dimethyl-(2-methylcarbamoyl-1-methyl-vinyl)-phosphat) chemisch verwandt:

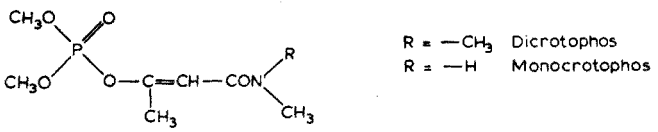


Beide haben als Insektizide mit systemischer, akarizider und Kontaktgift-Wirkung von breitem Wirkungsspektrum eine ausgedehnte Anwendung gefunden.

In dieser Arbeit werden zwei analytische Methoden zur spezifischen Gehaltsbestimmung von Dicrotophos und Monocrotophos beschrieben, die sowohl auf technische Wirkstoffe als auch auf deren Formulierungen anwendbar sind. Beide Verfahren benützen als ersten Schritt eine quantitative alkalische Hydrolyse der Ester gemäss der Gleichung

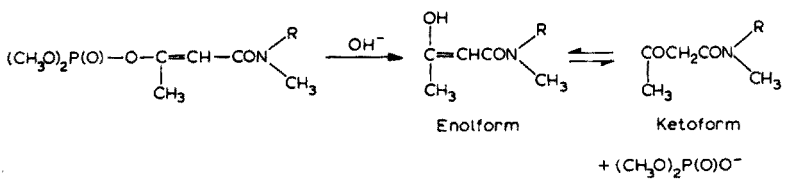


Das N,N-Dimethylacetoacetamid (DMA) und das N-Methylacetoacetamid (MMA) bilden als enolisierbare Verbindungen gefärbte Komplexe mit Eisen(III)-Ion (Abb. 1), worauf das erste Verfahren beruht. Die zweite Methode basiert auf der Fähigkeit dieser $\beta$-Diketoverbindungen, mit aromatischen Diazonium-Salzen gefärbte Derivate zu bilden. Technische Präparate können bereits kleine Anteile an DMA (in

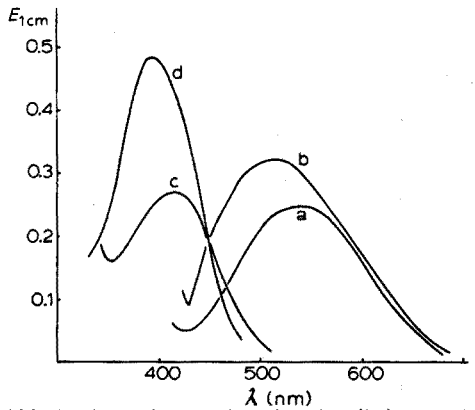


Abb. 1. Absorptionsmaxima der Eisen(III)-Komplexe des DMA und MMA (Kurven a und b) sowie der Farbverbindungen aus der Reaktion zwischen DMA bzw. MMA und dem Diazoniumsalz des 3-Chloro-4,6-disulfonamid-anilins (Kurven c und d). Konzentrationen: (a) $3.6 \cdot 10^{-5}$ *M* DMA (Wasser); (b) $3.6 \cdot 10^{-5}$ *M* MMA (Aethanol); (c) $3.6 \cdot 10^{-6}$ *M* DMA (Wasser); (d) $1.7 \cdot 10^{-6}$ *M* MMA (Wasser).

Dicrotophos) bzw. MMA (in Monocrotophos) enthalten; diese Nebenprodukte werden bei der Gehaltsbestimmung miterfasst, weshalb sie gesondert zu ermitteln und vom Gesamttiter in Abzug zu bringen sind. Bei der Bestimmung von Monocrotophos mit Eisen(III)-chlorid erfolgt die Bestimmung des freien MMA durch eine differentiell-kinetische Bestimmungsmethode, die die spezifische Erfassung von MMA neben α-Chlor-N-methylacetoacetamid ermöglicht; diese letzte Verbindung kann in sehr kleinen Mengen anwesend sein und gibt mit Eisen(III)-ion ebenfalls einen farbigen Komplex, dessen Bildung aber wesentlich langsamer erfolgt als im Falle von MMA. α-Chlor-N-methylacetoacetamid wird während der alkalischen Hydrolyse zu Verbindungen umgesetzt, die weder mit Eisen(III)-Ion noch mit einem Diazoniumsalz gefärbte Körper geben, es beeinflusst deshalb den Titer nicht.

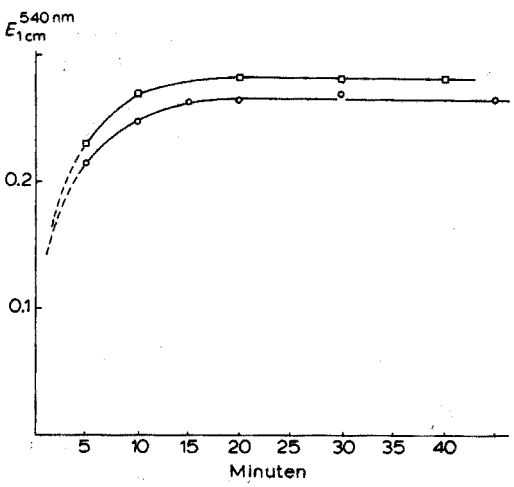


Abb. 2. Zeitlicher Ablauf der Hydrolyse von Dicrotophos (○) und Monocrotophos (□) in 1 *N* Natriumhydroxid, verfolgt durch Kolorimetrie der entstandenen DMA, bzw. MMA mit Eisen(III)-chlorid.

Für beide kolorimetrische Verfahren sind reines DMA, bzw. reines MMA als Referenzsubstanzen notwendig, deren Darstellung und Eigenschaften beschrieben werden.

*Hydrolyse der Phosphorsäureester*

Dicrotophos und Monocrotophos werden in 1 *M* Natriumhydroxid bei Raumtemperatur innert 15–10 min quantitativ hydrolysiert unter Aufspaltung der P–O–(Vinyl)-Bindung (Abb. 2). Die entstandenen N-Alkylacetoacetamide sind gegenüber dem Hydrolysiermittel bei Raumtemperatur während mindestens einer Stunde (2 Stunden beim MMA) vollkommen stabil. Die Hydrolyse bei mässig höheren Temperaturen (40–50°) führt zu unerwünschten Zersetzungen wie aus dem Spektrum der entsprechenden Eisen(III)-Farbkomplexe ersichtlich ist: es tritt eine starke bathochrome Verschiebung des normalen Absorptionsmaximums und Abnahme des Extinktionskoeffizienten auf.

*Zur Natur der Farbverbindungen*

*Komplex zwischen Acetoacetamiden und Eisen(III)-Ion.* Farbige Komplexverbindungen zwischen Enolen bzw. enolisierbaren Verbindungen oder Phenolen und Eisen(III)-Ion sind bekannt. Für den Farbkomplex DMA- bzw. MMA–Eisen(III) konnte ein Verhältnis Zahl der Zentralatome: Zahl der Liganden von 1 festgestellt werden. Es sind zwei Verfahren üblich, um dieses Verhältnis auf spektroskopischem Wege zu ermitteln, nämlich das klassische der "kontinuierlichen Variationen"[1] und das der "molaren Verhältnisse" (molar ratio)[2]. Die Abbildung 3 zeigt das durch die erste Methode gewonnene Resultat. Das Verfahren der molaren Verhältnisse dage-

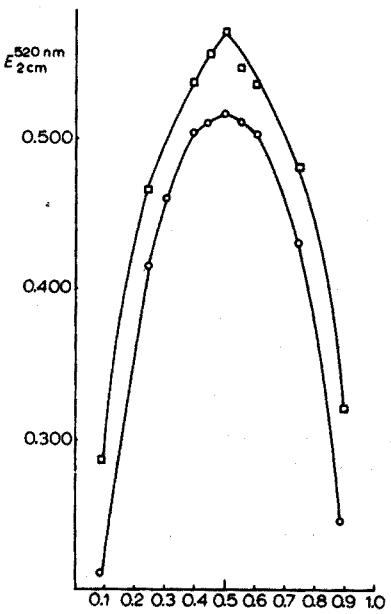


Abb. 3. Ermittlung des Verhältnisses Fe(III)/DMA und Fe(III)/MMA durch die Methode der kontinuierlichen Variationen, in Aethanol. [Fe(III)] + [DMA] = $2 \cdot 10^{-3}$ *M* (○); [Fe(III)] + [MMA] = $2 \cdot 10^{-3}$ *M* (□). Abszissenachse: [DMA]/[DMA + Fe(III)], bzw. [MMA]/[MMA + Fe(III)].

gen ergab Kurven, die sich nicht in eindeutigem Sinne auswerten liessen: mit zunehmendem Verhältnis Eisen(III)-chlorid : Enol steigt auch die Farbintensität laufend an, ohne dass der typische asymptotische Wert beobachtet wird. Aus solchen Kurven allein darf jedoch nicht auf die Unbestimmtheit der Struktur der jeweiligen Komplexe geschlossen werden[3]. Die DMA- und MMA-Komplexe mit Eisen(III)-Ion sind in wässriger oder äthanolischer Lösung bei mässig saurem pH und bei Zimmertemperatur während Stunden stabil. Zugabe von starken Säuren oder Elektrolyten wirkt farbvermindernd; in alkalischem Milieu wird der Komplex unter Fällung von Eisen-(III)-hydroxid zerstört.

Das Gesetz von Lambert und Beer ist für DMA- bzw. MMA-Konzentrationen bis zu 60 mg $l^{-1}$ erfüllt.

*Reaktion zwischen Acetoacetamiden und einem aromatischen Diazoniumsalz.* β-Diketone reagieren lediglich mit aromatischen Diazoniumsalzen zu Verbindungen, die als Monohydrazone von Triketonen angesehen werden können[4]. Die Reaktion verläuft wahrscheinlich über eine Zwischenstufe mit Diazo-Struktur:

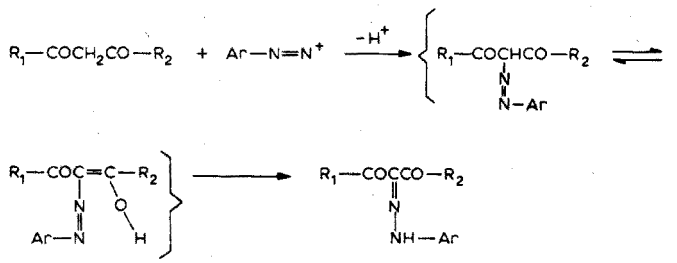

Zahlreiche solche Hydrazone sind bekannt, darunter z.B. die von N-Phenyl- und N-Naphthylderivaten des Acetoacetamids[5].

## KOLORIMETRIE MIT EISEN(III)-CHLORID

Die Ausführung der Kolorimetrie ist für Dicrotophos und Monocrotophos grundsätzlich dieselbe; als Lösungsmittel ergab jedoch im Falle des Monocrotophos Aethanol bessere Resultate als Wasser. In der in folgendem beschriebenen Prozedur verwendet man deshalb bei der Dicrotophosbestimmung die wässrige, bei der Monocrotophosbestimmung die äthanolische Eisen(III)-chlorid-Reagenzlösung. Sämtliche Verdünnungen werden bei der Analyse von Dicrotophos mit Wasser, bei derjenigen von Monocrotophos mit 96%igem Aethanol vorgenommen.

*Apparate und Reagenzien*

Es wurde das Spektrophotometer Modell Beckman DB-G verwendet.

*Reagenzlösung I (wässrig).* 27.0 g Eisen(III)-chlorid ($FeCl_3 \cdot 6\ H_2O$) in Wasser zu 1000 ml lösen.

*Reagenzlösung II (äthanolisch).* 27.0 g $FeCl_3 \cdot 6\ H_2O$ in 96%igem Aethanol zu 1000 ml lösen.

*Standardlösung für die Dicrotophosbestimmung.* 0.5 g DMA reinst (siehe unter *Darstellung und Reinigung*), mit Wasser auf 50.0 ml lösen.

*Standardlösung für die Monocrotophosbestimmung.* 0.4 g MMA reinst, werden mit Wasser auf 50.0 ml gelöst.

*Arbeitsvorschrift*

1 g Dicrotophos (Monocrotophos), wird mit Wasser auf 50.0 ml gelöst (Stammlösung). 10.0 ml dieser Lösung pipettiert man in einen 250 ml-Messkolben, versetzt mit 10.0 ml 2 *M* Natriumhydroxid und lässt das Gemisch 30 min bei Zimmertemperatur stehen. Nach Zusatz von Phenolphthaleinlösung als Indikator gibt man 1.5 *M* Salzsäure bis zum Farbumschlag zu und füllt mit Wasser (Aethanol) zur Marke auf. 10.0 ml dieser Lösung werden in einen 100 ml-Messkolben pipettiert. Nach Zugabe von 50 ml Wasser (Aethanol) und 10.0 ml Reagenzlösung I (Reagenzlösung II) füllt man mit Wasser (Aethanol) zur Marke auf (*Prüflösung*). Gleichzeitig stellt man eine *Vergleichslösung* her durch Vermischen von 10.0 ml Standardlösung DMA (MMA) mit 10.0 ml 2 *M* Natriumhydroxid und Zugabe von 1.5 *M* Salzsäure bis zum Farbumschlag auf Phenolphthalein. Es wird mit Wasser (Aethanol) auf ein Volumen von 250 ml aufgefüllt und gut durchgeschüttelt. 10.0 ml dieser Lösung werden in einen 100 ml-Messkolben abpipettiert, mit 50 ml Wasser (Aethanol) und 10.0 ml Reagenzlösung I (Reagenzlösung II) versetzt und mit Wasser (Aethanol) bis zur Marke aufgefüllt. Prüf- und Vergleichslösung lässt man 15 Min bei Raumtemperatur stehen, dann misst man die Extinktionen bei 530 (510) nm und 2 cm Schichtdicke gegen eine Blindlösung, die durch analoges Vermischen aller Reagenzien hergestellt wird.

*Berechnungen*:

$$\% \text{ Dicrotophos} = 183.8\ (E_1 W_2 / E_2 W_1) - K$$

$$\% \text{ Monocrotophos} = 194.0\ (E_1 W_2 / E_2 W_1) - K$$

$E$ = Extinktion der Prüflösung bei 530 (510) nm; $W$ = ursprüngliche Einwaage, Index 1 = Prüfmuster, Index 2 = Referenzsubstanz, in g; $K$ = Korrekturwert für freies DMA bzw. MMA (vgl. nächste Paragraphen).

*Bestimmung des freien DMA in Dicrotophos*

In ein 50 ml-Messkölbchen pipettiert man 5.0 ml der Stammlösung, gibt 5.0 ml Reagenzlösung I zu und füllt mit Wasser zur Marke auf (*Prüflösung*). *Vergleichslösung*: Aus einer frisch hergestellten Lösung von 20 mg reinem DMA, genau gewogen in 100.0 ml Wasser pipettiert man 5.0 ml in ein 50 ml-Messkölbchen, gibt 5.0 ml Reagenzlösung I zu und füllt mit Wasser zur Marke auf. Man misst die Extinktionen der Prüf- und Vergleichslösungen gegen eine geeignete Blindlösung etwa 5 Minuten nach deren Herstellung, bei 530 nm.

$$\% \text{ DMA} = 200\ (E_1 W_2 / E_2 W_1)$$

Korrekturwert $K$, der vom Gesamttiter in Abzug zu bringen ist:

$$K = 1.838 \cdot \% \text{ DMA}$$

*Differentiell-kinetische Bestimmung des freien MMA in Monocrotophos*

Man löst 0.6 g Monocrotophos in einem 50 ml-Messkolben mit Wasser und ergänzt zum Volumen. 5.0 ml dieser Lösung werden in einen 50 ml-Messkolben pipettiert und mit 30 ml Wasser versetzt. Aus einer Pipette lässt man rasch 5.0 ml Reagenz-

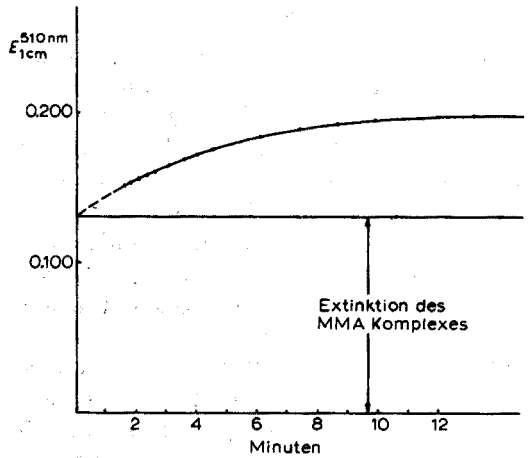


Abb. 4. Differentiell-kinetische Kolorimetrie zur spezifischen Bestimmung von MMA in Monocrotophos.

lösung I zufliessen, betätigt bei beginnender Zugabe eine Stoppuhr und füllt sofort mit Wasser zur Marke auf. Man schüttelt kräftig um und misst die Extinktion bei 510 nm in 2 cm Schichtdicke gegen eine Blindlösung, die man durch Verdünnen von 5.0 ml Reagenzlösung I mit Wasser auf 50.0 ml herstellt. Zunächst liest man die Extinktionswerte 4–6 mal in Intervallen von 15 Sekunden und anschliessend noch 4 mal in Intervallen von 1 Minute ab. Zwischen Zugabe der Reagenzlösung und der ersten Ablesung sollen nicht mehr als 1.5 min vergehen. Die Extinktionswerte trägt man in Funktion der Zeit in einem Koordinatensystem auf und extrapoliert auf die Zeit null. Der extrapolierte Extinktionswert ($E_1$) entspricht dem frei vorliegenden MMA. *Vergleichslösung*: 100 mg reines MMA werden mit dest. Wasser zu 100.0 ml gelöst; daraus pipettiert man 5.0 ml in einen 50 ml-Messkolben, setzt 30 ml Wasser und 5.0 ml Reagenzlösung I zu, füllt zur Marke auf und misst anschliessend die Extinktion bei 510 nm und 2 cm Schichtdicke ($E_2$). Berechnung

$$\% \text{ MMA} = 50\,(E_1 W_2 / E_2 W_1)$$

Korrekturwert $K$, der vom Gesamttiter in Abzug zu bringen ist:

$$K = 1.94 \cdot \% \text{ MMA}\,.$$

Die Abb. 4 zeigt an einem Beispiel die Aufstellung einer Extinktion–Zeit-Kurve, deren Aufnahme auch vorteilhaft mit Hilfe eines an das Spektrophotometer angeschlossenen logarithmischen Schreibers erfolgen kann.

### KOLORIMETRIE NACH REAKTION MIT EINEM AROMATISCHEN DIAZONIUMSALZ

*Reagenzien*

*Reagenzlösung.* 20 ml 1 *M* Salzsäure werden unter Eiswasserkühlung mit 5.0 ml der Aminlösung (0.8 g 3-Chlor-4,6-disulfonamidanilin in 100 ml Methanol) und 5.0 ml Natriumnitritlösung (4% in Wasser) versetzt. Man mischt gut durch, wartet 3 min und fügt 2 ml Sulfaminsäurelösung zu (10% in Wasser jeweils frisch herzustellen und innert 10 min zu verwenden).

*Standardlösungen.* 500 mg DMA reinst (für die Dicrotophosbestimmung) bzw.

150 mg MMA (für die Monocrotophosbestimmung) werden mit Methanol auf 50.0 ml verdünnt. 5.0 ml dieser Lösung werden mit Methanol auf 100.0 ml verdünnt. 10.0 ml der letzten Verdünnungen werden mit Methanol auf 100.0 ml verdünnt.

*Arbeitsvorschrift*

*Prüflösung.* 300 mg Dicrotophos, bzw. 150 mg Monocrotophos werden zu einem Volumen von 250.0 ml mit Methanol gelöst (Lösung A). 10.0 ml der Lösung A verdünnt man mit Methanol auf 100.0 ml (Lösung B). 10.0 ml der Lösung B werden in ein 100 ml-Messkölbchen pipettiert, mit 4.0 ml 1 *M* Natriumhydroxid versetzt und nach kurzem Umrühren während 45 min bei 20–25° stehen gelassen. Man gibt 4.0 ml 1 *M* Salzsäure, 8 ml 2 *M* Natriumacetat und 3 ml Reagenzlösung zu, schwenkt gut um und lässt das Gemisch während 10 min bei 20–25° stehen. Nach Zugabe von 10.0 ml 1 *M* Natriumhydroxid wird mit Wasser zu 100.0 ml aufgefüllt.

*Vergleichslösung.* 10.0 ml der entsprechenden Standardlösung pipettiert man in einen 100 ml-Messkolben ab und versetzt mit 4.0 ml 1 *M* Natriumhydroxid. Alle weiteren Operationen sind die gleichen wie oben beschrieben.

Man misst die Extinktionen der Prüf- und Vergleichslösung gegen eine durch Vermischen aller Reagenzien hergestellte Blindlösung bei 400 nm in 1 cm-Küvetten.

$$\% \text{ Dicrotophos} = 45.93\ (E_1 W_2 / E_2 W_1) - K$$

$$\% \text{ Monocrotophos} = 48.48\ (E_1 W_2 / E_2 W_1) - K$$

$K$ ist ein Korrekturfaktor für freies DMA (in Dicrotophos) bzw. freies MMA (in Monocrotophos) (vgl. nächsten Paragraphen).

*Bestimmung des freien DMA in Dicrotophos bzw. des freien MMA in Monocrotophos*

*Prüflösung.* 10.0 ml Lösung A (vgl. vorangehenden Paragraphen) werden in einem 100 ml-Messkolben mit 4.0 ml 1 *M* Salzsäure, 3.0 ml Reagenzlösung, 4.0 ml 1 *M* Natriumhydroxid und 8 ml 2 *M* Natriumacetat versetzt. Nach 10 min gibt man 10.0 ml 1 *M* Natriumhydroxid zu und füllt mit Wasser zur Marke auf.

*Referenzlösung.* In einem 100 ml-Messkolben werden 10.0 ml Standardlösung mit 4.0 ml 1 *M* Salzsäure, 3.0 ml Reagenzlösung, 4.0 ml 1 *M* Natriumhydroxid und 8 ml 2 *M* Natriumacetat vermischt. Nach 10 min setzt man 10.0 ml 1 *M* Natriumhydroxid zu und füllt mit Wasser auf. Die Messung erfolgt in 1 cm-Küvetten bei 400 nm.

$$\% \text{ DMA in Dicrotophos, bzw. MMA in Monocrotophos} = 2.5\ (E_1 W_2 / E_2 W_1)$$

für freies DMA $K = 1.84 \cdot \%$ DMA
für freies MMA $K = 1.94 \cdot \%$ MMA

*Darstellung und Reinigung der Referenzsubstanzen DMA und MMA*

Reines DMA gewinnt man aus seinen technischen wässrigen Lösungen durch Abtrennung des Wassers im Rotationsverdampfer und wiederholte Destillation des zurückbleibenden Oels im Vakuum. Die reine Substanz ist eine leicht gelbe Flüssigkeit mit Siedepunkt 90° (1 Torr). Die Reinheit dieser Referenzsubstanz kontrolliert man durch Gaschromatographie unter folgenden apparativen Bedingungen: Kolonne 1000/3 mm ∅, gefüllt mit Chromosorb Q 60–80 mesh, beladen mit 10% Etofat

60/25. Temperatur der Kolonne 140°. Detektor Katharometer, 200°. Verdampfertemperatur 150°. Trägergas Helium, 50 ml $min^{-1}$. Einspritzmenge 1–2 $\mu$l.

Mit der Zeit tritt beim DMA leichte Farbänderung auf und der Titer nimmt etwas ab; deshalb muss die Reinheit von Zeit zu Zeit durch Gaschromatographie kontrolliert werden.

Reines MMA kann aus den technischen wässrigen Lösungen nach Abdampfen des Wassers im Vakuum durch zwei- bis dreimaliges Umkristallisieren aus heissem Benzol gewonnen werden. Man erhält so farblose Kristalle vom Schmelzpunkt 50°.

DMA und MMA können prinzipiell auch aus den entsprechenden Phosphorsäureestern durch Hydrolyse in 2 *M* Natriumhydroxid bei Raumtemperatur gewonnen werden; nach sorgfältiger Neutralisation des Hydrolysates mit Salzsäure in der Kälte, Abdampfen des Wassers im Vakuum bei max. 50° und Extraktion des Rückstandes mit Benzol erfolgt die weitere Reinigung wie bereits beschrieben.

Wir danken den Herren O. Devillaz, F. Ehinger und Ch. Cherix für die sorgfältige Durchführung der experimentellen Arbeit und Herrn Dr. W. Büchler für die kritische Durchsicht des Manuskripts.

ZUSAMMENFASSUNG

Zwei kolorimetrische Verfahren zur spezifischen Gehaltsbestimmung der Vinylphosphatinsektizide Dicrotophos und Monocrotophos in technischen Wirkstoffen oder in Formulierungen werden beschrieben. Beide beruhen auf der quantitativen alkalischen Hydrolyse der Ester und der Bestimmung der entstandenen N-Alkylacetoacetamide, entweder als Eisen(III)/Enol Komplex oder als das Hydrazon, das durch Reaktion dieser Verbindungen mit einem diazotiertem aromatischem Amin entsteht.

SUMMARY

Two colorimetric assay methods for the vinyl phosphate insecticides Dicrotophos and Monocrotophos in technical concentrates or in formulations are described. They are based on the alkaline hydrolysis of the esters and the subsequent colorimetry of the resulting N-alkylacetoacetamides. In the first method, an iron(III) complex is formed with the enol form of these acetoacetamides. In the second the hydrolysis products are made to react with a diazotised aromatic amine to give a coloured hydrazone.

RÉSUMÉ

Deux méthodes colorimétriques spécifiques sont décrites pour le dosage des insecticides à structure phosphate de vinyle Dicrotophos et Monocrotophos, soit dans leurs concentrés techniques, soit dans leurs formulations. Elles sont basées sur l'hydrolyse alcaline quantitative de ces esters et le dosage colorimétrique des N-alcoyl acétoacétamides formées, soit sous forme de complexe avec l'ion ferrique, soit sous forme de l'hydrazone résultante de leur réaction avec le sel de diazonium d'une amine aromatique.

LITERATUR

1 P. JOB, *Ann. Chim.*, 9 (1928) 113; vgl. auch K. S. KLAUSEN UND F. J. LANGMYHR, *Anal. Chim. Acta*, 28 (1963) 335.
2 J. H. YOE UND A. L. JONES, *Ind. Eng. Chem., Anal. Ed.*, 16 (1944) 111.
3 Unauswertbare molar ratio Kurven treten oft bei starkdissoziierten Komplexen auf, vgl. z.B. A. E. HARVEY UND D. L. MANNING, *J. Amer. Chem. Soc.*, 72 (1950) 4488.
4 S. M. PARMERTER, in R. ADAMS *et al.*, *Organic Reactions, Vol. 10*, Wiley, New York, S. 9.
5 S. M. PARMERTER, in R. ADAMS *et al.*, *Organic Reactions, Vol. 10*, Wiley, New York, S. 60.

*Analytica Chimica Acta*
Elsevier Publishing Company, Amsterdam
Printed in The Netherlands

## SHORT COMMUNICATIONS

### Determination of selenium in glacial ice by radioactivation

Information on the selenium content of a Greenland ice sheet was desired[1]. In anticipation of finding only minute quantities of this element in glacial ice, the analysis was performed through radioactivation. The basic method of Bowen and Cawse[2] which measures neutron-induced $^{81}$Se was adopted. However, exclusive of a 3-min ashing step unnecessary in the present work, 33 min would have been required to process samples. Since $^{81}$Se decays with a half-life of 18.6 min, it was desirable to reduce the processing time.

This report describes the modified procedure devised, which permits the counting of samples within 12–14 min after irradiation and thereby effects a two-fold increase in sensitivity. The method of preparing the glacial ices for analysis and the results of their analysis are also given.

*Experimental*

*Samples.* The samples were collected by Dr. C. C. Patterson of the California Institute of Technology in connection with his work on lead[3]. Most samples were taken within the vicinity of Camp Century on the Greenland ice sheet and they were melted and stored in sealed polyethylene containers.

*Sample preparation.* Thirteen samples were analyzed in duplicate or triplicate. The sample volumes ranged from 1 to 4 l and the precise size was gravimetrically determined.

Each sample was transferred from the original polyethylene container to a round-bottom quartz flask that had been leached with hot concentrated nitric acid. To the sample were added 10 ml of concentrated nitric acid and a $^{75}$Se spike ($6 \cdot 10^3$ counts min$^{-1}$) that contained less than 0.06 ng of selenium carrier.

The flask was placed in a heated mantle and attached to a condenser by means of a quartz elbow; the volume was reduced to 20 ml at boiling temperature. The solution was transferred to a Teflon beaker and evaporated to a small drop of viscous consistency. To eliminate error from contamination by external sources, the evaporation was done within a glass enclosure that was maintained under slight positive pressure with a sweep of purified nitrogen gas. In preparation for irradiation, the residual drop was transferred with small portions of double-distilled water to a 1.3-ml polyethylene vial. The final solution volume, which was exactly determined by weighing, ranged closely about 1.1 ml. At this stage of the analysis, the $^{75}$ Se $\gamma$-ray activity of the sample was compared with that of a standard to estimate the combined losses in the evaporation and transfer steps.

*Blanks.* Four blanks were prepared which consisted of 20 ml of double-distilled water, 10 ml of concentrated nitric acid, and the $^{75}$Se spike. These constituents were contained in a Teflon beaker and processed from that point as described above for the samples.

*Comparators.* Comparators consisted of 1 ml of 0.16 *M* nitric acid containing 1 $\mu$g of selenium and the $^{75}$Se spike.

*Irradiation.* The samples, comparators, and blanks were irradiated for 30 min in a thermal flux of $1.8 \cdot 10^{12}$ n cm$^{-2}$ sec$^{-1}$, in the Lazy Susan of the Triga Reactor at the Gulf Energy and Environment Service facility in San Diego.

*Radiochemical purification.* The radiochemical purification process involved distillation, a precipitation of the selenium metal, its dissolution and re-precipitation[2]. The time-saving modifications in this purification were chiefly attained by dissolving the first selenium metal precipitate with a relatively large volume of concentrated nitric acid and by effecting the second selenium metal precipitation with hydroxyammonium chloride instead of sulfur dioxide. The larger quantity of nitric acid enabled an accelerated dissolution of the selenium metal. Since nitric acid inhibits the reduction of selenium to its metal with sulfur dioxide, the alternative method of reduction with hydroxyammonium chloride was introduced. This modification, besides providing conditions for an immediate precipitation, permitted direct filtration of the precipitated metal, whereas solutions treated with sulfur dioxide are not immediately filterable. The centrifugation, which would have been necessary had sulfur dioxide been used, results in a selenium metal deposit which firmly adheres to walls of plastic or glass composition even on treatment with ultra-sonics. Consequently the time involved to recover material in this condition also was avoided.

The purification procedure was as follows. To a 50-ml round-bottom flask were added 1 ml of selenium carrier (prepared by dissolving selenium dioxide in distilled water at a concentration of 10 mg Se ml$^{-1}$), 5-ml volumes of concentrated hydrochloric and hydrobromic acids, and 2 drops of each of these carriers: arsenic (10% sodium arsenate solution), manganese (50% manganese nitrate solution), phosphorus (10% ammonium dihydrogen orthophosphate solution), and tellurium (10% sodium tellurate in 1 *M* hydrochloric acid). The freshly irradiated solution was added to this flask; for samples and blanks a 1-ml aliquot was introduced while for comparators 0.50 ml were processed. The distillation head was promptly attached and the flask was heated with a small Bunsen burner for 3 min, during which time purified nitrogen gas was swept through the system. A centrifuge tube, which was used to collect the distillate, contained 15 ml of 4 *M* hydrochloric acid and 2 drops of manganese carrier.

After distillation, sulfur dioxide was bubbled through the collection tube for 30 sec. The resultant selenium metal precipitate was separated from the solution by a 1-min centrifugation. After the supernatant solution was discarded, 2 ml of concentrated nitric acid were added to the tube and it was immersed in a boiling water bath for 20–30 sec until the precipitate was completely dissolved. The solution was transferred to a beaker and after the addition of 0.1 ml of 30% hydrogen peroxide it was heated for 5–10 sec over a direct flame until effervescence ceased. Saturated hydroxyammonium chloride solution (10 ml) was added to the sample, and it was brought to steaming by heating over an open flame for about 20 sec.

After standing for 30 sec the precipitated selenium metal was collected by vacuum filtration onto a glass fiber disc. The disc was mounted on a brass planchet and $\beta$-rays were counted at frequent intervals for about 5 h in a gas-flow proportional counter. After counting, the samples were demounted, dissolved in nitric acid and the $^{75}$Se $\gamma$-ray activity was measured. By comparison of the sample count rate with that of the standard spike, the over-all selenium yield could be determined.

*Results*

Typical $\beta$-decay curves of a sample and a comparator are shown in Fig. 1. The long-lived tail, which is attributable to 57-min $^{81m}$Se and 120-day $^{75}$Se, was treated as a single component in the resolution of $^{81}$Se from the decay data. This approach

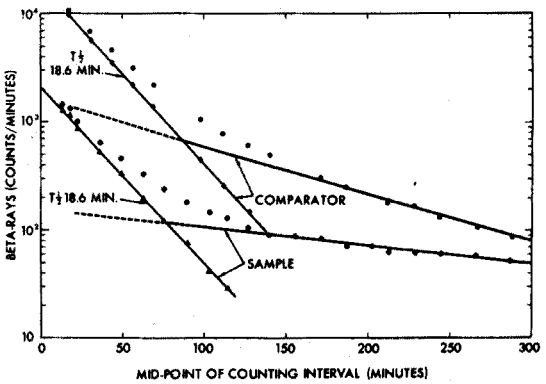


Fig. 1. $\beta$-Decay curves of a sample and a comparator and resolution of the $^{81}$Se component.

was sufficiently accurate to yield half-life values for $^{81}$Se which agreed, within several percent, with the accepted value. The difference between the sample and comparator in the apparent half-life of the tail is accountable to the relative proportions of the two longer-lived selenium radioactivities. Samples and comparators received the same quantity of $^{75}$Se spike; however, the absolute quantity of selenium in comparators was substantially greater than that of samples. The shorter half-life of the comparator tail reflects the relatively greater contribution of induced $^{81m}$Se to the total activity.

The results of the assay of the selenium content of glacial ices appear in Table I.

TABLE I

SELENIUM CONTENT OF GLACIAL SAMPLES

| *Sample*[a] | *Selenium* (*ng kg*$^{-1}$) | *Deviation from mean* (*ng kg*$^{-1}$) |
|---|---|---|
| 1 | 25.5 | 1.6 |
| 2 | 14.1 | 1.6 |
| 3 | 13.4 | 2.6 |
| 4 | 10.1 | 1.1 |
| 5 | 7.6 | 0.3 |
| 6 | 8.0 | 0.2 |
| 7 | 22.0 | 2.3 |
| 8 | 11.0 | 0.2 |
| 9 | 5.1 | 0.5 |
| 10 | 9.7 | 1.1 |
| 11 | 14.2 | 2.2 |
| 12 | 8.0 | 0.2 |
| 13 | 8.7 | 0.3 |

[a] Samples 4 and 11 were analyzed in triplicate, all others in duplicate.

The average deviation from the mean for all samples analyzed was 9.0%.

In the reduction of the sample volume to 1 drop and in its transfer to the

irradiation vial, about 10–15% of the selenium was lost. More serious loss was incurred when the sample was allowed to evaporate to dryness.

The final selenium yield (usually about 50%) as determined by measurement of the fraction of $^{75}Se$ spike ultimately recovered, is subject to a small error. In the case of the selenium comparators, the $^{75}Se$ activity induced during the irradiation was about 0.5% of the quantity added in the spike. Since the selenium content of the samples was considerably lower than that of the comparators, the error from this source was even less significant.

The results of the analysis of the comparators indicated that about 70 counts $min^{-1}$ of $^{81}Se$ per ng of selenium were realized at the end of the irradiation. With a $\beta$-ray background of 15 counts $min^{-1}$ for the counting system used, the limit of sensitivity is less than 1 ng. This sensitivity, coupled with the fact that blanks were devoid of detectable $^{81}Se$ activity, indicates that any contribution of selenium either through reagents or by contamination during processing was inconsequential.

I thank Professor Edward D. Goldberg of the Scripps Institution of Oceanography for the invitation to participate in this effort and Minoru Koide of that Institution for his generous assistance with the radiochemical separations.

*Naval Undersea Research and Development Center, San Diego, Calif. 92132 (U.S.A.)*

Herbert V. Weiss

1 H. V. Weiss, M. Koide and E. D. Golberg, *Science*, in press.
2 H. J. M. Bowen and P. S. Cawse, *Analyst*, 88 (1963) 721.
3 M. Murozumi, T. J. Chow and C. C. Patterson, *Geochim. Cosmochim. Acta*, 33 (1969) 1247.

(Received 18th January 1971)

*Anal. Chim. Acta*, 56 (1971) 136–139

## Liquid–liquid ion-exchange membrane electrodes with heteropoly compounds as the ion exchanger for the phosphate ion

In a search for an ion-selective electrode for the phosphate ion, it was thought that heteropoly complexes would be selective for the phosphate ion and could be used in a liquid–liquid membrane electrode. Phosphate is complexed by molybdate in acidic solution to form the heteropoly acid, 12-molybdophosphoric acid. Phosphate is also complexed by tungstate under acidic conditions to form the heteropoly acid, 12-tungstophosphoric acid[1]. A review on the structure and properties of heteropoly compounds of molybdenum and tungsten has been published by Tsigdinos[2].

The main problems in developing a successful liquid–liquid electrode are mechanical. The liquid ion exchanger must be in electrolytic contact with the sample solution, yet an actual mixing of the liquid phases must not occur to any great extent.

To prevent contamination of the sample, the exchanger material must be insoluble in the sample solution. The viscosity of the ion-exchange material should be high enough to prevent rapid flow across the interface. Other desirable characteristics of the ion exchanger include photochemical and thermal stability, moderate cost, availability in high purity, compatibility with the internal reference element, and high exchange capacity. Besides all of these stringent requirements, the need for high selectivity prevails[3].

Phosphotungstic acid and phosphomolybdic acid are very soluble in water and in organic solvents, especially if the solvent contains oxygen. Ethers, alcohols, and ketones, in that order, are generally the best solvents[2]. The non-aqueous solvent chosen for use in the liquid–liquid membrane electrode was *n*-pentanol. It has the desirable characteristics of very low miscibility with water, of low volatility (b.p. 137°), and of being oxygen-containing.

The free heteropoly molybdic and tungstic acids are fairly strong acids, with dissociation constants in the range $10^{-1}$–$10^{-3}$. All 12-heteropoly molybdates have high molecular weights (generally over 1800) and their tungsten analogs have molecular weights over 2800. Since the complexes are soluble in both the organic and the aqueous layer, a porous membrane was placed between the two layers, which could restrict the passage of the complex from the organic layer to the aqueous layer. This is based on the theory that a high-molecular-weight compound such as the heteropoly acid, could not diffuse through, but that smaller ions could penetrate quite easily.

In the presence of alkaline compounds, these complexes are degraded to products with few molybdenum or tungsten atoms. In order not to degrade the heteropoly, the pH of the sample solution must be kept well on the acidic side[2].

*Experimental*

*Apparatus.* A Beckman Research pH meter, used as a millivolt meter, coupled with a Sargent Recorder Model SRG was used in all measurements. The commercial nitrate-selective liquid–liquid membrane electrode, Orion Ionalyzer, model No. 92–07, was used as the electrode cell assembly. The non-aqueous compartment was filled with a heteropoly acid in *n*-pentanol. The membrane used in the electrode was that provided for the nitrate ion electrode, nitrate porous membranes, 92–07–04. In the reference compartment were placed 0.1 *M* potassium chloride and 0.1 *M* phosphoric acid.

*Reagents.* Phosphomolybdic acid ($P_2O_5 \cdot 24MoO_3 \cdot nH_2O$; Mallinckrodt), phosphotungstic acid ($P_2O_5 \cdot 24WO_3 \cdot nH_2O$; Baker) and *n*-pentanol (Baker) were used.

*Electrode preparation.* Phosphotungstic acid (1.2500 g) was dissolved in 10 ml of *n*-pentanol and placed in the non-aqueous compartment of the electrode. The electrode was used in conjunction with a reference calomel electrode. These electrodes were soaked in 0.1 *M* phosphoric acid for 24 h before evaluation.

*Results and discussion*

The results of varying the concentration of sodium dihydrogen phosphate with the phosphotungstic acid liquid–liquid membrane electrode are given in Fig. 1.

The selectivity over other anions was poor. The response was leveled by the presence of high electrolyte concentrations of other anions. The electrode was then

placed in 0.1 *M* phosphoric acid and soaked for 24 h. The results of varying phosphoric acid concentration can be seen in Fig. 2, Curve A. The selectivity obtained over other anions with this electrode was the best obtained in this study, but is still poor (Table I).

The results of varying the concentration of sodium dihydrogen phosphate with an electrode containing phosphomolybdic acid indicated that such an electrode was not usable. The calibration curves were not linear and the selectivity was poor. The results of varying phosphoric acid concentration are shown in Fig. 2. The selectivity was very similar to that of phosphotungstic acid.

However, within 24 h of evaluation, the phosphomolybdic acid was reduced to a blue color. The response characteristics of this electrode changed, indicating a non-reproducible system. In the case of phosphotungstic acid, the color remained unchanged for a period of at least 5 days. Calibration plots for the response of this electrode to phosphoric acid were made on successive days. The potentials changed

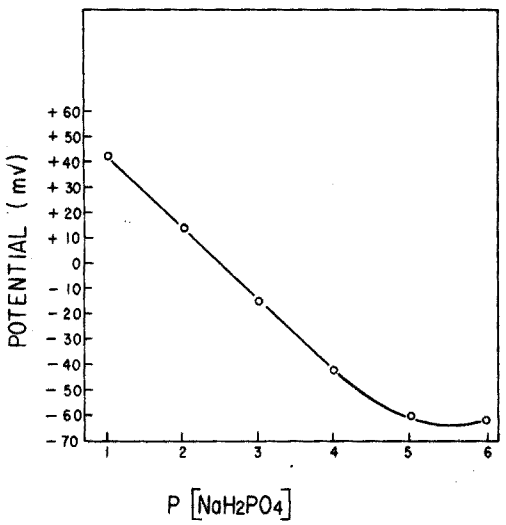


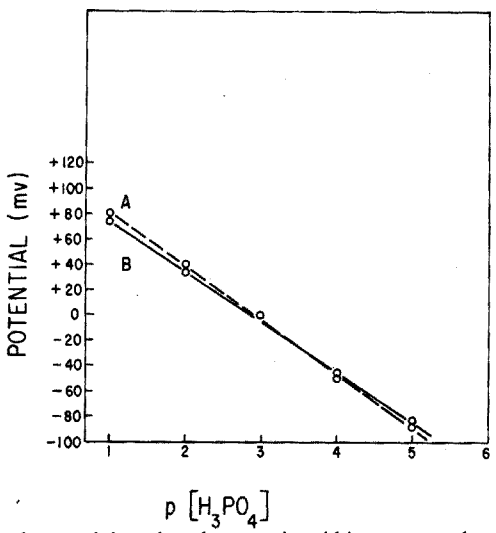


Fig. 1. Response of a liquid–liquid ion-exchange electrode containing phosphotungstic acid in *n*-pentanol to sodium dihydrogen phosphate. pH of all solutions = 4.67.

Fig. 2. Responses of various electrodes to phosphoric acid. (A) Liquid–liquid ion-exchange electrode containing phosphotungstic acid, (B) liquid–liquid ion-exchange electrode containing phosphomolybdic acid.

| *pH values* | *Dilutions* |
|---|---|
| 1.56 | 0.1 *M* $H_3PO_4$ |
| 2.06 | 0.01 *M* $H_3PO_4$ |
| 2.56 | 0.001 *M* $H_3PO_4$ |
| 3.06 | 0.0001 *M* $H_3PO_4$ |
| 3.56 | 0.00001 *M* $H_3PO_4$ |

slightly, but the slope remained the same. This was not an ideal situation, but it is the best that could be achieved.

Phosphotungstic acid was also placed in a silicone rubber membrane electrode. The selectivity obtained was poor.

TABLE I

SELECTIVITY RATIOS OF A PHOSPHOTUNGSTIC ACID LIQUID ION-EXCHANGE MEMBRANE ELECTRODE

| 0.1 *M* Salt | $\Delta mV$ | $K = \frac{E_{0.1\ M\ \text{anion}}}{E_{0.1\ M\ H_3PO_4}}$ |
|---|---|---|
| $H_3PO_4$ | 0 | 1.0 |
| KI | 36.2 | 0.550 |
| $KNO_3$ | 36.7 | 0.544 |
| $Na_2SO_4$ | 38.6 | 0.520 |
| NaBr | 45.0 | 0.440 |
| $NaClO_4$ | 45.4 | 0.435 |
| NaCl | 47.4 | 0.410 |
| $Na_2HPO_4$ | 51.7 | 0.366 |
| $NaH_2PO_4$ | 53.7 | 0.332 |
| NaOAc | 62.1 | 0.228 |

*Conclusions*

The results of this study tend to indicate that the desired selectivity could not be achieved by the above techniques. The heteropoly compounds are evidently not specific in their ion-exchange reactions. It appeared that the liquid–liquid membrane with phosphotungstic acid gave the best selectivity of all the electrodes fabricated in this study. However, the reproducibility was not as good as in the case of the iron phosphate silicone rubber electrode.

The financial support of the Fisher Scientific Company in the form of a Fellowship, Grant No. 346–83–9604, is gratefully acknowledged.

*Department of Chemistry,*
*Louisiana State University in New Orleans,*
*New Orleans, La. 70122 (U.S.A.)*

G. G. Guilbault
P. J. Brignac, Jr.*

1 S. R. Crouch and H. V. Malmstadt, *Anal. Chem.*, 39 (1967) 1084, 1090.
2 G. A. Tsigdinos, *Heteropoly Compounds of Molybdenum and Tungsten*, Climax Molybdenum Company, New York, Bull. No. Cdb-12a, 1966.
3 G. A. Rechnitz, *Chem. Eng. News*, 45 (25) (1967) 146.
4 G. G. Guilbault and P. J. Brignac, Jr., *Anal. Chem.*, 41 (1969) 1136.

(Received 20th September 1970)

* Present address: Northwestern State College, Natchitoches, La. 71457.

*Analytica Chimica Acta*
Elsevier Publishing Company, Amsterdam
Printed in The Netherlands



## Atomic absorption determination of yttrium in the nitrous oxide–acetylene flame

The determination of yttrium by atomic absorption spectroscopy with the nitrous oxide–acetylene flame has been investigated by Amos and Willis[1] and Manning[2]. Kinnunen and Lindsjo[3] have investigated the effects of relatively high concentrations (10 mg $ml^{-1}$) of mineral acids on the atomic absorption of yttrium. The present work presents a more detailed study of the interferences caused by sodium, sulphuric, nitric, phosphoric and perchloric acids when present in concentrations up to 5 mg $ml^{-1}$.

*Apparatus*

A Varian Techtron Model AA5 atomic absorption spectrophotometer was used for all measurements in conjunction with a Varian Techtron Type AB50 high-temperature premix burner. The light source used was an yttrium hollow-cathode lamp (Varian Techtron Pty. Ltd., No. CR912), which was operated at 15 mA. The analytical wavelengths employed were 410.2 nm and 407.7 nm. A spectral bandwidth of 0.17 nm was used throughout. The flow rates of nitrous oxide and acetylene were measured with calibrated flow meters. A scale expansion of approximately 3 was used for the absorbance measurements.

*Reagents*

All solutions were made up in a potassium chloride solution containing 1 mg $ml^{-1}$ of potassium for suppression of ionisation. A standard yttrium stock solution was prepared by dissolving analytical-grade yttrium oxide (Alfa Inorganics Inc., 99.9%) in warm dilute hydrochloric acid, evaporating to dryness and making up to volume. The acids used were reagent grade and their solutions were standardised against sodium tetraborate. All inorganic salts used were of analytical grade. The standard sodium solution was prepared from the chloride which was dried at 110° for 3 h. In studies on the interference of phosphoric acid it was found necessary to add hydrochloric acid to the solutions to prevent the precipitation of yttrium[4]. A check showed that at the concentration used (3.7 mg $ml^{-1}$) hydrochloric acid had no effect on the absorbance of yttrium. The yttrium concentration used for all measurements was 250 $\mu g$ $ml^{-1}$.

*Flame parameters*

It was found that the sensitivity for yttrium was markedly dependent on the flame composition. The following conditions gave maximal sensitivity: fuel–oxidant ratio 0.69; nitrous oxide flow rate, 5.2 l $min^{-1}$. Under these conditions the "red feather" was *ca.* 1 cm high. The height in the flame at which the measurements were made was 3 mm above the burner head, zero height being read when the burner head just began to cut out some of the light from the hollow-cathode lamp. The above gas flow rates gave rise to a nebulisation rate of 7.5 ml $min^{-1}$ with the adjustable nebuliser set for maximal uptake. The nebulisation rate was independent of the concentration of species in the solutions studied. These standard conditions produced maximal yttrium absorption. However, the effect of varying the flame composition, height in the flame above the burner head and spectral bandwidth was also investigated (see below); unless otherwise stated, the standard conditions will be as above.

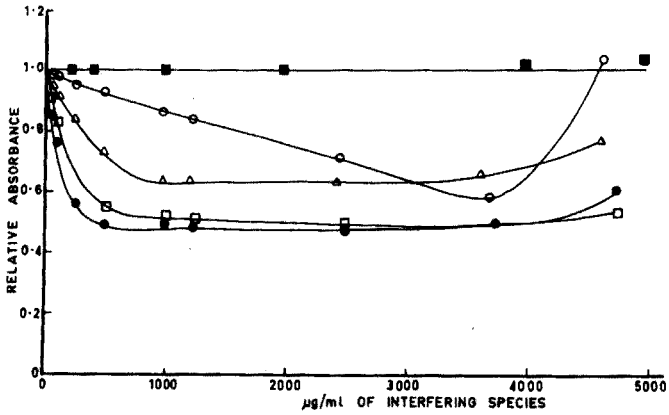


Fig. 1. Interferences on yttrium atomic absorption at 410.2 nm. (■) Na, (○) $HClO_4$, (△) $HNO_3$, (●) $H_2SO_4$, (□) $H_3PO_4$.

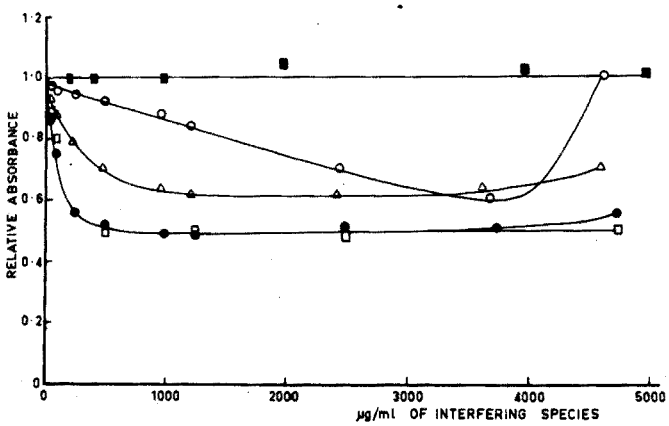


Fig. 2. Interferences on yttrium atomic absorption at 407.7 nm. Symbols as in Fig. 1.

*Results and discussion*

*Effect of acids.* The results shown in Figs. 1 and 2 demonstrate that sulphuric, nitric, phosphoric and perchloric acids interfere significantly with the absorption of yttrium for both the analytical spectral lines used. Sulphuric, nitric and phosphoric acids gave a decrease in absorbance over the concentration range studied with a region of essentially constant interference occurring between 1 and 4 mg $ml^{-1}$. The interferences of sulphuric and phosphoric acids were about the same.

Kinnunen and Lindsjo[3] also found that these two acids decreased the absorption of yttrium when they were present in concentrations greater than 10 mg $ml^{-1}$. However, the extent of the interference they found was significantly less than that reported here. For example, to check the effect of very high sulphate concentrations a solution containing 50 mg $ml^{-1}$ was nebulised; a relative absorption of 0.70 was obtained. Kinnunen and Lindsjo obtained a relative absorption of 0.92 for the same sulphate concentration for an yttrium concentration of 100 $\mu$g $ml^{-1}$ in the presence of 1 mg $Na^+$ $ml^{-1}$ as ionisation suppressant. However, such direct comparisons between the present work and that of Kinnunen and Lindsjo may be misleading, since these wor-

kers may have used a larger height in the flame for their observations. It was found in the present work that the use of larger heights in the flame gave similar, but reduced, interferences.

The interference for nitric acid was very similar to that found by Kriege and Welcher[5] for the effect of nitrate ion on the absorption of scandium. However, these workers observed an enhancement of the absorption of scandium by the sulphate ion, which is, of course, opposite to that found for the effect of sulphuric acid on the absorption of yttrium. Kinnunen and Lindsjo[3] found that nitric acid in the concentration range 10–100 mg $ml^{-1}$ produced an enhancement of the absorption of yttrium. Relative absorbance in this range rose from 1.22 to 1.31. The present work, however, shows that at lower concentrations nitric acid produces a decrease in absorbance, under the conditions used.

With perchloric acid, the absorbance initially decreased, but then increased and at concentrations of the order of 5 mg $ml^{-1}$, perchloric acid produced a slight enhancement of the signal. When present in a much higher excess, *i.e.*, 25 mg $ml^{-1}$, perchloric acid caused slight interference, the relative absorbance being 1.05 for both wavelengths. Kinnunen and Lindsjo[3] also found that perchloric acid produced an increase in the absorption of yttrium when present in the concentration range 10–100 mg $ml^{-1}$. The explanation for the increased signal at high perchloric acid concentrations may be related to an increase in flame temperature resulting from the additional oxidant provided by increasing amounts of perchloric acid. To test this idea the effect of an excess of perchloric acid on the interference caused by sulphuric acid was investigated. It was found that the sulphuric acid interference was reduced by about 15% in the presence of 25 mg of perchloric acid per ml. The interference was unaffected by similar concentrations of hydrochloric acid. Since the interference of sulphate is temperature-sensitive[1], it appears that the flame temperature is raised sufficiently by the excess of perchloric acid to reduce to some extent the interference caused by sulphuric acid. However, as yet there is no experimental evidence to show whether this increase in flame temperature occurs. The fuel–oxidant ratio was varied to observe the effect of this parameter on the interferences. The effects showed little change for the additional ratios of 0.73 and 0.77.

*Effect of sodium.* It was apparent that sodium had a negligible effect at both analytical wavelengths on the absorption of yttrium over the concentration range studied. In fact, sodium concentrations as high as 23 mg $ml^{-1}$ produced no significant interference. Yttrium should be partially ionised at the temperature of the nitrous oxide–acetylene flame but it appears that the 1 mg K $ml^{-1}$ used to suppress the ionisation was sufficient for the yttrium concentration taken. Consequently the added sodium produced no significant increase in the absorption.

The aspiration rate was not changed by the presence of such high concentrations of salt. This was checked by comparison with the aspiration rate in the absence of sodium chloride. This result is in agreement with the work of Ramirez-Munoz[6], who suggested that although the presence of large amounts of sodium chloride has no effect on the aspiration rate it could affect the droplet size. He proposed also that large concentrations of sodium chloride in the air–acetylene flame would make the conditions for proper diffusion and evaporation equilibria difficult to achieve. The results of the present work suggest that this effect may not be as serious for the nitrous oxide–acetylene flame, under the conditions used, as it was for the air–acetylene flame.

*Effect of spectral bandwidth and height above the burner.*

Increasing the spectral bandwidth from 0.17 nm to 0.33 nm also resulted in no significant change in the effect. At 407.7 nm the absorption band was significantly broadened by using the 0.33-nm spectral bandwidth, owing to the presence of an adjacent line. The use of the increased spectral bandwidth allowed lower settings of the coarse gain of the instrument to be employed. This led to an increase in the signal-to-noise ratio obtained.

For a fuel–oxidant ratio of 0.69, the absorption of yttrium showed a marked dependence on the height in the flame above the burner head. The effects of the four acids on the absorption at a height of 5 mm in the flame were studied. The shapes of the curves were essentially the same as before, but the degrees of interference were not as great.

Increased heights in the flame were not investigated because it was found that the yttrium absorption decreased rapidly. The large setting of scale expansion that subsequently had to be used led to a very noisy signal. For a fuel–oxidant ratio of 0.77, a height above the burner head of 8 mm was found to give the strongest absorption. A study showed that the effects of the acids remained essentially unchanged under these conditions.

We are grateful to the Australian Research Grants Committee for financial support.

*Department of Chemistry,*
*La Trobe University,*
*Bundora, Victoria 3083 (Australia)*

R. W. Cattrall
S. J. E. Slater

1 M. D. Amos and J. B. Willis, *Spectrochim. Acta*, 22 (1966) 1325, 2128.
2 D. C. Manning, *Atomic Absorption Newsletter*, 5 (1966) 127.
3 J. Kinnunen and O. Lindsjo, *Chemist-Analyst*, 56 (1967) 25.
4 R. C. Vickery, *The Chemistry of Yttrium and Scandium*, Pergamon Press, New York, 1960, p. 63.
5 O. H. Kriege and G. G. Welcher, *Talanta*, 15 (1968) 781.
6 J. Ramirez-Munoz, *Anal. Chem.*, 42 (1970) 517.

(Received 30th November 1970)

*Anal. Chim. Acta*, 56 (1971) 143–146

*Analytica Chimica Acta*
Elsevier Publishing Company, Amsterdam
Printed in The Netherlands



## The determination of boron in saline waters with Nile Blue A

Boron occurs widely distributed throughout the earth's crust, and figures have been obtained ranging from 0.013 p.p.m. in fresh water to 120 p.p.m. in marine plants[1]. Its function is somewhat obscure, but it seems essential for green algae and angiosperms[2,3]. In parts of California plants and animals may be poisoned by excessive amounts of boron in the soil; deficiencies in boron lead to poor crops in other areas[4]. Various methods have been suggested for the determination of boron in sea waters, titrimetric, spectrographic, fluorimetric[5] and spectrophotometric[6] procedures having been utilized.

Most recent work on the spectrophotometric determination of boron has centred around thionine derivatives, *e.g.* methylene blue[7], which form extractable complexes with the fluoroborate ion. Several dyestuffs and extractants have been investigated[8,9]; the complex formed with Nile Blue A[9] can be readily extracted with *o*-dichlorobenzene[10]. In the work described here, the method outlined by Gagliardi and Wolf[10] for mineral waters was reinvestigated and extended for the analysis of sea waters.

*Reagents and apparatus*

*Standard boron solution* (0.5 *mg B ml*$^{-1}$). Dissolve 0.7144 g of boric acid in water and dilute to 250 ml. Dilute this to give working solutions containing 2.5 $\mu$g B ml$^{-1}$.

*Nile Blue A.* Prepare a 0.1% (w/v) aqueous solution (Revector microscopical stain C.I. 51180, Hopkin and Williams Ltd., Chadwell Heath, Essex).

Polythene apparatus was used throughout, except for the final solution.

A Unicam S.P.800 spectrophotometer with a Philips external recorder was used.

*Procedure*

Pipette a suitable aliquot of the water sample (2.5–25 $\mu$g B) into a 70-ml polythene bottle and dilute to 10 ml with water. Add 10 ml of 2% (v/v) hydrofluoric acid solution, seal the bottle with a polythene screw cap and shake for *ca.* 2 h. Add 10 ml of aqueous 10% (w/v) iron(III) sulphate nonahydrate, and 1 ml of Nile Blue A solution. Extract the complex with one 10-ml and three 5-ml portions of 1,2-dichlorobenzene, removing the lower organic layer from the reaction vessel by means of a polythene bulb-pipette. Dilute to 50 ml in volumetric flasks and measure the absorbance at 647 nm.

*Interferences*

According to Gagliardi and Wolf, chloride ions interfere above 500 mg l$^{-1}$; in the investigations described here, interference was found with as little as 100 mg l$^{-1}$, and was directly proportional to chloride ion concentration over the range 100–600 mg l$^{-1}$. This interference could be completely removed by the addition of 0.025 *M* silver sulphate solution and centrifuging or filtering off the precipitate before the hydrofluoric acid addition. The volume of silver sulphate required could be calculated from a total halide titration, but a small excess had no effect on the absorbances of the final solutions.

As natural waters have a wide range of pH variation it is necessary to ensure that all sample aliquots and standards are at the same pH before the addition of the hydrofluoric acid. This avoids any difference in reaction time owing to different hydrofluoric acid concentrations. As stated by Gagliardi and Wolf, the Nile Blue A may be added as an acid–base indicator, and the solutions neutralised with *N* sodium hydroxide or *N* sulphuric acid.

*Results and discussion*

Two samples of English Channel water from Hove, Sussex, were taken under different tidal conditions and analysed for boron content. The boron contents were found to be 4.2 and 4.9 mg $l^{-1}$, respectively, with ratios of p.p.m. boron to chlorinity ($Cl^0/_{00}$) of 0.247 and 0.255; the standard deviation for the second of these analyses (twenty determinations) was 0.17 mg $l^{-1}$, giving a coefficient of variation of 3.5 %. The results obtained by Barnes and Parker[5], who used a fluorimetric method, on samples from the English Channel are 4.6 p.p.m. boron (Selsey) and 4.7 p.p.m. boron (Portland), with corresponding ratios to chlorinity of 0.237 and 0.244.

To increase sensitivity, it was decided to evaporate a larger quantity of sample, and to check this procedure for loss of boron, aliquots of standard boron solution containing 10 μg of boron were diluted to about 200 ml and evaporated under neutral, acid and alkaline conditions in PTFE beakers. After evaporation to somewhat less than 10 ml, all three gave peak heights equal to a 10-μg standard.

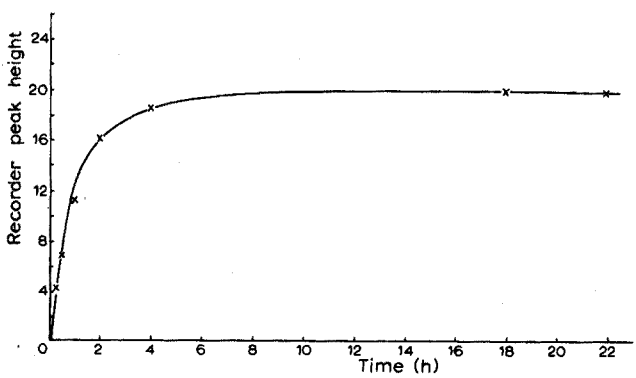


Fig. 1. Effect of reaction time. Boron added: 10 μg.

It was found, in the procedure, that the reaction time of 20 min used by Gagliardi and Wolf was insufficient for the complete formation of the fluoroborate ion. As is shown in Fig. 1, complex formation was not complete until about 18 h had elapsed, and this is borne out by other workers[7,8,11]. Even though the fluoroborate ion is slow to form in its entirety, this has no effect in routine analysis, provided that suitable standards are analysed with each batch of samples. If the boron content is extremely low it is advisable to allow the solutions to remain in contact with the hydrofluoric acid for at least 18 h, but for most concentrations, a time of 2 h suffices. The final solution of Nile Blue fluoroborate is stable for at least 72 h.

The author wishes to thank Mr. P. J. Moore for helpful discussion with this paper, and the Director of the Institute of Geological Sciences for permission to publish this work.

*Geochemical Division,*
*Institute of Geological Sciences,*
*London WC1 8NG (England)*

R. A. Nicholson

1 H. J. M. BOWEN, *Trace Elements in Biochemistry*, Academic Press, London and New York, 1966.
2 W. STILES, in W. RUHLAND, *Encyclopedia of Plant Physiology, Vol. 4*, Springer, Berlin, 1958, p. 558.
3 E. J. UNDERWOOD, *Trace Elements in Human and Animal Nutrition*, Academic Press, London and New York, 1962.
4 K. H. SCHUTTE, *The Biology of Trace Elements*, Crosby Lockwood, London, 1964.
5 W. J. BARNES AND C. A. PARKER, *Analyst*, 85 (1960) 828.
6 R. GREENHALGH AND J. P. RILEY, *Analyst*, 87 (1962) 970.
7 L. DUCRET, *Anal. Chim. Acta*, 17 (1957) 213.
8 L. C. PASZTOR AND I. D. BODE, *Anal. Chim. Acta*, 24 (1961) 467.
9 O. B. SKAAR, *Anal. Chim. Acta*, 32 (1965) 508.
10 E. GAGLIARDI AND E. WOLF, *Mikrochim Acta*, (1968) 140.
11 J. COURSIER, J. HURE AND R. PLATZER, *Anal. Chim. Acta*, 13 (1955) 379.

(Received 2nd April 1971)

*Anal. Chim. Acta*, 56 (1971) 147–149

## Gravimetric and spectrophotometric determination of mercury with thiosalicylamide

Thiosalicylamide has been found a useful analytical reagent for the determination of certain metal ions[1,2]. In the present investigation the reagent has been employed for the gravimetric and spectrophotometric determination of mercury(II). In dilute hydrochloric acid medium, the metal forms a light yellow precipitate with thiosalicylamide which can be weighed as $Hg(C_7H_7ONS)_2Cl_2$ after drying at 110–120°. The mercury precipitate is soluble in 50% ethanol; the ethanolic solution obeys Beer's law at 355 nm in the concentration range 3.90–23.40 $\mu g\ Hg^{2+}\ ml^{-1}$.

*Apparatus*

All the spectral transmittance measurements were carried out with a Carl Zeiss spectrophotometer Model PMQ II with 1-cm quartz cells. The pH values were measured with a Cambridge pH meter (Bench Model).

*Reagents*

*Standard mercury solution.* Dissolve an appropriate amount of mercury(II) chloride in 0.1 *M* hydrochloric acid and standardize by the periodate method.

*Solutions of diverse ions.* Standard solutions were prepared in distilled water, hydrochloric acid being added, where required, to prevent hydrolysis of the metal ions.

*Thiosalicylamide solution.* For the gravimetric method, prepare a 1% solution of thiosalicylamide in 20% ethanol. For the spectrophotometry, use a 0.02 *M* ethanolic solution of the reagent.

All the reagents used were of A.R. grade.

*Gravimetric determination of mercury*

The light yellow precipitate obtained by adding the thiosalicylamide solution to a hot solution of mercury(II) chloride in 1 *M* hydrochloric acid medium was slightly soluble in chloroform and carbon tetrachloride. It was stable towards nonoxidising

TABLE I

DETERMINATION OF MERCURY BY DIRECT WEIGHING OF MERCURY–THIOSALICYLAMIDE COMPLEX

| *Hg taken* (*mg*) | *Wt. of ppt.* (*mg*) | *Hg found* (*mg*) | *Error* (*mg*) |
|---|---|---|---|
| 4.95 | 14.3 | 4.951 | +0.001 |
| 4.95 | 14.2 | 4.930 | −0.020 |
| 9.90 | 28.5 | 9.896 | −0.004 |
| 9.90 | 28.6 | 9.924 | +0.024 |
| 19.80 | 56.9 | 19.740 | −0.060 |
| 19.80 | 57.0 | 19.770 | −0.030 |
| 29.70 | 85.6 | 29.700 | 0.000 |
| 29.70 | 85.7 | 29.730 | +0.030 |
| 39.60 | 114.1 | 39.590 | −0.010 |

TABLE II

SEPARATION OF MERCURY(II) FROM FOREIGN IONS

(19.80 mg of mercury(II) were used in each experiment)

| *Foreign ion added* (*mg*) | *Hg found* (*mg*) | *Error* (*mg*) |
|---|---|---|
| $Mn^{2+}$ (200) | 19.81 | +0.01 |
| $Co^{2+}$ (200) | 19.81 | +0.01 |
| $Ni^{2+}$ (200) | 19.81 | +0.01 |
| $Zn^{2+}$ (150) | 19.84 | +0.04 |
| $Cd^{2+}$ (100) | 19.81 | +0.01 |
| $Cr^{3+}$ (200) | 19.81 | +0.01 |
| $Ga^{3+}$ (200) | 19.81 | +0.01 |
| $In^{3+}$ (150) | 19.81 | +0.01 |
| $Al^{3+}$ (100) | 19.84 | +0.04 |
| $Fe^{3+}$ ( 50)[a] | 19.84 | +0.04 |
| $Ti^{4+}$ ( 50) | 19.77 | −0.03 |
| $Th^{4+}$ (100) | 19.81 | +0.01 |
| $Mo^{6+}$ ( 50) | 19.84 | +0.04 |
| $U^{6+}$ (100) | 19.81 | +0.01 |
| $Bi^{3+}$ ( 50) | 19.81 | +0.01 |
| $As^{3+}$ ( 50) | 19.81 | +0.01 |
| $Sb^{3+}$ ( 50) | 19.84 | +0.04 |
| $Pb^{2+}$ ( 20) | 19.84 | +0.04 |

[a] In presence of phosphoric acid.

acids but reacted readily with alkali. On analysis the pure complex was found to contain 34.70% Hg, 4.75% N, 11.12% S and 12.31% Cl (required for $Hg(C_7H_7ONS)_2Cl_2$: 34.72% Hg, 4.85% N, 11.08% S and 12.29% Cl). It decomposed at 204°.

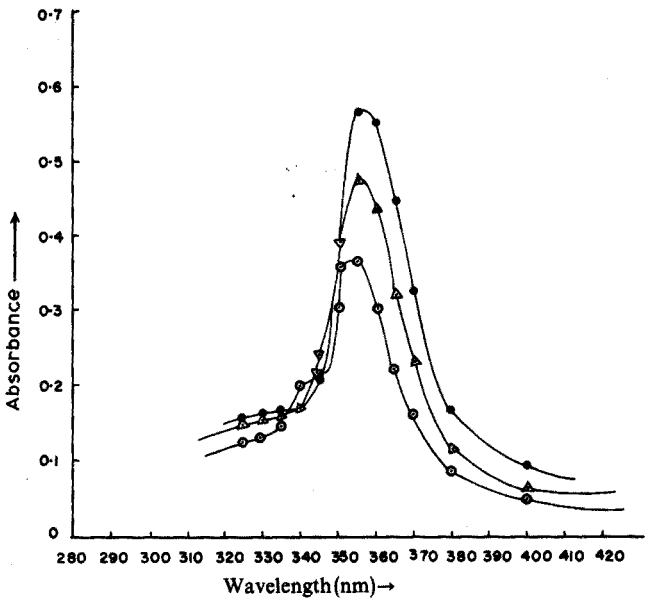


Fig. 1. Absorbance curves of mercury(II)–thiosalicylamide complex in 50% ethanol. (⊙) $[Hg^{2+}] = 11.70$ μg ml$^{-1}$; (△) $[Hg^{2+}] = 15.60$ μg ml$^{-1}$; (●) $[Hg^{2+}] = 19.50$ μg ml$^{-1}$.

For complete precipitation of mercury in 0.1–2.0 *M* hydrochloric acid medium, 1.5–3.5 times the theoretical amount of thiosalicylamide was required. At pH 4.0–5.0, mercury(II) formed a bright yellow precipitate with the reagent, which decomposed on standing. Mercury(I) produced a very unstable yellowish-white precipitate.

*Procedure.* Dilute the mercury(II) chloride solution to 120–150 ml and adjust the acidity to 0.2–1 *M* in hydrochloric acid. Heat to 50–60° and add 10–15 ml of the reagent solution. Digest on a hot water bath for 30 min with occasional stirring. Filter the precipitate on a no. 4 sintered glass crucible, and wash with hot 1% hydrochloric acid. Dry the precipitate at 110–120° to constant weight. Typical results are given in Table I.

*Effect of diverse ions.* Mercury was determined as above, without interference, in the presence of known amounts of Mn, Co, Ni, Zn, Cd, Fe(II), Cr(III), Ga, In, Al, Mo(VI), U(VI), As(III), Sb(III), Pb(II), Bi(III), Th or Ti (Table II). Addition of phosphoric acid was necessary to mask the interference of iron(III). Palladium, platinum and copper interfered.

*Spectrophotometric determination of mercury*

The absorbance curves of mercury–thiosalicylamide complex of varying concentrations of metal in 50% ethanol at pH 2.5 are shown in Fig. 1. The complex showed maximum absorbance at 355 nm.

*Procedure.* Place an aliquot of the mercury(II) solution in a 25-ml flask, and

adjust the pH to 2.5 with sodium acetate solution and dilute hydrochloric acid. Add 2.0–3.5 ml of 0.02 *M* thiosalicylamide solution, thoroughly mix and make up the volume with water and ethanol so that the final solution contains 50% ethanol. Measure the absorbance at 355 nm after 30 min against a reagent blank.

*Study of variables.* Solutions containing 78 μg of mercury(II) were separately mixed with 2 ml of 0.02 *M* solution of the reagent and the mixtures were adjusted to different acidities with dilute hydrochloric acid and sodium acetate solution, before

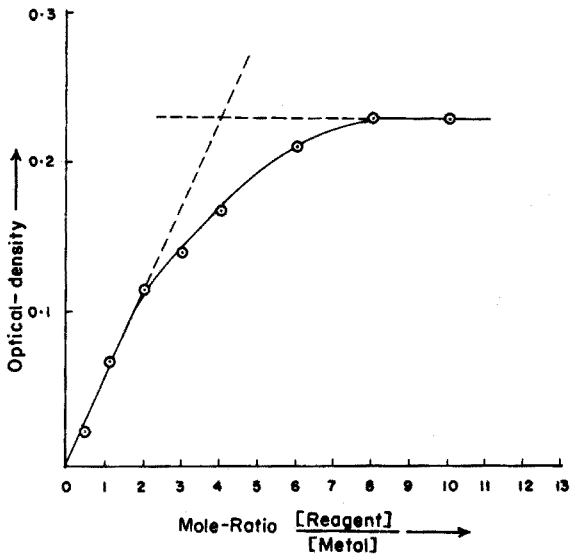


Fig. 2. Composition of the mercury(II)–thiosalicylamide complex in 50% ethanol (mole-ratio method).

dilution to 25 ml with ethanol and water. Maximal colour formation occurred between pH 2.0 and 2.95.

The absorbance of the mercury–thiosalicylamide complex in 50% ethanol was stable upto 12 h.

Beer's law was obeyed at 355 nm over the range 3.90–23.40 μg $Hg^{2+}$ $ml^{-1}$. According to Sandell's[3] recommendation, the optimal range for the determination was 6.83–23.40 μg Hg $ml^{-1}$. The sensitivity of the colour reaction and the molar absorptivity of the mercury–thiosalicylamide complex in 50% ethanol were found to be 0.034 μg $cm^{-2}$ and $5.878 \cdot 10^3$, respectively.

*Nature of the complex and its dissociation constant.* The empirical formula of the mercury complex was determined by the mole-ratio method[4]. The results (Fig. 2) indicated that mercury forms a 1:4 complex with thiosalicylamide.

The dissociation constant of the complex in 50% ethanol was found from the mole ratio curve (Fig. 2) to be $6.5 \cdot 10^{-18}$. The degree of dissociation was calculated from the curve as described by Harvey and Manning[5].

*Effect of diverse ions.* The tolerance limits for various diverse ions (Table III), are those concentrations of foreign ions which caused errors of less than ±2%. The interference of iron(III) was again avoided by adding small quantity of phosphoric acid.

TABLE III

EFFECT OF DIVERSE IONS ON THE SPECTROPHOTOMETRIC DETERMINATION OF MERCURY(II)
(190 $\mu$g of mercury(II) was taken)

| *Foreign ion added* | *Amount tolerated* ($\mu$g) | *Foreign ion added* | *Amount tolerated* ($\mu$g) |
|---|---|---|---|
| $Mn^{2+a}$ | 2000 | $Ti^{4+a}$ | 100 |
| $Ni^{2+a}$ | 2000 | $Th^{4+d}$ | 500 |
| $Co^{2+a}$ | 2000 | $W^{6+e}$ | 500 |
| $Zn^{2+a}$ | 1500 | $Mo^{6+e}$ | 500 |
| $Cd^{2+a}$ | 2000 | $UO_2^{2+d}$ | 400 |
| $Cr^{3+a}$ | 1000 | $Bi^{3+d}$ | 500 |
| $Ga^{3+b}$ | 500 | $As^{3+}$ | 500 |
| $In^{3+a}$ | 500 | $Sb^{3+b}$ | 600 |
| $Al^{3+a}$ | 600 | $Pb^{2+b}$ | 200 |
| $Fe^{3+b,c}$ | 50 | | |

[a] As sulphate. [b] As chloride. [c] In presence of phosphoric acid. [d] As acetate. [e] As sodium salt.

*Discussion*

Thiosalicylamide is an important addition to the numerous available organic reagents used for the determination of mercury(II). The reagent possesses some advantages over others such as thionalide[6], monalzine[7] and N-benzoyl-N-phenylhydroxylamine[8]. The procedure for the gravimetric and spectrophotometric determination of mercury with thiosalicylamide is simple. The mercury–thiosalicylamide complex is stable, can be obtained in a directly weighable form and has a high molecular weight. Thiosalicylamide is very soluble in hot water, so that the excess of reagent can be removed easily from the precipitate. Moreover, mercury can be determined with the reagent from dilute hydrochloric acid medium and a large number of foreign ions do not interfere with the procedure. The colour reaction between mercury(II) and thiosalicylamide is of high sensitivity.

*Chemistry Department,*
*Presidency College,*
*Calcutta (India)*

M. Mazumdar
S. C. Shome

1 S. C. Shome and M. Mazumdar, *Anal. Chim. Acta*, 46 (1969) 155.
2 K. Sur and S. C. Shome, *Anal. Chim. Acta*, 48 (1969) 145.
3 E. B. Sandell, *Colorimetric Determination of Traces of Metals*, Interscience, New York, 1959, p. 83.
4 A. S. Meyer and G. H. Ayres, *J. Amer. Chem. Soc.*, 79 (1957) 49.
5 A. E. Harvey and D. L. Manning, *J. Amer. Chem. Soc.*, 72 (1960) 4488.
6 R. Berg and W. Roebling, *Angew. Chem.*, 48 (1938) 430.
7 N. K. Dutta and B. K. Bhattacharyya, *Sci. Cult. (Calcutta)*, 29 (1963) 257.
8 B. Das and S. C. Shome, *Anal. Chim. Acta*, 35 (1966) 345.

(Received 16th March 1971)

*Analytica Chimica Acta*
Elsevier Publishing Company, Amsterdam
Printed in The Netherlands

## Iodometric determination of organic arsine compounds in aqueous acetic acid media

Conventional methods for the determination of arsenic in organic compounds are rather tedious[1], and titrimetric methods which are available for the determination of organic arsine derivatives are usually indirect[2]. A procedure for a series of water-insoluble compounds of this type was required, and a direct titration with iodine in aqueous acetic acid medium proved to be satisfactory. The equivalence points of the titrations can be determined visually or potentiometrically; satisfactory results can be achieved for samples weighing 10–100 mg.

*Experimental*

*Procedure.* Dissolve the sample (10–100 mg) containing arsenic(III) in 20–30 ml of anhydrous acetic acid. Add water dropwise until a slight milkiness appears and remove the turbidity by adding a few drops of the acetic acid. Heat the solution to 40–50° and titrate with an aqueous 0.05 *N* iodine solution from an accurate microburette with scale divisions of 0.01 ml, using starch as indicator. The end-point is shown by the appearance of a light violet colour instead of the usual blue colour.

Alternatively, detect the end-point potentiometrically with a platinum–calomel electrode pair.

*Standardization.* Standardize the iodine solution, prepared in the conventional manner, against sodium thiosulphate solution which has been previously standardized against potassium iodate. Use an aqueous medium and starch as indicator.

*Results and discussion*

The results obtained for different compounds analysed by this method are

TABLE I DIRECT DETERMINATION OF ORGANIC ARSINE COMPOUNDS

| *Compound* | *Weight taken (mg)* | *Weight found (mg)* | *Error (%)* | *End-point*[a] |
|---|---|---|---|---|
| Triphenylarsine | 50.60 | 50.36 | 0.47 | vis. |
| | 79.40 | 79.20 | 0.25 | vis. |
| | 12.40 | 12.51 | 0.89 | pot. |
| Tolylarsine | 59.00 | 59.07 | 0.12 | vis. |
| | 68.00 | 67.97 | 0.04 | vis. |
| | 12.20 | 12.22 | 0.15 | pot. |
| 1,4-Butylene bis-diphenylarsine | 20.50 | 20.43 | 0.34 | vis. |
| | 28.90 | 28.82 | 0.28 | vis. |
| 1,2-Ethylene bis-diphenylarsine | 20.60 | 20.46 | 0.67 | vis. |
| | 23.00 | 22.84 | 0.68 | vis. |
| *o*-Carboxyphenyl-dimethylarsine | 11.40 | 11.34 | 0.53 | vis. |
| | 23.60 | 23.53 | 0.30 | vis. |
| | 11.00 | 11.09 | 0.81 | pot. |
| *o*-Carboxyphenyl-diphenylarsine | 12.60 | 12.48 | 0.95 | vis. |
| | 20.00 | 19.89 | 0.55 | vis. |
| | 14.60 | 14.72 | 0.82 | pot. |
| *o*-Carboxyphenyl-ditolylarsine | 14.40 | 14.28 | 0.83 | vis. |
| | 30.40 | 30.28 | 0.39 | vis. |
| | 12.40 | 12.38 | 0.15 | pot. |

[a] vis. = visual; pot. = potentiometric.

given in Table I. Organic compounds of arsenic(III) are usually insoluble in water, but the present arsine compounds were readily soluble in acetic acid. The end-points of the titrations could not be satisfactorily detected in anhydrous acetic acid with starch solution, hence water was added to give a slight milkiness which was then removed by adding a few drops of acetic acid. Under these conditions, the end-points could be readily detected visually.

The potentiometric method of end-point detection was preferable, since it could also be used for coloured solutions. Typical titration curves are shown in Fig. 1. Moderate amounts of iodide, bromide and chloride did not interfere in these titrations.

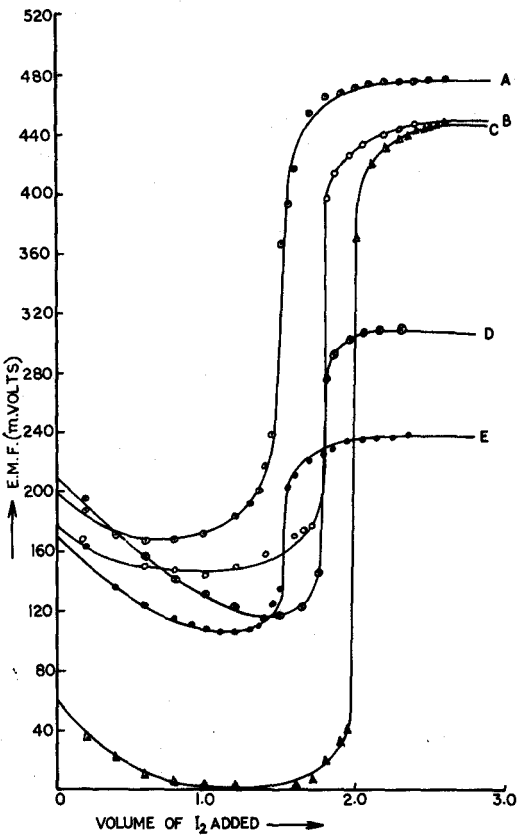


Fig. 1. Potentiometric titration curves for various arsine compounds. (A) *o*-Carboxyphenylditolylarsine, (B) triphenylarsine, (C) *o*-carboxyphenyldimethylarsine, (D) *o*-carboxyphenyldiphenylarsine, (E) tritolylarsine.

*Department of Chemistry,*
*Punjabi University,*
*Patiala (India)*

Sarjit Singh Sandhu
Sarvinder Singh Pahil
Krishan Dev Sharma

1 G. INGRAM, *Methods of Organic Elemental Analysis*, Chapman and Hall, London, 1964.
2 M. R. F. ASHWORTH, *Titrimetric Organic Analysis, Vol. 1 and 2*, Wiley–Interscience, London, 1964.

(Received 14th January 1971)

*Analytica Chimica Acta*
Elsevier Publishing Company, Amsterdam
Printed in The Netherlands

# ANNOUNCEMENTS

## 10th NATIONAL MEETING ON APPLIED SPECTROSCOPY

The Tenth National Meeting of the Society for Applied Spectroscopy will be held at Stouffer's Riverfront Inn in St. Louis, Missouri on October 18–22, 1971. Special symposia and general sessions on all areas of spectroscopy will be presented. For additional information please write to the General Chairman: Miss Joan E. Westermeyer, Titanium Pigment Division, National Lead Company, Carondelet Station, St. Louis, Mo. 63111 (U.S.A.).

## BIOCHEMICAL ANALYSIS PRIZE—PREIS BIOCHEMISCHE ANALYTIK

A prize of DM 10,000 is donated from Boehringer Mannheim and is awarded every two years at the conference "Biochemische Analytik" in Munich for outstanding work in the field of biochemical analysis. The donation will take place during the 1972 conference between 25 and 28 April. Papers, either published or accepted for publication between 1 January 1970 and 30 September 1971 may be sent in triplicate before 15 November 1971 to Dr. Rosmarie Vogel, Secretary of the "Preis Biochemische Analytik", D-8000 Munich 15, Nussbaumstr. 20, Deutsche Bundes Republik.

# CONTENTS

Determination of traces of arsenic by coprecipitation and X-ray fluorescence
T. M. REYMONT AND R. J. DUBOIS (Magna, Utah, U.S.A.) (Rec'd 18th January 1971) . . . . . 1

Ammonium 1-pyrrolidinedithiocarbamate as a reagent for bismuth
H. K. Y. LAU, H. A. DROLL AND P. F. LOTT (Kansas City, Mo., U.S.A.) (Rec'd 25th February 1971) . . . . . 7

Evaluation of some three-quarter-wave microwave cavities for the operation of electrodeless discharge lamps
D. O. COOKE, R. M. DAGNALL AND T. S. WEST (London, England) (Rec'd 10th April 1971) . . . . . 17

Description et performances d'une installation pour l'étude des sels fondus par spectrophotométrie d'absorption
G. LANDRESSE (Liège, Belgique) (Reçu le 18 mars 1971) . . . . . 29

Solvent extraction separations of the lanthanides and selected metal ions with 1,1,1,2,2,3,3-heptafluoro-7,7-dimethyl-4,6-octanedione
T. R. SWEET AND D. BRENGARTNER (Columbus, Ohio, U.S.A.) (Rec'd 1st February 1971) . . . . . 39

Observations sur le dosage du cobalt dans les métaux ferreux
R. BOULIN ET A. M. LEBLOND (St-Germain-en-Laye) et M. JEAN (Gif-sur-Yvette, France) (Reçu le 17 mars 1971) . . . . . 45

Spectrophotometric determination of small amounts of nitrate and nitrite by conversion to nitrotoluene and extraction into toluene
M. K. BHATTY AND A. TOWNSHEND (Birmingham, England) (Rec'd 30th March 1971) . . . . . 55

Instrumental neutron activation analysis of rocks with a low-energy photon detector
J. HERTOGEN AND R. GIJBELS (Ghent, Belgium) (Rec'd 1st April 1971) . . . . . 61

Fluorescence and phosphorescence of 5- and 8-aminoquinoline
S. G. SCHULMAN AND L. B. SANDERS (Gainesville, Fla., U.S.A.) (Rec'd 29th March 1971) . . . . . 83

Lowest excited singlet state $pK_a^*$ values of the isomeric aminopyridines
S. G. SCHULMAN, A. C. CAPOMACCHIA AND M. S. RIETTA (Gainesville, Fla., U.S.A.) (Rec'd 16th February 1971) . . . . . 91

Determination of diffusion coefficients from instantaneous current measurements and the Koutecky equation
J. L. JONES AND H. A. FRITSCHE, JR. (College Station, Texas, U.S.A.) (Rec'd 15th March 1971) . . . . . 97

Polarographic determination of chloramphenicol
K. FOSSDAL AND E. JACOBSEN (Oslo, Norway) (Rec'd 6th April 1971) . . . . . 105

Standardisation of dilute aqueous bromine solutions for reaction kinetics by incremental potentiometric titration with thiosulphate
R. E. EVANS AND D. R. MARSHALL (Bangor, Wales) (Rec'd 15th March 1971) . . . 117

Kolorimetrische Bestimmungsmethoden für die Vinylphosphatinsektizide Dicrotophos (Dimethyl-(2-dimethylcarbamoyl-1-methyl-vinyl)-phosphat) und Monocrotophos (Dimethyl-(2-methylcarbamoyl-1-methyl-vinyl)-phosphat)
J. ROSALES UND R. DOUSSE (Werk Monthey, U.S.A.) und A. BECKER (Basel, Schweiz) (Eing. den 31. März 1971) . . . . . 127

*(continued on page 4 of cover)*

*Continued from inside page of cover*

*Short Communications*

Determination of selenium in glacial ice by radioactivation
H. V. WEISS (San Diego, Calif., U.S.A.) (Rec'd 18th January 1971) . . . . . 136

Liquid–liquid ion-exchange membrane electrodes with heteropoly compounds as the ion exchanger for the phosphate ion
G. G. GUILBAULT AND P. J. BRIGNAC, JR. (New Orleans, La., U.S.A.) (Rec'd 20th September 1970) . . . . . 139

Atomic absorption determination of yttrium in the nitrous oxide–acetylene flame
R. W. CATTRALL AND S. J. E. SLATER (Bundora, Vict., Australia) (Rec'd 30th November 1970) . . . . . 143

The determination of boron in saline waters with Nile Blue A
R. A. NICHOLSON (London, England) (Rec'd 2nd April 1971) . . . . . 147

Gravimetric and spectrophotometric determination of mercury with thiosalicylamide
M. MAZUMDAR AND S. C. SHOME (Calcutta, India) (Rec'd 16th March 1971) . . . . 149

Iodometric determination of organic arsine compounds in aqueous acetic acid media
S. S. SANDHU, S. S. PAHIL AND K. D. SHARMA (Patiala, India) (Rec'd 14th January 1971) . . . . . 154

*Announcements* . . . . . 156